

**TUMOUR CHEMO SENSITIVITY ASSAYS:
AN INVESTIGATION INTO THE
SUSCEPTIBILITY OF CELLS TO
CHEMOTHERAPEUTICS**

SUSAN CATHERINE GILL

**A thesis submitted in partial fulfilment of the
requirements of Nottingham Trent University
for the degree of Doctor of Philosophy**

July 2009

This work is the intellectual property of the author, and may also be owned by the research sponsor(s) and/or Nottingham Trent University. You may copy up to 5% of this work for private study, or personal, non-commercial research. Any re-use of the information contained within this document should be fully referenced, quoting the author, title, university, degree level and pagination. Queries or requests for any other use, or if a more substantial copy is required, should be directed in the first instance to the author.

Dedication

This PhD is dedicated to my mum of whom I am forever proud. Memories of laughing, smiling and the unconditional love that you gave so freely and without compromise remain deep in my heart. Your strength inspired me so much, facing whatever challenges were put in your way and it is that strength that has motivated me to carry on. Your belief in me, amazing hugs, laughter and endless chats when I needed them most are sorely missed but never forgotten. I know one of your regrets would be not getting to see me become a 'doctor', but I know that you will be looking down so proud and smiling. I wish you were here and I miss you so much. I could not have done it without you.....thanks mum - I did it!!

Acknowledgements

Firstly, I would like to thank Lonza BioScience Ltd. for giving me the opportunity to undertake this PhD. Particularly, I would I would like to thank Claire Scholfield whose guidance in the cell assay development and research was invaluable. I would also like to thank my director of studies Professor Bob Rees for his guidance, and Dr Matharoo-Ball whose supervision over the last 18 months on the proteomics study has been fantastic. The proteomics group Baharak Vafadar-Isfahani, Clare Coveney and David Boocock were all so accommodating towards me and were always ready to lend a hand. Thanks must also go to James Hind, and Graham Ball in the Bioinformatics team who were also willing to help with server problems!!

Finally I would like to thank my support system; both friends and family. My parents and grandparents have always supported me, helping through my many long hours of research and the many hard times (miss you mum & granddad). Lastly, but certainly not least I would like to thank Simeon, my partner, whose support has been amazing (the endless cups of tea and supplies of cookies, chocolates and lots of hugs kept me going) and my two little boys (pugs) Bert and Ernie who have been by my side, keeping my feet warm through many late nights of writing. I cannot begin to explain how much love and support you have all given me over the last 7 years especially the latter few when times have been very difficult and I was ready to pack it all in – for that I am forever grateful.

TABLE OF CONTENTS

Dedication	I
Acknowledgements	II
Contents	III
Figures	X
Tables	XV
Abbreviations	XVII
Abstract	XIX
Chapter 1 Introduction	1
1.1 Cancer Development and Progression	1
1.1.1 Oncogenes and Tumour Suppressor Genes	3
1.1.2 Regulation of p53	8
1.1.3 Angiogenesis and Metastasis	10
1.1.4 Carcinogenesis	11
1.2 Cell Death	14
1.3 Cancer Therapy	19
1.4 Malignant Melanoma	22
1.4.1 Melanoma Treatment	27
1.4.2 Melanoma Tumourigenesis	30
1.5 Chemo Sensitivity Assays	32
1.6 Analysis of the Cancer Proteome	43
1.6.1 Mass Spectrometry	44
1.6.2 Bioinformatics Approaches for Data Analysis	51
1.7 Aims and Objectives	55

Chapter 2 Materials and Methods	58
2.1 Materials and list of Suppliers	58
2.2 Preparation of Buffers, Stains and Kits	60
2.2.1 Preparation of Phosphate Buffered Saline (PBS)	60
2.2.2 Preparation of Acridine Orange/Ethidium Bromide	60
2.2.3 JC-1 Staining	60
2.2.4 Preparation of Propidium Iodide	61
2.2.5 Preparation of Trypan Blue	61
2.2.6 ViaLight Plus Kit	61
2.2.7 ToxiLight Kit	61
2.2.8 CytoTox-ONE Kit	62
2.2.9 MycoAlert Kit	62
2.3 Cell Lines	63
2.3.1 Freezing and Thawing of Cells	63
2.3.2 Culturing Suspension Cells	63
2.3.3 Cell Lines Used	64
2.3.4 Culturing Adherent Cells	65
2.3.5 Counting Cells	65
2.3.6 Mycoplasma Testing	66
2.4 Structure, Mechanism and Preparation of Apoptosis Inducing Agents	67
2.4.1 Structure and Mechanism of Apoptotic Agents	67
2.4.2 Preparation of the Apoptosis Inducing Agents	71
2.4.3 Preparation of Apoptotic Models	71

2.4.4 Preparation of Necrotic Models	72
2.4.4.1 Freeze-Thawing of Cells	72
2.5 Cell Number Dilutions	73
2.6 Measuring ToxiLight with/without Cells	74
2.7 Preparation of Standards	74
2.7.1 ATP Standards	74
2.7.2 Myokinase Standards	75
2.8 Measurement of Cell Viability	76
2.8.1 Measuring Cell Permeability with Propidium Iodide	76
2.8.2 Uptake of Trypan Blue	76
2.8.3 Assays Used to Measure Cytotoxicity	77
2.8.3.1 ViaLight Plus Assay	77
2.8.3.2 ToxiLight Assay	78
2.8.3.3 Cyto-Tox-ONE Assay	79
2.8.3.4 WST-1 Assay	80
2.8.3.5 XTT Assay	80
2.8.3.6 MTS Assay	81
2.8.4 Inducing Necrotic Cell Death	82
2.8.5 Fluorescent Microscopy	83
2.8.5.1 Acridine Orange/Ethidium Bromide	83
2.8.5.2 JC-1	83
2.8.4 Preparation of Chromium release Cytotoxicity Assay	84
2.8.4.1 Tumour Therapy Procedure	84
2.8.4.2 Immunotherapy with DISC/mGM-CSF	84

2.8.4.3 Chromium Release Cytotoxicity Assay	84
2.9 Proteomic Samples	86
2.9.1 Sample Preparation	86
2.9.2 Protein Micro Assay	86
2.9.3 Control Samples Used in MALDI analysis	87
2.9.3.1 QC Samples	87
2.9.3.2 BSA Samples	87
2.9.3.3 Blanks	88
2.9.4 Sample Processing on the Xcise Robotic System	88
2.9.4.1 ZipTip Methodology	88
2.9.4.2 Preparation of Calibrants	89
2.9.4.3 MALDI-MS Set-up and Analysis	90
2.9.4.4 Identification Using MALDI MS-MS	90
2.9.5 Bioinformatics Analysis	91
2.9.5.1 ANN Analysis	92
Chapter 3 A Novel Bioluminescent Assay for Necrotic Cell Death	
3.1 Introduction	93
3.2 Results	104
3.2.1 Formulation and Measurement of AK	104
3.2.2 Measuring AK within Cells	105
3.2.3 ToxiLight With/Without Cells	108
3.2.4 Suitability of the ToxiLight Assay Compared To Traditional Assays	110
3.2.4.1 Comparison with LDH Release	110

3.2.4.2 Enzyme Stability	115
3.2.4.3 Comparison with Propidium Iodide Uptake	117
3.2.4.4 Comparison with Chromium ⁵¹ Release	119
3.2.4.5 Measuring Cell Viability	121
3.2.4.6 Measuring ATP as a Cell Marker	125
3.2.5 Optimisation of ToxiLight	127
3.2.6 Combination of ToxiLight and ViaLight Plus Assays	131
3.3 Discussion	133
3.3.1 Optimisation of ToxiLight Assay	133
3.3.2 ToxiLight Compared to Traditional Assays	133
Chapter 4 Utilising Bioluminescent Assays to Assess Cell Death in Melanoma Cells	
4.1 Introduction	138
4.2 Results	144
4.2.1 Measuring ATP and AK as a Cell Marker in Melanoma Cells	146
4.2.1.1 Effect of Chemo Toxic Agents on Assays	146
4.2.1.2 Effect of Chemo Toxic Agents on Melanoma Cells	148
4.2.2 Effect of Trichostatin A on Melanoma Cells	162
4.2.2.1 Effect of Trichostatin A on MEWO cells	163
4.2.2.2 Effect of Trichostatin A on Ma Mel 28 cells	168
4.2.2.3 Effect of Trichostatin A on Ma Mel 26a cells	173
4.3 Discussion	178
4.3.1 Effect of Doxorubicin of Melanoma cells	179

4.3.2 Effect of Cisplatin and Vindesine on Melanoma Cells	180
4.3.3 Effect of Trichostatin A on Melanoma Cells	181
Chapter 5 Identification of Important Ions using Proteomics and Bioinformatics Analysis which could be Associated with Drug Response	
5.1 Introduction	184
5.2 Results	192
5.2.1 Protein Quantification of Melanoma Samples	192
5.2.2 Sample Optimisation	192
5.2.3 MALDI-TOF-MS	193
5.2.4 MALDI-TOF-MS on Ma Mel 26a Cells	195
5.2.4.1 Bioinformatics Analysis of Ma Mel 26a Cells	199
5.2.4.2 Validation of ANNs	202
5.2.5 MALDI-TOF-MS on Ma Mel 28 Cells	204
5.2.5.1 Bioinformatics Analysis of Ma Mel 28 Cells	207
5.2.5.2 Validation of ANNs	210
5.2.5.3 Identification using MALDI MS-MS	210
5.2.6 MALDI-TOF-MS on MEWO Cells	217
5.2.6.1 Bioinformatics Analysis of MEWO Cells	220
5.2.6.2 Validation of ANNs	223
5.2.6.3 Identification using MALDI MS-MS	223
5.3 Discussion	227
5.3.1 Sample Preparation and Analysis by MALDI MS	227

5.3.2 Importance of QC in MALDI-MS analysis	228
5.2.3 MALDI-MS analysis	229
5.3.4 Analysis by ANNs	230
5.3.5 Clinical relevance of identified ions	233
5.3.6 Conclusion	239
Chapter 6 Conclusions and Further Study	
6.1 ToxiLight and its Use as a Cytotoxicity Assay	240
6.2 Cytotoxicity Assays and Melanoma Study	242
6.3 The Use of Trichostatin A in the Treatment of Melanoma	244
6.4 Use of Cancer Cell Lines in Proteomics	246
6.5 Use of Bioinformatics as a Tool in Biomarker Identification	248
6.6 Personalised Medicine	250
References	252

Figures

Figure 1.01	Diagram of the cell cycle	1
Figure 1.02	Regulation of p53	8
Figure 1.03	Growth arrest and p53	9
Figure 1.04	Illustration of a normal cell progressing into apoptosis	14
Figure 1.05	Photograph with acridine orange / ethidium bromide	16
Figure 1.06	Schematic to show intrinsic and extrinsic apoptotic pathways	17
Figure 1.07	Structure of a pro-caspase	18
Figure 1.08	Photograph to show the “ABCD” signs of melanoma	24
Figure 1.09	Examples of up-regulated and down-regulated apoptotic factors in melanoma	31
Figure 1.10	Formula for Chromium ⁵¹ detection	35
Figure 1.11	Example of propidium iodide staining on FACScan machine	36
Figure 1.12	Illustration of how cells scatter light and emit fluorescence	37
Figure 1.13	LDH reaction	38
Figure 1.14	Electron transport chain	39
Figure 1.15	Photograph of north-American firefly <i>Photinus pyralis</i>	41
Figure 1.16	Formula for ATP detection	42
Figure 1.17	Illustration of the procedure used in this study for MALDI-MS	45
Figure 1.18	A SELDI ProteinChip	46
Figure 1.19	Flow diagram of MALDI-MS and SELDI-MS	47
Figure 1.20	Example of spectra from MALDI-MS	48

Figure 1.21	Work flow of mass spectra analysis	53
Figure 2.01	Formula for counting cells	65
Figure 2.02	Structure of camptothecin	67
Figure 2.03	Structure of vindesine	67
Figure 2.04	Structure of doxorubicin	68
Figure 2.05	Structure of cisplatin	69
Figure 2.06	Structure of dexamethsone	70
Figure 2.07	Structure of trichostatin A	70
Figure 2.08	Summary workflow of cell sample processing	90
Figure 2.09	Summary workflow of Bioinformatics analysis	91
Figure 3.01	To show the different markers of cell viability and apoptosis <i>in vitro</i>	94
Figure 3.02	Schematic diagram to show the LDH reaction	97
Figure 3.03	The luciferase reaction (ATP)	101
Figure 3.04	The adenylate kinase reaction (AK)	102
Figure 3.05	The adenylate kinase reaction resulting in conversion of ATP to light	103
Figure 3.06	Graph to show myokinase standard detection	105
Figure 3.07	Graph to show 384 well versus 96 well detection of AK	107
Figure 3.08	Graph illustrating ToxiLight with/without cells	109
Figure 3.09	Graph to compare LDH and ToxiLight	111
Figure 3.10	EC ₅₀ comparisons of LDH and ToxiLight	112
Figure 3.11	Comparison of cell sensitivity with LDH and ToxiLight	114
Figure 3.12	Graph to show enzyme stability of AK	115

Figure 3.13	Graph to show enzyme stability of LDH	116
Figure 3.14	Graph comparing PI uptake and ToxiLight	118
Figure 3.15	Graph comparing Chromium release and ToxiLight	120
Figure 3.16	Graph to show the sensitivity of WST-1, MTS and XTT	121
Figure 3.17	Graph to show the sensitivity of alamarBlue	122
Figure 3.18	Graph of ToxiLight versus alamarBlue	123
Figure 3.19	Graph to show the sensitivity of ViaLight Plus and ToxiLight	125
Figure 3.20	Graph to show the ToxiLight Lysis Reagent	127
Figure 3.21	Graph illustrating 100% control	128
Figure 3.22	Graph to compare % LDH and AK release	129
Figure 3.23	Graph illustrating the need for combination assays to assess cellular toxicity	131
Figure 4.01	Illustration of trichostatin A interaction	142
Figure 4.02	Graph to show the effect of cytotoxic agents on ToxiLight and ViaLight Plus assays	147
Figure 4.03	Graph to show the effect of doxorubicin on COLD 794, ESTDAB 005, WM 1205 and MEWO cells	149
Figure 4.04	Graph to show the effect of doxorubicin on Ma Mel 28 and Ma Mel 26a cells.	150
Figure 4.05	Graph to show the effect of cisplatin and vindesine on ESTDAB 005 cells	151
Figure 4.06	Graph to show the effect of cisplatin and vindesine on COLD 794 cells	152
Figure 4.07	Graph to show the effect of ciplatin and vindesine on WM 1205 cells	153

Figure 4.08	Graph to show the effect of cisplatin and vindesine on MEWO cells	155
Figure 4.09	Graph to show the effect of ciplatin and vindesine on Ma Mel 28 cells	156
Figure 4.10	Graph to show the effect of cisplatin and vindesine on Ma Mel 26a cells	157
Figure 4.11	Graph to show the effect of ara-C, dexamethasone, and camptothecin on Ma Mel 28 and Ma Mel 26a cells	160
Figure 4.12	Graph to show the effect of trichostatin A on MEWO cells	163
Figure 4.13	Photographs of trichostatin A treated MEWO cells	164
Figure 4.14	Graph comparing PI uptake and ToxiLight	167
Figure 4.15	Graph to show the effect of trichostatin A on Ma Mel 28 cells	168
Figure 4.16	Photographs of trichostatin A treated Ma Mel 28 cells	169
Figure 4.17	Graph comparing PI uptake and ToxiLight	172
Figure 4.18	Graph to show the effects of trichostatin A on Ma Mel 26a cells	173
Figure 4.19	Photographs of trichostatin A treated Ma Mel 26a cells	174
Figure 4.20	Graph comparing PI uptake and ToxiLight	176
Figure 5.01	Flow diagram to show the procedure of mass spectrometry	186
Figure 5.02	Structure of the multi-layer perceptron ANN	187
Figure 5.03	Schematic flow chart outlining the methodology used for biomarker identification	190
Figure 5.04	Graph illustrating a BSA standard curve	192
Figure 5.05	Graph to illustrate the reproducibility of MALDI-MS	194

Figure 5.06	Spectra of Ma Mel 26a cells treated with 1 μ M trichostatin A	197
Figure 5.07	Spectra of Ma Mel 26a cells treated with 5 μ M trichostatin A	198
Figure 5.08	Spectra of Ma Mel 28 cells treated with 1 μ M trichostatin A	205
Figure 5.09	Spectra of Ma Mel 28 cells treated with 5 μ M trichostatin A	206
Figure 5.10	Population chart to show the predictive capability of ANNs	209
Figure 5.11	Spectrum illustrating the observed intensity differences of ions at m/z 1439.8 in Ma Mel 28 cells	214
Figure 5.12	Spectrum illustrating the observed intensity differences of ions at m/z 1541 in Ma Mel 28 cells.	215
Figure 5.13	Spectrum illustrating the observed intensity differences of ions at m/z 1884.04 in Ma Mel 28 cells	216
Figure 5.14	Spectra of MEWO cells treated with 1 μ M trichostatin A	218
Figure 5.15	Spectra of MEWO cells treated with 5 μ M trichostatin A	219
Figure 5.16	Population chart to show the predictive capability of ANNs	222
Figure 5.17	Spectrum illustrating the observed intensity differences of ions at m/z 1439.8 in MEWO cells	226

Tables

Table 1.01	Oncogenes and their function	5
Table 1.02	Tumour Suppressor Genes and their function	7
Table 1.03	The fundamental differences between apoptosis and necrosis.	15
Table 1.04	An example of treatment for melanoma	29
Table 1.05	Advantages and disadvantages of necrotic assays	33
Table 1.06	Advantages and disadvantages of viability assays	34
Table 2.01	List of materials used within this study and their supplier	59
Table 2.02	Cell lines used	64
Table 2.03	Cytotoxic drugs used	71
Table 2.04	Cell models used to induce cell death	72
Table 2.05	Necrotic cell model	73
Table 2.06	Cell number dilutions	73
Table 2.07	ATP standards	74
Table 2.08	AK standards	75
Table 3.01	To illustrate the fundamental cytotoxicity assays	95
Table 3.02	Oxidation reduction potentials in the electron transport system	98
Table 3.03	Cell lines tested for assay optimisation	106
Table 3.04	Summary of conclusion drawn from ToxiLight and ViaLight Plus assays	132
Table 4.01	Treatments used and how they target melanoma	140
Table 4.02	The six melanoma cell lines chosen and the three cytotoxic drugs used	144
Table 4.03	MEWO cells treated with trichostatin A	165

Table 4.04	Ma Mel 28 cells treated with trichostatin A	170
Table 4.05	Ma Mel 26a cells treated with trichostatin A	175
Table 4.06	Summary of results	177
Table 5.01	Artificial neural network results of Ma Mel 26a cells	201
Table 5.02	Artificial neural network results of Ma Mel 28 cells	209
Table 5.03	Identified peptides by MS/MS	214
Table 5.04	Artificial neural network results of MEWO cells	222
Table 5.05	Identified peptides by MS/MS	226
Table 5.06	Clinical information of the cell lines used	239

Abbreviations

ACN	Acetonitrile
ADP	Adenosine diphosphate
AK	Adenylate kinase
AKDR	AK Detection Reagent
AMP	Adenosine monophosphate
AMR	ATP Monitoring Reagent
ANNs	Artificial Neural Networks
ATP	Adenosine triphosphate
Abs	Absorbance unit
BP	Back Propagation
BSA	Bovine Serum Albumin
CGD	Conjugate Gradient Descent
CV	Coefficient of Variation
Da	Daltons
DMEM	Dulbecco's minimum essential media
DMSO	Dimethyl sulphoxide
DNA	Deoxyribonucleic acid
DTT	Dithiothreitol
FCS	Foetal calf serum
FLU	Fluorescent Light Units
HDACs	Histone Deacetylators
JC-1	5,5', 6,6'-tetrachloro-1, 1', 3,3'-tetraethylbenzimidazolocarboxyanide iodide
LDH	Lactate dehydrogenase
MALDI-MS	Matrix-Assisted Laser Desorption Ionisation Mass Spectrometry
MS	Mass Spectrometry
MTS	3-(4,5-dimethylthiazol-2-yl)-5-(3-carboxymethoxyphenyl)-2-(4-sulfophenyl)-2H- tetrazolium, inner salt

MTT	3-(4,5-dimethylthiazol-2-yl)-2,5-diphenyl-tetrazolium bromide
<i>m/z</i>	Mass-to-charge ratio
NRR	Nucleotide Releasing Reagent
OGP	Octyl- β -D-glucopyranoside
PCA	Principal Components Analysis
PI	Propidium iodide
PMF	Peptide Mass Fingerprinting
RLU	Relative Light Units
RNA	Ribonucleic acid
RPMI	Roswell Park Memorial Institute
RT	Room Temperature
SA	Sinapinic Acid
SD	Standard deviation
SELDI MS	Surface-Enhanced Laser Desorption Ionisation Mass Spectrometry
SEM	Standard Error of the Mean
SPS	SPSYVYHQF (Peptide)
SVM	Support Vector Machines
TFA	Tri-Fluoro Acetic Acid
TNF	Tumour necrosis factor
TOF	Time-of-Flight
TPH	TPHPARIGL (Peptide)
WST-1	4-[3-(4-iodophenyl)-2-(4-nitrophenyl)-2H-5-tetrazolio]-1,3-benzene Disulfonate
XTT	sodium 3'-[1-(phenylaminocarbonyl)-3,4-tetrazolium]-bis (4- methoxy-6-nitro) benzene sulfonic acid hydrate

Abstract

To evaluate and identify new candidate cancer drug targets, there is an ongoing need for a reliable, sensitive and quantitative assay that enables the analysis of larger numbers of compounds in preclinical research. This thesis has developed, and optimized a sensitive enzyme-release assay for monitoring natural cytotoxicity. It measures the release of the intracellular enzyme adenylate kinase into the culture supernatant after membrane rupture and is evaluated as an indicator of cell death. This assay was proven to correlate and compete with currently used methodologies for the assessment of cytotoxicity and with its superior sensitivity; convenience and in expense, it should be applicable to the study of other cytotoxicity reactions. The resulting ToxiLight® kit is now being sold world-wide and rapidly became the top selling product for Lonza Bio Science with many references to its use in publications.

It was proven from this investigation that to truly comprehend the effect a cytotoxic drug has on cells, two assays are required in combination; one to measure cytotoxicity and a second to measure viability. The two most sensitive kits tested in this study, the ViaLight® Plus assay and the newly designed ToxiLight® assay were used in combination to monitor the effect of commonly used cytotoxicity drugs on melanoma cells. It was hoped to find both a sensitive and resistant cell line for further analysis by MALDI-MS. The study revealed how cells of the same histological and tissue type can respond differently to the same anticancer drug with one cell line revealing cell death after treatment and another remaining unaffected. This is representative of how individual patients may respond differently to the treatments given *in vitro* and explains the vast biochemical heterogeneity of tumour cells and the complexity involved in developing anticancer drugs that will specifically kill tumours arising from a given cell. The primary melanoma cells used for the research were representative of the clinical situation and were a kind gift from the

OYSTER (Outcome and Impact of Specific Treatment in European Research in melanoma) tissue bank; with the established cell lines obtained from ESTDAB. A selection of three of these cell lines (Ma Mel 28, Ma Mel 26a and MEWO) were chosen after investigating their sensitive/resistant nature to certain chemotherapeutic drugs and were further investigated with a novel agent currently in its early stages of drug trials, the histone deacetylase inhibitor, trichostatin A.

To investigate this resistance further, MALDI-MS was performed on the chosen melanoma cell lysates. The results demonstrated that good quality proteomic data could be achieved from cell lines and that it is possible to generate discriminatory protein profiles that correlate with the cytotoxicity assays when analysed using artificial neural networks (ANNs). Through the analysis of the proteome the ANNs was able to train itself using the raw dataset from the MALDI-MS analysis and distinguish differences between those samples that were drug-treated and those that were left untreated. The differences between the two classes of treated and untreated cells revealed biomarkers that may correlate to cell death and thus the effect of the drug trichostatin A. These findings could lead to the discovery of proteins that are up regulated when a patient is responding to therapy. This could be of prognostic and therapeutic benefit to patients enabling them to find out in the early stages of treatment if they are responding to a given treatment; the long term outcome leading to personalised treatments for individuals in which a decision can be made on the best suited treatment.

Chapter 1 – Introduction

1.1 Cancer Development and Progression

Cancer is one of the most intractable diseases to man and comprises over 200 different forms. Together, they account for approximately one fifth of all deaths in the industrialized countries of the Western World (Schulz, 2007). Cancer is an extremely complex disease resulting from changes in gene expression of previously normal cells, where ‘checkpoints’ control cell cycle progression. The cell cycle consists of four distinct phases: G₁, S (synthesis), G₂ (collectively known as interphase) and M phase (mitosis; figure 1.01). M phase is composed of two tightly coupled processes: mitosis, in which the cell’s chromosomes are divided between the two daughter cells, and cytokinesis, where the cell’s cytoplasm divides forming distinct daughter cells (Weinberg, 1994). The activation of each phase is dependent on the correct progression and completion of the previous phase. Cells that have temporarily or reversibly stopped dividing are said to have entered a state of quiescence called G₀ phase.

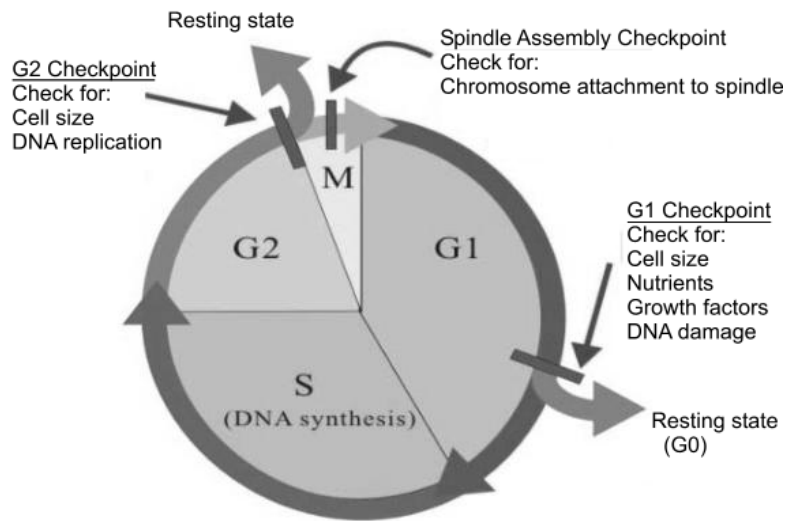


Figure 1.01: Cell Cycle adapted from Kiaris, 2006

As the cell progresses from one phase to another, cell cycle checkpoints take place to ensure that damaged or incomplete DNA is not passed on to daughter cells. If damage is detected the cycle is halted, allowing for either repair or for programming the cell to die (apoptosis). There are two main checkpoints in the cycle: the G₁/S checkpoint and the G₂/M checkpoint (figure 1.01). The tumour suppressor gene, p53 plays an important role in triggering the control mechanisms at both G₁/S and G₂/M checkpoints, halting further progression if damage is detected (Klatt and Kumar, 2009). If the cells are not halted when damage occurs or fail to repair any DNA damage, it may result in continued growth of 'faulty' DNA which continues to proliferate 'unchecked', resulting in the potential for unrestricted growth and tumour formation (Fenech, 2002).

Although in theory three mutations could lead to cancer, it is thought that most common adult cancers result from five or more mutations. More than 100 cancer genes have been found, but many more are thought to yet be discovered (Weinberg, 2007). Most of the 100 known genes have been found in the relatively rare leukaemias and lymphomas, which account for less than 10 % of all human cancers. For the common adult epithelial cancers of the breast, colon, prostate, lung and ovary, which account for 80 % of the cancer burden, over 100 oncogenes are known (Richards, 2007).

The key difference between cancerous and normal cells is that despite the abnormalities formed within the cancer cell, it continues to reproduce in an unrestricted manner. In addition to this continued growth, when cells become confluent, they continue to replicate, thus contradicting the normal laws of contact inhibition. Without contact inhibition to stop their progress, cancer cells are free to grow and although signs of differentiation may be observed, the cancer cells are not governed by the normal rules of cell or tissue growth. There are six main changes,

considered which are considered to be the 'hallmarks of cancer' (Hanahan and Weinberg, 2000) which include:

- self-sufficiency in growth signals
- insensitivity to anti-growth signals
- evasion of apoptosis
- limitless replicative potential
- sustained angiogenesis
- tissue invasion and metastasis

1.1.1 Oncogenes and Tumour Suppressor Genes

In the last forty years, two classes of genes now known to play a key role in cancer formation were discovered: the oncogenes and tumour suppressor genes. The first oncogene (the src gene: for sarcoma) was discovered as an oncogene in a chicken retrovirus induced tumour (Gonda *et al.*, 1982). Since then, more than one hundred oncogenes have been discovered (Richards, 2008). An oncogene, upon mutation, may increase protein production or biological activity resulting in the transformation of a normal cell to a cancerous cell. It was demonstrated in 1976, (Bishop and Varmus) that oncogenes were in fact defective proto oncogenes; caused by relatively small modifications of their original function, which could be either quantitative or qualitative changes. Proto oncogenes promote growth but they function under tight genetic control where tumour suppressor genes may function to restrict cell division (Weinberg, 1994). Any changes in either one or both of these sets of genes will result in uncontrolled growth and potentially cancer (Hodgson, 2008). Quantitative changes in the proto-oncogenes result from point mutations that cause a modification in the protein structure leading to an increase in the activity of the protein and reduced regulation. In addition, an increase in the stability of a protein can prolong its existence and

therefore its activity. Qualitative changes result from a conversion from proto oncogene to a transforming gene (or cellular oncogene (c-onc)) with altered nucleotide sequence (Weinberg, 1994). An activated oncogene can cause a cell that would normally undergo a programmed form of cell death to survive and proliferate. Examples of oncogenes involved in breast cancer formation are shown in table 1.01.

Myc (table 1.01) is among the most, if not the most potent human oncogene in terms of its ability to elicit tumourigenesis. The original implication of *myc* in carcinogenesis was suggested following its identification as a target of translocation in primary Burkitt's lymphomas that results in over expression. Subsequently, it became clear that over expression of *myc* is common in human tumours, by mechanisms that involve its transcriptional activation, with the majority not being accompanied by amplification. Virtually all signalling pathways activated in carcinogenesis result in the direct induction of *myc* expression. *Ras* oncogenes (table 1.01) are among the most prominent oncogenes and are widely used as transforming proteins. They control divergent processes such as proliferation, angiogenesis and malignant transformation.

ONCOGENE	FUNCTION	TARGETED THERAPY (2004)
<i>HER-2</i>	Tyrosine kinase receptor	Anti HER-2 antibodies (trastuzumab, pertuzumab) Kinase inhibitors (CI-1003, EKB-569, Lapatinib) E1A adenoviral gene therapy
<i>Ras</i>	G-protein	Farnesyl transferase inhibitors (tipifarnib)
<i>PI3K</i>	Kinase	Rapamycin/rapamycin analogues (CCI-779, RAD 001, AP23573)
<i>Akt</i>	Kinase	Rapamycin/rapamycin analogues (CCI-779, RAD 001, AP23573)
<i>EIF-4E</i>	Initiator of protein translation	No therapy
<i>Cyclin D1</i>	Cell-cycle mediator	Flavopiridol, UCN-01 (7- OH staurosporine),
<i>Cyclin E</i>	Cell-cycle mediator	Ro 31-7453, specific CDK inhibitors
<i>c-myc</i>	Transcription factor	Antisense
<i>c-fos</i>	Transcription factor	Antisense

Table 1.01: Oncogenes, their functions, and targeted therapies in breast cancer (Osbourne *et al.*, 2004)

The second class of genes involved in carcinogenesis is tumour suppressor genes (anti-oncogenes) which play a role in inhibiting both growth and tumour formation. If a cell divides excessively, inhibiting factors act directly to prevent further cell cycle events (Weinberg, 1994). Unlike the dominant oncogenic changes, tumour suppressor genes are usually recessive requiring mutation to occur on both alleles, or loss of heterozygosity plus a mutation in a second allele which alter cell surface receptors involved in cell signalling (Schulz, 2007). They can also disable proteins, for example the tumour suppressor protein p53, a transcription factor encoded by the TP53 gene. This gene is known to trigger the cell to commit suicide (undergo apoptosis) if DNA damage occurs, or when signalling cascades are altered. Mutated p53 is found in 70% of colon cancers, over 30% of breast cancers and 50% of lung cancers and is also involved in leukemia, lymphomas, sarcomas and neurogenic tumours. Examples of tumour suppressor genes involved in breast cancer are illustrated in table 1.02.

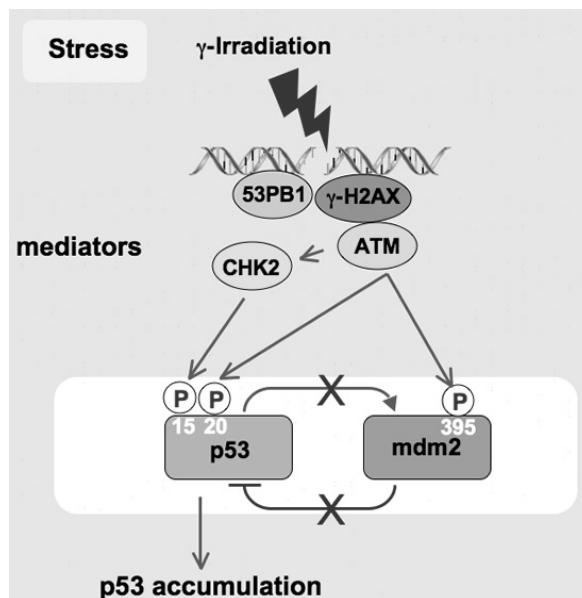
Two nuclear proteins known to be the most important regulators of the cell cycle are Rb and the previously mentioned p53 (table 1.02). Rb is responsible for G1 arrest and prevents entrance to the S phase of the cell cycle by inactivating E2F transcription factors (Ginsberg *et al.*, 2002). Inactivation of Rb by phosphorylation is mediated by specific CDKs (cyclin dependent kinases), especially CDK4 and CDK6 that are under negative regulation (inhibition) of the p16 tumour suppressor gene (Jiao *et al.*, 2008). P53 is the fundamental protein for encoding for a 53 kDa transcription factor that is considered the main mediator of the response of the cell to stress triggered by DNA-damaging agents, hypoxia, activated oncogenes and other genotoxic stress inducing factors (Rieber *et al.*, 2001). Its activation results in cell cycle arrest or apoptosis by binding onto specific regulatory regions in the promoters of target genes, causing induction or suppression of their activity.

TUMOUR SUPPRESSOR GENE	FUNCTION	TARGETED THERAPY (2004)
<i>p53</i>	Induces cell-cycle arrest, cell-cycle checkpoint activation Triggers/facilitates apoptosis	Phase II p53 peptide vaccine with or without interleukin.
<i>p27</i>	Inhibit cyclin-dependent protein kinases; arrest cell cycle in G ₁ phase	Phase II trials with CCI-779 and RAD 001
<i>BRCA-1</i>	Regulates DNA transcription; acts to repair damaged DNA	Phase II clinical trial with carboplatin
<i>BRCA-2</i>	Repairs damaged DNA	No therapy
<i>CHK2</i>	Cell cycle checkpoint kinase, activates p53 after DNA damage	No therapy
<i>ATM</i>	Checkpoint kinase, activates CHK2	No therapy
<i>PTEN</i>	Phosphatase, negative regulator of Akt kinase	No therapy
<i>Rb</i>	Retinoblastoma gene, repressor of cell cycle and protein translation	No therapy
<i>c-fos</i>	Transcription factor	No therapy

Table 1.02: Tumour suppressor genes, their functions, and targeted therapies in breast cancer (Suter and Marcum, 2007; Osbourne et al., 2004).

1.1.2 Regulation of p53

P53 normally exists bound to a protein called MDM2 or HDM2 in humans (Alacon-Vargas and Ronai, 2002). Under normal circumstances, p53 is under tight control through its partnership with mouse double minute-2 (Mdm2). The Mdm2 oncogene not only binds and blocks the N terminus of p53 but also targets p53 degradation via the ubiquitin-proteasome pathway (figure 1.02 (b)), by acting as an E3 ligase (Kiaris, 2006; Alacon-Vargas and Ronai, 2002). Both p53 and Mdm2 (together with other key components of the network) are controlled through a series of regulatory post-translational modifications, for example changed by phosphorylation and dephosphorylation. Phosphorylation reactions are carried out in the cell by a family of enzymes called protein kinases (figure 1.02 (d)) and are dephosphorylated by protein phosphatases (Alacon-Vargas, D. and Ronai, 2002). Any change in MDM2 phosphorylation status consequently affects the activity of p53.



(a) Mdm2 is activated by p53

(b) Binding of p53 by Mdm2 can trigger the degradation of p53 via the ubiquitin system

(c) Phosphorylation of p53 will disrupt its binding with Mdm2.

(d) DNA damage may activate protein kinase to phosphorylate p53 thereby increasing p53 level and subsequently Mdm2

After the DNA damage is repaired, the ATM kinase is no longer active. P53 will be quickly dephosphorylated and destroyed by the accumulated Mdm2.

Figure 1.02: Regulation of p53 adapted from Hainaut and Wiman, 2007

In normal replicating cells p53 remains dormant. Active p53 is induced after the effects of various cancer-causing agents such as UV radiation, oncogenes and some DNA-damaging drugs (figure 1.02). DNA damage is sensed by 'checkpoints' in a cell's cycle, and causes proteins such as ATM (Westphal *et al.*, 1997), CHK1 and CHK2 (Gottifredi *et al.*, 2001) to phosphorylate p53 at sites that are close to or within the MDM2-binding region of the protein. Oncogenes also stimulate p53 activation, mediated by the protein p14ARF. Some oncogenes can also bring about the transcription of proteins which bind to MDM2 and inhibit its activity. Once activated, p53 initiates the expression of several genes including one encoding for p21 which binds to molecules important for the G1/S transition in the cell cycle inhibiting their activity as shown in figure 1.03 (Gottifredi *et al.*, 2001).

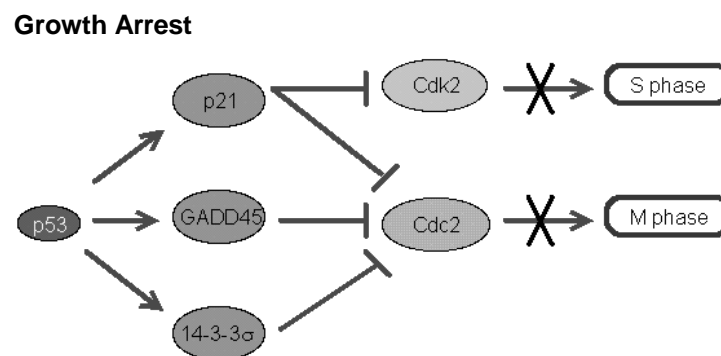


Figure 1.03: Regulation of p53

In its mutated form, p53 can no longer bind DNA in an effective way, and as a consequence the p21 protein is not made available to act as the 'stop signal' for cell division. Thus cells divide uncontrollably, and form tumours. The progression into the M phase requires Cdc2 which can be inhibited by p21, GADD45 or 14-3-3s (see figure 1.03).

1.1.3 Angiogenesis and metastasis

Other genes that play a role in carcinogenesis include angiogenic and metastatic genes (Aalinkeel *et al.*, 2004). As the cancer cells become confluent and proliferation continues the daughter cells produce a mass. As this mass expands, an increase in the supply of oxygen and nutrients is required to maintain continued growth. Without extra nutrients, the cells will be unable to continue to grow and remain at a steady-state size where the number of new cells is balanced by the number of dying cells. These small carcinomas can remain in the body for months or years without gaining size, but upon further gene mutations in regulating angiogenesis, an increased supply of nutrients re-establishes cell and mass expansion. Angiogenesis is a normal process involved in the growth and development of new blood vessels (DeWitt, 2005) as well as being involved in wound healing. However, it is also a fundamental step in the transition of tumours from a dormant to a malignant state. When this occurs, new capillaries are formed around the tumour, allowing it to gain the supplies it needs to grow in size (Pecorino, 2005). Whereas normal cells are generally restricted to a certain tissue and stop proliferating and die if they become detached; a cancer cell can acquire mutations in genes involved in metastasis that enable the cell to undergo tissue and basement membrane invasion and spread to other parts of the body.

1.1.4 Carcinogenesis

The possibility of developing cancer is, in the main, unpredictable; however, certain risk-factors can increase the chance of cell transformation due to:

- Chemical carcinogens
 - Age and decrease in immunosurveillance
 - Lifestyle factors
 - Radiation
 - Oncogenic viral infection
 - Genetic pre-disposition
- (Pecorino, 2005)

It is estimated that viral infections contribute to over 15% of all human cancers (Esteller *et al.*, 2007; McLaughlin-Drubin *et al.*, 2007). Three DNA viruses' have been linked to tumours in humans; the human papillomaviruses (HPV), the Epstein-Barr virus (EBV) and the hepatitis B virus. Throughout the world the majority of the population are infected with these diseases; some develop into the disease and a few eventually obtain a viral-related cancer (e.g. lymphoma, liver cancer, cervical cancer). It is important to understand the molecular mechanisms of these infections and their ability to cause some cancers so new methods can be developed in attacking the virus and consequently preventing malignancies. There are many types of HPV which are known to be a high risk including types 16, 18, 31 and 45. These can lead to cervical, anal, vulvar and penile cancer (Parkin, 2006). HPV type 16 in particular has been shown to be linked with oropharyngeal squamous-cell carcinoma or head and neck cancer (D'Souza *et al.*, 2007). HPV causing cancers generally have viral sequences integrated into the cellular DNA.

The protein products of genes E6 and E7 (known as early genes of HPV), bind to the protein products of two tumour suppressor genes that are crucial in cell apoptosis. E6 binds to the protein product of p53 and E7 to RB, resulting in their loss of action allowing the cell to grow and divide (Horner *et al.*, 2004).

The first virus to be identified as cancer causing is the Epstein-Barr virus, also called the human herpes virus 4 (HHV-4). It is widespread in all human populations, occurring generally during childhood but can be seen during adolescence resulting in infectious mononucleosis or glandular fever (Baumforth *et al.*, 1999). The virus has been implicated in four human tumours: the African form of Burkitt lymphoma, B-cell lymphomas in individuals whose immune systems are blighted due to human immunodeficiency virus (HIV) or the use of immunosuppressant drugs in organ transplantation, nasopharyngeal carcinoma, and some kinds of Hodgkins disease (Thompson and Kurzrock, 2004; Carbone *et al.*, 2008). It has been detected in approximately 10% of gastric tumours (Young and Rickinson, 2004; Truong *et al.*, 2009). In addition, the virus has been shown to infect B lymphocytes, which play a key role in infection-fighting (white blood cells) by transforming the cells into lymphoblasts which have an indefinite life span rendering these cells immortal.

Southeast Asia and sub-Saharan Africa have the highest occurrence of hepatocellular carcinoma (HCC) and liver cancer in the world. This is linked to the hepatitis B virus which is endemic throughout these countries (Seeff and Hoofnagle, 2006). Both hepatitis B and C viruses (HCV) are global health problems; they can lead to cirrhosis and liver cancer and cause millions of deaths each year (Sagnelli *et al.*, 2009). The role hepatitis B and C play in developing liver cancer is not yet understood, with the virus carrying no known oncogenes. There is evidence to suggest that the presence of multiple integrated viral genes

create genomic instability in the host and may lead to loss of heterozygosity for tumor suppressor genes. Curing these infections has proved very difficult with the focus more on prevention than treatment (Lindenbach *et al.*, 2005). A vaccine against HBV has been available since 1982, and early childhood vaccination programs have been the most effective strategy for reducing the prevalence of infection in high-risk populations. Prevention of hepatitis C (HCV) infection is more challenging due to HCV eliciting a weak immune response; however progress is being made (Kaplan and Chang, 2006). Universal precautions against exposure to blood borne infectious agents are the primary means of prevention.

One key area of current research involves epigenetic properties of genomes. Epigenetics (greek for over/above (epi) genetics) refers to changes that occur in the phenotype (appearance) or gene expression as a result of mechanisms other than those occurring in the DNA sequence. The viral genome can be exposed to chemical modification revealing variations in different tissues of the same individual, between identical twins and in disease states. Dr. Manel Esteller of the Bellvitge Institute for Biomedical Research in Barcelona has determined the complete map of DNA methylation, a specific type of chemical modification, for the entire genome of the Epstein-Barr virus, the human papilloma virus, and the hepatitis B virus. Importantly, the researchers compared the DNA "methylomes" of asymptomatic carriers of each virus, patients with active infections, and patients harbouring cancerous tumors. When they looked at asymptomatic carriers of the virus compared to intermediate stages of the disease and established associated cancer, the genome of the virus did not change that much but its epigenome was completely different. It was discovered that the genomes of the virus become progressively methylated in patients who had developed cancer (Esteller *et al.*, 2007).

1.2 Cell Death

In the recent literature, cell death is said to occur by two alternative pathways: apoptosis, a programmed, managed form of cell death, and necrosis, an unordered and accidental form of cell death. Cells may die by either of these two mechanisms depending on the cellular context, or stimulus (Fiers *et al.*, 1999; Tsujimoto *et al.*, 1997). Apoptosis, is a multistep and highly organised process which avoids an immune inflammatory reaction by the activation of phagocytic cells (McCarthy, 2002), autophagy which involves bulk degradation of cellular proteins, a process essential during both the growth and development of the organism, oncosis, an accidental form of cell death caused by the failure of the ionic pumps of the plasma membrane resulting in swelling. In comparison, necrosis is a violent form of cell death producing cellular debris and the induction of an immune response within the organism (McCarthy and Bennet, 2002). Apoptosis is characterized by membrane blebbing, shrinking and condensing of the cell and its organelles and internucleosomal DNA degradation. The cell finally disintegrates, and apoptotic bodies are consumed by phagocytes or neighbouring cells (Wyllie, 1980; figure 1.04).



Figure 1.04: Cytospin preparations of HL60 cells stained and examined by light microscopy. The slide shows a cell with normal appearance progressing into apoptosis. The picture is taken from *Techniques in Apoptosis; a user's guide* (Gorman *et al.*, 1994).

Both apoptotic and necrotic cell death have been observed within the same cell culture population. The severity of the initial insult or damage to

the cell is usually the deciding factor between necrosis and apoptosis (Hirsch *et al.*, 1998). This would imply that there is a common pathway between these two modes of death until they are eventually triggered towards either necrosis or apoptotic demise. It has been proposed that cells exposed to the same stimulus undergo a necrotic death as opposed to an apoptotic death when ATP stores are depleted (Leist *et al.*, 1997), Tsujimoto *et al.*, 1997). The necrotic morphology does not involve DNA and protein degradation and is accompanied by swelling of the entire cytoplasm and mitochondrial matrix, which occurs shortly before the cell membrane ruptures (Kroemer *et al.*, 1998); this process is not genetically controlled and results from injury or infection (Cooper, 1997). The fundamental differences are summarised in table 1.03 below:

APOPTOSIS	NECROSIS	SECONDARY NECROSIS
Physiological or Pathological	Accidental; always pathological	Cytolysis secondary to apoptosis (when dying cells fail to be removed by heterophagy).
No mitochondrial swelling	Mitochondrial swelling	
Susceptibility tightly regulated	Unregulated or poorly regulated	
Plasma membranes near-to-intact until late	Plasma membrane destroyed early	
No leakage of cell content; little or no inflammation.	Leakage of cell content; inflammation.	
Chromatin condensation	Swelling of the entire cytoplasm	
Cell shrinkage		
Nuclear fragmentation		
DNA fragmentation		
Selective protein degradation		
Subtle changes in plasma membrane		

Table 1.03: The fundamental differences between apoptosis and necrosis

Visual examples of the morphology of cells during apoptosis and necrosis are shown in figure 1.05. Jurkat cells were stained with acridine orange (which will fluoresce green when bound to DNA) and ethidium bromide (which will fluoresce red when bound to DNA). Acridine orange is permeable to the cell membrane whereas ethidium bromide is excluded from cells with intact membrane. Using the two fluorochromes combined it is possible to distinguish between viable cells (green fluorescence with intact nucleus), early apoptotic (green fluorescence with chromatin condensation) and necrotic cells (orange fluorescence with an intact nucleus (Gorman *et al.*, 1996)).

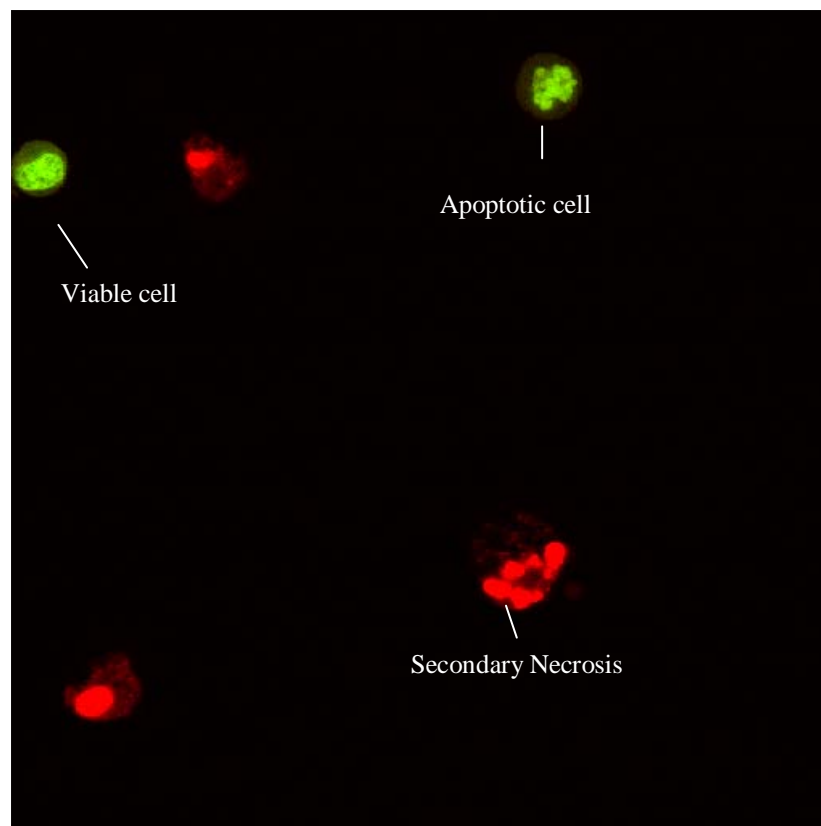


Figure 1.05: The above image was taken as part of the work in this thesis and shows Jurkat cells treated with vincristine; a mitotic inhibitor; stained with acridine orange and ethidium bromide and observed by confocal microscope (x 63 magnification).

Two principal pathways of apoptotic cell death have been described; (McCarthy and Bennett, 2002) the 'extrinsic pathway' which is initiated by specific death receptors that are activated by their ligands (tumour necrosis factor or TNF family) and the 'intrinsic pathway' involving the mitochondrion. Both pathways are shown in figure 1.06 which demonstrates the implementation of the apoptotic response in both intrinsic and extrinsic pathways involving the activation of specific proteases, termed caspases (Lamkanfi *et al.*, 2003; Finucane *et al.*, 1999). Caspases are indispensable as initiators and effectors of apoptotic cell death and are involved in many of the morphological and biochemical features of apoptosis.

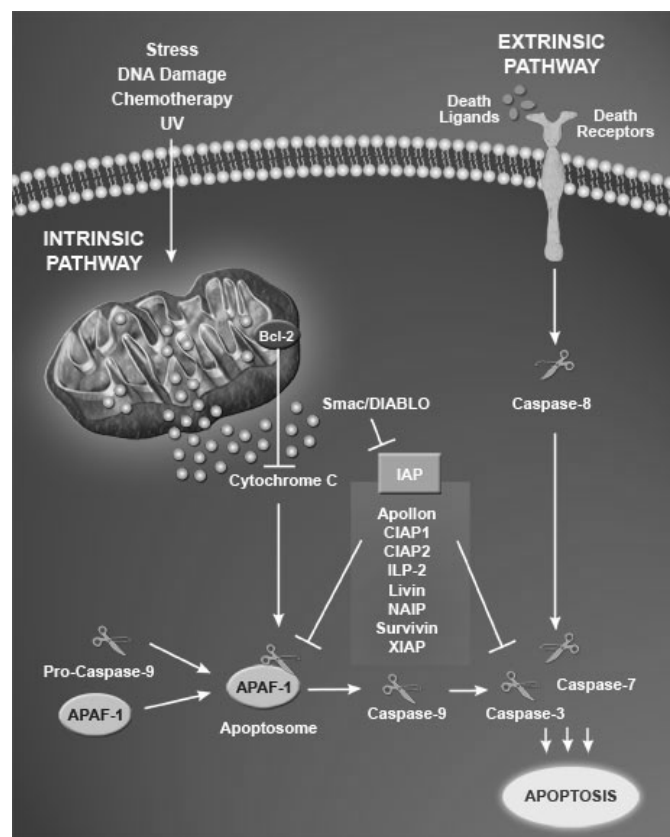


Figure 1.06: To illustrate the two principal pathways of apoptotic cell death: intrinsic and extrinsic where IAP proteins are shown to be inhibiting by binding to activated caspases (taken from IMGENEX).

The name 'caspase' comes from the 'c' denoting a cysteine protease and the 'aspase' referring to the ability of these enzymes to cleave after an aspartic (Asp) acid residue (Nicholson, 1999). Cells contain inactive zymogen forms of pro-caspase that become activated following cleavage at aspartic acid residues.

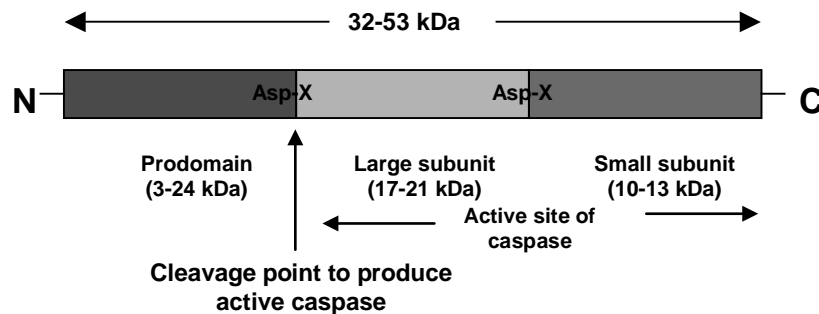


Figure 1.07: Structure of a procaspase (Nicholson, 1999).

There are two major subfamilies of the caspase proteins; the ICE subfamily and the ced-3 subfamily (Nicholson, 1999), and further divisions can be made depending upon the length of their pro-domain (figure 1.07). The ICE family contains the group I caspases which are involved in inflammation: caspase 1, 4, 5 and 13 (Nicholson, 1999). The ced-3 family contains both group II; caspase 2, 3 and 7 (effector caspases) and group III; caspase 6, 8, 9 and 10 (initiator caspases) both involved in apoptosis (Roy and Cardone, 2002). Caspases form an enzyme cascade with initiator caspases which instigate the processes (initiator caspases, activator caspases, upstream caspases), and others acting as downstream caspases involved in the execution of cell death (executioner caspases, effector caspases) (Taylor *et al.*, 2008).

In vitro studies of cell death in cell lines have revealed that inhibition of the classical caspase-dependent apoptotic pathway leads, in several cases to necrotic cell death. Thus, the same cell death

stimulus can result either in apoptotic or necrotic cell death, depending on the availability of activated caspase. Therefore, death domain receptors may initiate an active caspase-independent necrotic signalling pathway (Chautan *et al.*, 1999).

1.3 Cancer Therapy

The majority of patients with cancer will require treatment with therapeutic agents at some point in the course of their disease. In principle, a range of different therapies can be employed but the choice depends strongly on the classification of the cancer by certain criteria (Wittig *et al.*, 2002) including the patient's age, history and lifestyle. Currently clinical studies carried out on large patient populations provide an individual patient with a probability for effective recovery based on clinically observed response rates. There are currently many different ways to treat cancer by.

- Surgery
- Radiotherapy
- Chemotherapy
- Hormone therapy
- Immunotherapy
- Chemo immunotherapy
- Gene therapy

The objectives of cancer therapies are to prevent proliferation (cytostatic effect) and to kill the cancer cells (cytotoxic effect). Surgery or radiation is the treatment choice for localised cancers, in contrast, leukaemias and metastatic or locally advanced carcinomas require drug therapy, which in some cases is supplemented by surgery or radiotherapy (Pecorino, 2005). Conventional chemotherapy, used in most cancer treatments, uses chemicals that target DNA, RNA and protein to disrupt the cell cycle in rapidly dividing cancer cells. Although conventional chemotherapies

have resulted in treating cancers and continue to extend lives, at the same time their efficiency remains low with debilitating side effects.

Hormone therapy is being used for some cancer treatment including cortisone, used to treat some leukemia's and lymphomas, and 'androgen-ablation therapy' (which uses drugs to lower the amount of the male sex hormone testosterone) to treat prostate cancer (Mostaghel *et al.*, 2009). In addition, immunotherapy treatment is currently underway with many clinical trials being conducted. Antibodies specific for cancer cell-surface antigens can be useful in different ways; they can stop the cancer from growing by stopping other essential 'growth factors' from sticking to it and they can 'tag' the cancer for destruction by the immune system. The cancer drugs or radioactive particles are attached to the antibody; it can deliver them directly to the cancer cell without harming the rest of the body. An enzyme (a type of protein that can promote chemical reactions) can be attached to an antibody, and then given to a patient along with a chemical that can be turned into a powerful drug by the enzyme. This directs the drug to the cancer, and minimizes side effects. This process is known as Antibody-directed Enzyme/Pro-drug Therapy (ADEPT). Several antibody-based therapies are available, including the breast cancer drug Herceptin (Subramanian and Mokbel, 2008).

In addition to immunotherapy, gene transfer approaches have found many applications at preclinical and clinical levels, in particular for the study and treatment of tumors, cardiovascular diseases and angiogenesis, infectious and other acquired diseases (AIDS, viral hepatitis), genetic disorders (e.g. cystic fibrosis) and various degenerative, chronic, inflammatory, and age-related diseases (Alzheimer's, Parkinson's, and Huntington's diseases). Vectors based on a new class of virus, the adeno-associated virus (AAV), have emerged as favoured gene vehicles (Shih *et al.*, 2009). AAV is non-pathogenic,

replication-defective small human parvovirus (25 nm in diameter). In gene therapy the retrovirus is modified so that it is no longer capable of causing disease, but is able to insert new genes into a patient's chromosomes. However, there are many concerns over the safety of modifying a patients' DNA. To date, no successful gene-based treatment has been approved for routine use on cancer patients, but a large amount of research is being carried out in this area. Even where the full range of modern cancer therapies is available, many cancers still cannot be cured today (Dolken, 2001). In the majority of patients with malignant disease, state of the art therapies are at best palliative. Part of the explanation is believed to be tumour heterogeneity arising through genetic diversity as responsiveness to individual chemotherapeutic agents varies widely between tumours of the same histological type. This heterogeneity is present at the molecular, cellular, histological and clinical level and makes the choice of patients' treatment extremely difficult since a given drug may work extremely well only for a subset of patients (Alexandrova, 2001). Remarkable progress is being made in the development of therapeutic agents; however, an enormous amount of time and money must be invested before an agent is approved for clinical use (Kawada *et al.*, 2002).

1.4 Malignant Melanoma

Melanoma is the rarest and most aggressive form of skin cancer and has been the focus of the majority of the research in this thesis. It was chosen due to the current lack of available treatments in metastatic melanoma and an opportunity arose to look into primary melanoma samples through collaboration with OYSTER (Outcome and Impact of Specific Treatment in European Research in melanoma) tissue bank. There are 3 types of skin cancer based in the epidermis of the skin; melanoma (the most aggressive form), basal cell skin cancer and squamous cell skin cancer. Melanoma has become increasingly prevalent over the last few decades with around 160,000 new cases diagnosed worldwide each year; mainly among caucasians (Ries *et al.*, 2003). The median age of melanoma diagnosis is 45 years, almost twenty years prior to most other tumours (O'Day *et al.*, 2001). The occurrence of the majority of melanoma cases is in normal skin; with a small percentage diagnosed in the eye (intraocular or ocular melanoma) or rectum (mucosal melanoma).

The development of melanoma occurs from the pigment producing (melanin) cells of the skin (melanocytes), which upon transformation begin to grow and divide more quickly than usual spreading into the surrounding surface layers of the skin (Meyskens *et al.*, 1999). Melanin, in humans is the primary determinant of skin, hair colour, and the pigmented tissue underlying the iris. Melanocytes insert granules of melanin into specialized cellular vesicles called melanosomes that are incorporated into dendrites and transferred by phagocytosis into the other skin cells (keratinocytes) of the human epidermis (Burns *et al.*, 2004). The melanosomes in each recipient cell accumulate above the cell nucleus to protect the nuclear DNA from mutations caused by the ionising radiation of the sun's ultraviolet rays. There are two major forms of melanin produced in the epidermis and hair follicles - eumelanin and pheomelanin.

Eumelanin is brown to black in colour while pheomelanin is yellow to red. People whose ancestors lived for long periods in the regions of the globe near the equator generally have larger quantities of eumelanin in their skins (Berwick *et al.*, 2004), affording protection against high levels of exposure to the sun, which more frequently results in melanomas in lighter skinned people. The four most common types of skin melanoma are:

- superficial spreading melanoma (SSM) - the most common form (approximately 70%) of cutaneous melanoma (Forman *et al.*, 2008)
- nodular melanoma - most aggressive form of melanoma (approximately 15%) which grows quickly in a vertical direction from the outset.
- lentigo maligna melanoma - usually found on chronically sun damaged skin such as the face and the forearms of the elderly (approximately 10%).
- acral lentiginous melanoma - observed on the palms, soles and under the nails. It is the most common form of melanoma diagnosed amongst Asian and Black ethnic groups but constitutes less than 5% of overall cases (Krementz *et al.*, 1982).

(Reed and Martin, 1997)

As melanoma is the most aggressive form of skin cancer due to its high resistance to currently available therapy early detection remains the best treatment (Peltonen *et al.*, 2005). The ABCD rules illustrated in figure 1.08 are the key changes to monitor during regular skin self-examinations.

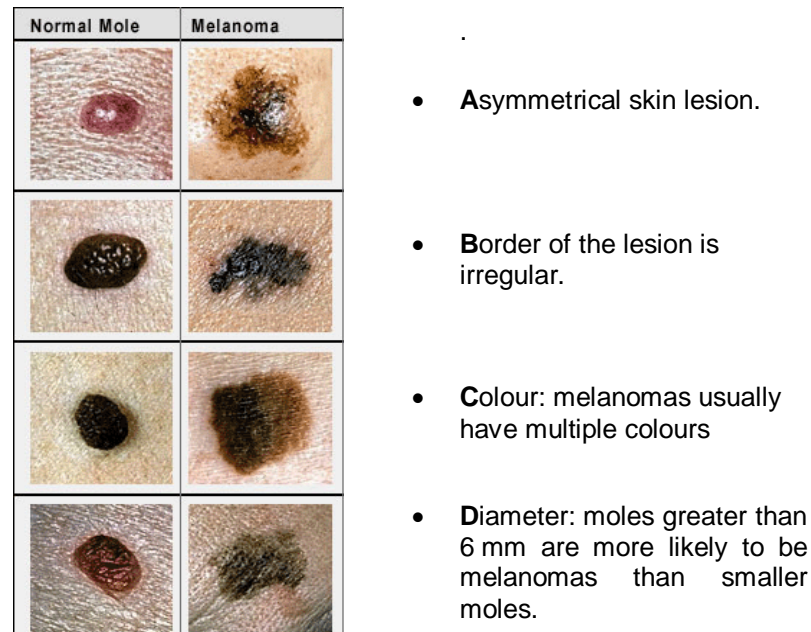


Figure 1.08: To show the “ABCD” method for remembering the signs and symptoms of melanoma adapted from the National Cancer Institute.

The contributing factor bringing about the onset of basal and squamous skin cancer is exposure to ultra violet (UV) light, through natural sunlight or artificially from sun beds or lamps resulting in damage to the DNA (genetic material) in skin cells (Zanetti *et al.*, 1992; Harrison *et al.*, 1994). UV light can directly induce melanocytic lesions and melanoma in human skin grafts (Sauter *et al.*, 1998; Berking *et al.*, 2002; Wolnicka-Glubisz and Noonan, 2006). The mechanism, however, whereby UV light induces melanoma has not been determined, causing debate over whether melanoma is actually caused by UV light. Despite many reports that UV light damages the DNA in our skin cells causing melanoma, a recent report by Sam Shuster (2008) claims that there is insufficient evidence linking UV exposure to melanoma with 75% of melanomas occurring on relatively unexposed sites, especially the feet of dark skinned Africans. Previous reports have also reported this fact (Ragnarsson-Olding, 2004).

The detection of melanoma is mainly visible using the ABCD methodology shown in figure 1.08. The diagnosis of melanoma requires experience, especially in its early stages when it may look identical to harmless moles or not have any colour at all. Confirmation of its malignant potential is carried out with a skin biopsy performed under local anesthesia and assists in defining the severity of the melanoma. Currently researched biomarkers including lactate dehydrogenase (LDH), S100B and melanoma-inhibitory activity (MIA) are being looked at but lack sensitivity (Matharoo-Ball *et al.*, 2008). No blood test is available for detection, although an increase in LDH has been observed in metastatic disease often indicating spread of the disease to the liver (Agarwala *et al.*, 2009). It is used to follow-up cancer (especially lymphoma) patients, as cancer cells have a high rate of turnover with destroyed cells leading to an elevated LDH activity. However, many patients with metastases (even end-stage) have normal LDH levels.

One of the main problems in detecting the progression of melanoma is its vertical growth through the skin. It is this “unseen” spread and growth that affects prognosis. Diagnostic and staging criteria includes tumour thickness in millimeters (Breslow's depth), depth related to skin structures (Clark level), type of melanoma, presence of ulceration, presence of lymphatic/perineural invasion, presence of tumour infiltrating lymphocytes (if present, prognosis is better), location of lesion, presence of satellite lesions, and presence of regional or distant metastasis (Berger *et al.*, 2003).

From this information melanoma can be staged:

Stage 0: Melanoma in Situ (Clark Level I), 99.9% Survival

Stage I/II: Invasive Melanoma, 85-95% Survival

- T1a: Less than 1.00 mm primary, no ulceration, Clark Level II-III
- T1b: Less than 1.00 mm primary, ulceration or Clark Level IV-V
- T2a: 1.00-2.00 mm primary, no ulceration

Stage II: High Risk Melanoma, 40-85% Survival

- T2b: 1.00-2.00 mm primary, ulceration
- T3a: 2.00-4.00 mm primary, no ulceration
- T3b: 2.00-4.00 mm primary, ulceration
- T4a: 4.00 mm or greater primary, no ulceration
- T4b: 4.00 mm or greater primary, ulceration

Stage III: Regional Metastasis, 25-60% Survival

- N1: Single positive lymph node
- N2: 2-3 positive lymph nodes or regional skin/in-transit metastasis
- N3: 4 positive lymph nodes or lymph node and regional skin/in transit metastases

Stage IV: Distant Metastasis, 9-15% Survival

- M1a: Distant skin metastasis, normal LDH
- M1b: Lung metastasis, normal LDH
- M1c: Other distant metastasis or any distant metastasis with elevated LDH.

(Balch *et al.*, 2001)

Upon diagnosis, a treatment plan can be devised. For primary melanoma, the main treatment is complete surgical excision of the tumour resulting in >95% complete remission (O'Day *et al.*, 2002; Soengas and Lowe, 2003)

For regional and distant metastases, chemotherapy, radiotherapy and biological therapy is given to patients.

1.4.1 Melanoma Treatment

Treatment of melanoma can involve:

- Initial Surgical Treatment (Wide-excision). The surgical removal of additional surrounding skin is necessary to reduce the risk of tumor regrowth, which is called "wide-excision."
- Sentinel Lymph Node Biopsy – test to determine which lymph node may be involved with tumour
- Surgical Treatment of Lymph Nodes
- Chemotherapy
- Radiation therapy
- Biologic therapy
- Chemoimmunotherapy

Many clinical trials have and are still being carried out to determine the effects of drugs in single and combination therapy. Dacarbazine is the only one single-entity drug which has been approved in the UK for treatment of late-stage melanoma, but provides complete remission in only 2% of patients. The disappointing results of single-agent therapy led to the development of combination therapy in the 1980's. Two published regimes have been trialled, the Dartmouth regimen (carmustine, cisplatin, vinblastine and dacarbazine) and CVD (cisplatin, vinblastine and dacarbazine) used for metastatic disease with some encouraging results but durable remissions remained very rare (O'Day *et al.*, 2002). The F.D.A. (federal agency charged with overseeing the safety of drugs, medical devices, food, cosmetics and many other health-related products) has approved both dacarbazine and Interleukin 2 (IL-2) for clinical use. IL-2 was approved in the US based on a 6% complete response rate in a 270-patient phase II study data set (O'Day *et al.*, 2002). The absence of any phase III data demonstrating the benefit of any dose of IL-2 in

metastatic melanoma prevented approval in Europe, and it is unlikely that IL-2 would be approved at present as it is difficult to predict which patients will respond.

Combination therapy with IL-2 has been an active area of research, with a recently completed phase I clinical trial funded by the Cancer Vaccine Institution (CVI). This was to determine the efficacy of Aldara and IL-2 injections into lesions of melanoma. Aldara Cream activates the immune system and clinical results revealed that Aldara treatment was effective in controlling the growth of approximately 50% of cutaneous melanoma lesions (Green *et al.*, 2007). In addition, a recent trial has currently ended for the investigation of stage IV melanoma patients, who have failed chemotherapy, using a dendritic cell vaccine approach. This was developed by the Baylor Institute for Immunology Research (BIIR). Dendritic cells were loaded with melanoma cells from a cell line treated with heat prior to loading. This methodology of killing the cells initially has been shown to be more efficient in priming the melanoma specific CD8+ cells. Results demonstrated that patients with low volume disease demonstrated longer survival compared with other therapies (Cancer Vaccine Institute, 2009). A variety of other agents have been used (e.g. carmustine (BCNU), vinblastine, cisplatin), including drug trials combined with hormonal based therapy, tamoxifen, but with no significant increase in patient response observed (O'Day *et al.*, 2002). Another chemotherapy drug, temozolomide (Temodal), taken in capsule form, has been used in trials for melanoma (Plummer *et al.*, 2005) and was thought to have benefits over dacarbazine (Darkes *et al.*, 2002), offering better protection from the development of brain metastases and with the advantage of being orally administered. It is not however currently licensed for metastatic melanoma and continues to be investigated both as a single and combined agent in therapy (Plummer *et al.*, 2005). With the exception of the above mentioned trials, the actual treatment for

melanoma has remained unchanged for many years. No agent has been shown to have a significant impact on survival with stage IV melanoma which remains a very poor prognosis; a median survival of only 6-9 months (Dothager *et al.*, 2005).

THERAPY FOR PRIMARY MELANOMA	THERAPY FOR REGIONAL METASTASES	THERAPY FOR DISTANT METASTASES
Complete surgical excision of primary tumour	Surgery	Surgery
Elective lymph node dissection	Isolated limb perfusion	Radiotherapy
Sentinel lymph node biopsy	Adjuvent therapy (radiotherapy, chemotherapy, regional limb perfusion. IFN-alpha)	Chemotherapy (single agent or combination including Dacarbazine (DTIC), Carmustine (BCNU), Loustine (CCNU), Trichostatin-A, Vindesine, taxanes, platinum compounds. Chemoimmunotherapy (IFN-alpha + chemotherapy) Biologic therapy (IFN-alpha, IL-2, monoclonal antibodies, melanoma vaccines.

Table 1.04: An example of treatment for melanoma
(Adapted from Logovic *et al.*, 2005; Kim *et al.*, 2002)

1.4.2 Melanoma Tumourigenesis

Several genes have been shown to be involved in malignant melanoma including germline mutations in *cdkn2A*, *Arf*, *cdk4* and somatic mutations in *Pten* and *BRAF* but many are currently being researched (Dahl and Guldberg, 2007). As already mentioned UV light is specifically carcinogenic and can damage skin cells which then need to be eliminated by apoptosis (when the skin peels). The tumour suppressor p53 protein (previously mentioned and discussed earlier in this chapter) is an important regulator of apoptosis. However mutations to p53 have not been linked to melanoma but only to squamous and basal cell carcinoma (Pecorino, 2005). Inactivation of the *INK4a/ARF* (or *CDKN2a*) locus is a common and critical genetic event in the development of human and mouse melanoma. This locus engages the Rb and p53 tumor suppressor pathways through its capacity to encode two distinct gene products, p16^{INK4a} and p14^{ARF}. These two pathways are of potential importance in mediating UV-induced melanoma (Sharpless *et al.*, 2003).

Intermittently sun-exposed skin accounts for the majority of this cancer in caucasians and has been associated with *BRAF* mutations. Chronic sun damaged skin (lentigo maligna melanoma) seems to have significantly fewer chromosomal aberrations compared to acral and mucosal melanomas, with an absence in *BRAF* mutations but frequent gains in *CCND1* and regions of chromosome 22, and losses from chromosome 4q. Acral and mucosal melanomas occur in sun protected areas and have infrequent *BRAF* mutations and show greater numbers of chromosomal aberrations (Nouri, 2007).

There is also growing evidence suggesting that certain histone modifications and associated altered chromatin remodeling activities can play a key role in melanoma tumour progression. These epigenetic events are involved in different aspects of tumorigenesis including cell cycle control, apoptotic pathways (figure 1.09), cell signaling, tumor cell invasion and metastasis, drug resistance, and immune recognition. These findings suggest a promising future for the utility of drugs such as histone deacetylase (HDAC) inhibitors, in treating patients with evidence of histone deacetylation.

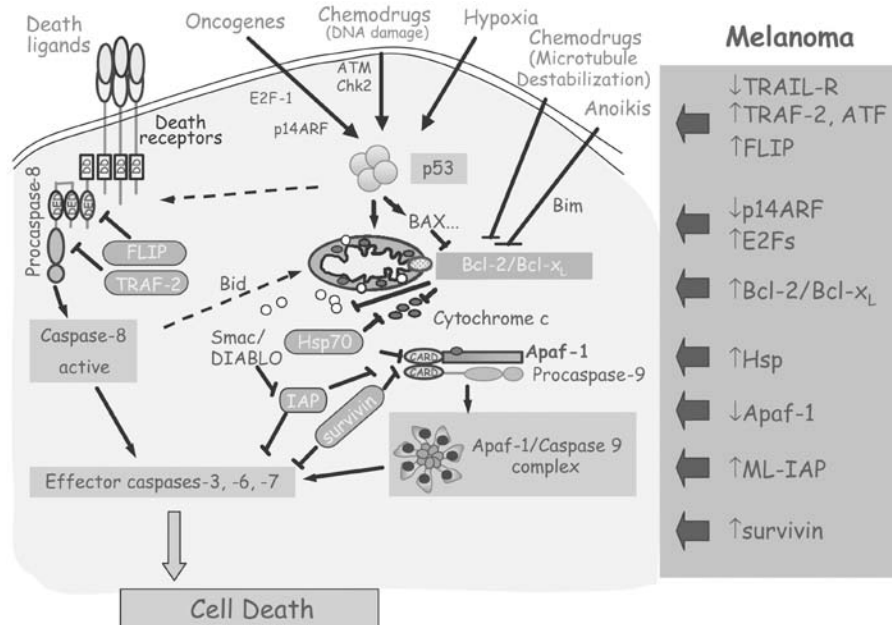


Figure 1.09 Simplified schematic of apoptotic pathways in mammalian cells of both extrinsic (death receptor-mediated) and intrinsic (mitochondrial) apoptosis pathways. Examples of up regulated and down regulated apoptotic factors in melanoma are indicated on the right panel (Soengas and Lowe, 2003).

1.5 Chemo Sensitivity Assays

Upon the development of chemotherapeutic agents reaching the clinical trial stage, rapid tests of drug sensitivity are of utmost importance for selecting the most promising agents for cancer treatments. A high percentage of patients with leukaemia, lymphoma and solid tumours achieve complete remission after initial treatment, but the majority of these patients will finally relapse due to the presence of residual tumour cells detectable in clinical remission only by the most sensitive methods (Cree 1998; Campana and Coustan-Smith, 2004; Kurth, 1997). These residual cells need to be detected and eradicated for the treatment to be successful.

Assays of chemo-sensitivity are of the utmost importance to pharmaceutical companies as part of their strategy to discover new chemotherapeutics. Commercially, cytotoxicity assays are used to detect the killing of tumour cell lines by newly discovered or existing cytotoxic drugs. An important feature required for these assays is the ability of the assays to detect 100% cell death of a tumour population. If the results of an assay reveal all cells have been killed by a potential cytotoxic agent when in actual fact there are residual viable cells still present that the assay has been unable to detect, then these cells will eventually reform into a new tumour within a patient. Current assays used to demonstrate chemo sensitivity, have not been able to evaluate whether a given drug successfully targets 100% of a tumour cell population (Dworzak, 2001). The methods currently utilised to detect cell killing lack sensitivity, often as a result of high background readings and an unacceptable signal; noise ratio; it is therefore difficult to confirm the complete (100%) killing of tumour cells (Collie-Duguid *et al.*, 2007; Motoko and Akihiro, 2004). There are several assays currently employed that can potentially be used for prediction of patient responses to single agent and combination therapy.

These include:

1. Measurements of cellular necrosis:

- Chromium-51 release
- Propidium Iodide uptake
- Lactate dehydrogenase (LDH) assessment

Assay	Advantages	Disadvantages
Chromium-51	Stable Sensitive	Radioactive High spontaneous release Time consuming
Propidium Iodide uptake	Very sensitive User friendly	Requires specialist training Can be time consuming
LDH	User friendly Sensitive Rapid	High signal:noise levels Affected by culture reagents containing pyruvate Stability of only 9 hours

Table 1.05: Advantages and disadvantages of necrotic assays.

2. Measurements of cell viability:

- AlamarBlue
- 3-(4,5-dimethylthiazol-2-yl)-2,5-diphenyltetrazolium bromide, a tetrazole); MTT
- 3-(4,5-dimethylthiazol-2-yl)-5-(3-carboxymethoxyphenyl)-2-(4-sulfophenyl)-2H-tetrazolium); MTS
- 2,3-bis (2-methoxy-4-nitro-5-sulfophenyl)-5-[(phenylamino) carbonyl]-2H-tetrazolium hydroxide); XTT
- 2-[4-iodophenyl]-3-[4-nitrophenyl]-5-[2,4-disulfophenyl]-2H tetrazolium monosodium salt; WST-1
- Adenosine triphosphate; ATP

<i>Assay</i>	<i>Advantages</i>	<i>Disadvantages</i>
Alamar Blue	User friendly	Lacks sensitivity Time consuming
MTT/MTS	User friendly	Lacks sensitivity Time consuming
XTT	User friendly	Lacks sensitivity Time consuming
WST-1	User friendly	Lacks sensitivity Time consuming
ATP	Sensitive Fast User friendly Rapid	No substantial evidence of cell death

Table 1.06: Advantages and disadvantages of viability assays.

Chromium-51(Cr^{51}), a radioactive element, has the ability to be taken up by healthy cells as an internal label. Target cells are pre-labelled with Cr^{51} which is released for detection when cells are induced to lyse by effector cells (i.e. cytotoxic T cells, NK cells or activated macrophages). Upon lysis of the cell, the chromium is released and this can then be measured using a gamma scintillation counter (Bachy et al., 1999).

The specific lysis was determined according to the formula:

$$\text{Total Lysis (\%)} = 100 \times \frac{(\text{Exp} - \text{Spo})}{(\text{Max} - \text{Spo})}$$

Where:

Exp = experimental release; Spo = spontaneous release; Max = maximum release.

Figure 1.10: Formula for chromium⁵¹ detection

Fluorescent dyes are a safe and convenient alternative to radioactive labels such as chromium for monitoring the fate of cells *in vivo*. The number of dead cells in a suspension is often estimated by counting the cells which take up an acidic dye, such as trypan blue. Assessment of cell viability by flow cytometry, using propidium iodide (PI) can also be used (Ormerod, 1999). PI is excluded by viable cells and when taken up by dead or dying cells, binds to nucleic acids and fluoresces red. Flow cytometry is a well established, multi-disciplinary technique in standard use in biological and clinical research. A typical flow cytometer will consist of an optical, electronic and fluidic system, which provides a visual picture of their relative size, granularity and fluorescent properties on a computer screen (Ormerod, 1999). The fluidic system contains an air pump, pressure regulator, sheath fluid reservoir, sample regulator, flow cell and a waste reservoir, where the speed at which the cells pass the laser can

be controlled by either increasing or decreasing the pressure (Becton Dickinson, 1997). This technology has been used to measure many processes during apoptosis and necrosis and measurements are recorded for each individual cell to obtain the percentages of necrotic or apoptotic cells within a population (Ormerod, 1998). The size, granularity and fluorescent properties of a cell can be investigated by the analysis of their forward scatter (FSC-H) indicating cell size, side scatter (SSC-H) showing granularity of the cell and different fluorescent parameters (FL-1, FL-2, FL-3) (Ormerod, 1998; Becton Dickinson 1997). Figure 1.11 is representative of the forward scatter and side scatter dot plot for a typical healthy population of cells when analysing for plasma membrane integrity (red; FL-2) (Becton Dickinson, 1997).

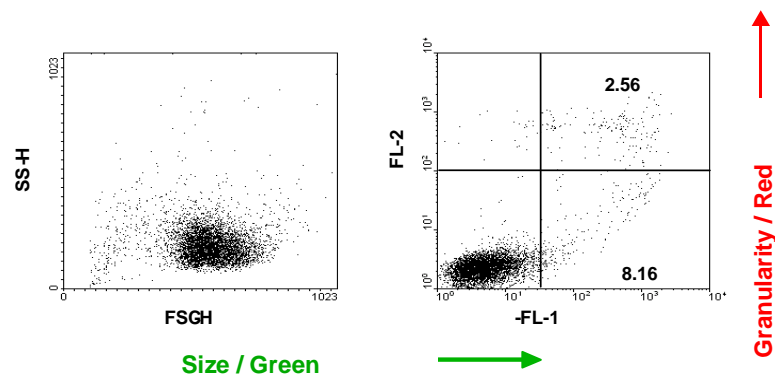


Figure 1.11: Forward scatter (size) and side scatter (granularity) dot plot and FL-1 (green) and FL-2 (red) dot plot showing a typical picture of healthy Jurkat cells stained with propidium iodide (red fluorescence) detecting loss of plasma membrane integrity, where each dot represents a single cell.

The properties of the cell are clarified by the way in which the cells scatter the incident light (as demonstrated in figure 1.12) and emit fluorescence. Side scatter is proportional to granularity and is measured when the light is reflected at high angles (at 90° to the incident light axis (Becton Dickinson, 1997)). As cells become apoptotic they become increasingly granular as their chromatin becomes more condensed thereby showing an increase in side scatter (McCarthy, 2002). Low angle forward scatter is

roughly proportional to the diameter of the cell and is detected when light is diffracted at angles of between 1 and 10 degrees measured across the axis of the incident light (Becton Dickinson, 1997).

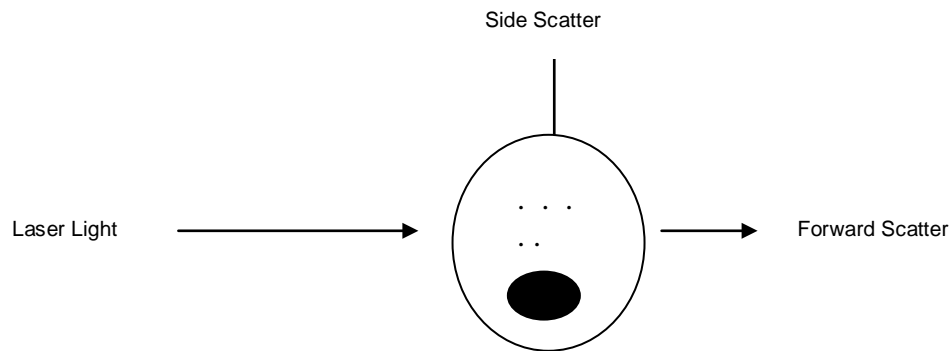


Figure 1.12: Diagram to illustrate how cells scatter light and emit fluorescence in flow cytometry.

FL-1 and FL-2 are detected through the absorbance of energy from the laser by fluorochromes added to the cell sample. This absorbance of energy elevates the fluorochrome to a higher energy level when the cell has passed by the laser this energy is released in the form of a photon of light emitting in the red or green spectra (Becton Dickinson, 1997).

In addition to these methodologies, the LDH (CytoTox One™, Promega) fluorescent assay measures necrosis by the release of the enzyme lactate dehydrogenase into the culture medium. LDH is a stable enzyme normally found in the cytosol of all cells, converting lactic acid to pyruvic acid (figure 1.13) in the electron transport chain (Ewaschuk *et al.*, 2005; Herrera *et al.*, 2008). This assay measures the released LDH from cells with damaged membranes. Released LDH is measured directly in the cell culture wells with a coupled enzymatic assay that results in the conversion of a non-fluorescent compound (resazurin) to a fluorescent compound (resorufin), which can be detected by fluorometry (Korzeniewski and Callewaert, 1983; Decker and Lohmann-Mathes,

1988; Sasaki *et al.*, 1992).

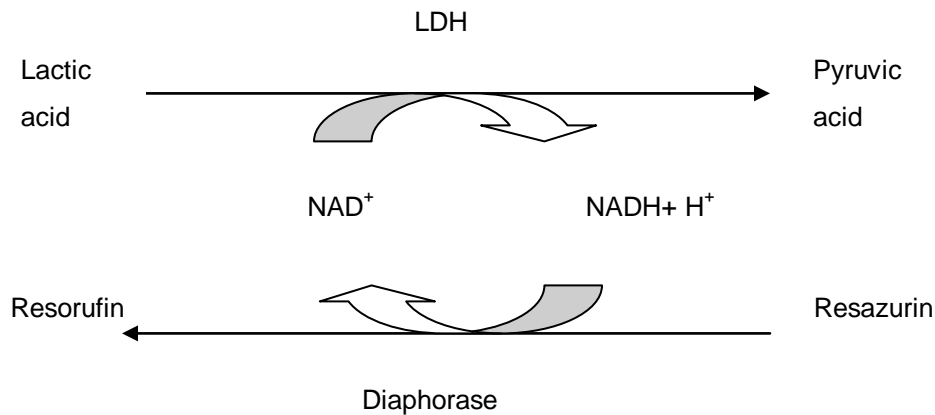


Figure 1.13: Detection of LDH demonstrated by the conversion of resazurin to a fluorescent compound, resorufin.

Many assays utilise the electron transport chain illustrated in figure 1.14 to measure changes within cells. ATP, the energy source of all cells is produced from the donation of H^+ ions from the reduction of NADH and FADH_2 . It is this reaction that the LDH assay is monitoring converting the resazurin to resorufin. The electron transport chain consists of four complexes:

- NADH dehydrogenase complex
- cytochrome reductase complex
- cytochrome oxidase complex
- ATP synthetase complex

(*Alberts et al.*, 1989)

During electron transport, the enzymes of the electron transport chain (e.g. NADH, FADH_2) create a proton gradient across the inner mitochondrial membrane. This proton gradient is subsequently used by the enzyme ATP synthase to produce ATP (*Alberts et al.*, 1989).

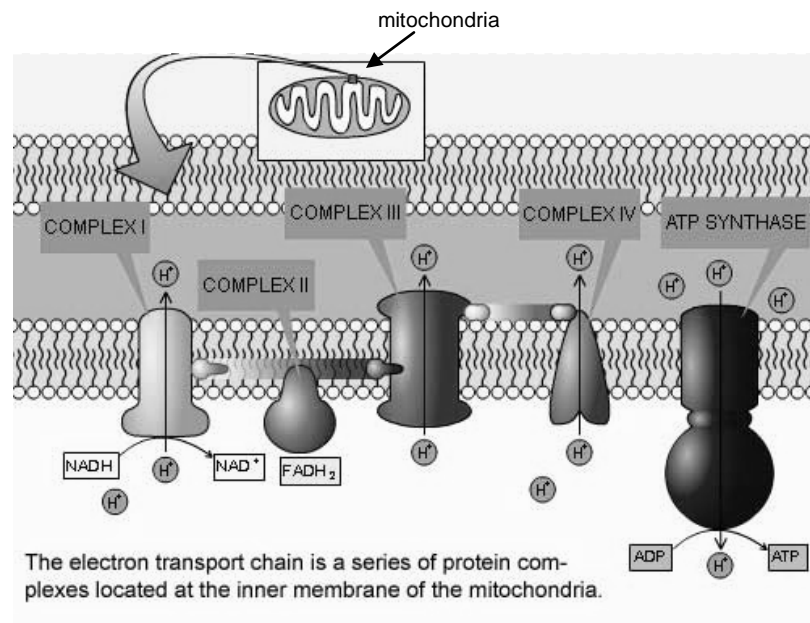


Figure 1.14: Illustration of the Electron Transport Chain (taken from HOPES website: Huntington's outreach project for education at Stanford).

Another fluorescence assay, alamarBlue, along with the absorbance assays WST-1, MTT and MTS also utilise the natural reducing power of living cells to measure cell viability. Unlike the LDH assay which measures cell permeability, these are viability assays. AlamarBlue is a non-toxic metabolic indicator of viable cells that becomes fluorescent upon mitochondrial reduction (Nociari *et al.*, 1998). The alamarBlue indicator detects changes in oxidation as a result of the electron transport chain (figure 1.14) by monitoring the change of a blue and non-fluorescent dye resazurin, to a pink and fluorescent dye resorufin in response to chemical reduction of growth medium resulting from cell growth. Continuous cell growth maintains a reduced environment while inhibition of growth maintains an oxidised environment. Reduction related to growth causes the REDOX indicator to change from the oxidized blue form to the reduced pink form.

The colorimetric or absorbance assays (MTT, XTT, WST-1) measure the intracellular reduction of a soluble yellow tetrazolium dye to a purple product, based on the cleavage of a tetrazolium salt by mitochondrial dehydrogenases in viable cells (Marshall, 1995). Upon reduction by electrons flowing through the electron transport system and by superoxide radicals produced, this change of colour can be detected. The formazan dyes derived from each tetrazolium salt are completely different in terms of solubility. The MTT assay contains insoluble crystals and must be solubilised with surfactants or organic reagents. The XTT and MTS assays are soluble but the most water-soluble and stable of the salts is WST-1 (Clontech, 2007).

All living cells contain ATP produced by the electron transport chain (Krebs, 1970), making it a good presumptive marker for cell number and cell condition (Crouch *et al.*, 1993). Assessment of ATP, using established methods, enables the measurement of the effects of cytotoxic agents on cell lines and tumours to determine the cellular outcome after treatment. These effects could be apoptotic, growth inhibiting or no effect at all therefore resulting in continued proliferation (Cree, 1995). When cells are subjected to stress; the process of oxidative phosphorylation breaks down, so that ATP is no longer produced. It has been observed that apoptotic and necrotic cells give out different ATP relative light units (RLUs) when measured by bioluminescence. These changes in the ATP levels brought about by programmed cell death may be early indicators of apoptotic or necrotic changes within the cells (Crouch *et al.*, 1993; Bradbury *et al.*, 2000; Tsujimoto, 1997). Bioluminescence is the production of light by living organisms. Bioluminescence is used by fireflies to attract mates, anglerfish to lure prey, railroad worms to scare predators and pelagic squid as camouflage (Pazzagli *et al.*, 1988). Probably the best known example of bioluminescence is in the North America Firefly (*Photinus pyralis*, shown in figure 1.15), whose

development of a highly efficient bioluminescent system is employed when attracting a mate (Lundin, 1982 and Lundin, 1993).



Figure 1.15: The male species of the north-American firefly *Photinus pyralis* is shown emitting the familiar yellow-green light.

Luciferase is a generic term for an enzyme that can generate light as a product in luminous organisms. These luminous organisms have over 700 genera representing 17 phyla including plants, fish, bacteria, worms and beetles (Hastings, 1983). The first applications using luciferase were based upon biomass measurement in the food industry for microbial contamination in food products such as milk, (Bossuyt, 1982) carbonated drinks, (Little and LaRocco, 1986) and meat (Stannard and Wood, 1983).

A typical detection system for the measurement of ATP using bioluminescence is the luminometer. This consists of a sample chamber, a photomultiplier tube (PMT) for the detection of the light produced and a means of recording the amount of light released. The sample chamber is responsible for receiving and presenting the microplate to the detector. It is important that this is completely sealed to minimise interference from ambient light. In order to produce precise, rapid measurements the sample chamber must be positioned as close to the detector as possible

as this positioning gives the optimal signal to noise ratio. The detection system of the luminometer consists of a photomultiplier tube (PMT) where a single photon of light triggers a rapid amplified cascade of electrons. The resulting electrical current created when the photons strike the PMT is measured by the luminometer and expresses this information as arbitrary light units, referred to as relative light units (RLUs). Luminometers can detect an even collection of light from the smallest of samples, obtained by either positioning the PMT side on or end on within the machine. The bioluminescent ATP assay, ViaLight HS (Lonza Bioscience Inc.), was developed to detect ATP released from cells as an indication of viable cell number in the following reaction:

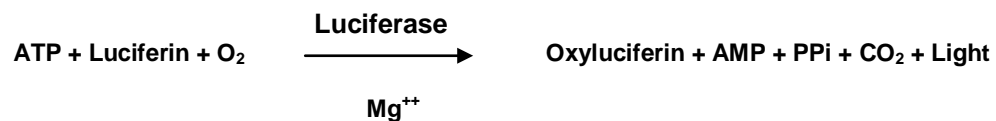


Figure 1.16: The reaction resulting in conversion of ATP to light

Samples of cells are treated with a lysis reagent (detergent based) and a formulation of luciferase, luciferin and magnesium is then added to the lysate to measure the light emitted. The light produced is directly proportional to the amount of ATP, which in turn is proportional to the number of viable cells. If all factors in the above reaction mechanism are saturated it can be deduced that the light emission is linearly related to the concentration of ATP present within the sample. The emitted light is then detected by a luminometer and expressed as the relative light units (RLUs).

1.6 Analysis of the Cancer Proteome

The cancer proteome is now becoming a significant area of research for many researchers, with early detection remaining the most promising approach to improve long term survival for patients with cancer (Diamandis, 2004; Zhang *et al.*, 2004). Wilkins and colleagues in the early 1990's used the terms 'proteomics' and the 'proteome', reflecting the area of 'genomics' and the 'genome' (Liebler, 2002; Baak *et al.*, 2003). Genomics (the study of the human genome) and proteomics (the analysis of the protein complement of the genome) now play a major role in advancing scientific understanding, diagnosis, prognosis and potentially also the treatment of cancer (Baak *et al.*, 2003). Methodologies in proteomics are being enhanced year on year for the analysis of the serum proteome in identifying signature biomarker patterns that may be symptomatic of cancer. Blood contains many proteins which could represent potential biomarkers for a particular cancer type or stage (i.e. primary or metastatic cancer). Overexpression of carcinoembryonic antigen or CEA was first reported by Gold and Freedman in 1975 (Fuks *et al.*, 1975). It is a protein molecule that can be found in many different cells of the body, but is typically associated with certain tumours mainly of the gastro intestine. Another example is the isolation and purification of prostate specific antigen or PSA which is currently the only biomarker for prostate cancer (Leman and Getzenberg, 2009). Blood and urine is routinely analysed for potential or known biomarkers that could reflect the state of an individual. From blood samples serum, plasma and peripheral blood mononuclear cells (PBMCs) can be extracted and routinely monitored for undefined or renowned biomarkers for diagnostic and therapeutic purposes (Mian *et al.*, 2005).

1.61 Mass Spectrometry

One of the main reasons proteomics has become an extremely active area of research for biomarker discovery in recent years is the development of mass spectrometer technologies. Conventionally two-dimensional polyacrylamide gel electrophoresis (2D-PAGE) is used in the discovery of proteins associated with disease (Petricoin and Liotta, 2003; Li *et al.*, 2002)). The negative side to this methodology, despite its ability to identify thousands of proteins, is that it is labour-intensive and necessitates considerable amounts of protein. Recent progress made in mass spectrometry is beginning to offer an alternative to 2D-PAGE (Li *et al.*, 2002). Mass spectrometers represent an analytical tool used for measuring the molecular mass/weight (MW) of a sample and are able to measure bio molecules to within an accuracy of 0.01% of the total MW of the molecule (Ashcroft, 2005). There are many different mass spectrometers currently employed in the analysis of the human cancer proteome that are used for early detection, therapeutic targeting and patient-tailored (personalised) therapy (Petricoin and Liotta, 2003). Identification of a protein biomarker may not only enable the development of assays for the early detection of cancer, but its physical properties and function may be used as a target for therapy or to predict a patient's likely response to a particular drug or treatment. The majority of studies carrying out this research use Matrix Assisted or Surface Enhanced Laser Desorption Ionisation Time of Flight Mass Spectrometry (MALDI-TOF-MS or SELDI-TOF-MS) (Cazares *et al.*, 2008).

The term matrix-assisted laser desorption ionization (MALDI) was first utilised in 1985 by Franz Hillenkamp, Michael Karas and colleagues (Karas *et al.*, 1987). The sample preparation of MALDI includes the mixing of the protein or peptide sample with a matrix in solution. This mixture is then spotted in small amounts onto a specialised 384 target

plate and allowed to dry. The sample and matrix co-crystallise as the solvent evaporates (Mann *et al.*, 2001). The main purpose of a matrix is to stabilise the proteins in the sample on the plate which would otherwise be destroyed by the laser upon analysis. The target plate is then inserted into the mass spectrometer which is sealed and a vacuum created. The research team at the Nottingham Trent University has employed a combination of automated robotic chromatographic ZipTip format and MALDI-ToF-MS producing a powerful and sensitive analysis of pre-fractionated samples, a whole protein based top-down separation strategy for the identification of markers (Matharoo-Ball *et al.*, 2007). The originality of this method is the ability to be able to measure the samples at the protein level for screening biomarkers, followed by tryptic digestion of the same sample (bottom-up) as shown in figure 1.17. This methodology helps identification of biomarkers by measuring tryptic peptides which can be separated out better due to their smaller size by MALDI-MS (reflectron mode) than whole protein based studies.

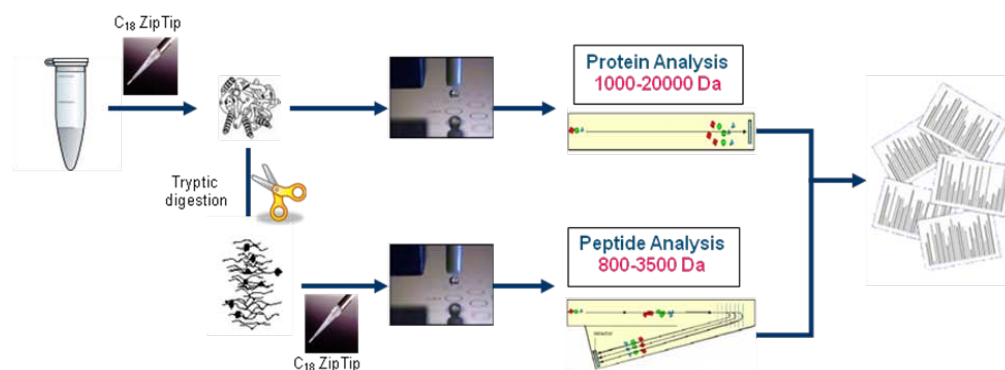


Figure 1.17: A flow diagram to illustrate the procedure of mass spectrometry

In comparison, SELDI technology, developed by William T. Hutchens at Baylor College of Medicine later in 1993 uses a target modified to achieve biochemical affinity with the analyte compound. This is carried out by preparing a specialised chip that contains different chemical

functional groups individually spotted onto the chip and then mixed with the protein sample to be analysed (Hutchens and Yip, 1993). Chip surfaces that are available include; hydrophobic ProteinChip, weak cation exchange ProteinChip, strong anion exchange ProteinChip, immobilised metal affinity ProteinChip (IMAC) and an immobilized copper ProteinChip (IMAC3).

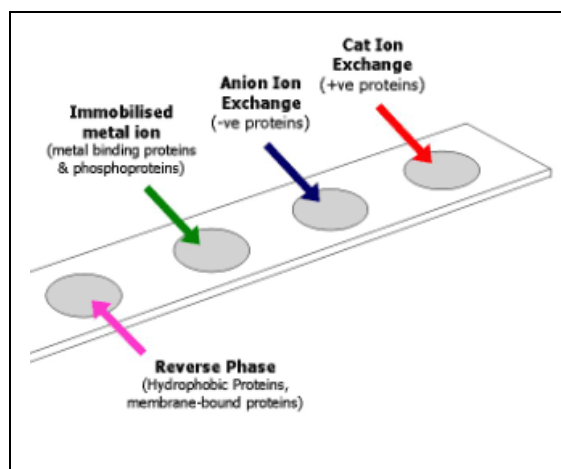


Figure 1.18: A SELDI ProteinChip

The proteins contained within the sample will bind to the different surfaces on the chip, depending on their specialised structures. Some proteins in the sample will bind to the surface, while others are removed through washing (Li *et al.*, 2002). Only proteins complementary to the chip surface are retained and analysed (figure 1.18). As with the MALDI methodology, matrix is applied to the surface after washing and allowed to crystallise with the sample peptides. Binding to the SELDI surface acts as a separation step and the subset of proteins that bind to the surface are easier to analyse. An overview of the processes involved in both MALDI and SELDI mass spectrometry are illustrated in figure 1.19.

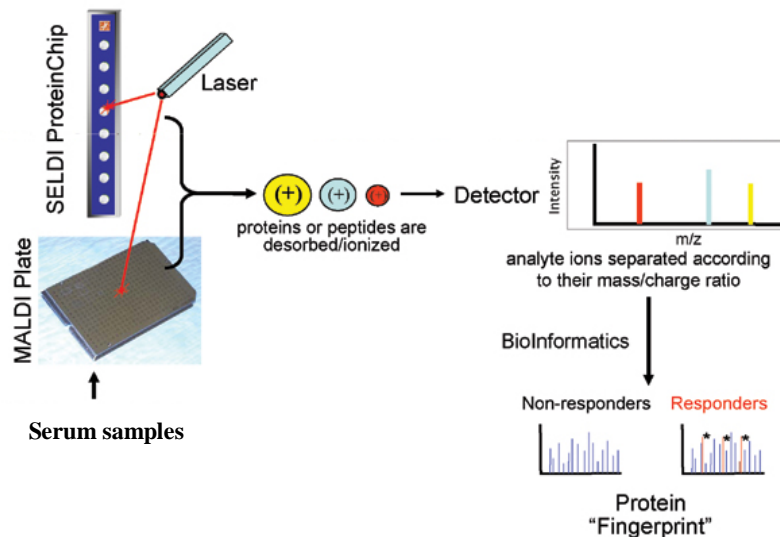


Figure 1.19: A flow diagram to outline SELDI and MALDI mass spectrometry edited from Sidawi and Derra, 2009.

The 'high throughput robotic sample processing', illustrated in figure 1.19 is used to standardise procedures prior to sample analysis. These robotic systems can precisely pipette, mix and spot samples, reducing the amount of time, improving the dimensionality of the data and the reproducibility of experiments.

Mass spectrometry (MS) is an analytical technique for determining the composition of a sample or molecule and consists of three modules; the ion source, mass analyzer and the detector. Initially, the sample is ionised and vaporised by a laser in the ion source, which converts it into electrically charged particles. These particles then enter a mass analyser, which contains electric and magnetic fields. By Newton's second law of motion, lighter ions are deflected more and travel faster than the heavier ions. Both the speed and direction of the charged particle can be increased or decreased while passing through the electric field but the magnitude of the deflection is dependent on the ions mass-to-charge (m/z) ratio. It is this ratio that identifies individual proteins or peptides (Henrickson and Pandey, 2001). The streams of

sorted ions pass from the analyser to the detector (figure 1.19), where the results are recorded and illustrated as peaks grouped together in a 'spectrum' representing the protein or peptide fingerprints. A typical spectrum obtained from mass spectrometry is shown in figure 1.20 below where the m/z ratios of the prominent ions are labeled.

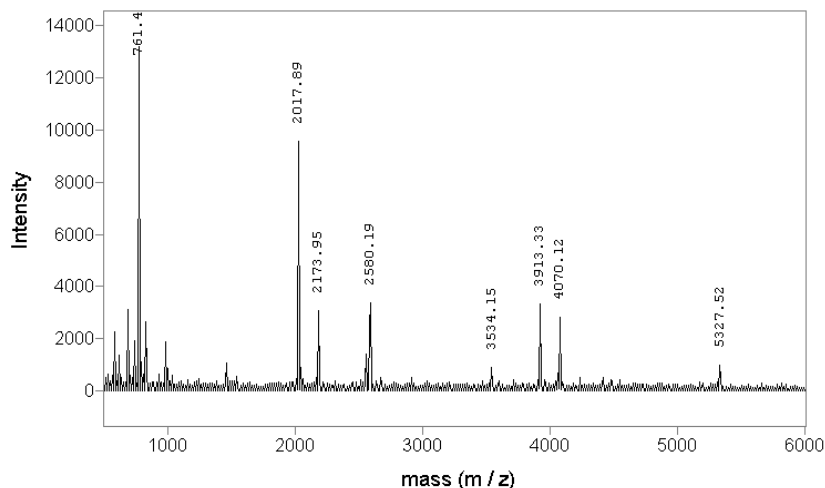


Figure 1.20: Example of spectrum seen after mass spectrometry analysis.

The sample can be measured directly by the mass spectrometer or it can be fractionated to make sample identification more sensitive. This usually involves the mass spectrometer being coupled directly to a high pressure liquid chromatography (HPLC), gas chromatography (GC) or capillary electrophoresis (CE) separation column, separating the sample into a series of components which are measured by the mass spectrometer sequentially for individual analysis (Petricoin and Liotta, 2003; Diamandis, 2004).

MALDI has been used as a high throughput and extremely sensitive tool to generate proteomic patterns from a variety of biological samples ranging from serum, plasma, cerebrospinal fluid and urine to tissue in order to detect biomarkers of disease (Veenstra *et al.*, 2005). Many

biomarkers have been identified in prostate (Adam *et al.*, 2003), polycystic ovary syndrome (Matharoo-Ball *et al.*, 2007), breast (Mian *et al.*, 2003; Traub *et al.*, 2005), ovarian (Petricoin *et al.*, 2002), colorectal (de Noo *et al.*, 2006) and melanoma (Matharoo-Ball *et al.*, 2007; Hutchens and Yip, 1993). MALDI-MS is an ideal methodology for analysing simple peptide mixtures but for more complex samples, especially for protein identity, liquid chromatography-electrospray ionisation combined with mass spectrometry (LC-ESI-MS) may be required (Huang *et al.*, 2002; Karas and Hillenkamp, 1988). One of the major limitations of the MALDI-based technique is its relative poor reproducibility in measuring m/z abundances (peak intensity), which may be essential in biomarker discovery. In addition, LC-MALDI-TOF/TOF analysis generally takes a long time, which is hardly practical when analysing large numbers of samples. However, this technique is recognized for its high mass accuracy (typically in the range of 5 ppm to 20 ppm routinely). Another area of contention is the tools used to analyse the complex data in MALDI. Re-analysis of the raw data from Petricoin's study in 2002 with different bioinformatics tools failed to validate the initial findings causing much dispute over techniques and validation used on data sets (Baggerly *et al.*, 2004; Sorace *et al.*, 2003).

The development of electrospray ionisation for the analysis of biological macromolecules was awarded the Nobel Prize in Chemistry to John Bennett Fenn in 2002. There are a wide range of basic electrospray techniques primarily microspray and nanospray but they all involve the transfer of ions from solution to a gas phase (Kearle, 2000). There are many variations on the basic electrospray technique. Microspray and nanospray have better sensitivity due to the reduction in the flow rate of the analyte containing liquid. The main process involves applying an electric field to the tip of a capillary which contains a solution of electrolyte with the substance or analyte to be studied (Karas and

Hillenkamp, 1988). The solvent used is normally much more volatile than the analyte which exists as an ion in solution (either an anion or a cation). Volatile acids, bases or buffers are added to this solution and due to forces of charge repulsion, the liquid pushes itself out of the capillary and forms a 'mist' of droplets approximately 10 μm across. This forces the molecules together which are continually trying to repel each other as they evaporate, thus breaking up the droplets. This is known as Coulombic fission because it is driven by repulsive Coulombic forces between charged molecules (Kearle, 2000). This continues until the analyte is free of solvent and enters the mass analyser to be measured, and shown on spectra containing peaks as previously demonstrated in figure 1.20.

1.62 Bioinformatics approaches for data analysis

With the introduction of mass spectrometers and the vast amounts of data produced; analysing the data became a minefield, introducing a high degree of complexity into the results (Lancashire *et al.*, 2005). However, recent advances in computer algorithms and informatics, combined with biological knowledge are enabling this data to be analysed (Ball *et al.*, 2002; Diamandis, 2004). This requires the use of highly sophisticated statistical methods with high computational power such as Bayesian analyses, fuzzy logic and artificial neural networks or ANNs (Matharoo-Ball *et al.*, 2007). There are many proteomics tools that can be employed providing a wealth of information and rapid interpretation of the large quantities of data analyzed (Bensmail *et al.*, 2005). There has to be an accurate interpretation of the 'curse of dimensionality' (Ball *et al.*, 2002) which refers to the asymmetry seen between the number of input features (e.g. peaks) and the number of exemplary features (e.g. samples). Overcoming this problem is challenging but necessary and some of the bioinformatics tools developed to successfully analyse complex data sets include:

1. Artificial neural Networks (ANNs) – identifies peaks that are statistically different between two groups. Links are used within the computer model which are strengthened or weakened depending on their frequency of use (Lancashire *et al.*, 2005).
2. Principle Component Analysis or PCA – used to sort data by finding the fewest dimensions. Data is sorted into axes that best represent the differences between groups and represented visually on 2D or 3D scatter-plot graph (Lesk, 2005).
3. Cluster Analysis – involves placing data into distinct groups based on the similar characteristics shared between individuals.

4. Support Vector Machines (SVM) – correctly separates into classes but can also identify classifications not supported by the data.
5. Decision Trees – can be applied to problems such as protein function.

Generally data mining approaches fall into two categories: unsupervised and supervised. Unsupervised data (e.g. PCA and cluster analysis) do not take into account class labels, while supervised (e.g. ANNs, SVMs) approaches do. For initial assessment of the quality of data unsupervised approaches can be carried out to visualize the overall distribution of the data (Fung *et al.*, 2005). They can also provide a qualitative assessment of the data by superimposing the sample labels. All of these tools have the capability to aid the researcher in accurately identifying biomarkers from data retrieved from mass spectrometry (Fogel, 2004). Prior to analysis of the data by informatics, data are manipulated or preprocessed by removing any unwanted and inconsistent data as shown in figure 1.21. This involves selecting peaks and removing any m/z ratios that are outside the targeted range (Fung *et al.*, 2005). The data are smoothed to allow comparisons between spectra and baseline corrected to eradicate insignificant datasets.

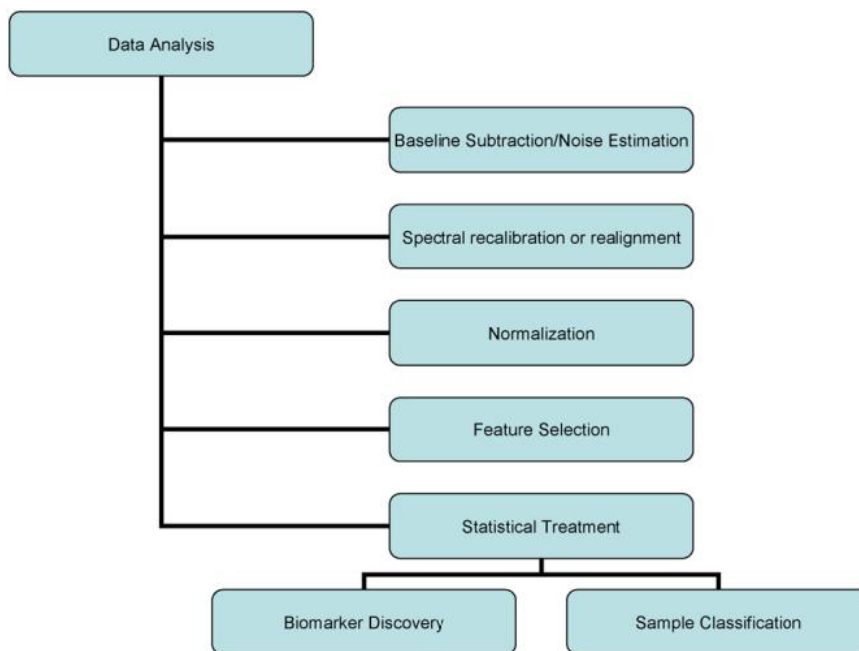


Figure 1.21: Mass spectra analysis work flow taken from Norris *et al.*, 2007.

Analysis of MALDI data can be separated into two distinct steps: pre-processing and processing or statistical analysis. Pre-processing has been the focus of much variance within a data set. This procedure plays a key role in reducing experimental variance, and preparing the subsequent data for statistical analysis. The spectra obtained are conditioned through the removal of background, normalization of intensity, and alignment. The analytical goals of profiling experiments can be two-fold: the classification of samples into two or more classes such as diseased/non-diseased, and the identification of biomarkers characteristic to each class (Yanagisawa *et al.*, 2003). Identification of disease specific proteins could reveal much information from protein mechanisms to potential diagnostic markers or drug targets. Recognising this importance is highlighted in comparative analyses of profile spectra (Markey *et al.*, 2003), whereby varied biostatisticians all reported an accuracy >90% in classifying the same profile spectra from either tumour or non-tumour samples. The controversy however lies in identifying which ions are the most significant

to determine the classifications in which there was little to no agreement. These inconsistencies cause much consternation particularly since these same ions are prime candidates for further identification and study as disease biomarkers. This debate over data interpretation limits mass spectrometry as a powerful technique which needs to be taken into account when analysing data (Westhead and Twyman, 2002)

Upon finding important peaks using computer algorithms, that have significant differences between cancer and control groups, the next step is to characterise and identify the proteins that they represent. There are several web-based databases e.g. Mascot, ProFound or MOWSE (Matharoo-Ball *et al*, 2007) that provide complete listings of all known proteins' sequences. Intact proteins are incompatible with these databases; therefore a digest of the protein is carried out using a specific protease such as trypsin. The mass measurements of the digested fragments are more precise, whereas the various forms of proteins that exist due to post-translational modifications make identification by this method unclear (Wu *et al.*, 2002). Where such modifications are known, exact mass differences between unmodified and modified amino acids can be predicted. Algorithms such as SEQUEST have built-in parameters for detecting such modifications. The presence of a modified residue should always be confirmed experimentally (Westhead and Twyman, 2002). Imperfect matches can also result because the actual protein does not exist on the database but a close homolog from the same species does exist. This is often the case if a protein contains a single nucleotide polymorphism leading to two or more variants. Another technique often used for identity is electrospray ionisation tandem mass spectrometry (EITMS) which produces amino acid sequences of each peptide fragment based on its net charge, which can be entered into the online data bases and compared to all known proteins.

1.7 Aims and Objectives

Cancer is a complex disease that presents many challenges to clinicians and cancer researchers who are constantly searching for more effective ways to combat its often devastating effects. The majority of patients with cancer will require treatment with chemotherapeutic agents at some point in the course of their disease. A significant percentage of these patients can achieve a complete remission after initial treatment but a high proportion of these will finally relapse due to the presence of residual tumour cells that resist drug treatment (Dolken, 2001). The methods used to detect cell killing, lack sensitivity, often as a result of high background readings and the unacceptable signal: noise ratio. This means it is often difficult to confirm the complete (100%) killing of tumour cells.

The initial aim of this research was to produce a novel assay that would be a quick, safe and highly sensitive alternative to traditional assays such as MTT or chromium-51 that is historically used to measure cell viability. With the increase in the use of ATP as a detection system for viable cells (due to ease of use and the speed and accuracy of the detection) an investigation was conducted into an extension of this technology. A paper was found by Squirrel and Murphy (1997) which looked into the use of adenylate kinase (AK) for hygiene monitoring in the food and beverage industry. One molecule of AK could turn over 1000 molecules of ATP. As ATP had already been shown to be sensitive in detecting cell viability, the measurement of AK leakage from cells could result in a more sensitive assay for measuring cell death. It was therefore decided to produce a novel assay using AK and if successful, compare its sensitivity against the well-established methodologies. AK belongs to the class of enzymes known as phosphotransferases, specifically those that use a phosphate group as an acceptor (Rosenfelt and Hubler, 1999). It is a ubiquitous protein present in all eukaryotic cells. The principle behind the assay is based on the leakage of the enzyme into the culture supernatant through

lysis of the cell membrane (Squirrel and Murphy, 1997). Due to its small size (36 KDa), measurement of this enzyme should be more accurate and sensitive for the determination of cytotoxicity and cytolysis, than those presently available (i.e. LDH is 140 KDa). An AK detection reagent (named 'ToxiLight' in this thesis), would be designed to be added to a cell culture and allow for the detection of AK leakage from damaged cells by bioluminescence. The detection limits of this assay will be investigated and compared to the commonly used cytotoxicity assays.

The second part of the research was to utilise the most responsive assays tested in the initial investigation to establish sensitive and resistant melanoma cell lines. The cell lines will be chosen based on their responses to various well-known chemotherapeutic drugs using the chosen assays. When a resistant and sensitive cell line has been chosen, the investigation will be continued to test the effects of the drug trichostatin A (a reversible inhibitor of the histone deacetylase (HD)) upon these cells. The effects of trichostatin A has been researched widely on melanoma cells including its investigation into the role of p53 (Halaban *et al*, 2009) and p21 (Boyle *et al*, 2005) with evidence suggesting that it may play an important role in carcinogenesis. Trichostatin A has been shown to induce differentiation in acute myeloid leukemia and displays potent antitumor activity against prostate and breast cancer cells *in vitro* and *in vivo*. This experiment would involve treating the chosen melanoma cells with trichostatin A, testing them with the cytotoxicity assays with further confirmation by using PI uptake, light microscopy and trypan blue. The cell lysates from these drug-treated and untreated melanoma cell lines would be frozen down and utilised for further research.

The final part of this study was to utilise the frozen lysates obtained from the cytotoxicity experiments to assess the molecular effects of trichostatin A on the melanoma cells by MALDI-TOF-MS. By identifying patterns in

proteomic profiles it may be possible to identify possible biomarkers reflecting differences between sensitive and resistant drug-treated cell lines. The spectra obtained from the MALDI-MS analysis will then be analysed using ANNs to determine if patterns can be found within the data that can classify blind samples according to drug-treated and untreated cells. The MALDI spectra will be analysed using the same ANNs parameters and the results of the analyses with the MALDI methods compared to the previous cytotoxicity assays.

Chapter 2 – Materials and methods

2.1 Materials

Material	Supplier
FACS Flow FACSscan tubes	BD BioSciences Between Towns Road Oxford
5,5',6,6'-tetrachloro-1,1',3,3'- tetraethylbenzimidazolylcarbocyanine iodide (JC-1)	Cambridge BioScience Newmarket Road Cambridge
Dimethyl sulphoxide (DMSO) Foetal Bovine Serum (FBS)	Harlan Sera Labs Loughborough Leicestershire
Acetonitrile (ACN):HPLC grade Trifluoroacetic acid (TFA): HPLC grade	Fisher Scientific Bishop Meadow Road Leicestershire
α -cyano-4-hydroxycinnamic acid (CHCA) Peptide calibration mix Protein calibration mix 2 Sinapinic acid	Laser Bio Labs Cedex France
ATP ToxiLight ViaLight HS	Lonza BioScience Wokingham Berkshire
ADP Camptothecin Dexamethasone Vindesine	Merck BioSciences Ltd Beeston Nottingham
Zip Tip pipette tips	Millipore UK Ltd Units 3 and 5 The Courtyards Hatters Lane Watford
Bovine Serum Albumin (BSA)	MP Biomedicals Wellington House Cambridge
96 well cell culture plates 96 well luminometer plates	Porvair Sciences Ltd Govett Avenue Sheperton

Material	Supplier
Cytotox One MTS	Promega UK Chilworth Science Park Southampton
WST-1 XTT	Roche Switzerland
Cell culture flasks (T25 and T75) Sterile universal tubes (25ml and 50ml) 10ml pipettes	Sarstedt Ltd Beaumont Leys Leicestershire
12 well tissue culture plates	Scientific Laboratory Supplies Wilford Industrial Estate Nottingham
Acridine orange Cisplatin Dacarbazine Dimethylsulfoxide (DMSO) Dithiothreitol (DTT) Doxorubicin Ethidium bromide L-Glutamine Myokinase Standards n-octyl-beta-D-gluco-pyranoside (OGP) PBS tablets Penicillin and Streptomycin Propidium Iodide RPMI-1640 Trichostatin A Trypan Blue	Sigma-Aldrich Poole Dorset
Axima CFR ⁺ MALDI TOF mass spectrometer 384 MALDI target plate	Shimadzu Manchester
Statistica 7.0 software	StatSoft Inc. Tulsa OK

Table 2.01: List of materials used within this study and their supplier.

2.2 Preparation of buffers, stains and kits

2.2.1 Preparation of phosphate buffered saline (PBS)

1 tablet was dissolved in 200 mL of dH₂O to give 0.01 M phosphate buffer, 0.0027 M potassium chloride and 0.137 M sodium chloride at pH 7.4 (25°C).

2.2.2 Preparation of Acridine Orange/Ethidium bromide and fluorescent microscopy

Preparation of stock solution.

The stock included: 15 mg Acridine orange, 50 mg Ethidium bromide which was dissolved in 1 mL of 95% (v/v) ethanol. 49 ml of d.H₂O were added.

Preparation of working solution.

The stock solution was diluted 1:100 with PBS to give a final working concentration of 3 µg.ml⁻¹ Acridine orange and 10 µg.ml⁻¹ Ethidium bromide.

2.2.3 Preparation of JC-1 Staining (5,5',6,6'-tetrachloro-1,1',3,3'-tetraethylbenzimidazolcarbocyanide iodide)

Preparation of stock solution.

JC-1 was dissolved in DMSO to give a 1mg.ml⁻¹ solution.

Preparation of working solution.

The stock solution was diluted 1:50 in PBS and filtered using a 0.45 µm filter.

250 µl of the filtered JC-1 was added to 125 µl of the cell suspension and incubated for 30 minutes at 37°C in a 5% (v/v) CO₂, humidified incubator.

2.2.4 Preparation of Propidium iodide (PI) – PI was reconstituted in DMSO to give a stock of $1\text{mg}\cdot\text{ml}^{-1}$ which was diluted 1:20 in PBS to give a working concentration of $50\ \mu\text{g}\cdot\text{ml}^{-1}$.

2.2.5 Preparation of Trypan Blue – Trypan Blue was obtained ready to use at a 0.4% (w/v) solution (0.81% (w/v) sodium chloride and 0.06% (w/v) potassium phosphate).

2.2.6 Preparation of ViaLight® Plus kit

- Nucleotide Releasing Reagent – Provided ready to use.
- Tris Acetate Buffer – Provided ready to use.
- ATP Monitoring Reagent (AMR) – AMR was reconstituted by the addition of 50 mL of Assay Buffer to the bottle. This was equilibrated for 15 min at room temperature to ensure complete rehydration, as to the manufacturers' specifications.

2.2.7 Preparation of ToxiLight® kit

- AK Assay Buffer – Proprietary information.
Provided ready to use.
- Adenylate Kinase Detection Reagent (AK-DR) - Proprietary information.
AK-DR was reconstituted by the addition of 10 mL of AK Assay Buffer to the bottle.

This equilibrated for 15 min at room temperature to ensure complete rehydration, as to the manufacturer's specifications.

2.2.8 Preparation of CytoTox-ONE kit

- CytoTox-ONE assay buffer – Provided ready to use.
- CytoTox-ONE Reagent – CytoTox-ONE was reconstituted by the addition of 10 mL of CytoTox-ONE assay buffer to the bottle. This was then allowed to equilibrate for 15 min, as to the manufacturers specifications.
- Stop solution – Provided ready to use.

2.2.9 Preparation of MycoAlert kit

- MycoAlert Assay Buffer – Provided ready to use.
- MycoAlert Substrate - substrate was reconstituted by the addition of 6000 μ L of MycoAlert Assay Buffer to the bottle.

This equilibrated for 15 min at room temperature to ensure complete rehydration, as to the manufacturer's specifications.

2.3 Cell lines

The cell lines used in this study were all obtained from ECACC apart from the melanoma cell lines, which were a kind gift from Professor Rees at Nottingham Trent University.

2.3.1 Freezing and thawing of cells

The cells were frozen in 1ml aliquots at concentrations between 2 - 5 x 10⁷ cells.ml⁻¹ in the appropriate media, containing 10% (v/v) foetal calf serum (FCS) and 10% (v/v) dimethyl sulphoxide (DMSO). The cells were thawed in a 37°C water bath and washed in warmed media and centrifuged for 5 minutes at 400 x g to remove any excess DMSO. The cells were then placed in 10 mL of fresh media and then into a T25 tissue culture flask.

2.3.2 Cell culturing Suspension Cells

All cells were cultured in a humidified, 5%(v/v) CO₂ incubator at 37°C in the appropriate complete media containing 10% (v/v) FCS, 2 mM L-Glutamine, 50 units mL⁻¹ penicillin and 50 µg.ml⁻¹ streptomycin. The cell lines were sub cultured twice weekly or when they had reached an approximate cell density of 1 x10⁶ mL⁻¹.

2.3.3 Cell lines Used

Cells	Cell Type	Culture Media	Suspension/Adherent	Source
Jurkat	Acute human T cell lymphoblast	RPMI	Suspension	ECCAC
U937	Human histiocytic lymphoma	RPMI	Suspension	ECCAC
K562	Human chronic myelogenous leukaemia	RPMI	Suspension	ECCAC
CEM-7	Human acute T cell lymphoblast	RPMI	Suspension	ECCAC
HL60	Human promyelocytic leukaemia	RPMI	Suspension	ECCAC
FM-3	Human breast mammary cells		Adherent	ECCAC
A549	Human small cell lung cancer cells	DMEM	Adherent	ECCAC
Hep G2	Hepatocellular carcinoma	DMEM	Adherent	ECCAC
Ma Mel 26a	Melanoma (human)	RPMI	Adherent	Nottingham Trent University (OYSTER)
Ma Mel 28	Melanoma (human)			
MEWO	Melanoma (human)	RPMI	Adherent	Nottingham Trent University (ESTDAB)
COLD 794	Melanoma (human)	RPMI	Adherent	
ESTDAB-105	Melanoma (human)	RPMI	Adherent	
WM 1205	Melanoma (human)	RPMI	Adherent	

Table 2.02: Cell Lines Used

2.3.4 Culturing Adherent Cells

With the exception of the melanoma cell lines which were cultured in the same media as the suspension cells above, all of the adherent cell lines were cultured in 75 cm² cell culture treated flasks in Dulbecco's Modified Eagles Medium (DMEM) media supplemented with 10% (v/v) heat inactivated foetal bovine serum, 1% (v/v) L-Glutamine (2 mM), 1% (v/v) penicillin (50 U.ml⁻¹) / streptomycin (50 µg.ml⁻¹). The culture supernatant was carefully poured off and discarded. Enough trypsin EDTA solution (100 mg porcine trypsin, 40 mg EDTA) was added to cover the bottom of the flask in use. The flask was then placed at 37°C in 5% (v/v) CO₂ in a humidified atmosphere until the cells became detached from the bottom. The detached cells were transferred to a sterile universal tube (25 cm²), media added to wash off the trypsin and centrifuged for 5 minutes at 400 x g. The supernatant was removed from the tube and the cell pellet re-suspended in fresh media. The cells were sub cultured from this into a fresh flask containing media. Generally a 1:10 dilution is carried out.

2.3.5 Counting cells

50 µl of cells were diluted with 50 µl of 0.4% (w/v) trypan blue and the cells were counted on a haemocytometer. This 1:2 dilution factor was incorporated into the calculation below. The cells with damaged membranes take up trypan blue and appear violet in colour. Normal cells do not take up trypan blue and appear colourless when viewed with the aid of a light microscope. Cell counts were taken both of viable and non-viable cells by:

Average of number of cells x dilution factor x 10⁴ = cell count per mL.

Figure 2.01: Calculation for the counting of cells (Sigma).

2.3.6 Mycoplasma Testing

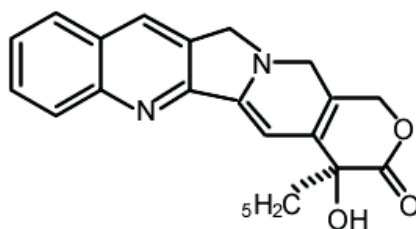
Mycoplasma species can be found in many research laboratories. A cell culture with mycoplasma occurs due to contamination from individuals or contaminated cell culture medium ingredients. As they are physically small ($< 1 \mu\text{m}$) and cause no visible changes to the cell culture media, they are very difficult to detect with only a conventional microscope. Eventually severe *mycoplasma* contamination will destroy the cell line. MycoAlert® has been designed to detect cellular contamination by bioluminescence within 15 min.

All reagents were initially brought up to room temperature prior to reconstituting the MycoAlert® substrate in 600 μl of MycoAlert® assay buffer. After 15 min of rehydration, 2 mL of cell culture was transferred into a centrifuge tube and the cells spun at 200 g for 5 min. 100 μL of supernatant was then transferred into a luminometer cuvette and the luminometer programmed to take a 1-second integrated reading. 100 μL of MycoAlert® Reagent was added to each sample and after 5 min a reading taken (reading A). 100 μL of MycoAlert® substrate was added to the same tube and after 10 min a second reading is taken (reading B). The ratio of reading B to A is used to determine whether a cell culture is contaminated by *mycoplasma*. The test is designed to give a ratio of less than 1 with uninfected cultures and a ratio of greater than 1 for cells infected with *mycoplasma*.

2.4 The structure, mechanism and preparation of the Apoptosis inducing agent

The following apoptosis inducing agents were well known cytotoxic agents used by Lonza Bio Science. The required cytotoxic concentrations of the drugs with the majority of cell lines assayed in this project had already been researched and were reliable cell models that could be used in the work-up of the ToxiLight™ assay.

2.4.1 Structure and mechanism of apoptotic agents



Camptothecin

Figure 2.02: Structure of Camptothecin

Camptothecin is a pale yellow solid and a DNA topoisomerase I inhibitor. The unique mode of action for this potent cytotoxic compound was found to be the inhibition of an enzyme known as DNA topoisomerase I. Camptothecin traps this enzyme, inhibiting DNA replication and killing the cancer cells. (Calbiochem, 1999)

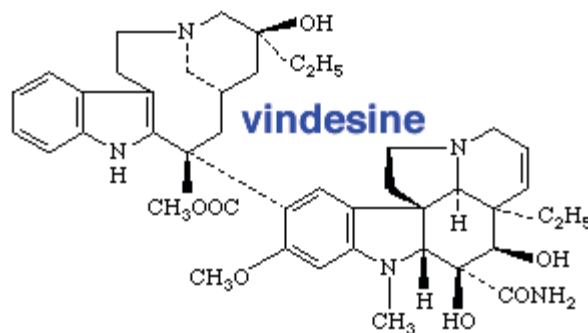


Figure 2.03: Structure of Vindesine

Vindesine is a vinca alkaloid, which is a synthetic derivative of vinblastine. It binds to the microtubular proteins of the mitotic spindle, leading to crystallisation of the molecule and mitotic arrest or cell death in metaphase. The vinca alkaloids are considered to be cell cycle phase-specific.

Doxorubicin

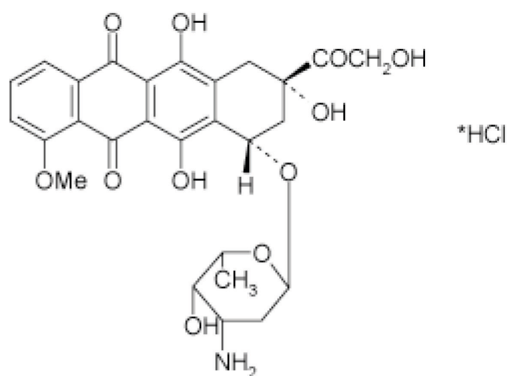


Figure 2.04: Structure of Doxorubicin

Doxorubicin is an anthracycline antibiotic produced by the fungus *streptomyces peucetius*. Doxorubicin damages DNA by intercalation of the anthracycline portion, metal ion chelation, or by generation of free radicals. It has also been shown to inhibit DNA topoisomerase II which is critical to DNA function. Cytotoxic activity is cell cycle phase-nonspecific. (Thakkar and Potten, 1993).

Cisplatin

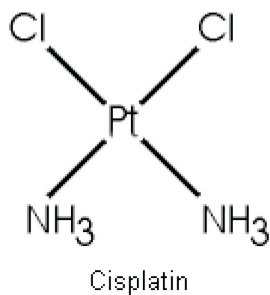
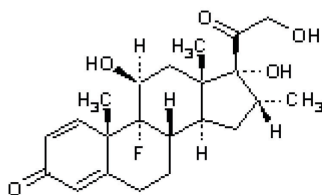


Figure 2.05: Structure of Cisplatin

Cisplatin was first synthesised in 1845, but its cytotoxic properties were not described until 1965. Cisplatin is an inorganic complex formed by an atom of platinum surrounded by chlorine and ammonia atoms. Intracellularly, water displaces the chloride to form highly reactive charged platinum complexes. These complexes inhibit DNA through covalent binding leading to intrastrand, interstrand, and protein cross-linking of DNA. Experimental and clinical data suggest that cisplatin enhances radiation therapy effects. Early studies suggested that cisplatin was cell cycle phase-nonspecific, while more recent studies have shown complex and variable effects on the cell cycle.

Dexamethasone



9-Fluoro-11 β ,17,21-trihydroxy-16 α -methylpregna-1,4-diene-3,20-dione

Figure 2.06: Structure of Dexamethasone

This white solid is an active and highly stable glucocorticoid. It inhibits the expression of inducible but not constitutive nitric oxide synthase in vascular endothelial cells. Dexamethasone is also known to enhance active cation transport in aortic smooth muscle cells by stimulating the sodium-potassium pump. It is a drug used to induce apoptosis in human thymocytes.

Trichostatin A

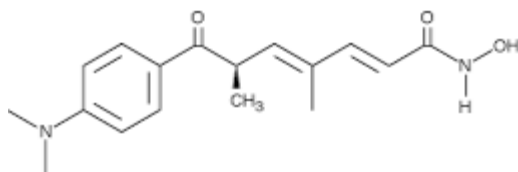


Figure 2.07 Structure of Trichostatin A

Trichostatin A is a potent reversible inhibitor of histone deacetylase (HD) and selectively inhibits the removal of acetyl groups from the amino-terminal lysine residues of core histones, which modulates the access of transcription factors to the underlying genomic DNA. Trichostatin A mediates the activation of O⁶-methylguanine-DNA methyltransferase (MGMT). It may be involved in cell cycle progression of several cell types, inducing cell growth arrest at both G₁ and G₂/M phases. In some cases it can induce apoptosis.

2.4.2 Preparation of the apoptosis inducing agents

All the cytotoxic agents below were reconstituted in DMSO to produce the stock concentrations listed:

Cytotoxic Agent	Stock Concentration
Camptothecin	5 mM
Cisplatin	1 mg. ml ⁻¹
Dacarbazine	20 mM
Dexamethasone	25 mM
Doxorubicin	10 mg.ml ⁻¹
Trichostatin A	1 mM
Vindesine	1 mg. ml ⁻¹

Table 2.03: Table to illustrate the cytotoxic drugs used.

2.4.3 Preparation of apoptotic models

The cells were seeded at 5×10^5 cells.ml⁻¹. 1 ml of the cell suspension was transferred into 8 wells of a 12 well plate and the cells were dosed with the following concentrations of cytotoxic drug depending upon the model being prepared.

Following dosing, the cells were incubated at 37°C in a humidified atmosphere of 5% (v/v) CO₂, 95% (v/v) air for the required incubation time indicated in table 2.04.

<i>Cytotoxic Drug</i>	<i>Incubation Time (h)</i>	<i>Dosing Range (μM)</i>
Camptothecin	24	0, 0.5, 0.1, 1, 2, 5, 10
Cisplatin	24, 48, 72	0, 0.1, 0.2, 0.5, 0.8, 1
Dacarbazine	24, 48, 72	0, 0.03, 0.06, 0.13, 0.25, 0.5, 1, 2
Dexamethasone	72	0, 10, 25, 50, 75, 100, 150, 200
Doxorubicin	24, 48, 72	0, 0.1, 0.2, 0.5, 0.6, 0.8, 0.9, 1
Trichostatin A	24, 48, 72	0, 0.2, 0.4, 0.6, 0.8, 1, 2, 5
Vindesine	24, 48, 72	0, 0.2, 0.5, 1.0, 2, 5

Table 2.04: Table to show the cytotoxic cell models used to induce cell death.

2.4.4 Preparation of Necrotic model

2.4.4.1 Freeze-thaw Method

2mls of suspension (1×10^6 cells.ml⁻¹) were placed into two cryotubes. Another 2 mL was placed in a 25 ml universal tube and left at room temperature to give healthy control cells. The cryotubes were placed in liquid nitrogen until frozen and then immediately immersed in a water bath at 37°C. This was repeated six times until all the cells had burst open. Using trypan blue exclusion the viability of the cells was checked. When 100% cell death had occurred the healthy and necrotic cells were mixed as shown in table 2.05 to make up 1 ml samples and 100 μl placed in triplicate into a 96 well white walled plate.

The cells were then mixed as per the following table (for a total 1 ml volume). A 100 μl volume was taken and placed in triplicate into a 96 well white walled plate for analysis.

% Necrosis	0	10	30	50	60	80	90	100
Volume necrotic cells (μl)	0	100	300	500	600	800	900	1000
Volume healthy cells (μl)	1000	900	700	500	400	200	100	0

Table 2.05: Table to show the volumes required for differing percentage necrosis samples.

2.5 Cell Number Dilutions

Cells were diluted 1:10 in complete media as per the table below. A 100 μl sample was placed in triplicate into a 96 well white walled plate for analysis.

Cell Number (mL^{-1})	Volume of cell suspension (μl)	Volume of complete media (μl)
1×10^6	1000	0
1×10^5	100 (of above)	900
1×10^4	100 (of above)	900
1×10^3	100 (of above)	900
1×10^2	100 (of above)	900
1×10^1	100 (of above)	900
0	0	1000

Table 2.06 Table to show the volumes required for a cell number curve.

2.6 Effect of measuring the ToxiLight® assay with / without cells present in the test sample.

Two tubes containing K562 cells seeded at 5×10^5 cells.ml⁻¹ were spun down to eradicate any cells present in the media. One tube was sampled for the supernatant in 100 µl volumes in triplicate into a 96 well plate. The second tube was vortexed to re-suspend the cells, then sampled in 100 µl volumes in triplicate as per the first tube. The samples in the 96 well plate were then analysed by ToxiLight® as described in section 2.8.3.3.

2.7 Preparation of Standards

2.7.1 ATP Standards

From a stock concentration of 10 µmol.ml⁻¹, ATP was diluted 1:10 in Tris Acetate Buffer or complete media as shown in the table below to produce the required concentrations of ATP. A control was set up consisting of Tris Acetate Buffer or complete media alone.

<i>ATP Standard (nmol.ml⁻¹)</i>	<i>Volume of ATP (nmol.ml⁻¹) (µl)</i>	<i>Volume of complete media or Tris acetate buffer (µl)</i>
10,000	1000	0
1000	100 (of above)	900
100	100 (of above)	900
10	100 (of above)	900
1	100 (of above)	900
0.1	100 (of above)	900
0	0	1000

Table 2.07: Table to show the dilutions and volumes required for ATP standards.

The standards were left on ice throughout the procedure until required when 100 μl was placed in triplicate into a 96 well white-walled bioluminescent plate.

2.7.2 Myokinase standards

AK standards from a stock concentration of 1 M were diluted down 1:2 from $1 \times 10^{-3} \text{ U} \cdot \mu\text{l}^{-1}$ in Tris Acetate Buffer as shown in table 2.08 to produce the following concentrations of AK with a blank consisting of Tris Acetate Buffer. The standards were left on ice throughout the procedure until required when 100 μl was placed in triplicate into a 96 well white-walled plate.

<i>AK Standard ($\text{U} \cdot \mu\text{l}^{-1}$)</i>	<i>Volume of AK ($\text{U} \cdot \mu\text{l}^{-1}$) ($\mu\text{l}$)</i>	<i>Volume of Tris acetate buffer (μl)</i>
$1 \times 10^{-2} \text{ U} \cdot \mu\text{l}$	1000	0
$1 \times 10^{-3} \text{ U} \cdot \mu\text{l}$	400 (of above)	3600
$5 \times 10^{-4} \text{ U} \cdot \mu\text{l}$	2000 (of above)	2000
$2.5 \times 10^{-4} \text{ U} \cdot \mu\text{l}$	2000 (of above)	2000
$1.25 \times 10^{-4} \text{ U} \cdot \mu\text{l}$	2000 (of above)	2000
$6.25 \times 10^{-5} \text{ U} \cdot \mu\text{l}$	2000 (of above)	2000
0	0	2000

Table 2.08: Table showing the dilutions and volumes required for differing AK standards

Methods

2.8 Measurement of cell viability

The ability of the cell to exclude various dyes indicates the maintenance of the cell membrane integrity and hence the viability of the cell.

2.8.1 Measuring Cell Permeability with PI

PI is also used to assess plasma membrane integrity and cell viability. 200 μl of cell suspension was placed into a round bottom FACScan tube and 200 μl of PI ($50 \mu\text{g.mL}^{-1}$) added, mixed and incubated for 10 min at room temperature. The cells were analysed to assess PI uptake with a Becton Dickinson FACScan™ Flow Cytometer where 5,000 events were counted. The compensation settings were not required due to only one fluorescent dye being monitored in this project (*Darzynkiewicz et al., 1992*).

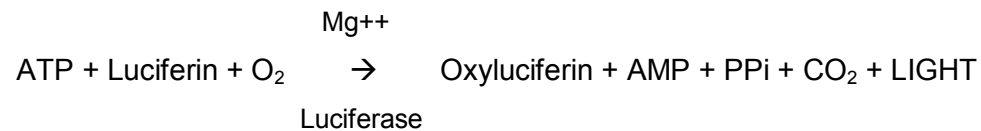
2.8.2 Uptake of Trypan Blue

Cells were mixed with Trypan blue as detailed in section 2.3.5. The cells were counted and analysed under a light microscope. Membrane integrity was assessed by the number of cells that could take up the dye (appearing blue under the microscope (*Gorman et al., 1996*)).

2.8.3 Assays used to measure cytotoxicity

2.8.3.1 Measurement of ATP (ViaLight HS, Lonza BioSciences)

ATP was measured using bioluminescence based on the luciferin-luciferase reaction:



ATP was measured using the ViaLight BioAssay Kit (Lonza BioScience) according to the manufacturer's instructions. Briefly, 100 µl of Nucleotide Releasing Reagent (NRR) were added manually to 100 µl of cells and incubated at RT for 5 minutes. If cells had been grown up in volumes greater than 100 µl, an equal volume (to the culture volume) of NRR were added and the sample incubated for 5 minutes at RT. 180 µl of the cell lysate was subsequently transferred to a luminometer compatible plate. The plate was read in a luminometer, programmed to inject 20 µl of reconstituted ATP Monitoring Reagent (AMR) to each well and an immediate 1-second integrated reading was taken and expressed as relative light units (RLUs). Data were expressed as mean +/- SD of triplicates.

2.8.3.2 Measurement of ATP (ViaLight Plus, Lonza BioSciences)

This method was used as an alternative to the original ViaLight Plus in the latter parts of the study. The ideology is the same but the methodology slightly different. It was used due to its good stable readings in comparison to ViaLight Plus, making it more flexible.

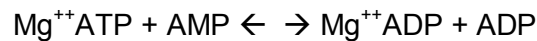
Briefly, 100 μ l of cells to be measured were added manually into a cell culture plate. If an experiment is already set up then a total well volume of 100 μ l is required. 50 μ l of cell lysis reagent is added to the wells and incubated at RT for 10 minutes. 100 μ l of the reconstituted ViaLight Plus reagent is then added manually to the wells and after 5 min incubation at RT the amount of ATP in the cell was measured on a luminometer, using a 1 second integral reading and expressed as relative light units (RLUs). Data were expressed as mean \pm SD of triplicates.

2.8.3.3 Measurement of Adenylate Kinase (AK) (ToxiLight, Lonza BioScience)

The adenylate kinase assay was developed over an initial period of two years as part of my PhD research and was undertaken by myself. The optimisation of the assay was carried out using various concentrations of luciferin, luciferase, ADP, and magnesium (proprietary information) with a preliminary release of the assay (ToxilightTM) at the end of 2002. The second phase of the assay included the optimisation of the assay buffer to improve the signal stability along with the introduction of a 100% cell lysis reagent prior to a second launch in 2004. Due to confidentiality with respect to the product formulation, the initial work-up and concentrations tested are not shown in this thesis but the assay performance and steps undertaken at each level is shown at each point of assay development.

The basis of the novel AK assay was to measure the release of the enzyme adenylate kinase (AK) from cytolytic cells using bioluminescence based on the conversion of ADP to ATP. This is detected by the luciferin-luciferase reaction and measured as light:

AK



This was measured using the Toxilight BioAssay Kit (Lonza Bio Science) according to the manufacturer's instructions. Briefly, 100 μl of reconstituted AK Detection Reagent (AKDR) were added manually to triplicate samples of 100 μl or 20 μl of experimental cell supernatant in a 96 well plate. After a 5-min incubation period, the amount of AK released from the cell was measured on the luminometer, using a 1 s integral reading and expressed as relative light units (RLUs). Data were expressed as mean +/- SD of triplicates.

2.8.3.4 CytoTox-One™ Homogenous Membrane Integrity Assay (LDH)

LDH released from cytolytic cells was measured using CytoTox-One™ Homogenous Membrane Integrity Assay (Promega) according to the manufacturer's instructions. The experiments were either set up in triplicate in 96 well clear bottom plates in the case of adherent cells or 12 well or 6 well clear, tissue culture plates when using suspension cell cultures. The suspension cultures were pipetted into 96 well plates after treatment.

To each well of the 96 well plate containing 100 μl of cell suspension 100 μl of CytoTox-One™ Reagent were added and incubated at room temperature for 10 min. At the end of 10 min, 50 μl of stop solution were added and the fluorescence was measured at an excitation wavelength of

590 nm. The amount of LDH release was measured using the Wallac Victor2 1640 work station and expressed as fluorescent light units (FLUs).

2.8.3.5 Cell Proliferation Reagent WST-1 assay (4-[3-(4-iodophenyl)-2-(4-nitrophenyl)-2H-5-tetrazolio]-1,3-benzene disulfonate)

The ability of viable cells to metabolise a formazan dye to induce a colour change was measured using WST-1 (Roche) according to their instructions. Cells were cultured in 100 µl volumes in clear-bottomed 96 well plates.

After the incubation period, 10µl of cell proliferation reagent WST-1 was added to each well and the cells were incubated for a further 30 min to 4 h in a humidified atmosphere.

The plate was then shaken for 30 s and read on a spectrophotometer at an absorbance of 470 nm. The cell viability was measured and expressed as the absorbance (Abs.) Data were expressed as mean +/- SD of triplicates.

2.8.3.6 Cell Proliferation assay XTT (sodium 3'-[1-phenylamino)-carbonyl]-3,4-tetrazolium]-bis(4-methoxy-6-nitro)benzene-sulfonic acid hydrate)

The ability of viable cells to metabolise a formazan dye to induce a colour change was measured using XTT, a colourimetric assay available from Roche according to their instructions. The experiments were either set up in triplicate in 96 well clear bottom plates or 12 well or 6 well clear, tissue culture plates. If in 12 or 6 well plates, the suspension cultures were then pipetted into 96 well plates.

XTT labelling reagent and electron coupling reagent were prepared by adding 0.1 mL of electron coupling reagent to a test tube containing 5mls of XTT labelling reagent and swirling to mix thoroughly.

To each well containing 100 μ L of cells 50 μ L of XTT labelling mixture was added. The plate was incubated for 4 to 24 h in a humidified 5% CO₂ (v/v) atmosphere. Readings were taken using a spectrophotometer at a wavelength between 450 to 500 nm. The cell viability was expressed as the absorbance (Abs.). Data were expressed as mean +/- SD of triplicates.

2.8.3.7 Cell Titer 96 Aqueous Non-Radioactive Cell Proliferation Assay

The ability of viable cells to metabolise a formazan dye to induce a colour change was measured using the Cell Titer 96 assay. It works by utilising the tetrazolium compound, MTS ([3-(4,5-dimethylthiazol-2-yl)-5-(3-carboxymethoxyphenyl)-2-(4-sulfophenyl)-2H-tetrazolium, inner salt; MTS) (Promega) and the electron coupling reagent phenazine methosulfate (PMS). MTS is chemically reduced by cells into formazan, which is soluble in tissue culture medium. The assay measures dehydrogenase enzymes found in metabolically active cells.

The assay was carried out according to the manufacturer's instructions. The experiments were either set up in triplicate in 96 well clear bottom plates or 12 well or 6 well clear, tissue culture plates. The suspension cultures were then pipetted into 96 well plates. If in 12 or 6 well plates, the suspension cultures were then pipetted into 96 well plates.

100 μ l of the PMS solution were added to the test tube containing 2 mL of MTS solution and swirled to completely mix the MTS and PMS solution.

To each well containing 100 μ l of cells 20 μ l of combined MTS/PMS solution were added. The plates were incubated for 1 – 4 h at 37°C in a humidified, 5% CO₂ (v/v) atmosphere. Following this, the absorbance was measured at 490 nm using an ELISA plate reader.

2.8.3.8 Inducing Necrotic Cell Death

To obtain 100% cell death by primary necrosis several methods were employed:

- Freeze-thaw fracture - the cells were frozen in a 1ml cryotube and immersed in the container containing liquid nitrogen for 5 min, followed by thawing in a water bath at 56°C. This process was repeated five to six times to ensure that all the cells are lysed. This was checked using Trypan Blue exclusion, which can rapidly assess cell viability and thus confirm whether or not 100% necrosis had occurred. (Necrotic cells are stained blue by this dye).
- Heating at 56°C (in a water bath) for an hour assessed by Trypan Blue exclusion
- Lysis with detergent – to the wells containing culture sample, 100 μ l of detergent (nucleotide releasing reagent) was added and left for at least 10 min at room temperature.

2.8.3.9 Fluorescent Microscopy Assessment

2.8.3.9.1 Acridine Orange/Ethidium bromide and fluorescence microscopy

Staining of suspension culture cells.

The cell suspension was spun at 400 x g for 5 min and the supernatant carefully removed. 100 µl of the working solution (3 µg.mL Acridine orange and 10 µg.mL Ethidium bromide) was added. Approximately 50 µl of stained cell suspension was placed onto a slide and covered with a cover slip. The edges of the cover slip were sealed with clear nail varnish and examined using a fluorescent microscope.

Staining of adherent cells.

The adherent cells were cultured on chamber slides. The culture medium was removed and replaced with just enough working solution (3 µg.mL Acridine orange and 10 µg.mL Ethidium bromide) to cover the slides. It was mounted with a cover slip and sealed round the edges with nail varnish. The slide was examined as soon as possible using a fluorescence microscope.

2.8.3.9.2 JC-1 Staining

Staining cells.

250 µl of the filtered JC-1 were added to 120 µl of the experimental cells to be analysed prior to incubating for 30 min at 37°C in a 5% (v/v) CO₂, 95% (v/v) air humidified incubator.

The percentage of red and green fluorescence was estimated by flow cytometry or by fluorescence microscopy.

2.8.4 Preparation of Chromium⁵¹ release Cytotoxicity Assay

This assay was carried out by Murrium Ahmad as part of her PhD work at the Nottingham Trent University under Home Office approval. No radioactive suite was available at Lonza Bio Science.

The project licence number was 40/2414.

2.8.4.1 Tumour Therapy Procedure

CT26 tumour cells were cultured until they reached 75-80% confluence in a T75 tissue culture flask. The cells were harvested and used to inject the mice by shaving the site of injection. Subcutaneous CT26 tumours were induced by injection of 8×10^4 cells into the shaved right hand side flank of the animal. The tumours were allowed to develop for approximately 7 days prior to the initiation of immunotherapy.

2.8.4.2 Immunotherapy with DISC/mGM-CSF

At the time of therapy (day 7-10), the tumours were approximately 0.04-0.36 cm in diameter. The animals were injected intratumourally with approximately 2.5×10^7 PFU (plaque forming units) of DISC/mGM-CSF. A second injection was administered 3 days later. The animals were monitored for tumour growth and general health twice weekly.

2.8.4.3 Chromium Release Cytotoxicity Assay

Splenocytes were harvested, washed twice in serum-free medium, counted, re-suspended in CTL media at the appropriate concentration and used as the effector cells. The target cells were harvested by trypsinisation (for adherent cells), washed and labelled with chromium-51 (Amersham, UK) for 1 hour in a 37°C water bath. The cells were washed

twice in serum-free media and centrifuged at 400 x g for 3 minutes to yield a cell pellet. The cells were re-suspended in CTL media to the appropriate concentration and used as the target population. The effector and target cells were co-cultured in a 96 well plate for 4 hours in a humidified lead container. Following the standard 4 hour Chromium release assay at 37°C, approximately 50µl of supernatant was transferred to a lumaplate (Packard, UK) and dried overnight in a drying cabinet prior to being counted on a Top-Count scintillation counter (Packard).

The percentage cytotoxicity was determined using the following formulae:

Percentage Cytotoxicity =

$$\frac{(\text{Experimental release} - \text{Spontaneous release})}{(\text{Maximum release} - \text{Spontaneous release})} \times 100\%$$

2.9 Proteomic Samples

2.9.1 Sample Preparation

The cell samples obtained from the experiments were lysed and frozen at -80°C for MALDI-MS analysis. The cells were lysed in a lysis buffer containing 9.5 M urea, 2% (w/v) DTT (dithiothreitol) and 1% (w/v) OGP (n-octyl-beta-D-gluco-pyranoside). This enabled all the required proteins to be released from the cells ready for measurement.

Prior to MALDI-MS analysis, the cells were thawed out, sonicated and put on ice. Repetitive freezing and thawing of the samples were prevented by aliquoting the samples in the required volumes for each experiment and thawing just prior to analysis on ice.

2.9.2 Protein Micro assay

A Bio-Rad protein micro assay was used to determine the protein concentration of all of the samples used in this study, aside from the serum samples. This assay proved to be the most appropriate to use as most other kits available were not compatible with the 9.5M urea present in the lysis buffer.

A BSA protein standard was made up to concentrations of 0, 2, 4, 6, 8, 10, 12, 14, 16, 18, 20 μg in water to a total volume of 800 μl . Two eppendorf tubes were set up for every sample with 795 μl of water and 5 μl of sample. 5 μl of cell lysis buffer and 795 μl of water were used as the negative control. 200 μl of undiluted Bio-Rad protein assay dye concentrate was added to each eppendorf and left to incubate for 15 min at room temperature. 100 μl of sample from each eppendorf was then aliquoted into a 96 well plate and the absorbance determined using a spectrophotometer at 595nm.

2.9.3 Control samples used in MALDI analysis

2.9.3.1 QC samples

QC samples were required on all MALDI test plates to ensure the good quality of the data. The samples used were obtained from human blood where serum was extracted, a well studied and recognised QC methodology used at the Nottingham Trent University. To obtain the serum, healthy donor blood samples were collected. After clotting at RT for 30 min, the collected blood was centrifuged at 2500 g for 15 min. The separated serum was aliquoted and stored at -80°C.

An aliquot of a QC sample was diluted in 0.1% (v/v) TFA at a ratio of 1:20 and processed along with other samples. After data acquisition by MALDI-MS, the spectra were checked visually.

The profiles of these QC controls could be checked on each run to check for any potential sample processing errors both on the MALDI-MS and the Xcise. For every 50 samples in an experiment, five QC samples were included in the run.

2.9.3.2 BSA samples

BSA samples were fundamental controls on the MALDI plate. These ensured the trypsin was in good working order for the tryptic digest and therefore peptide analysis. Five BSA samples were included for every fifty samples run. The BSA was made at a concentration of 0.1 mg.ml⁻¹ in water and stored at -80°C.

2.9.3.3 Blanks

Blanks, which consisted of 0.1% (v/v) TFA, were used to detect any contamination on the MALDI plate. As all the samples had been diluted in 0.1% TFA, analysing these blanks played a vital role in investigating the peaks obtained in the sample profiles. Ten blanks were included for every 50 samples, in each run.

Contamination can also occur due to unclean MALDI plates. The MALDI target plates are repeatedly used, and therefore the control blanks will reveal any contamination on the plate (i.e. from the previous samples).

2.9.4 Sample processing on the Xcise robotic system

An automated sample processor Xcise robotic system was utilised for sample preparation and processing prior to MALDI-TOF analysis. The cell samples from control and treated melanoma samples were diluted to 0.1 $\mu\text{g}.\text{ml}^{-1}$ in 0.1% (v/v) trifluoroacetic acid (TFA) for the Ma Mel 26a cells. A more concentrated amount was used for Ma Mel 28 and MEWO cells where the cells were diluted to 0.5 $\mu\text{g}.\text{ml}^{-1}$ in 0.1% (v/v) trifluoroacetic acid (TFA).

2.9.4.1 ZipTip Method

25 μl volumes of the samples were placed into a 96 well plate. The positions of the samples in the 96 well plates were randomly selected using a Microsoft Excel computer program. They were then processed on the Xcise robotic system and the ZipTipping procedure was carried out. The samples were bound to the ZipTip with 25 cycles of binding, followed by two washes in 0.1% TFA, where the washes were discarded. The samples were eluted off of the ZipTip in 4 μl of 80% ACN + 0.1% TFA. At the end of the Xcise run, 1 μl of eluted samples had been spotted onto

the MALDI target plate followed by 1 μ l of sinapinic (SA) matrix solution containing 12 mg of sinapinic acid (SA) in 1 ml of 50% (w/v) ACN, 50% (w/v) TFA. In the case of tryptic peptides, 1 μ l of the eluted sample contained 1 μ l of matrix solution of 12 mg α -cyano-4-hydroxycinnamic acid (CHCA) in 1 mL of 50% (w/v) ACN. The samples were randomly spotted in duplicate on the MALDI target and then analysed by MALDI-TOF MS.

2.9.4.2 Preparation of the control calibration mixtures for MALDI-MS

Calibration mixtures were used in the study to calibrate the instrument for accurate mass measurements of the proteins. Every 4 spots of samples were calibrated according to one calibration spot in the middle.

Two separate calibration mixtures were used. For proteins, protein calibration mix 2 (Laser Bio Labs, Cedex France), which contained Cytochrome C (horse heart) m/z 12361.12, Myoglobin, (horse) m/z 16181.06, Trypsinogen m/z 23981.98 and Insulin beta chain m/z 3494.65 (5 μ l of 5mM). In the analysis of tryptic peptide samples, peptide calibration mix 4 (Laser Bio Labs, Cedex France) was used. This mixture is based on monoisotopic masses and contains Bradykinin fragment 1-5 m/z 573.31, Angiotensin II m/z 1046.54, Neurotensin m/z 1672.91, ACTH clip (18-39) m/z 2465.19 and Insulin B-chain oxidized m/z 3494.65.

To spot the calibration mixtures onto the MALDI plate, equal volumes of the appropriate calibration solution was mixed with the relevant matrix (10 $\text{mg}\cdot\text{ml}^{-1}$ Sinapinic acid (SA) in 50% (w/v) Acetyl nitrate (ACN) and 50%(w/v) Trifluoroacetic acid (TFA) for protein and 10 $\text{mg}\cdot\text{ml}^{-1}$ α -cyano-4-hydroxycinnamic acid (CHCA) in 50%(w/v) ACN/50%(w/v) TFA for peptide calibration mix). Subsequently, 1 μ l of this solution was spotted

manually on the plate in the middle of every 4 sample spots. The calibration mixture was made-up fresh, spotted on the plate and dried overnight at room temperature prior to MALDI-MS analysis.

2.9.4.3 MALDI-MS set-up and analysis

The samples were analyzed using Axima CFR⁺ MALDI-TOF mass spectrometer (Shimadzu, Manchester UK) operated in linear mode for protein analysis with a mass range of 1000-20000 Da and reflectron mode for peptides analysis with a mass range of 800-3500 Da. The instrument was externally calibrated using a standard mixture of proteins or peptides in which 1 calibration spot was allocated for every 4 sample spots. Mass spectra acquisition was performed using autoquality mode for the peptides.

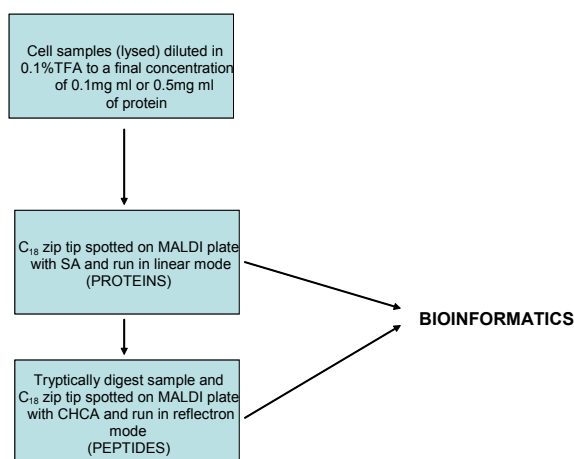


Figure 2.08: Summary workflow for cell sample processing and analysis using Xcise sample processor and MALDI-MS for mass analysis.

2.9.4.4 Identification using MALDI MS-MS

The original samples containing the ions of interest were manually zip-tipped using a C₁₈ column. The column was conditioned twice with 200 μ l of 80% ACN and 200 μ l of 0.1% TFA. The sample was then bound to the column at 1mg/ml and eluted off with increasing concentrations of ACN

diluted in 0.1% TFA. Concentrations used for elution were 5%, 10%, 20%, 30%, 35%, 40%, 43%, 45%, 48%, 50%, 60%, 70%, 80% and 90% of ACN. Each of the eluted samples were analysed by MALDI MS- MS.

2.9.5 Bioinformatics analysis

The spectra obtained from the samples were visually checked and the m/z values for the peptides from 800 to 3500 Da were used. The approved spectra were imported to a format called ASCII files and the data was smoothed and merged to reduce the dimensionality using SpecAlign software which is available online. The data was also baseline corrected to remove any background noise from the spectra. Using an in-house programme designed by Nottingham Trent University, the data was investigated using stepwise analysis. This determines minimum inputs for correct classification of data and provides ion interaction.

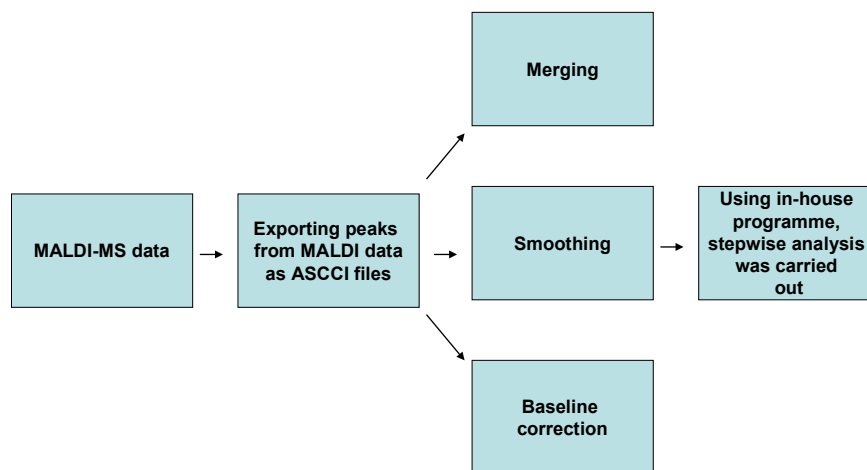


Figure 2.09: Summary workflow of Bioinformatics analysis

2.9.5.1 ANN analysis – step wise approach

The inputs into the ANNs consisted of 23001 variables specifying the intensity at given binned m/z values for every sample analysed by MALDI. The samples were split into training (60%), test (20%) and validation or blind (20%) data sets. The ANNs were trained using the training set and the network error with regards to the predictive performance was monitored with the test data set, which was unseen during training. Once this error failed to improve for a pre-determined number of training events (epochs), training was terminated and the model validated on the blind data set. A linear regression output function was used to map the output variables, where the sum-squared error function was used. The training was performed using a back-propagation (BP) algorithm until the error no longer improved for 10,000 epochs, followed by a conjugate gradient descent (CGD) algorithm for 3000 epochs at a learning rate of 0.1 and a momentum of 0.5. Once this error failed to improve for a pre-determined number of training events, training was terminated and the model validated on the blind data set. This process was repeated 50 times so that each sample was treated as truly blind a number of times, enabling confidence intervals to be calculated for the network predictions on blind data. The inputs were ranked in ascending order based on the mean squared error values for the test data and the input which was performed with the lowest error was selected for inclusion into the subsequent step. Next, each of the remaining inputs were then sequentially added to the previous best input, creating $n-1$ models each containing two inputs. Training was repeated and performance evaluated. The model which showed the best capabilities to model the data was then selected and the process repeated, creating $n-2$ models each containing three inputs. This continued until no significant improvement was gained from the addition of further inputs resulting in a final model containing the proteomic pattern which most accurately predicted between the two outcomes.

Chapter 3: A novel bioluminescent assay for necrotic cell death

3.1 Introduction

There are several assays currently employed that can potentially be used for prediction of patient responses to single agent and combination cancer therapy. Current treatment recommendations depend on carefully designed clinical studies in large patient populations and provide an individual patient with a probability for response based on clinically observed response rates. Complete remission does not mean that cancer cells are totally eradicated from the body but that their level is beyond the sensitivity of the assays used to detect them (Cree, 1998; Dawson and Whitfield, 1996; Kurth, 1997). These assays measure cell death in two different ways. There are those which are based on the detection of viable cells left in a population, the assumption being that any remaining cells have died, which may not be the case in all instances. ATP, MTS and resazurin measurements in figure 3.11 reveal detection only in viable cells, and in the early stages of apoptosis. Alternatively, there are assays which are based on the detection of enzymes 'leaked' from cells or the ability of dyes to pass into cells when the cell membrane has been compromised (necrotic). LDH release is illustrated in figure 3.01 with detection only seen when the cell is permeabilised. The latter, are true assays of cell death as once the cell membrane is permeabilised the cell cannot recover.

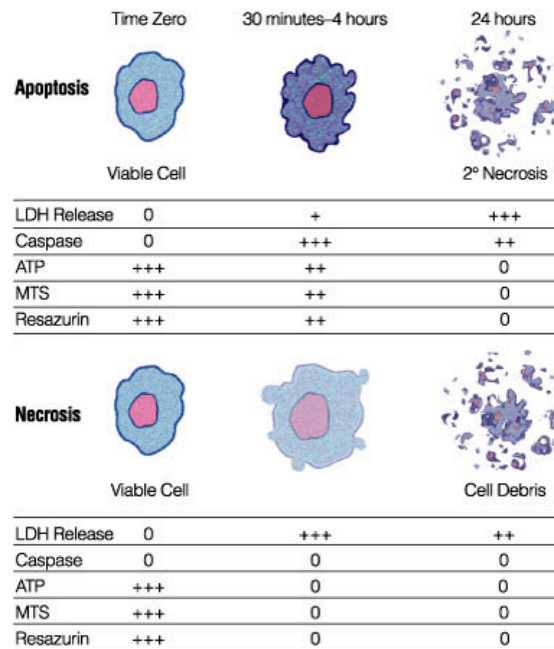


Figure 3.01: To show how the mechanisms of cell death can be determined by measuring different markers of cell viability and apoptosis in vitro.

The assays commonly used are the necrotic endpoint measurements of cell death including chromium-51 release (Bachy *et al.*, 1999); Propidium Iodide uptake by cells (Ormerod, 1998); or measurement of lactate dehydrogenase (LDH) release from cells (Korzeniewski and Callwaert, 1983; Decker and Lohmann-Mathes 1988; Sasaki *et al.*, 1992). Alternatively, the assays which are based on the detection of viable cells left in a population include the fluorometric assay known as Alamar Blue (or resazurin); the colorimetric assays, WST-1, XTT and MTS (Petty *et al.*, 1995; Marshall *et al.*, 1995) and the bioluminescent measurement of ATP (table 3.01).

There are many cytotoxicity assays but the principle techniques are listed below in table 3.01.

<i>Viability Assays</i>	<i>Necrotic Assays</i>
Alamar Blue	Chromium ⁵¹
WST-1	Propidium Iodide
XTT	LDH
MTS	
ATP	

Table 3.01: To illustrate the fundamental cytotoxicity assays.

There are several drawbacks to these assays. Chromium-51 (Cr^{51}) involves the labeling of the target cells with radioactive material which is released upon the lysis of the cell and the resultant radioactivity measured. Apart from the major disadvantages associated with the handling of radioactive elements (Bachy *et al.*, 1999), it also assumes that there has been 100% efficient loading of the target cells with the label. In addition, there is a great deal of spontaneous chromium⁵¹ release by cells, whether alive or dead, occasionally exceeding 50% over a three hour period. Thus, it is difficult to determine with precision how much chromium release is due to the drug and how much is caused by damage to tumor cells as opposed to non-tumor cells. Finally, because of the rapid spontaneous release, the duration of the assay is constrained to a period of only several hours. This means that long incubations with a cytotoxic drug is more problematic and when carrying out cell mediated cytotoxicity assays with target and effector cells large concentrations of the immune effectors is a necessity for a quick kill.

Flow cytometry is the conventional method for measuring cell death (Ormerod, 1998). Propidium Iodide (P.I), a fluorochrome that fluoresces red when it binds to DNA or double-stranded RNA, can be used to measure percentage apoptosis in fixed cells and cell viability and membrane permeability on unfixed cells. The size, granularity and fluorescent properties of a cell can be investigated by the analysis of their forward scatter (FSC-H) indicating cell size, side scatter (SSC-H) showing granularity of the cell and green (FL-1) and red fluorescent (FL-2) markers after staining with either one or two fluorometric dyes (Ormerod, 1998; Becton Dickinson, 1997).

Flow cytometry technology has been used to measure many of the processes during apoptosis and necrosis as it measures cells on a per cell basis (Ormerod, 1998). The cells of interest can be further analysed by the use of cell analysing technology using, for example the FACScaliber. Many of the proteins involved in apoptosis, such as the anti apoptotic protein Bcl-2 (Steck *et al.*, 1996), have been detected and quantified. The correlation between the expression of Bcl-2 to Bax has also been successfully investigated where peripheral blood lymphocytes from a chronic lymphocytic leukaemia patient were stained with antibodies to Bcl-2, Bax and the general B-cell marker CD19. This data showed the tumour cells to have higher expression of the anti apoptotic protein Bcl-2 (Ormerod *et al.*, 1998). In addition, lactate dehydrogenase (LDH) release is commonly used as a marker for necrotic cell death (Valentovic and Ball, 1998; Lash *et al.*, 1995). Most cells contain LDH and when these cells are lethally injured, loss of membrane integrity can be assessed by monitoring activity of LDH in the incubation medium. It is measured by an enzymatic assay that results in the conversion of resazurin into resorufin and can be measured on a fluorometer. This LDH reaction is illustrated in figure 3.02 below:

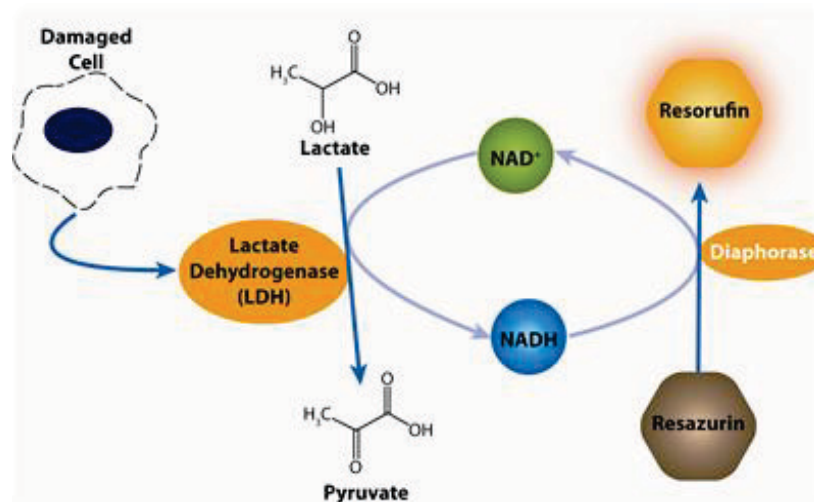


Figure 3.02: A schematic diagram to show the LDH reaction

The addition of LDH assay reagent directly to cells in culture eliminates the need to transfer an aliquot of medium to a separate plate. The simplified procedure reduces errors introduced by multiple pipetting steps and conserves the time and expense of an extra assay plate. LDH (140kD) is relatively stable in culture medium once it is released from cells with compromised membranes. However, its half-life is still only 9-10 h, making the interpretation of data over a prolonged period difficult when measuring precise quantitative measurements of cytotoxicity. In addition to measuring cell death, it is also possible to measure total cell numbers of a cell population. The procedure requires the addition of a lysis solution to rupture the cell membranes, followed by measuring the total amount of LDH present:

$$\% \text{ Cytotoxicity} = \frac{\text{Experimental LDH (OD490)} - \text{Background values (OD490)}}{\text{Maximum LDH release (OD490)} + \text{Background values (OD490)}}$$

Another disadvantage of the LDH assay is that culture media supplemented with pyruvate will slow the rate of appearance of the fluorescent signal because it slows the conversion of lactate to pyruvate by LDH. An assay containing pyruvate may require up to 30 min incubation to reach its optimal signal compared to the normal 10 min.

As illustrated in table 3.02 below, the amount of cell killing over a given period of time can be determined using dyes that are reduced or oxidised by the electron transport chain. These assays are measured by evaluating the remaining viable cells in a population after their exposure to these dyes. AlamarBlue® is a proven cell viability indicator that uses the natural reducing power of living cells to convert resazurin to the fluorescent molecule, resorufin. The active ingredient of alamarBlue® (resazurin) is a nontoxic, cell permeable compound that is blue in colour and virtually non-fluorescent. Upon entering cells, resazurin is reduced to resorufin, which produces very bright red fluorescence. Viable cells continuously convert resazurin to resorufin, thereby generating a quantitative measure of viability and cytotoxicity.

Half-reaction		Eo' (mV) pH7.0 25°C	
NAD+2H ⁺ +2e ⁻	↔	NADH+H ⁺	-320
NADP+2H ⁺ +2e ⁻	↔	NADPH+H ⁺	-320
FAD+2H ⁺ +2e ⁻	↔	FADH ₂	-220
FMN+2H ⁺ +2e ⁻	↔	FMNH ₂	-210
MTT _{OX} + 2H ⁺ + 2e ⁻	↔	MTT _{RED}	-110
cytochromes _{OX} +1e ⁻	↔	cytochromes _{RED}	+80 to +290
alamarBlue [®] _{OX} +2H+2e ⁻	↔	alamarBlue [®] _{RED}	380
O ₂ +4H ⁺ +4e ⁻	↔	2H ₂ O	820

Table 3.02: Oxidation reduction potentials in the electron transport system and alamarBlue®. The midpoint redox potential (Eo') values determined at pH 7.0, at 25°C.

The alamarBlue® indicator is ideally set up to detect oxidation by the whole of the electron transport chain. As can be seen from table 3.02, the midpoint potential of alamarBlue® is greater than that of any of the other components of the electron transport chain. alamarBlue® will be reduced by FMNH₂, FADH₂, NADH, NADPH and cytochromes, since their midpoint potentials are lower than that for alamarBlue®. Therefore, alamarBlue® is an excellent detector of reduction of all the elements of the electron transport chain (chapter 1). Given that alamarBlue® has a midpoint potential greater than the midpoint potential of the cytochromes, it can detect oxidation by all the components of the electron transport chain and it does not interfere with any of the redox reactions of the electron transport chain.

An alternative redox indicator is tetrazolium salt (MTT, MTS or WST-1). MTT has a midpoint potential of -110 mV (table 3.02), which enables MTT to be reduced by the electron donors FMNH₂, FADH₂, NADH and NADPH. However, since the midpoint potential of MTT is intermediate between that of the electron donors and cytochromes, MTT will not be reduced by cytochromes. Furthermore, if MTT is reduced by FMNH₂, FADH₂, NADH or NADPH and the electrons released by these donors will not be passed to the cytochromes as would normally happen in the electron transport chain. This shuts down the respiratory chain. These assays detect cell proliferation and cell viability in a cell population, based either on the red colour change resulting from cleavage of a tetrazolium salt by mitochondrial dehydrogenases in viable cells (Kawada *et al.*, 2002; Marshall *et al.*, 1995) or the reduction of the Alamar Blue to produce a bright fluorescent red colour. As well as the above assays for measuring viability, measurement of ATP, using the luciferase-luciferin reaction, is an established method to assess chemotoxicity in cell lines and tumours and to determine tumour growth inhibition by cytotoxic agents. ATP is essential for all cells to carry out their specific activities

including programmed cell death, as it serves as the primary donor of free energy.

Apoptosis is an energy driven process that requires ATP to carry out its specialized functions (Cree, 1998). Reports have indicated the requirement for ATP during Fas mediated apoptosis for active nuclear exchange of large molecules across the membrane (Yasuhara *et al.*, 1997) it has also been suggested that whilst programmed cell death requires ATP, it is not necessary during necrosis (Tsujiimoto *et al.*, 1997). Depletion in cellular ATP levels is therefore an accurate indicator of the viability of a cell, as all cells have an absolute requirement for ATP (Crouch *et al.*, 1993).

The acknowledgement in 1947 by McElroy that the luciferase reaction in the Firefly (*Photinus pyralis*) required ATP led to an extensive investigation into the use of bioluminescence as a measure of ATP within cells. It was not until the 1980's however that bioluminescence became more widely used within laboratories. Up until this time only crude luciferase / luciferin reagents were available to the researcher; this, combined with the poor methods of extraction of ATP and the lack of commercially available luminometers, led to extensive analytical problems (Lundin, 1993) and halted progress within this field. The development of a purified luciferase with a stable light emission in the late 1970's however led to bioluminescence becoming the most widely used method of measuring ATP due to its ease, reproducibility and sensitivity over other assays.

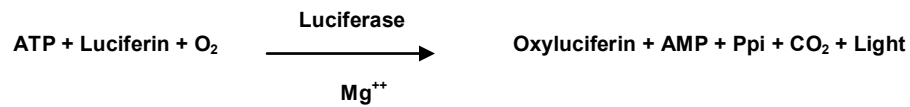


Figure 3.03: The luciferase reaction resulting in conversion of ATP to light

The basic luciferin-luciferase reaction involves the presence of ATP (released by a detergent which renders cells permeable), luciferin, luciferase and magnesium as illustrated in figure 3.03. If all the factors in the reaction mechanism are constant it can be deduced that the light emission is linearly related to the concentration of ATP present within the sample. The emitted light is then detected by a luminometer and expressed as the relative light units (RLUs).

It became apparent from the literature that all of the assays referred to above have their limitations either in the sensitivity of their detection limits, in the actual assay procedure requiring specialist knowledge and making them unsuitable for all users or indeed by the fact they required certain assumptions to be made in advance. The aim of the current research was to produce a novel assay involving the measurement of the enzyme adenylate kinase (AK) by bioluminescence. It is a ubiquitous enzyme and is integral to cellular function, being found in a diverse number of organisms. It is present in both eukaryotes and prokaryotes and has a low molecular weight of 20-25 kDa. It is most abundant in the mitochondria of tissues such as liver and muscle in which there is considerable energy turnover (Squirrell and Murphy, 1997). It catalyses the equilibrium reaction:

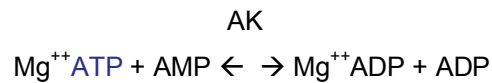


Figure 3.04: The adenylate kinase reaction resulting in conversion of ADP to ATP

Squirrell and Murphy (1995) proposed the use of the intracellular enzyme AK as a bacterial marker in place of ATP. They used ADP as the substrate to drive the reaction in the direction of ATP synthesis (figure 3.04). In addition, Squirrell and Murphy showed that AK can act as an alternative to ATP as a cell marker for bacteria providing a 10-fold increase in detection of sensitivity. A micron-sized bacterial cell contains about 10^{-21} moles of AK compared to 10^{-18} moles of ATP, so there are approximately 1,000 molecules of ATP for every molecule of AK. The small size of the AK would suggest that it may offer advantages in early detection and assay sensitivity of cytotoxicity compared to the current available assays which detect the leakage of much larger enzymes e.g. LDH (140kD). The assay sensitivity and suitability would be compared against the currently used assays.

The aim of the research in this chapter was to use AK as a cell marker with ATP bioluminescence as the end detection point for cytotoxicity. As AK was revealed to be a very promising marker in the paper by Squirrell and Murphy (1995) it was discovered that this enzyme could be used in conjunction with the luciferase assay that Lonza Bio Science had already designed for detecting ATP in cells and had good sensitivity. If this novel assay had the potential to be even more sensitive than ATP, then its potential use as a cytotoxicity assay could be enormous. Due to proprietary information the specifics of the assay work-up cannot be shown in this thesis but the experimental processes and assay performance is demonstrated with various known cell lines used by

pharmaceutical companies in drug discovery. An AK detection reagent (named 'ToxiLight®' in this thesis), would be designed so it could be added to a cell culture and allow for the detection of AK leakage from damaged cells. The ToxiLight® assay would be based on bioluminescent detection using the reaction shown in figure 3.05. The light emitted would then be detected by a luminometer or Beta Counter and expressed as relative light units (RLUs).

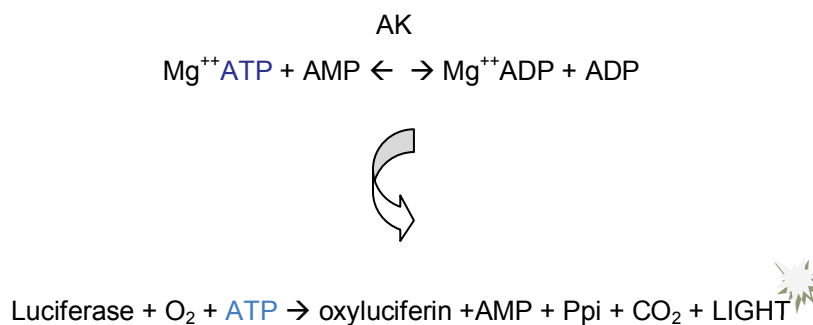


Figure 3.05: The adenylate kinase reaction resulting in conversion of ATP to light

The sensitivity of the developed ToxiLight® reagent would be investigated using enzyme standards (AK; myokinase from chicken muscle) followed by its suitability in cell-based assays. These cell models are standard cytotoxicity models used by Lonza Bio Science and the cells are those used by many drug discovery companies. The comparison of this novel bioluminescent measurement of cell death to currently used methodologies will be investigated and the sensitivity and informative value of all of these assays assessed.

Therefore the initial aims of my research would be to:

- Develop and optimise the assay.
- Miniaturize the assay for high throughput screening.
- Compare its suitability for use in cytotoxicity screening.

3.2 Results

3.2.1 Formulation and Measurement of AK

Initial experiments were carried out to determine the optimal concentrations of ADP, magnesium, luciferase and luciferin in the AK Detection Reagent using myokinase standards (as demonstrated in figure 3.06). Initial experiments did not show a good linear response and the reagent had to be optimised by altering the concentrations of both ADP and magnesium substrates. Eventually it was discovered that the ADP was causing the stability problems due to contamination of ATP within it. The ADP therefore had to be purified and then re-analysed within the reagent. In addition, the AK assay buffer had to be optimised and tested using various buffers until a stable signal was produced. This work was carried out over an 18 month period using both myokinase standards and cells. The assay was later optimised further to obtain improved signal stability by altering the AK assay buffer. The results in this chapter show the optimised reagent named ToxiLight® after formulation (which cannot be shown due to company confidentiality).

The linearity of the ToxiLight® assay was verified by performing AK standard curves using the enzyme 'myokinase', a pure AK isolated from chicken muscle from a starting concentration of $25 \mu\text{mole}^{-1}\text{ml}^{-1}$. The standards were serially diluted 1:1 in distilled water and plated into a 96 well white luminometer plate in 100 μl aliquots in at least triplicates. The plate was measured using a Berthold MPL3 Luminometer, following 5 min of incubation at room temperature. The results from the serial dilutions (figure 3.06) show a linear detection response ($R^2=0.999$). As the concentration of myokinase standard increased, the amount of AK measured by the assay also increased (shown by an increase in Relative Light Units (RLUs) detected).

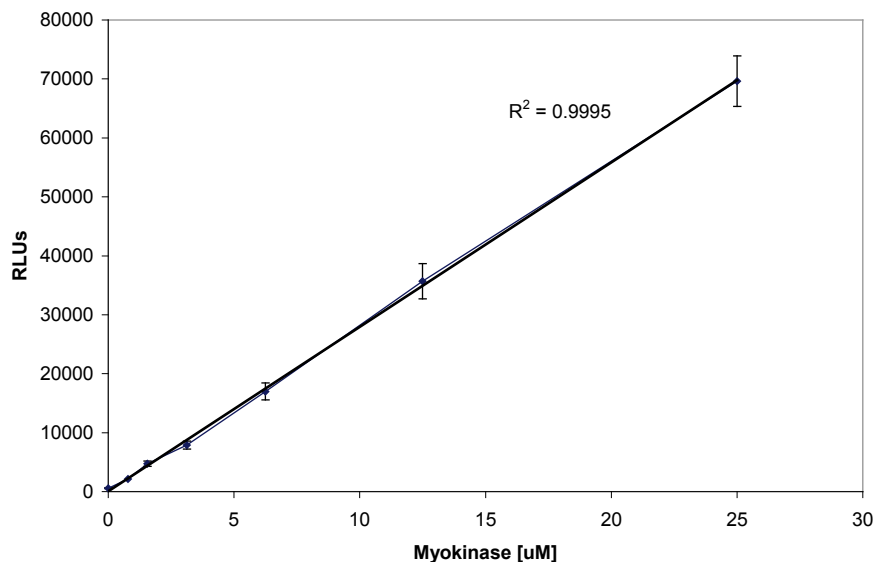


Figure 3.06: Myokinase standard (chicken muscle) was serially diluted 1:1 from 25 $\mu\text{mole}^{-1}\text{ml}^{-1}$, in dH_2O . A 100 μl volume of detection reagent was then added to a 20 μl sample of myokinase and the sensitivity observed. The resulting RLUs were measured using bioluminescence on an MPL-2 luminometer to obtain an ATP/RLU +/- the standard error of the mean (n=7).

N = number of experiments

3.2.2 Measuring AK within cells

As the ToxiLight® assay had shown excellent sensitivity with myokinase standards, the assay testing was extended to its use with cell lines and also to assess if sensitivity could be affected by different volumes of a test sample. Experiments were conducted using known cytotoxicity models routinely used by Lonza BioScience, Nottingham. The main cell lines used are revealed in table 3.03.

<i>Suspension cell lines</i>	<i>Adherent cell lines</i>
Human Histiocytic Lymphoma, U937	Human breast cancer cell line FM-3
Human acute T-Lymphoblastic leukaemic, Jurkat	Human Hepatocyte Carcinoma cells HepG2
Human Chronic Myeloid Leukaemic, K562	

Table 3.03: Cell lines tested for assay optimisation.

Cells were either dosed with the topoisomerase I inhibitor, camptothecin or with the alkylating agent mitomycin-C. Suspension cells were seeded at 5×10^5 cells.ml⁻¹ whereas adherent cells had an initial cell density of 1×10^5 cells.ml⁻¹. Various concentrations of the drugs were added to the cells (See Chapter 2 for details) and after incubation for the required period the culture medium was sampled and measured for the release of the enzyme AK. For the initial testing on cell lines, U937 cells were used and dosed with camptothecin over a 20-h incubation period. U937 cells are small and therefore contain less AK than other cells. If AK can be detected in these cells then the assay sensitivity in other cells would be very good. After incubation a 100 µl volume sample of the cell culture medium was transferred into a 96 well luminometer plate. In conjunction with this a 20 µl sample was transferred into a 384 well plate to assess potential miniaturization.

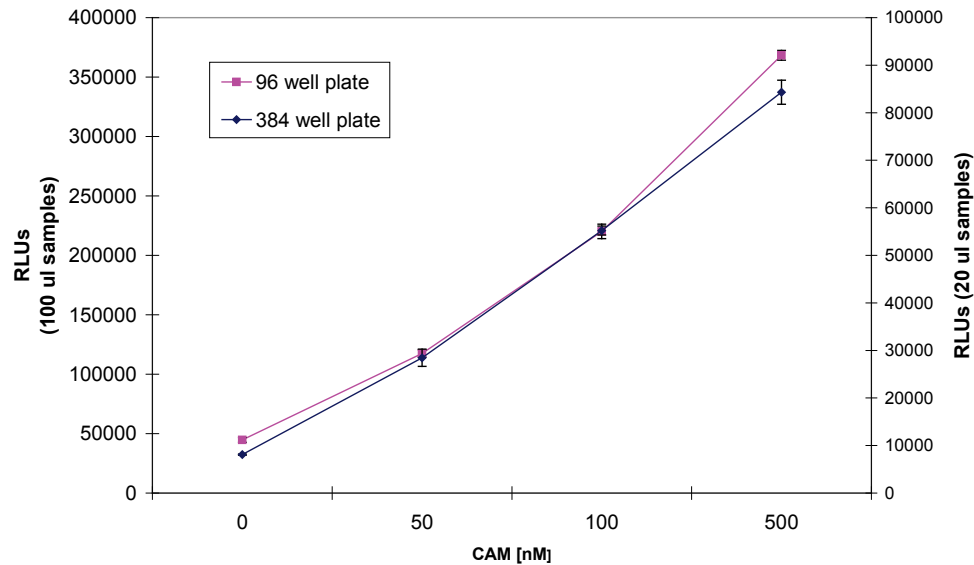


Figure 3.07: U937 cells dosed with camptothecin and incubated for 20 h. Samples of the culture supernatant containing cells were removed into fresh luminometer plates and were measured using the ToxiLight® assay on the TECAN ULTRA luminometer. The y-axis on the left represents the RLUs for the 100 µl samples whereas the y-axis on the right hand side has the 20 µl samples. ATP/RLU +/- the standard error of the mean (n=4)

Correlation between 96 and 384 well plate: $R^2 = 0.9963$
 N = number of experiments

Figure 3.07 shows a concentration dependent effect with a rise in the RLUs with increasing dosage of the drug. This means the RLUs generated denotes leakage of the enzyme AK from drug induced damaged cells showing the validity of this assay to detect necrotic cell death. In addition, these results revealed that the reaction had the potential for miniaturization. The correlation between the 96 and 384 well plate was >0.99 . The 20 µl sample volumes in the 384 wells (shown on the right hand axis) produced less light than the 100 µl culture volumes (shown on the left axis) in the 96 well plates but this was predicted. The difference seen is due to the ratio of AK present in the samples tested. There is more AK present to turn over the reaction in the 100 µl sample than the 20 µl sample; hence you see a higher level of RLUs.

3.2.3 Effect of measuring the ToxiLight® assay with / without cells present in the test sample.

The addition of the ToxiLight® assay reagent directly to cells grown in culture plates would eliminate the need to transfer an aliquot of medium to a separate plate. This simplified procedure reduces errors introduced by multiple pipetting steps and saves the time and expense of an extra assay plate. However, some cells are naturally suspended in the media and would be present in the assay wells tested as in figure 3.07. Does the presence of these cells affect the results of the assay or would the media have to be spun down to eradicate these cells? K562 cells were the chosen cell lines in this experiment due to their large size and therefore large quantities of intracellular AK. If the presence of viable cells in media did have an affect on the background levels of the assay, it would be seen in K562 cells.

To determine whether the presence of cells did have an adverse effect on any results obtained in figure 3.07, K562 cells were seeded at 5×10^5 cells.ml⁻¹ and spun down to eradicate any cells present in the media (chapter 2.6 for methodology).The results were compared to samples from another tube treated in the same manner i.e. were spun down and then the cells re suspended back into the media, to ensure that spinning down the cells had no effect, on producing a false result. Both of these tubes were sampled in 100 µl volumes in triplicate. The results in figure 3.08 show no significant difference in the RLUs when measuring the ToxiLight® assay with or without cells present in the test sample.

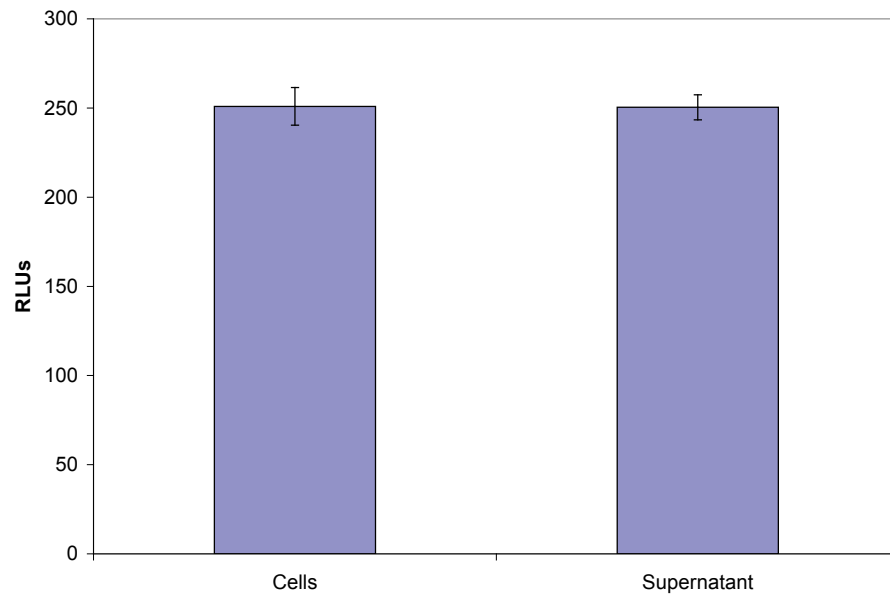


Figure 3.08: K562 cells sampled both with and without cells present in the media. 100 μ l samples were tested in triplicate using the ToxiLight[®] assay on the MPL-2 luminometer. The data is expressed as RLUs \pm the SEM (n=5).

N= number of experiments

3.2.4 Suitability of the ToxiLight® assay compared to traditional assays

There is no gold standard assay used in pharmaceutical companies for drug screening but assays that are chosen have to be suitable for high through-put (HTS) use. Pharmaceutical companies test thousands of potential drug therapies on a weekly basis and cannot therefore use assays that are time-consuming, inefficient and lack sensitivity. At the moment for cell-based HTS, the lactate dehydrogenase (LDH) assay is one of the most widely used in monitoring cytotoxicity.

3.2.4.1 Measuring LDH release from necrotic cells

Traditionally LDH, an enzyme leaked from dying cells when their cell membrane loses its integrity has been used as a measure of necrotic cell death. The enzyme can be detected by either a colorimetric or fluorescent detection mechanism requiring either a spectrophotometer or a fluorimeter. As ToxiLight® also detects an enzyme released from dying cells (AK), but by means of bioluminescence, it was considered important to assess this new methodology against the measurement of LDH release. Both adherent and suspension cell models were tested in both methods to compare and contrast the results obtained.

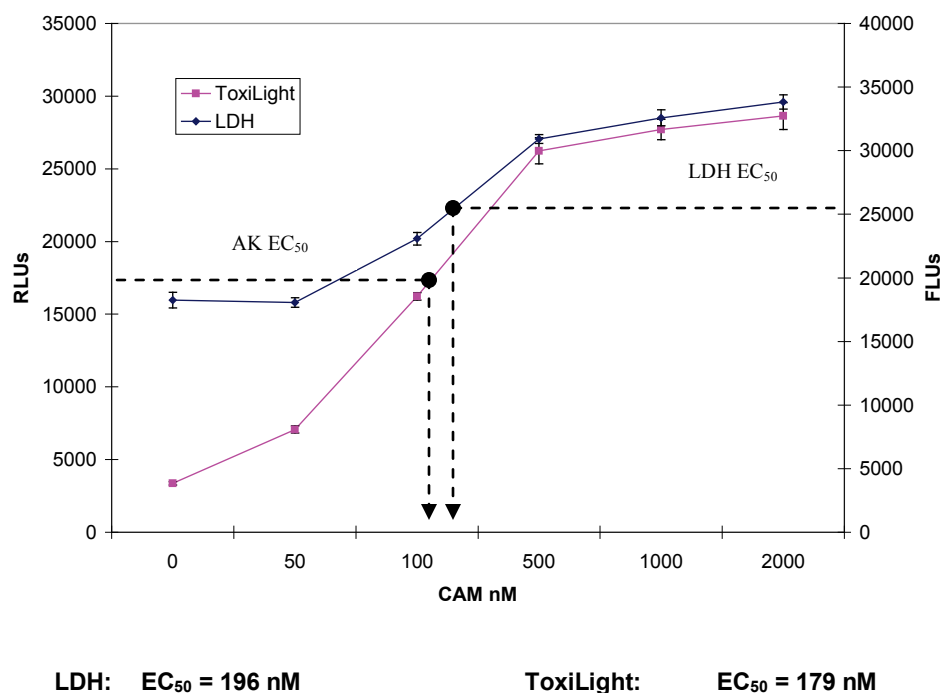


Figure 3.09: Jurkat cells in suspension were dosed for 48 h with the topoisomerase I inhibitor, camptothecin. The release of AK from the cell due to cytolysis was measured using the ToxiLight® assay on the MPL-2 luminometer. The data is expressed as RLUs +/- the SEM (n=4). It is directly compared to the LDH assay, data expressed as FLUs +/- the SEM (n=4) measured using the Victor 2 fluorometer.

N = number of experiments

Figure 3.09 illustrates four cytotoxicity experiments (n=4) using Jurkat cells dosed with camptothecin. Jurkat cells were chosen due to their small size like U937 cells. They are small cells in comparison to many used and are known to be problematic with the LDH assay. This model would reveal whether or not the assays could detect small releases of cellular enzyme after drug treatment and was deemed as a good test for the ToxiLight® assay. The results in figure 3.09 revealed that the signal to noise ratio was better in the ToxiLight® assay with a background of 3000 RLUs and the sensitivity levels showed detection of AK release down to the lowest 50 nM drug dosage. This was a promising result when compared to the LDH assay which had a background level of 160,000 FLUs and did not appear to indicate any cytolysis in the cells at 50 nM.

This improved sensitivity of the ToxiLight® assay would prove to play an important role in measuring the EC₅₀ of the drug. As can be seen in figure 3.09, the EC₅₀ of camptothecin was shown to be only 179 nM with the ToxiLight® assay but 196 nM when measuring LDH release due to the lack of detecting cell death in small numbers of cells within the population. The EC₅₀ is defined as the concentration of cytotoxic agent that provokes a response halfway between the baseline (bottom) and maximum response (top). The EC₅₀ in the LDH assay was therefore misleading and inaccurate. Further experiments were carried out on adherent cells to back up this data and to ensure the ToxiLight® assay was still as sensitive with these cells. Hep G2 cells were chosen due to their frequent use in biotechnology and pharmaceutical companies. As revealed by figures 3.09 and 3.10, the results shown were reproducible.

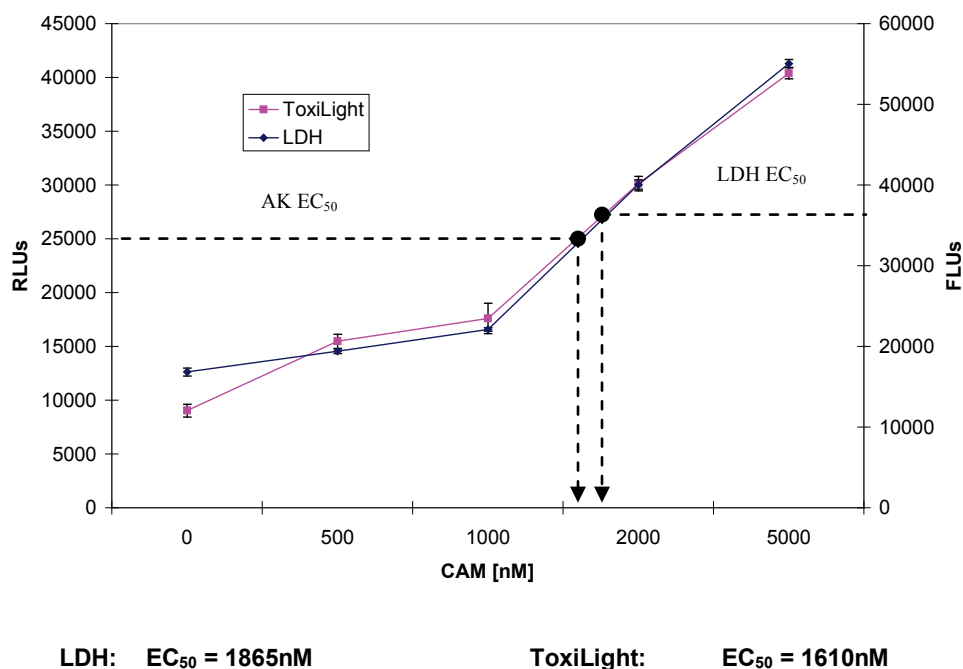


Figure 3.10: HepG2 cells were dosed for 48 h with the topoisomerase I inhibitor, camptothecin. The release of AK from the cell due to cytolysis was measured using the ToxiLight® assay on the MPL-2 luminometer. The data is expressed as RLUs +/- the SEM (n=4). It is directly compared to the LDH assay, data expressed as FLUs +/- the SEM (n=4) measured using the Victor 2 fluorometer. Correlation between ToxiLight® and LDH: R² = 0.99

N = number of experiments

Figure 3.10 illustrates the results obtained with adherent Hep G2 cells dosed with camptothecin over a 48 h period assessed using ToxiLight® and the LDH assays. Results validate the correlation between the two assays which was shown to be 0.99. Yet again, the signal to noise ratio was better in the ToxiLight® assay with consistently lower background levels in each experiment (7,000 RLUs) compared to 18,000 FLUs). In addition, the ToxiLight® assay revealed a larger dynamic range between concentrations of drug. This was illustrated by the ToxiLight® RLUs which increased 5 times above the control, whereas the FLUs from the LDH assay were less than 3 times greater than the background levels. Additionally, as can be noted in figure 3.09, the EC₅₀ of camptothecin was shown to be lower with the ToxiLight® assay than the LDH assay. It can also be observed from this data that the EC₅₀ varied significantly between the suspension and adherent cell model. The adherent cells showed an immense increase in the EC₅₀ of camptothecin when compared to suspension cells showing how the same drug can have different effects depending on the cells being tested.

The sensitivity of the ToxiLight® assay was investigated further to determine how many necrotic cells could be detected. Human histiocytic lymphoma U937 cells were lysed by freeze-thaw fracture, and cell viability determined with trypan blue. After showing 100% necrosis, the cells were diluted down from 10,000 cells to only 5 cells with a media background. The samples were assessed using both ToxiLight® and the CytoTox One™ Assay.

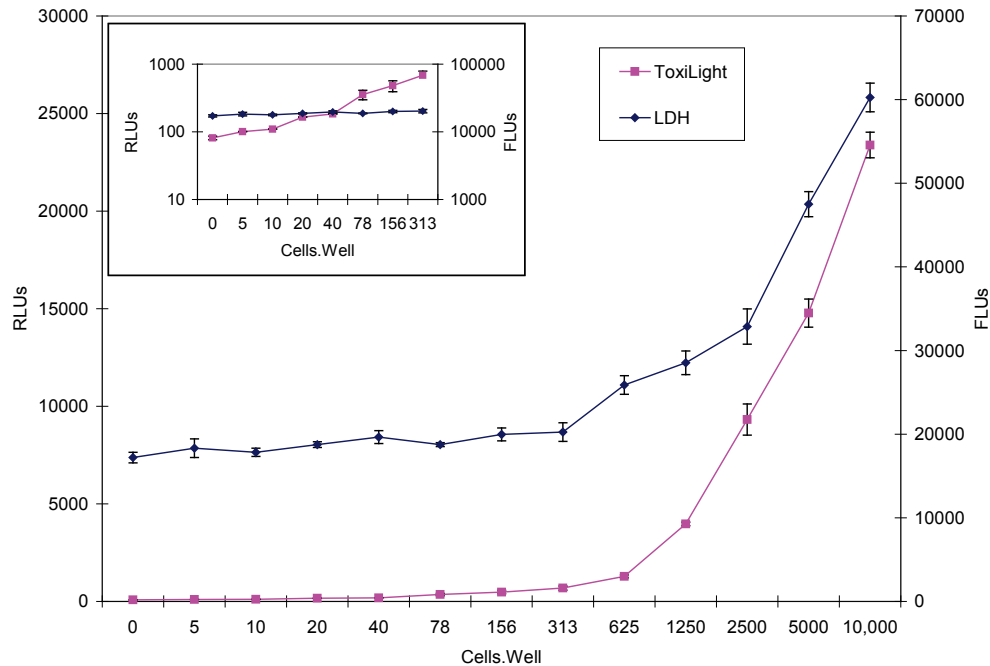


Figure 3.11: U937 cells were lysed by freeze-thaw fracture. The cells were then serially diluted 1:2 and then analysed by both the LDH and ToxiLight® assays. The release of AK from the cell due to cytolysis was measured using the ToxiLight® assay on the Wallac Betajet luminometer. The data is expressed as RLUs +/- the SEM (n=4). It is directly compared to the LDH assay, data expressed as FLUs +/- the SEM (n=4) measured using the Victor 2 fluorometer.

N = number of experiments

Figure 3.11, illustrates the how the LDH assay could no longer detect any significant differences above background below 313 cells per well i.e. from 313 cells per well down to 5 cells per well the fluorescent reading remains constant. The ToxiLight® assay showed significant differences between each cell number down to 5 necrotic cells per well above the background level. The reported detection limit of LDH routinely is 500 cells per well (Promega, 2004) but at best, detection was observed down to 50 cells per well in this research. The sensitivity of the ToxiLight® assay routinely observed was 10 cells per well; this would indicate that on average it is 50 times more sensitive than measuring LDH release.

3.2.4.2 Enzyme Stability

As LDH and AK are released into cell culture media it was important to assess the stability of the released enzymes. The reported half life of LDH is approximately 9 h in culture (Promega, 2004). This would indicate that any LDH released from dead cells more than 9 h before the assay point will have been degraded to some extent. To assess the stability of released AK and LDH, the adherent HepG2 cells were dosed with camptothecin and monitored for the release of the enzymes over a period of 4 days.

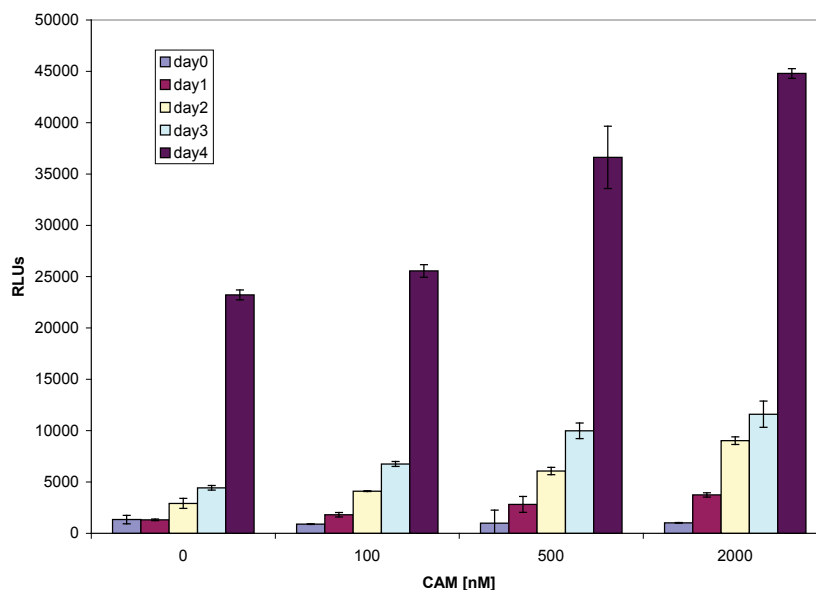


Figure 3.12: Hep G2 cells were dosed with the topoisomerase I inhibitor, camptothecin. The release of AK from the cell due to cytolysis was measured over 4 days using the ToxiLight® assay on the MPL-2 luminometer (n=1). The data is expressed as RLUs +/- the SD.

N = number of experiments

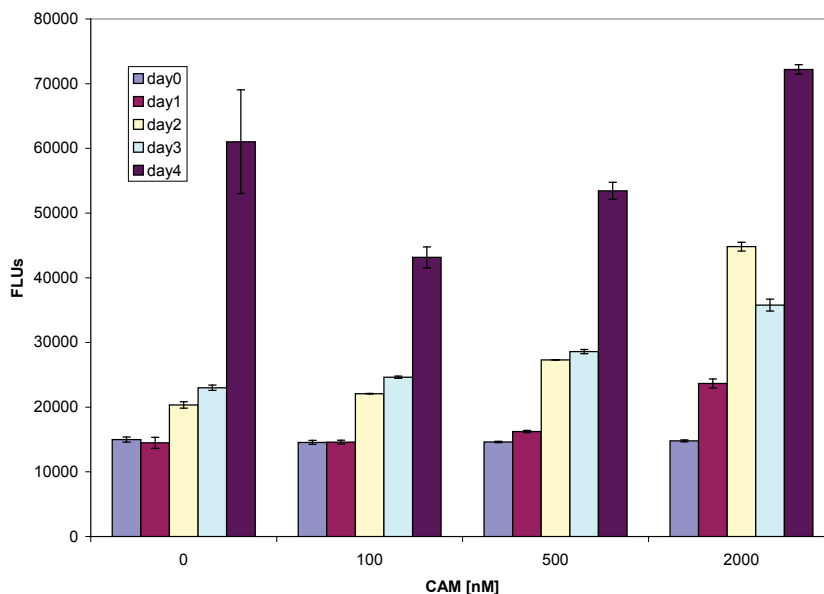


Figure 3.13: Hep G2 cells were dosed with the topoisomerase I inhibitor, camptothecin. The release of LDH from the cell due to cytolysis was measured over 4 days using the CytoTox One™ assay on the Victor 2 fluorometer, data expressed as FLUs +/- the SD (n=1).

N = number of experiments

Figure 3.12, shows AK release over 4 days. 100 µl volumes were sampled in triplicate to assess the enzyme stability. As observed from the results, a good concentration dependent effect can be seen with an increase in AK release as the dose of camptothecin becomes more concentrated. Over the 4 day period the AK continued to increase insinuating that no AK had been degraded in the culture media which was still being measured effectively. These results proved AK to be very stable in culture with no drop in concentration observed at any of the data points. This was promising for experiments where prolonged exposure to drugs would be required. In comparison figure 3.13 represents the release of LDH. As seen with the ToxiLight® assay there was a good concentration dependent increase in FLUs as the drug concentration increased within each experiment on days 1 to 3. As in previous

experiments the 100 nM drug concentration did not detect any cell death above background on day 1 unlike the ToxiLight® assay. By day 2 and 3, there was a significant difference between all concentrations of drug both within each experiment and over the 2 days. However, a drop in FLUs was noted by day 3 in the higher concentration of drug (2000 nM) when compared back to the previous day. This could be due to degradation. By day 4, the results become non-interpretable with a fluctuation in FLUs in all concentrations when compared to the control cells. These control cells were also shown to have become necrotic by day 4 due to a lack of space and nutrients to grow. This meant the experiment could not be monitored for more than 4 days.

3.2.4.3 Measuring Propidium Iodide uptake by necrotic cells

As Propidium Iodide or P.I. uptake is a recognised method for observing the state of cells the efficiency of the ToxiLight® assay could only be verified by comparison with this methodology. Visualization of the cells can be carried out by P.I. on a FACScan machine, thereby obtaining percentages of viable and necrotic cells. Jurkat cells were lysed through freeze-thaw fracture, checked by trypan blue uptake for necrosis and mixed with a healthy population of Jurkat cells to make 100%, 90%, 80%, 60%, 50%, 30%, 10% and 0% necrotic mixtures. These cells were then sampled in both 100 µl and 20 µl volumes for the ToxiLight® assay and P.I. uptake was measured in correlation on a FACScan machine.

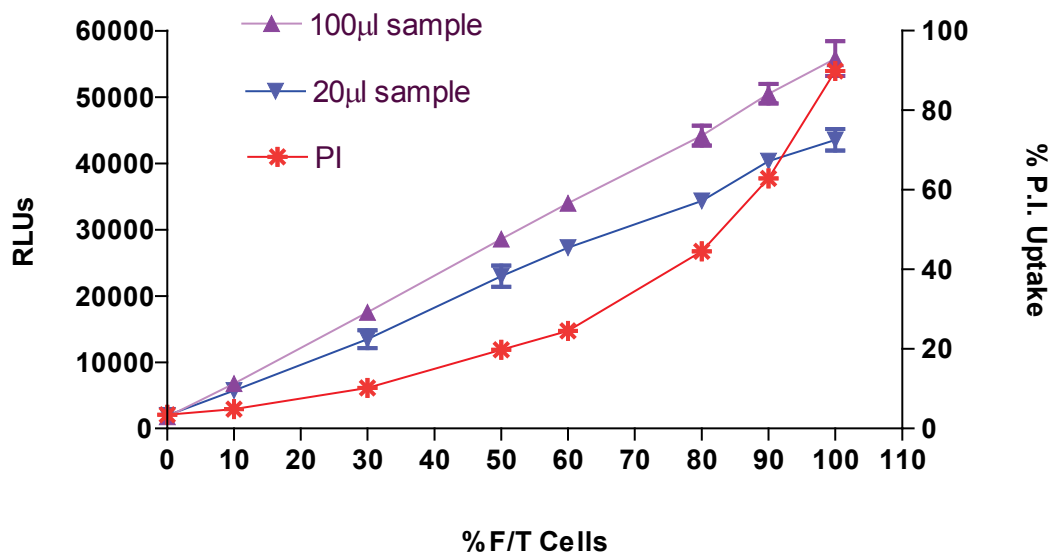


Figure 3.14: Jurkat cells were lysed by freeze-thaw fracture and mixed with various percentages of healthy cells. The release of AK due to cytolysis from 100 µl and 20 µl sample volumes were taken and measured using the ToxiLight® assay on the MPL-2 luminometer. The data is expressed as RLU's +/- the SEM (n=4). It is directly compared to the Propidium Iodide assay where % P.I. uptake was obtained from the FACScan machine.

Correlation between 100 µl sample (ToxiLight®) and P.I. Staining: $R^2 = 0.92$
 Correlation between 20 µl sample (ToxiLight®) and P.I. Staining: $R^2 = 0.92$

As can be seen in figure 3.14, the uptake of P.I. by FACScan analysis showed a close correlation with ToxiLight® ($R^2 = 0.92$). 20 µl and 100 µl volumes of culture medium were sampled for the ToxiLight® showing identical changes in RLU's as the AK levels increased and the percentage of freeze-thaw cells increased. The RLU's were slightly lower when measuring the 20 µl sample as expected due to less AK being presented to the assay in the well.

3.2.4.4 Measuring Chromium-51 release from necrotic cells

Historically the “gold standard” for cell mediated cytotoxicity studies has been the chromium⁵¹ release assay. It was thought it may be possible to utilise the ToxiLight® assay for cell-mediated cytotoxicity assays. As there were no radioactive laboratories available at ;Lonza Bio Science, the assay was carried out in conjunction with a PhD student Murriam Ahmad at Nottingham Trent University. The project was looking at immune-mediated cytotoxicity and resulted in incorporating the experiments in monitoring Toxilight® assay. Target cells are prelabelled with Cr⁵¹ which is released for detection when the cells are induced to lyse by effector cells. In collaboration with Nottingham Trent University, splenocytes were harvested from a mouse immunized against CT26, washed twice in serum-free medium, counted and resuspended in CTL medium and used as effector cells. Target cells used were the CT26+SPS (relevant peptide for kill) and CT26 TPH (irrelevant peptide for kill). SPS is a known murine leukaemic virus gp70-derived H2-L^d restricted peptide AH-1 (SPSYVYHQF). It is an immunodominant peptide for CT26 cells. TPH or TPHPARIGL is a control β-galactosidase H2-L^d peptide. (The chromium experiment was prepared in collaboration with Dr Murriam Ahmad, Nottingham Trent University).

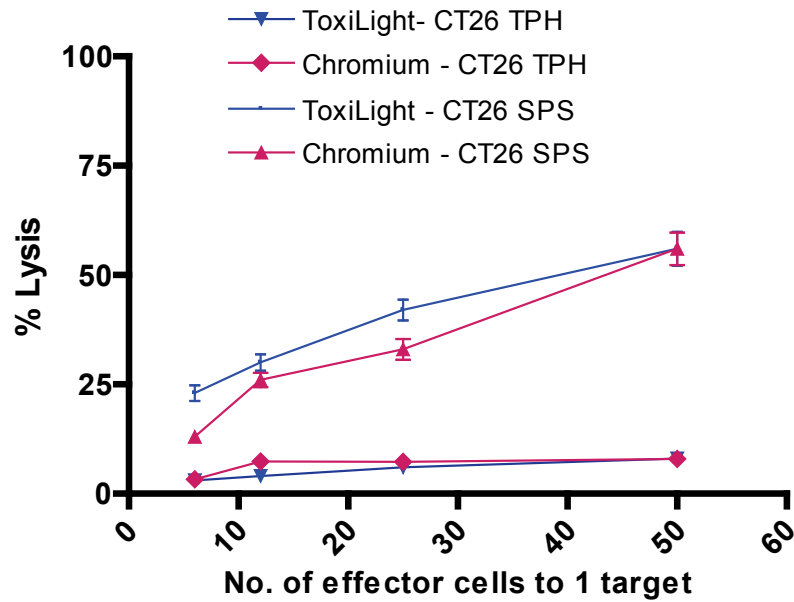


Figure 3.15: The CT26 SPS pulsed CTLs were used as the effector cells in the assay. The targets were the CT26+ SPS (relevant peptide). The release of AK from the cell due to cytolysis was measured using the ToxiLight® assay on the MPL-2 luminometer. The data is expressed as percentage of cells lysed +/- the SEM. It is directly compared to the chromium release assay, data expressed as percentage lysed cells +/- the SEM and measured on a beta counter (n=3).

N = number of experiments

Correlation between ToxiLight® and chromium (SPS); $R^2 = 0.98$

Figure 3.15 compares the ToxiLight® assay with the well-established chromium⁵¹ assay. The results are plotted as percentage release of either chromium or AK into the culture. As seen in the figure 3.15, it was revealed that the ToxiLight® data correlated with the chromium very reliably with R^2 values > 0.98 with the CT26 SPS. The TPH results also correlated showing little increase in RLU and absorbance readings (Chromium) with the irrelevant peptide and thus meant no cell death occurred.

3.2.4.5 Measuring Cell Viability

Other well-known assays were tested to determine their sensitivity compared to the ToxiLight® assay. These included the MTS, WST-1, XTT and the alamarBlue® colorimetric assays. As these assays measure viability rather than cell death the ToxiLight® assay cannot be compared directly. All of these assays were tested for their sensitivity to observe how many viable cells could actually be measured. Jurkat cells were diluted 1:2 in complete media from 1×10^6 cells.ml⁻¹ down to background levels.

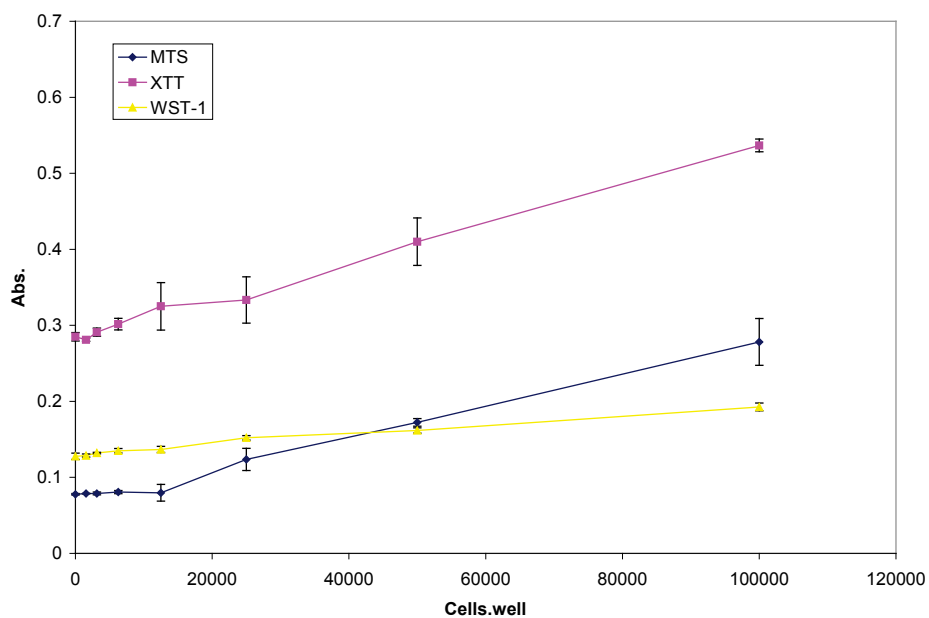


Figure 3.16: Jurkat cells were diluted 1:2 in complete media from 1×10^6 cells.ml⁻¹. The absorbance assays WST-1, XTT and MTS were measured on an ELISA plate reader at 450nm wavelength to obtain absorbance values +/- the SEM where n=5.

N = number of experiments

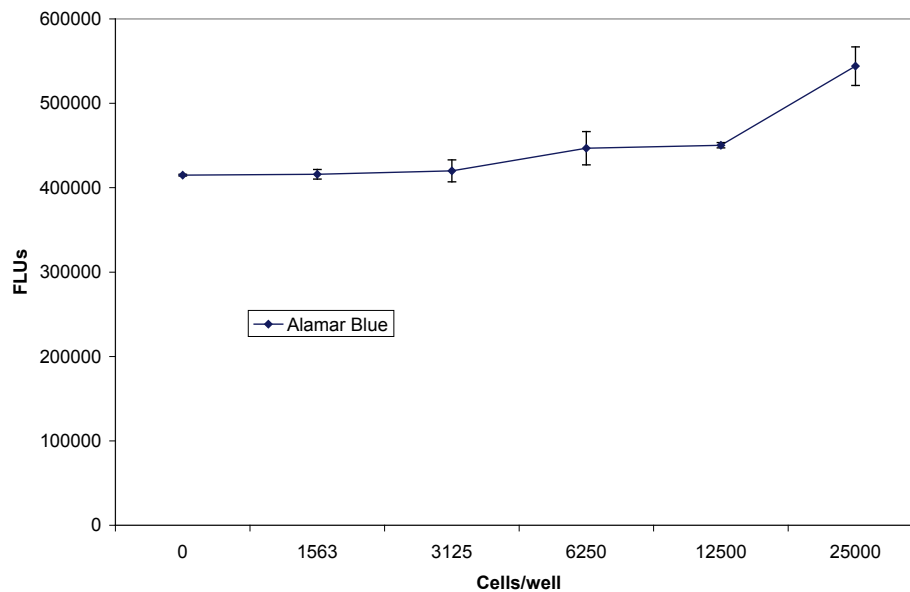


Figure 3.17: Jurkat cells were diluted 1:2 in complete media from 1×10^6 cells.mL⁻¹. The above figure represents only the lower values from 25,000 cells.mL⁻¹ to background levels. The alamarBlue® assay was carried out and measured using the Victor 2 fluorometer. The data is expressed as FLUs +/- the SEM (n=3).

N = number of experiments

The results in figure 3.16 revealed a lack of sensitivity for all of these 3 assays. The MTS and WST-1 assays could not detect below 10,000 cells per well when compared against background levels. The XTT assay was slightly better but still only had sensitivity down to 5,000 cells per well. After this point, the assay was only reading background levels. These three methods would not therefore be suitable indicators of cytotoxicity, as many viable cancer cells would be left undetected. Figure 3.17 shows the results from the alamarBlue® assay which proved to be much better than the colorimetric assays. Although still not sensitive enough, detection was much improved, measuring down to 3000 cells per well.

As the alamarBlue® assay proved to be the best of these viability assays, it was tested in a mixed cell population with a mixture of both necrotic and viable cells. Jurkat cells (at 10,000 cells/well) were lysed through freeze-thaw fracture, checked by trypan blue uptake for necrosis and mixed with a healthy population of Jurkat cells to make 100%, 90%, 80%, 60%, 50%, 30%, 10% and 0% necrotic mixtures. The alamarBlue® assay was monitored for its detection of viable cells and the ToxiLight® assay tested in comparison for detecting cell death.

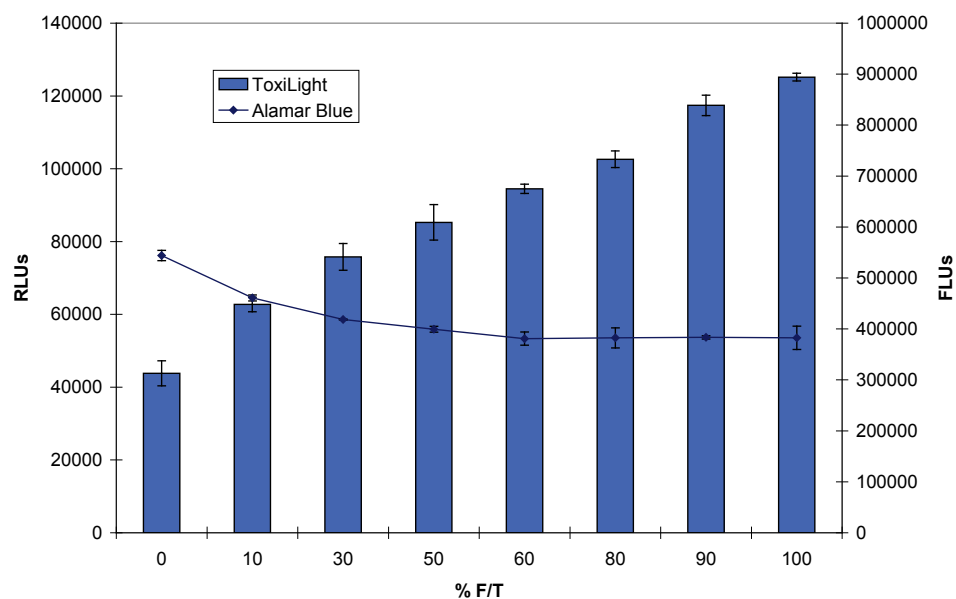


Figure 3.18: Jurkat cells were lysed by freeze-thaw fracture and mixed with various percentages of healthy cells. The release of AK due to cytolysis from different sample volumes were taken and measured using the ToxiLight® assay on the MPL-2 luminometer. The data is expressed as RLUs +/- the SEM (n=4). It is directly compared to the alamarBlue® assay where viable cells were measured using the Victor 2 fluorometer. The data is expressed as FLUs +/- the SEM (n=4).

N = number of experiments

As the results in figure 3.18 reveal, the alamarBlue® assay proved to detect 40% of the viable cells (or 60% F/T on the graph) in the mixed cell population. As the number of viable cells had decreased considerably by this point this assay could no longer detect anymore in the 80 and 90% F/T population. The assay therefore proved it could detect cell death but

only down to a limited number of cells, which would result in these viable cells being left undetected.

3.2.4.6 Measuring ATP as a Viability Cell Marker

In this study, the ViaLight® Plus kit was used by adding a Nucleotide Releasing Reagent (NRR). NRR contains a non ionic detergent that permeabilises the cell membrane and allows for the release of the nucleotides within the cells. The cells used in this investigation were a human leukaemic cell line K562 (in suspension) diluted 1:2 from a seeding density of 5×10^3 cells.ml⁻¹ in complete media (CM). The amount of ATP was then measured using the ViaLight® Plus kit in the following luciferin: luciferase reaction:

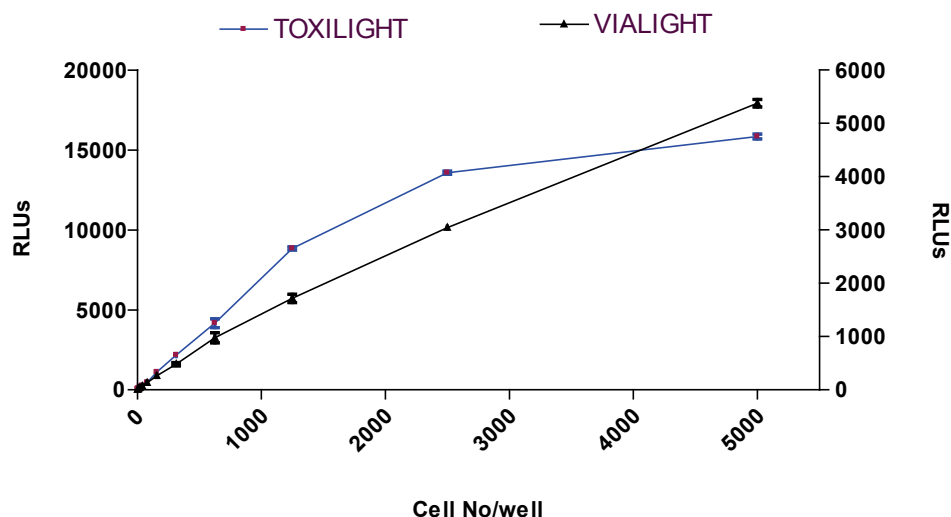
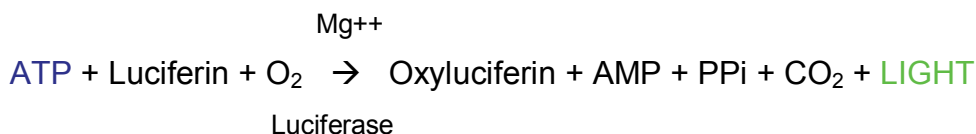


Figure 3.19: K562 cells were lysed with detergent and serially diluted 1:2 in complete medium. The release of AK from the cell due to cytolysis was measured using the ToxiLight® assay on the Wallac Betajet luminometer. The data is expressed as RLU +/- the SEM (n=3). It is directly compared to the ViaLight® Plus assay on the Wallac Betajet luminometer, data expressed as RLU +/- the SEM (n=3).

N = number of experiments

Correlation between ViaLight® and ToxiLight®: $R^2 = 0.96$

Results from the ViaLight® Plus assay, showed an excellent correlation with the ToxiLight® assay >0.96 (figure 3.19). K562 cells were diluted down from 5,000 to 5 cells per well. The ViaLight® assay showed sensitivity down to 10 cells per well (60 RLUs above background). The ToxiLight® assay detected 5 cells per well (120 RLUs above background levels). These results proved the ViaLight® Plus assay to be the best viable assay with the extreme sensitivity required for chemotoxicity studies.

After carrying out experiments comparing the ToxiLight® assay with available assays on the market, the results were encouraging. The ToxiLight® assay was able to directly compete with all other assays and had the ability to be more sensitive than any assay currently used; the only method giving comparable results was the ViaLight® Plus assay. In addition to measuring cell death, the reagents needed optimising to measure total cell numbers of a cell population. This would require the production of a lysis reagent that would be compatible with the ToxiLight® assay, measuring the total amount of AK present.

3.2.5 Optimisation of ToxiLight® assay

To complete the optimisation of the ToxiLight® assay it was necessary to obtain a control (100%) lysis solution that all values could be referenced to in order to express them as percentage cytolysis. The formulation of this reagent is proprietary information and therefore not shown in the chapter. The effect of the newly designed lysis buffer was tested on cells and compared to a control population of cells that had been lysed by freeze thaw. The human chronic myeloid leukaemic K562 cells were lysed and checked by trypan blue uptake for viability. A volume correction reagent was added to the freeze-thaw samples to ensure the volumes were the same in both test wells.

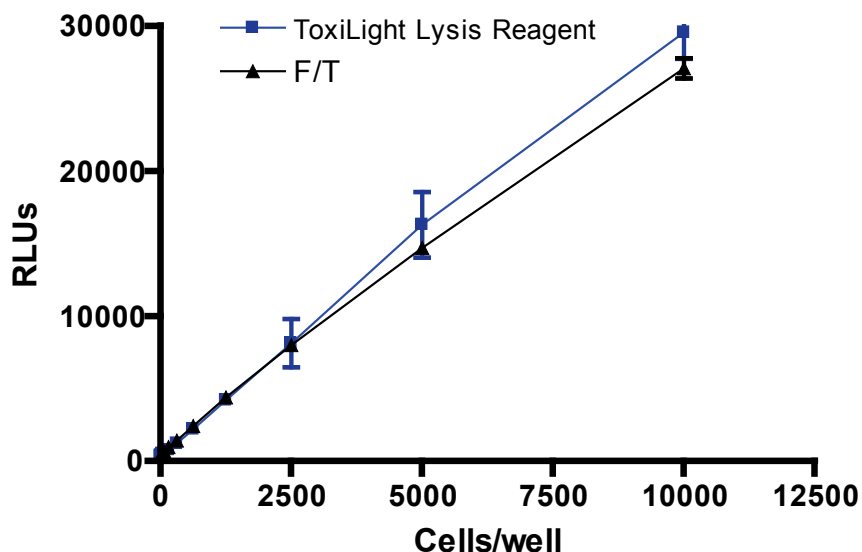


Figure 3.20: K562 cells were lysed through ‘freeze-thaw fracture’ (F/T) or ‘ToxiLight® Lysis Reagent.’ The release of AK from the cell due to cytolysis was measured using the ToxiLight® assay on the MPL-2 luminometer. The data is expressed as RLUs +/- the SEM (n=7).

N = number of experiments

Correlation between F/T and 100% lysis control (ToxiLight®): $R^2 = 0.99$

As figure 3.20 demonstrated, the ToxiLight® Lysis Reagent was able to successfully lyse the cells. In addition to this, it proved to match the results seen in the freeze-thaw cell population representing in 100% lysis of the cells. The correlation was shown to be > 0.99 . The lysis reagent was tested on all in-house cell lines at Lonza Bio Science using both adherent and suspension cells and trialed at a separate site prior to launch. No cell line has yet to be found to be incompatible. The testing of all cell lines used in this project, the results all showed >0.99 correlation with the freeze-thaw control. To illustrate its use, the lysis reagent was to be tested in a cell model whereby U937 cells were dosed with camptothecin. Prior to measurement, a control well was lysed with the ToxiLight® Lysis Reagent and to back-up the data, a second control sample was freeze-thawed.

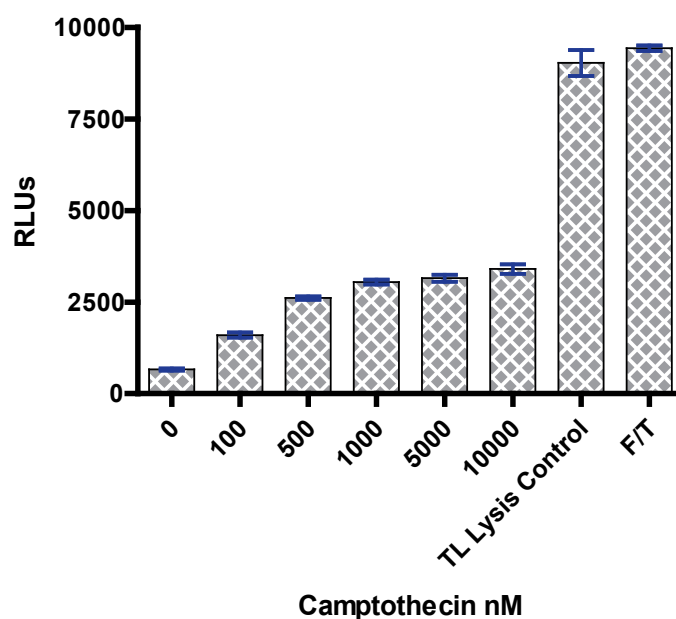


Figure 3.21: U937 cells dosed for 24 h with the topoisomerase I inhibitor, camptothecin. The release of AK from the cell due to cytolysis was measured using the ToxiLight® assay on the MPL-2 luminometer. The data is expressed as RLU \pm the SEM (n=4). The ToxiLight® lysis control is compared to F/T cells which were measured at the same time point.

N = number of experiments

Figure 3.21 demonstrated how well the ToxiLight® Lysis Reagent worked and therefore could be used as a 100% control for measuring total populations of cells. The results were nearly identical to the freeze-thaw control. This meant that a drug can be tested on a cell population and its effectiveness can be recorded as ‘percentage kill’ of the cells.

The ToxiLight® Lysis Reagent was finally compared to the LDH assay which also utilised a 100% control data point for total LDH release. A U937 and camptothecin model was incubated for 24 h before measuring using both the LDH and the ToxiLight® assay, including the appropriate lysis controls.

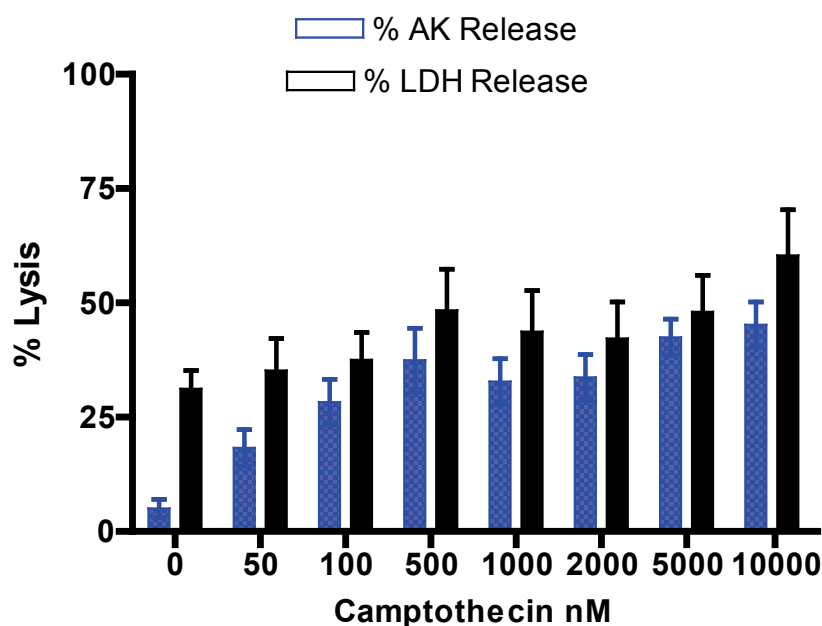


Figure 3.22: U937 were dosed for 24 h with the topoisomerase I inhibitor, camptothecin. The release of LDH from the cell due to cytolysis was measured using the LDH assay on the Victor 2 fluorometer, data expressed as percentage lysed cells. It is directly compared to the ToxiLight® assay on the MPL-2, data expressed as percentage lysed cells (n=3).

N = number of experiments

Correlation between ToxiLight® and LDH: $R^2 = 0.9$

The ToxiLight® assay proved to be a good competitor for the LDH assay in measuring the percentage of cell death. The results correlated exceptionally well with an R^2 value of 0.9. Figure 3.22 also showed the ToxiLight® assay to have a greater dynamic range than the LDH assay. This was seen in the percentage lysis which increased from 6% (control population) up to 48% necrosis with 10,000 nM camptothecin in the ToxiLight® assay. The LDH assay showed 28% necrosis in the control to 60% necrosis at 10,000 nM. The control was high in the LDH assay making the results questionable. Both trypan blue and propidium iodide staining showed the control cells to be no more than 12% necrotic.

3.2.6 Response of ToxiLight® and ViaLight® Plus Assay to Cytostatic cells

As the ToxiLight® assay measures only necrotic cells; it was decided to establish a model that would result in growth arrest from previous work carried out at Lonza Bio Science. Melanoma cells were seeded at 1×10^5 cells.ml⁻¹ and dosed with the alkylating agent dacarbazine. As the ViaLight® Plus proved to be the most sensitive viable assay tested, this was to be used in conjunction with the ToxiLight® assay.

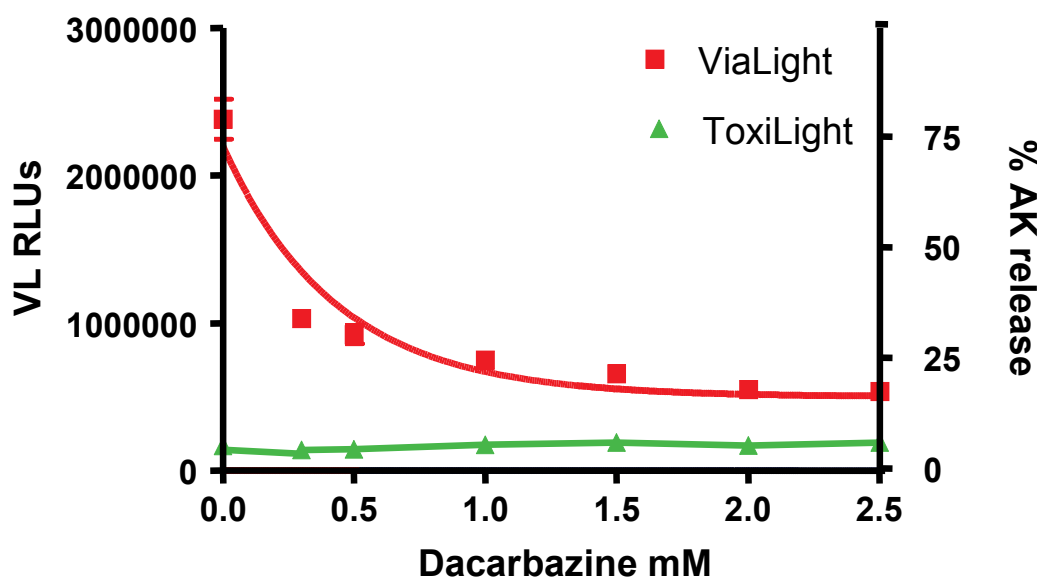


Figure 3.23: Ma Mel 28 cells were dosed for 72 h with the alkylating agent dacarbazine. The release of AK from the cell due to cytolysis was measured using the ToxiLight® assay on the MPL-2 luminometer, data expressed as RLU \pm the SEM (n=4). It is directly compared to the ViaLight® Plus assay on the MPL-2 luminometer, data expressed as RLU \pm the SEM (n=4).

N = number of experiments

The results in figure 3.23 show the ViaLight® Plus assay to measure a reduction in ATP levels with increased dacarbazine concentrations. This could imply that the cells are undergoing cell death. However, the ToxiLight® results revealed that no cell death was occurring. The ToxiLight® assay results alone would suggest that the drug was having no effect on the cells at all. The ViaLight® Plus assay results however revealed the opposite i.e. the drug ‘was’ having an affect on the cells and cell death was occurring. If the cells were not dying but then it became difficult to determine what a drop in ATP actually meant. After measuring these cells by a FACScan to assess the cells growth cycle, it was revealed that the cells were in fact in growth arrest.

In conclusion, through the above work performed on these melanoma cells, it became clear that one assay alone was insufficient to divulge the effect any drug has on a cell population. The use of only one assay can be misleading; and ideally both a viable and necrotic assay should be used.

*Compared to untreated control	Unresponsive	Proliferative	Cytostatic	Cytotoxic
ViaLight	→ RLU remain constant	↑ RLU Increase	↓ RLU Decrease	↓ RLU Decrease
ToxiLight	→ RLU remain constant	→ RLU remain constant	→ RLU remain constant	↑ RLU Increase

Table 3.04: Summary of the results drawn from the study.

Table 3.04 summarises the use of the ToxiLight® and ViaLight® assays, and represents the best necrotic and viable assays established by this research. The table highlights the responsiveness of these assays when exposed to defined conditions and demonstrates the ideology of how two assays would work better in combination than one assay alone.

3.3 Discussion

The work included in this chapter has examined the potential of using a novel bioluminescent assay with view to solving the lack of sensitivity in detecting low cell numbers associated with cytotoxicity assays.

3.3.1 Optimisation of ToxiLight® assay

The main focus of this study was to develop a novel assay based on AK release that could improve on the current assays already used. The ToxiLight® assay developed was shown to efficiently detect the release of AK both in a cell free system by myokinase standards (AK, chicken muscle) and from cell lines. All cell lines and cytotoxic agents used by Lonza BioScience, Nottingham UK were analysed successfully with the ToxiLight® assay and subsequently backed up by either P.I. uptake or the CytoTox One™ (LDH) assay. The assay demonstrated how it can be easily miniaturized down to 384 well plates for high throughput screening with equally effective results. In addition, the assay is simple to run; taking in total 5 min to obtain the required data, and potentially can be used in any situation where cytotoxicity is suspected. A 100% control lysis reagent was also effectively produced which compared significantly to AK released from freeze-thawed cells ($R^2 = 0.99$).

3.3.2 ToxiLight® assay compared to traditional assays

The study so far has incorporated data from well-established assays and techniques used for proliferation and cytotoxicity studies. Over the last decade colorimetric assays based on the reduction of tetrazolium salts have been promoted in the form of several commercial kits aimed at measuring cell proliferation (Petty *et al.*, 1995; Kawada *et al.*, 2002; Marshall *et al.*, 1995). This is a high-throughput method and is proposed as a preferable alternative to techniques such as those based upon the

uptake of ^3H -thymide or chromium release, both of which are radioactive. This study however, has shown that even the colorimetric assays are insufficient in detecting very low cell numbers. Their detection at best was only 10,000 cells per well, and represents a significant number of cells that would proliferate into a new tumour population, thus providing misleading results suggesting that the treatment successfully killed all of the cells.

The alamarBlue® assay proved to be the most sensitive after the colorimetric assays, detecting 3000 cells above the background levels. As shown in table 3.02, the midpoint potential of alamarBlue® is greater than that of any of the other components of the electron transport chain. This explains its superiority over the colorimetric assays as it will be reduced much better. The midpoint potential of MTT is intermediate between that of the electron donors and cytochromes meaning that MTT will not be reduced by cytochromes. Even though the alamarBlue® assay proved superior, it still lacked sufficient sensitivity and as with the colorimetric assays, it also proved to be time consuming.

The developed ToxiLight® assay was monitored alongside other well-established methods. This study revealed that the best assays on the market were the LDH, ViaLight™ Plus®, and the ToxiLight®™ assays, in terms of ease of use, speed and sensitivity. When ToxiLight® was compared to each of these assays, the correlation was >0.9 for all experiments performed. This revealed the assay to be very reproducible. LDH is relatively stable but for prolonged periods of incubation in culture media can result in unreliable results due to its degradation after 9 h (Promega, 2004). It is a cytosolic enzyme that is present in animal cells. Moreover, it is a rapid method and reagent kits for clinical screening are commercially available and relatively inexpensive (Sasaki *et al.*, 1991). However, the LDH assay was not as responsive as the new ToxiLight® assay; low concentrations of drugs showed little toxicity in comparison

and the cell number detection was 50 cells per well compared to the 5 cells per well of the ToxiLight® assay. Although LDH detection proved to be fast and efficient, the sensitivity was not comparable to AK release with the LDH enzyme being less stable in culture.

Propidium Iodide (P.I.) uptake is a widely used technique for measuring both hypodiploid peaks for cell cycle analysis and in monitoring cell permeability (Ormerod, 1998). It is much smaller in size (668 Da) than AK (36 kD) and thus measurement should be more sensitive. The disadvantage however, is that measuring P.I. uptake is time consuming and requires specialist knowledge. The results showed the ToxiLight® assay to be as sensitive as P.I. uptake (figure 3.14) in this research detecting down to as few as 5 cells per well (figure 3.11) and identifying cell death in very low concentrations of drug.

ViaLight® Plus offers many benefits over the conventional assays by avoiding the use of radioisotopes and showing greater sensitivity and reproducibility (Crouch *et al.*, 1993; Bradbury *et al.*, 2000; Tsujimoto, 1997). Due to the speed and ease of use of this method it lends itself particularly well to high throughput assays and drug screening like the ToxiLight® assay. When compared to the ToxiLight® assay, the sensitivity of both these assays was excellent. Figure 3.19 demonstrated with lysed K562 cells how both assays could measure small amounts of ATP (10 cells per well) or AK (5 cells per well) released above background. Although both assays measured different forms of cell death they shared the sensitivity required in detecting changes within a cell.

The data presented in this study suggests that ToxiLight® can be used as an indicator of necrotic cell death and is very sensitive compared to the conventional assays. An interesting finding was that when melanoma cells were dosed with dacarbazine, neither the ToxiLight® assay nor the

ViaLight® Plus assays on their own could identify the effects of the drug on the cells. It was only when the two assays were used in conjunction with each other that a conclusion could be drawn from the experiment (figure 3.23). The ToxiLight® assay implied no cell death was present. However, the ViaLight® Plus assay revealed a dramatic change with a large reduction in ATP levels leading to the assumption that cell death was in fact occurring. FACScan analysis revealed that the drug had a cytostatic effect on the cells which proved both assays to be correct. The ViaLight® Plus assay was merely showing fewer cells in culture due to growth arrest thus the lower levels of ATP with increasing drug and the two assays performed together would provide a definitive answer.

In conclusion, this study revealed that although the ToxiLight assay proved to be very sensitive, it should not be used alone unless purely looking for cell membrane damage or necrosis. Both a viability assay and an assay to detect necrosis is the best combination to use when analyzing the effects of a cytotoxic drug on a cell population. Ideally a cytolysis assay such as ToxiLight® and a proliferation assay such as ViaLight® Plus would be a desirable combination. As these assays are highly sensitive, slight changes within the cell population would be revealed. They would show both cell lysis, proliferation and any cytostatic effects over time. Detecting cytostatic effects are just as important in studies as the detection of toxicity and cell death.

Convenient methods for the quantification of cell numbers in culture have proven very difficult in the past. For example, the simple and direct techniques such as cell counting with haemocytometer chambers or electronic particle counters are unsuitable for the processing of large numbers of samples (Marshall *et al.*, 1995). All published reports describe assays utilised for the detection of either cell death or proliferation that are not sensitive enough in detecting any remaining resistant populations

of cells that are living in small cell numbers within a tumour population. It is this lack of sensitivity that results in cells being left undetected and allows them to proliferate into a new tumour population over time.

Resistance is known to occur with many chemotherapy drugs. Experimentally, acquired resistance developed to various compounds has been demonstrated (Kerbal *et al.*, 2001). Goldie and Coldman (1979) suggest that spontaneous mutations during tumour evolution are responsible for the presence of intrinsically resistant cells before exposure of a tumour to a cytotoxic drug. This could present itself by cell cytostasis or continued proliferation. Assays detecting this effect are crucial to clinicians before the commencement of treatment to prevent the patient being exposed to a drug that will not be beneficial. The ToxiLight® and ViaLight® Plus assays may help in studying these areas of cancer research.

The next stage of this study was to use both the ToxiLight® and ViaLight® Plus assays on both primary and continuous melanoma cell lines. These cells would be exposed to a number of known chemotherapeutic drugs and monitored with various doses over time. The assays would be used to assess the affects of these drugs and sensitive and resistant cell lines were identified using the ViaLight® Plus and ToxiLight® assays and selected for further research.

Chapter 4: Utilising bioluminescent assays to assess cell death in melanoma cells.

4.1 Introduction

The incidence of melanoma has more than doubled over the last decade and early detection is vital to reduce mortality in these patients; surgery curing 95% of early stage disease (Testori *et al.*, 2009). Balch *et al.* (1997) reported the survival rate for patients with loco regional disease to be 24 months and for patients with metastatic disease to be 6 months. This statistic has not improved today due to ineffective treatment for advanced melanoma. Anticancer agents commonly used in the treatment of melanoma do not result in clinically meaningful responses in most patients (Garbe, 1993), suggesting a high drug resistance for unknown reasons. Resistance to antineoplastic agents is a major obstacle in successfully treating metastatic malignant melanoma (Viatcheslav *et al.*, 1999; Wittig *et al.*, 2002; Dong *et al.*, 2002; Amiri *et al.*, 2004) and common anti-cancer drugs such as taxol, cisplatin (Sersa *et al.*, 2000; Leonetti *et al.*, 1999), etoposide (Wittig *et al.*, 2002; Lage *et al.*, 2001), doxorubicin (Panneerselvam *et al.*, 1987) and vindesine have shown no efficacy in large randomised trials (Soengas *et al.*, 2003). This lack of selectivity of chemotherapeutic agents has raised the call for the development of new drug delivery systems, such as enhanced delivery of drugs to tumour cells by electroporation (electrochemotherapy). This mode of delivery has been shown to be more effective for drugs such as cisplatin and bleomycin and increases drug delivery to the cells, with insignificant side effects due to the low cisplatin doses. However resistance has been observed after four cycles of chemotherapy (Sersa *et al.*, 2000).

Multidrug resistance (MDR) is a major obstacle for cancer therapy; the cancer may be either inherently untreatable (intrinsic resistance) or have progressed to develop resistance to a wide variety of anticancer agents over the course of treatment (acquired resistance) (La Porta, 2007). In general, the vast majority of anticancer drugs operate through induction of cell cycle arrest and cell death in either the DNA synthesis (S) or mitosis (M) phase of the cell cycle (Shabbits *et al.*, 2003). Table 4.01 illustrates how many of the resistant drugs tested target melanoma cells.

As previously mentioned in the introduction (chapter 1), it is well established that cancer is not caused by a mutation in a single gene, but requires genetic alterations affecting several pathways (Hanahan and Weinberg, 2000). P53 is one of the most commonly mutated genes in human cancers (>50%) and its role in malignant melanoma has been the subject of intense investigation (Rieber *et al.*, 2001). An increased p53 level due to decreased degradation of the mutant protein has been observed (Le *et al.*, 2003) in metastatic melanomas but not primary melanomas. In 1998, Li and his research team compared the responses of four melanoma cell lines containing the wild-type p53 and four cell lines carrying the mutant p53 when exposed to cisplatin, vincristine and camptothecin. Results revealed low percentages (<18%) of cell survival with wild-type p53 compared with a greater than 55% survival of the cells with mutant p53 (Li *et al.*, 1998).

Agents	Mode of Action	Specific cellular effects
Nitrosoureas Carmustine	Alkylation of nucleic acids and proteins	ssDNA breaks
Lomustine Semustine		DNA crosslinking Carbamoylation of proteins
Nitrogen mustard Cyclophosphamide		Alkylation of nucleic acids
Triazenes Dacarbazine	Alkylation and methylation of nucleic acids	Inhibition of nucleic acid and protein synthesis
Temozolomide		
Antibiotics Anthracyclines Doxorubicin (adriamycin)	DNA intercalating agent Free radicals	ssDNA breaks DNA crosslinking
		Inhibition of DNA and RNA replication
Plant-derived products Vinca alkaloids Vincristine	Microtubule disruption (prevent assembly)	Altered cell division, motility
Vinblastine		Intracellular transport
Epidodophyllotoxins Etoposide	Inhibition of topoisomerase II	DNA breaks
Taxanes Taxol Paclitaxel Docetaxel	Microtubule disruption (prevent depolymerisation)	Altered cell division, motility
		Intracellular transport
Hormonal analogs Antiestrogen Tamoxifen	Competitive inhibitor of endogenous estrogens	Altered estrogen signaling
Platinum drugs Cisplatin Carboplatin	DNA and protein crosslink	ssDNA and dsDNA breaks Changes in DNA structure Inhibition of DNA and RNA synthesis

Table 4.01 To illustrate treatments used and how they target melanoma

Recent research has looked into epigenetic events that affect cell transformation (Schwabe and Ubbert, 2007), which refers to changes in phenotype (appearance) or gene expression caused by mechanisms other than changes in the underlying DNA sequence. There is no alteration in the underlying DNA sequence of the organism; instead, non-genetic factors cause the organism's genes to behave (or "express themselves") differently. The irreversible changes that occur within the human DNA sequence, including chromosomal deletions, amplifications, and gene mutations, have all been implicated in the development and progression of melanoma (La Porta, 2007). The most common epigenetic phenomenon in malignancy appears to involve histone modification and DNA methylation. On the whole, epigenetic profiling of melanoma is still in its infancy, posing an enormous challenge for researchers and clinicians. Histone deacetylase (HDAC) inhibitors are a promising group of compounds inducing differentiation, growth arrest and apoptosis in tumour cells in preclinical studies (Peltonen *et al.*, 2005). The cellular effects of trichostatin A have been monitored in many studies (La Porta, 2007). It is an organic compound that serves as an antifungal antibiotic and selectively inhibits the class I and II mammalian HDAC families of enzymes, preventing progression of the eukaryotic cell cycle during the beginning of the growth stage (Kim *et al.*, 2000). Histone acetylation is carried out by HATs, while HDACs remove acetyl groups. Inhibitors of HDAC, such as trichostatin A (TSA) push the equilibrium towards the acetylated, transcriptionally active state as shown in figure 4.01. Increased histone acetylation leads to reversible decondensation of dense chromatin subcompartments (Toth *et al.*, 2004).

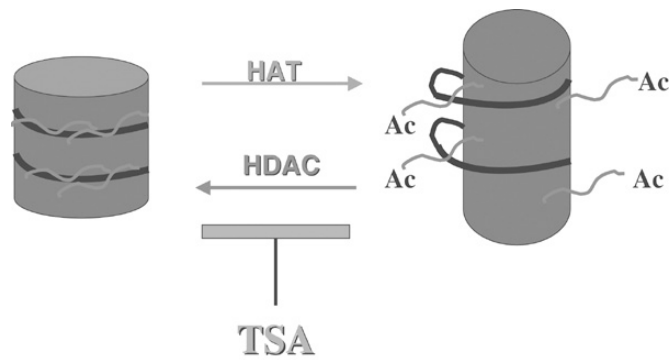


Figure 4.01 To illustrate how the HDAC inhibitor trichostatin A interacts (Scotto, 2003)

The relationship of trichostatin A with p53 (Halaban *et al.*, 2009; Peltonen *et al.*, 2005), p21^{WAF1/Cip1} (Boyle *et al.*, 2005), p27^{Kip1}, Fas/FasL (Kramer, 2007; Klisovic, *et al.*, 2003), E2F (Katsura, 2008), MHC class I and II (Bazhin, 2007) has been researched and shows much promise in melanoma treatment. Accumulating evidence has suggested that the histone deacetylases play a very important role in carcinogenesis, and histone deacetylase inhibitors (HDACIs) are being extensively studied for the treatment of various cancers (Muscolini *et al.*, 2008; Habold *et al.*, 2008; Katsura *et al.*, 2008). HDACIs cannot only induce growth inhibition, cell cycle arrest and apoptosis in cancer cells, but also increase the sensitivity to chemotherapy and ionizing radiation (Munshi *et al.*, 2005).

The aim of the research in this chapter was to use the most sensitive assays available for testing tumour chemo sensitivity assays. The assays to be used were determined in chapter 3 of this thesis; the ToxiLight® and ViaLight® Plus kits. These will be used in parallel for a study involving primary and immortalised melanoma cells cultured *in vitro*. The cells were obtained by Nottingham Trent University as part of the OISTER (Outcome and Impact of Specific Treatment in European Research in melanoma project (EU number QLKS-CT-2000-40643) involving seven partners across Europe and were designed to collect tissue, serum samples and culture cell lines from melanoma patients with known clinical outcome for analysis. The remaining cell lines were obtained from ESTDAB (european searchable tumour cell line database; EU number QLRT-2000-01325). The ToxiLight® and the ViaLight® Plus kits would be used to acquire sensitive and resistant cell lines to various cytotoxic drugs. These selected cell lines will then be tested with the histone deacetylase drug trichostatin A for further proteomics studies undertaken (chapter 5). The results will be analysed by FACScan analysis, light microscopy and trypan blue uptake to ensure the validity of the assays.

Therefore the aims of this chapter will be to:

- Test the library of melanoma cell lines with the ToxiLight® and ViaLight® Plus kits with some known chemotoxic drugs used in previous melanoma studies.
- Select sensitive and resistant cell lines to trial the histone deacetylase inhibitor, trichostatin-A, for its potential use in melanoma treatment.
- Validate the data by FACScan analysis, trypan blue uptake and light microscopy.

4.2 Results

The primary melanoma cells selected for this aspect of the research were obtained from the OYSTER (Outcome and Impact of Specific Treatment in European Research in melanoma) tissue bank; the established cells were obtained from ESTDAB. All of the cell lines were dosed with a range of chemo toxic drugs; known agents that have been investigated in many melanoma studies over the years. Table 4.02 summarises the cells and the drugs used:

Melanoma Cells Used	Chemo Toxic Drugs Used and their mechanism of action
ESTDAB 005 (established)	<u>Vindesine</u> Plant alkaloid that inhibits microtubule assembly.
COLD 794 (established)	<u>Cisplatin</u> Alkylating agent which interferes with DNA replication.
WM 1205 (established)	<u>Doxorubicin</u> Anti-tumour antibiotic. Binds to DNA and inhibits reverse transcriptase and RNA polymerase.
MEWO (established)	
MA MEL 28 (primary)	
MA MEL 26A (primary)	

Table 4.02: A summary of the six melanoma cell lines chosen and the three cytotoxic drugs used on them.

Cell cultures freshly initiated from tissues or organ pieces are called primary cell cultures. Cell lines may be obtained from the primary culture by renewed disruption of the cell layers with trypsin or any other suitable agent and fresh inoculation of a limited number of cells containing fresh medium. This process, which is repeated normally every three to four

days, is called cell passage or subcultivation and yields secondary cells. After approximately 70 sub cultivation steps the cell line is called an established cell line. Primary cells with an extended capacity to replicate are called immortalised cells. Such immortalised cells frequently arise spontaneously after adaptation to tissue culture conditions. These cells possess an extended proliferative capacity *in vitro*, but usually possess an unstable genotype and may not express the same phenotypic markers as those observed in primary cells, having lost some or many of the features observed in primary cells.

Initial experiments were carried out to ensure that all the melanoma cell lines were clear from mycoplasma contamination. This can result in possible cellular changes, including chromosome aberrations, changes in metabolism and cell growth which then affects any research data obtained on the cell lines (Lonza Ltd, 2006). All cell lines used were screened for mycoplasma and found to be negative (materials and methods – chapter 2.3.6).

4.2.1 Measuring ATP and AK as a Cell Marker in melanoma cells.

The most effective assays for measuring cell death/viability which were determined in chapter 3 (the ToxiLight® and ViaLight® Plus assays), were further utilised in experiments conducted on both primary and established melanoma cell lines. The cells were exposed to a number of known chemotherapeutic drugs to assess their effects on melanoma cells, in order to identify drug-sensitive and drug-resistant cell lines for further analysis.

4.2.1.1 Effect of chemotoxic drugs on the ToxiLight® and ViaLight® Plus assays.

Initial studies were conducted using both the Vialight® Plus and ToxiLight® assays to ensure there would be no interference from the chemotherapeutic agents on the assay themselves. ATP and AK (myokinase) standards were diluted in complete media: 0.1 μM ATP for the ViaLight Plus assay; and 25 μM AK for the ToxiLight® assay. 10 $\mu\text{g}\cdot\text{mL}^{-1}$ of vindesine; cisplatin or doxorubicin (the highest drug concentration used in the experiments) was added to the prepared standards; with control standards retained containing no drugs. 100 μL volumes of standards with and without the drug were sampled for both the ToxiLight® and ViaLight® Plus assays. From the results obtained in figure 4.02, it is clearly shown that none of these drugs had any adverse effect on either the ToxiLight® or the ViaLight® Plus kits. The RLUs for the control standards (labelled '0') in figures 4.02 A, B and C was not significantly different to the RLUs where the drugs were present (labelled '10').

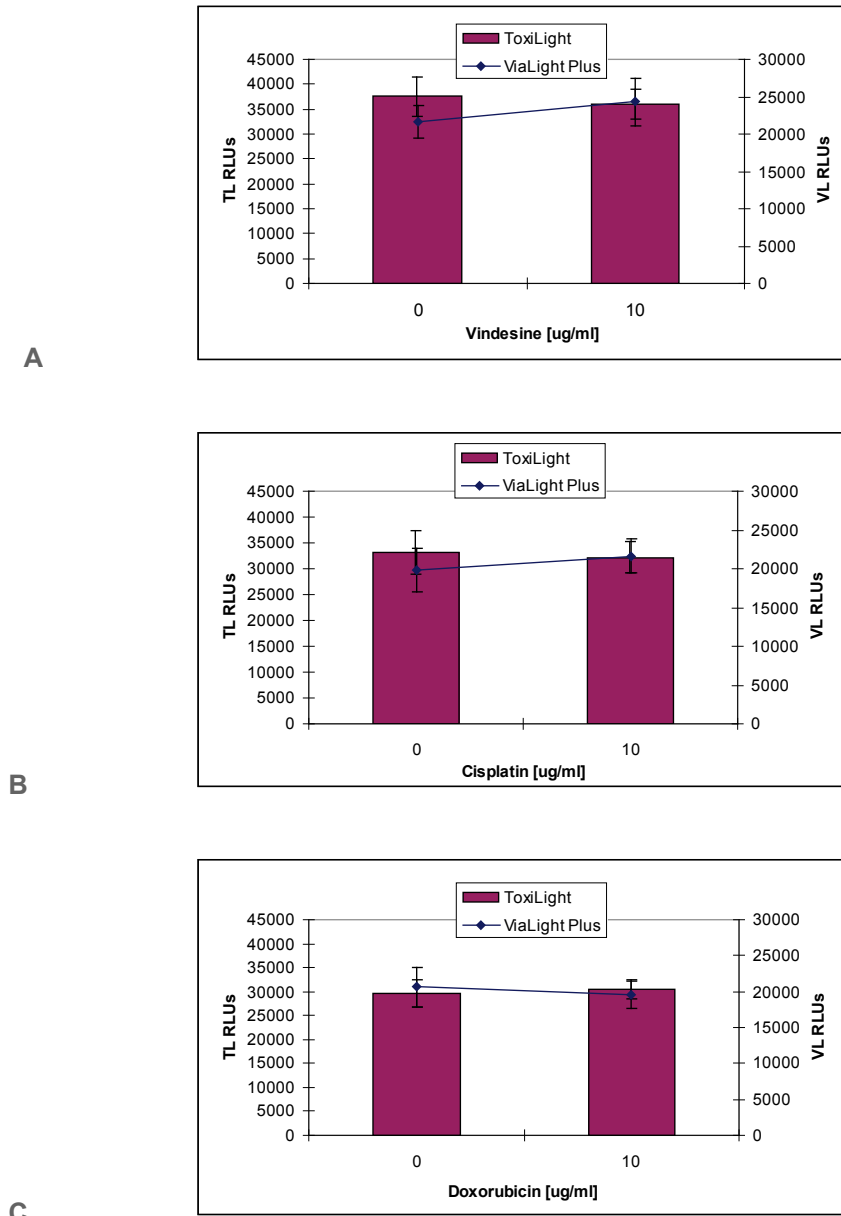


Figure 4.02: The effects of vindesine (A); cisplatin (B) and doxorubicin (C) on the ToxiLight® and ViaLight® Plus kits. ATP standards were used at 0.1 μM for the ViaLight® Plus assay and myokinase standards (AK) at 25 μM used to test the ToxiLight® assay. Both drugs were diluted in the standards and compared against control standards only. The resulting RLU were measured using bioluminescence on a Berthold MPL-2 luminometer to obtain an ATP/RLU (VL RLU) and an AK/RLU (TL RLU) \pm the standard error of the mean ($n=3$).

4.2.1.2 Effect of the chemo toxic agents on melanoma cells

The primary Ma Mel 28 and Ma Mel 26a cells and the four established melanoma cell lines (COLD 794, ESTDAB 005, WM 1205 and MEWO) were dosed with the anti-tumour antibiotic, doxorubicin. All cells were prepared in 100 μl volumes in a 96 well culture plate with an initial cell density of $1 \times 10^5 \text{ cells.ml}^{-1}$. Doxorubicin was used at 0, 1, 5 and $10 \mu\text{g.ml}^{-1}$ and the effect of the drug monitored with both the ToxiLight® and ViaLight® Plus kits at 24, 48 and 72 h. Doxorubicin has been shown to have no efficacy in melanoma patients in large randomised trials, but it was hoped that using these two detection assays in conjunction with each other, the *ex-vivo* effect of doxorubicin could be determined.

The results obtained in figure 4.03 with the immortalised cells dosed with the doxorubicin agent revealed that cell lines were sensitive to doxorubicin even in the lowest dose of the drug ($1 \mu\text{g.ml}^{-1}$). The ATP RLU's dropped significantly in all the cells tested after 48 h in culture. The ToxiLight® assay also revealed the RLU's to increase significantly after 48 hours, indicating that doxorubicin was inducing cell death. The most toxic effects were seen with MEWO cells (figure 4.03; D) where the increases in RLU's at 72 hours increased from 225 in the control to 3761 RLU's with $10 \mu\text{M}$ doxorubicin approaching sixteen times the control value. COLD 794 cells (figure 4.03; A) proved to be the least drug sensitive line only 1331 RLU's in the control and 2684 RLU's with $10 \mu\text{M}$ doxorubicin; only twice the increase of the control.

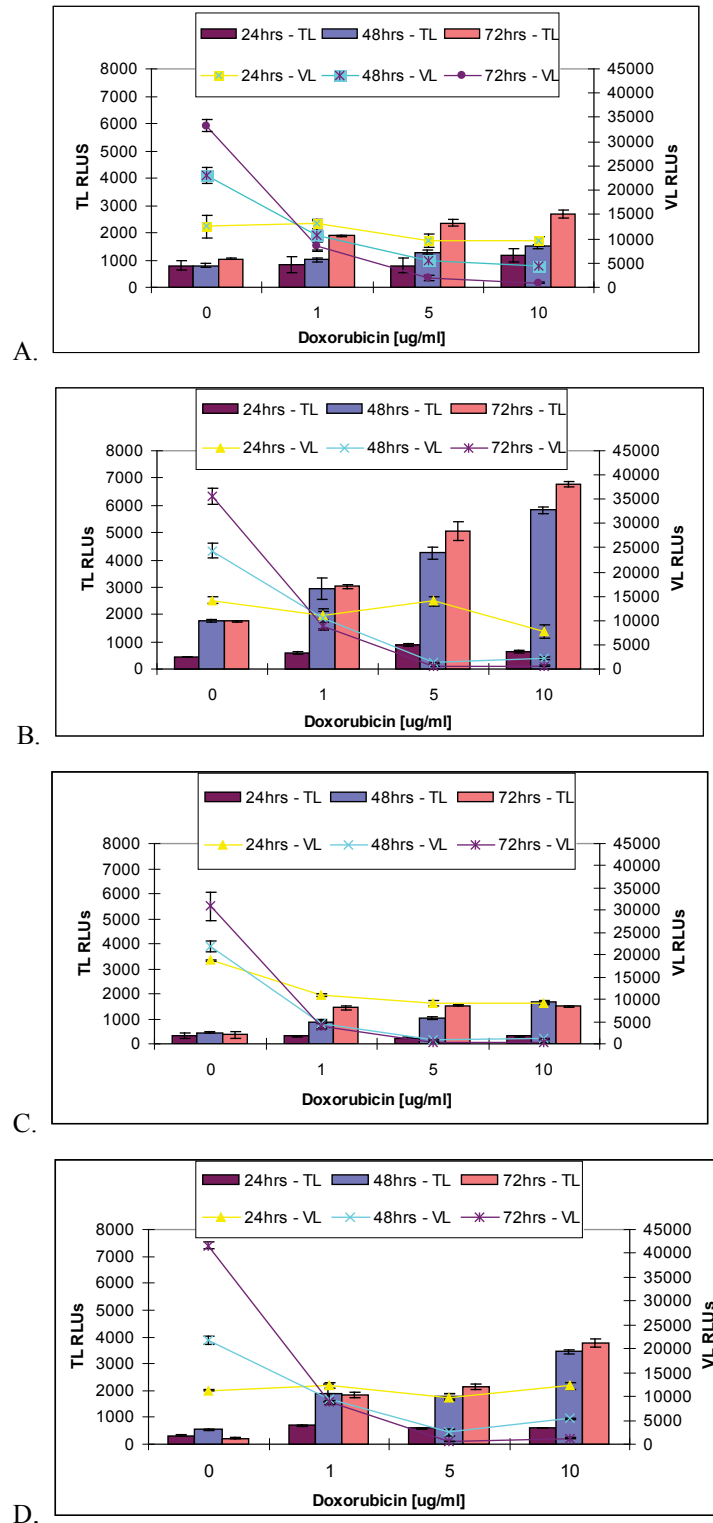


Figure 4.03: The effects of doxorubicin on COLD 794 cells (A), ESTDAB 005 cells (B), WM 1205 cells (C) and MEWO cells (D) tested using the ToxiLight® and ViaLight® Plus kits. The resulting RLUs were measured using bioluminescence on a MPL-2 luminometer to obtain an ATP/RLU (VL RLUs) and an AK/RLU (TL RLUs) +/- the standard error of the mean (n=3). N = number of experiments.

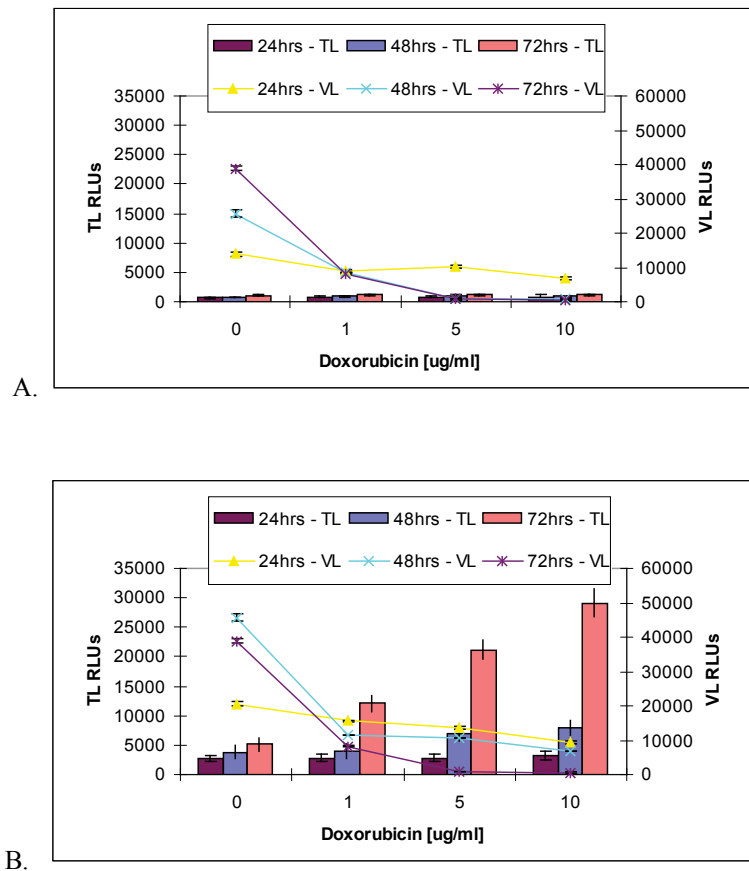


Figure 4.04: The effects of doxorubicin on Ma Mel 28 cells (A), and Ma Mel 26a cells (B), tested using the ToxiLight® and ViaLight® Plus kits. The resulting RLU's were measured using bioluminescence on a Berthold MPL-2 luminometer to obtain an ATP/RLU (VL RLU's) and an AK/RLU (TL RLU's) +/- the standard error of the mean (n=3).

N = number of experiments.

The Ma Mel 26a cells (figure 4.04; B) dosed with doxorubicin showed a similar effect, as previously seen in figure 4.04 with a reduction in ATP values after 24 hours. The ToxiLight® assay demonstrated cell death due to the increase in RLU's (four times above the control after 72 h) showing AK release from the necrotic cells. In comparison, the Ma Mel 28 cells (figure 4.04; A) demonstrated a reduction in ATP values; however the ToxiLight® RLU's showed no significant change when compared to the control throughout the experiment. As the plasma membrane was still

intact in these cells this result implied that the cells were in growth arrest (cytostasis) without direct cytotoxicity.

Due to the varying results obtained with doxorubicin dosing, it was decided to repeat these experiments on all the melanoma cells with two additional drugs; the alkylating agent, cisplatin and plant alkaloid, vindesine. As in the previous experiment, all cells were prepared in 100 μl volumes in 96 well culture plates with an initial cell density of 1×10^5 cells. ml^{-1} . Cisplatin and vindesine at 0, 1, 5 and 10 $\mu\text{g ml}^{-1}$ were used and tested with the ToxiLight® and ViaLight® Plus kits at 24, 48 and 72 h.

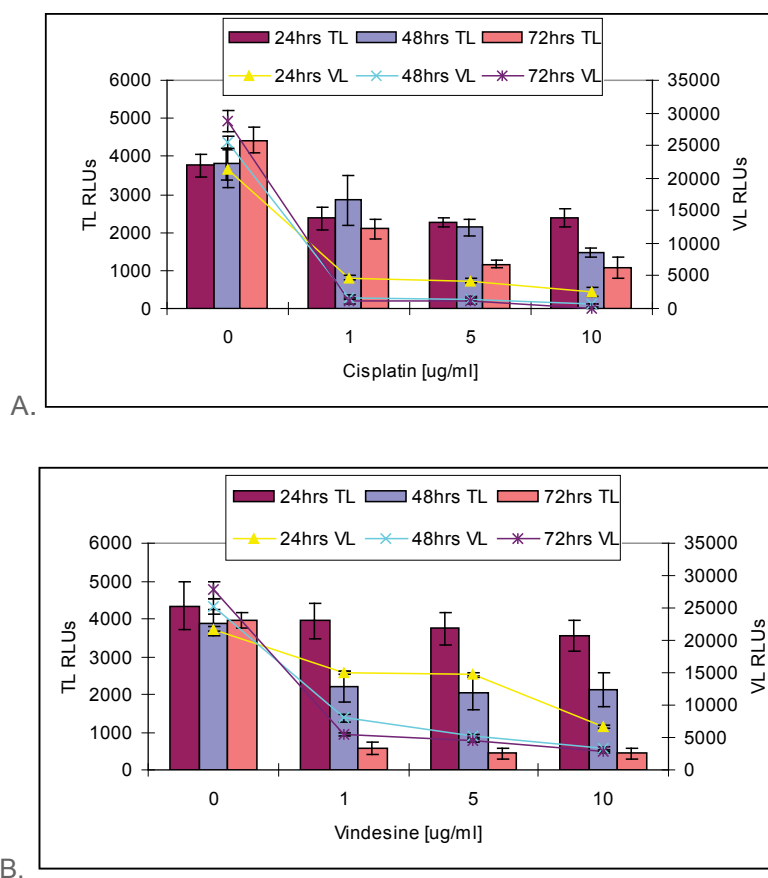


Figure 4.05: The effects of cisplatin (A) and vindesine (B) on ESTDAB 005 cells tested using the ToxiLight® and ViaLight® Plus kits. The resulting RLU were measured using bioluminescence on the Berthold MPL-2 luminometer to obtain an ATP/RLU (VL RLU) and an AK/RLU (TL RLU) \pm the standard error of the mean (n=3).

N = number of experiments.

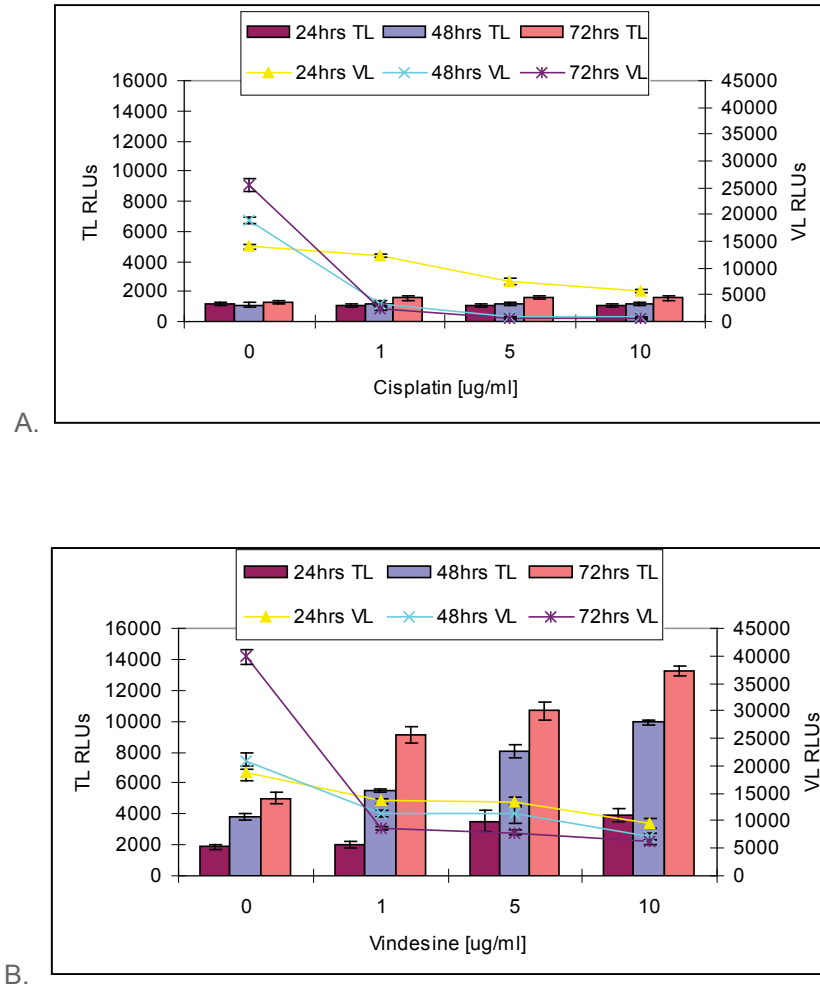


Figure 4.06: The effects of cisplatin (A) and vindesine (B) on COLD 794 cells tested using the ToxiLight® and ViaLight® Plus kits. The resulting RLU were measured using bioluminescence on the Berthold MPL-2 luminometer to obtain an ATP/RLU (VL RLU) and an AK/RLU (TL RLU) +/- the standard error of the mean (n=3).

N = number of experiments.

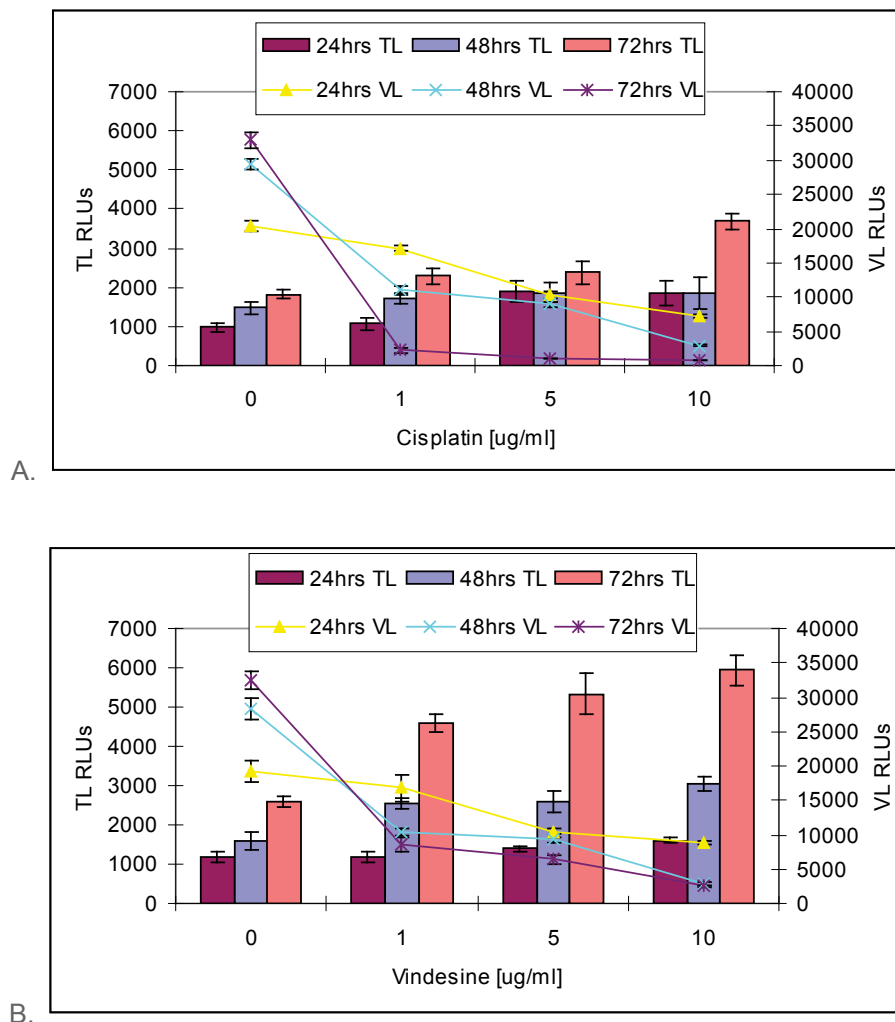


Figure 4.07: The effects of cisplatin (A) and vindesine (B) on WM1205 cells tested using the ToxiLight® and ViaLight® Plus kits. The resulting RLUs were measured using bioluminescence on the Berthold MPL-2 luminometer to obtain an ATP/RLU (VL RLUs) and an AK/RLU (TL RLUs) +/- the standard error of the mean (n=3).

N = number of experiments.

The results in figures 4.05 represent the ESTDAB 005 cells, figure 4.06 the COLD 794 cells and figure 4.07 the WM 1205 cells. All three cell lines revealed a concentration dependent effect with cisplatin when tested with the ViaLight® Plus assay. The ATP RLUs reduced in correlation with increasing drug exposure with a drop in RLUs at 24, 48 and 72 h after drug treatment. In addition, the resulting data with vindesine demonstrated a concentration dependent effect using the ViaLight® Plus

assay with all three cell lines revealing the same cellular effects regarding ATP reduction. However, the overall reduction in ATP RLUs after 72 h with vindesine was not as great as that observed with cisplatin.

Results obtained from the ToxiLight® assay (figures 4.05, 4.06 and 4.07) demonstrates the importance of having both ToxiLight® and ViaLight® Plus assays carried out in parallel. The ViaLight® Plus assay measuring viable cells and changes in ATP levels. If there is a reduction in RLUs, there are fewer cells present and the normal assumption is that they have been killed. By combining ToxiLight® and ViaLight® Plus assays, you can establish if this is an accurate assessment. If there is no increase in ToxiLight® there has been no compromise of the plasma membrane and the cells remain intact, but not proliferating. Therefore compared to healthy control cells which proliferated over the time course of the experiment, there are less cells per well. The previous ViaLight® Plus results with ESTDAB 005 cells (figure 4.05) implied the cisplatin and vindesine to induce cell death with the reduction in ATP. However, results from the ToxiLight® assay demonstrated that the RLUs were not increasing but actually reducing, inferring that no cell death was occurring in the cells. Again, the results of the two assays combined demonstrate cytostasis; the reduction in AK release with increasing doses being due to reduced background AK as fewer cells are present within the well.

The data obtained with COLD 794 cells and the drug cisplatin (figure 4.06; A) did not show significant cell death. Small increases in RLUs could be seen with the ToxiLight® assay after 72 h, revealing some cell death had occurred, but the majority of cells appeared to be cytostatic. In comparison, the results obtained with COLD 794 and vindesine (in figure 4.06; B) revealed that cell death had occurred with a significant increase in RLUs and therefore AK was released from the cells. WM 1205 cells were the only cell line to show significant amounts of cell killing with the drug cisplatin (in figure 4.07; A), with the RLUs doubling after 24 h

although no further cell death appeared to occur after this time (assayed at 48 and 72 h) with the RLUs remaining double that of the control throughout the experiment. This could be due to a mixed population of sensitive and resistant cells within the population. With vindesine exposure (in figure 4.07; B), WM 1205 cells were affected to the same extent as with cisplatin, with only a small increase in ToxiLight® RLUs and thus cell death at 24 h. After 48 h, the RLUs were double that of the control however, no further cytotoxic effects were observed from 48 to 72 h, which could imply the presence of a mixed population of sensitive and resistant cells as observed with cisplatin dosing.

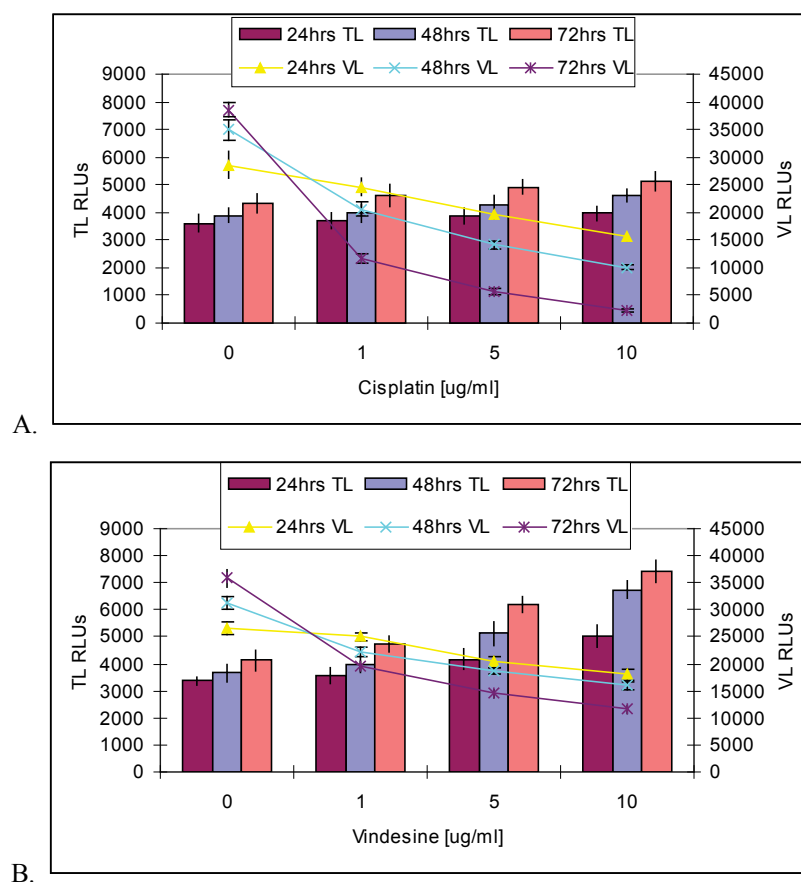


Figure 4.08: The effects of cisplatin (A) and vindesine (B) on MEWO cells tested using the ToxiLight® and ViaLight® Plus kits. The resulting RLUs were measured using bioluminescence on the Berthold MPL-2 luminometer to obtain an ATP/RLU (VL RLUs) and an AK/RLU (TL RLUs) +/- the standard error of the mean (n=3).

N = number of experiments.

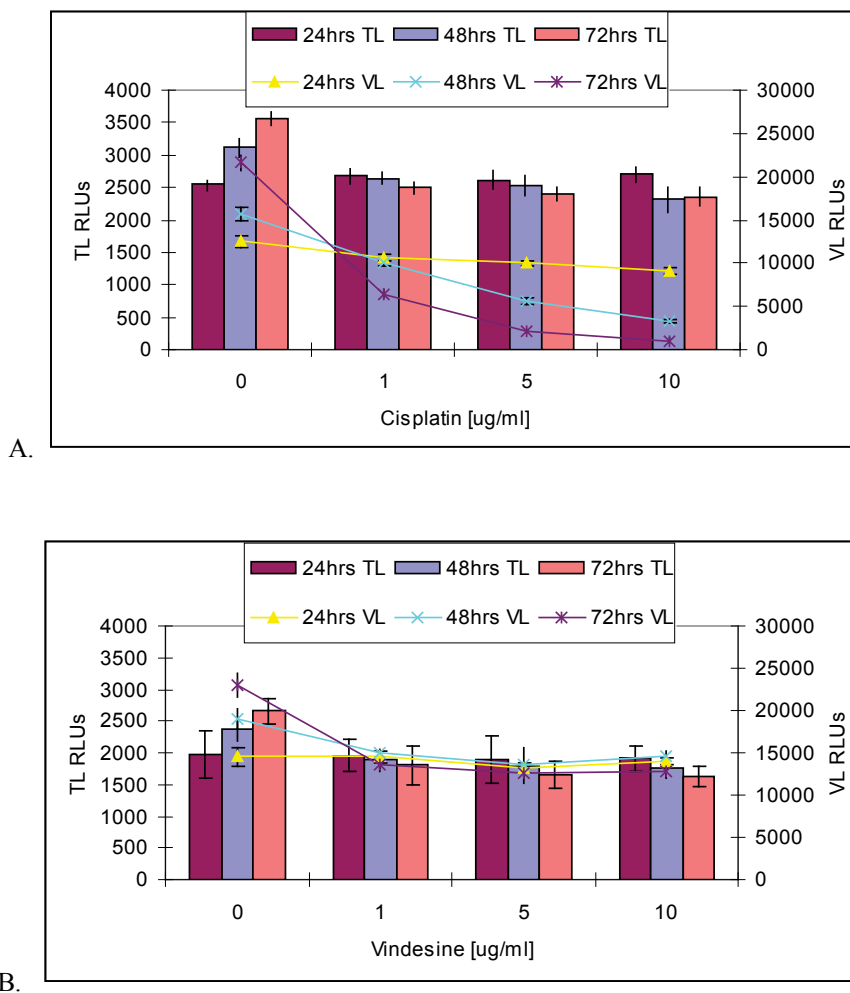


Figure 4.09: The effects of cisplatin (A) and vindesine (B) on Ma Mel 28 cells tested using the ToxiLight® and ViaLight® Plus kits. The resulting RLUs were measured using bioluminescence on the Berthold MPL-2 luminometer to obtain an ATP/RLU (VL RLUs) and an AK/RLU (TL RLUs) +/- the standard error of the mean (n=3).

N = number of experiments.

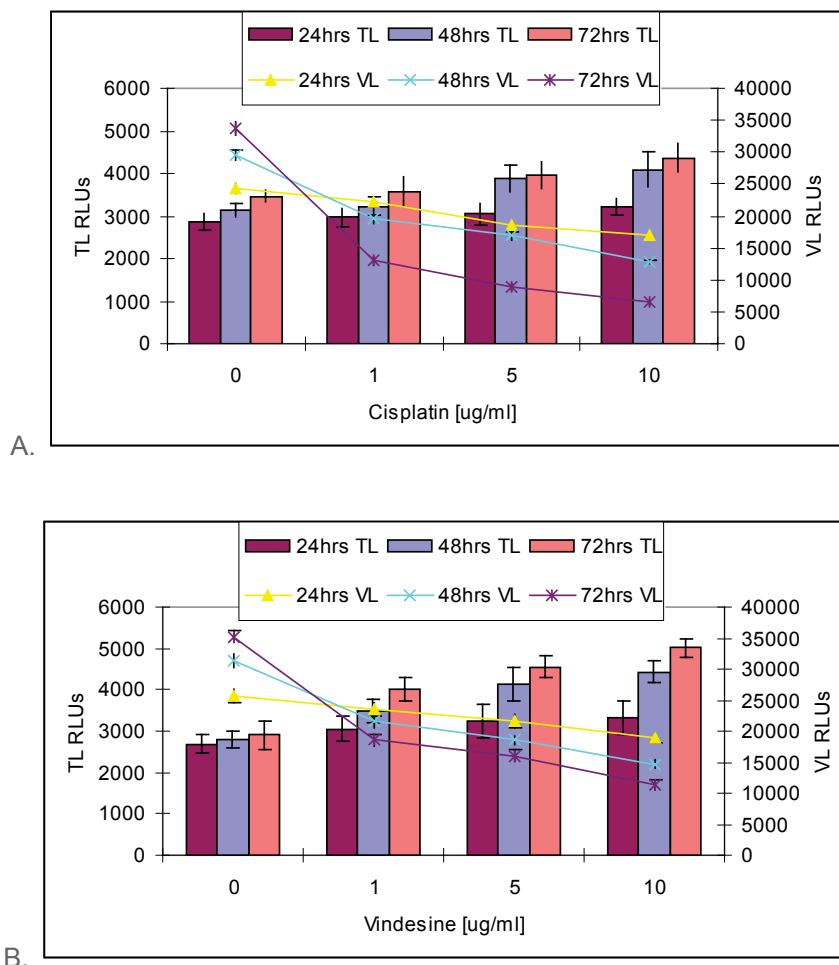


Figure 4.10: The effects of cisplatin (A) and vindesine (B) on Ma Mel 26a cells tested using the ToxiLight® and ViaLight® Plus kits. The resulting RLUs were measured using bioluminescence on the Berthold MPL-2 luminometer to obtain an ATP/RLU (VL RLUs) and an AK/RLU (TL RLUs) +/- the standard error of the mean (n=3).

N = number of experiments.

The three remaining cell lines, MEWO (figure 4.08), Ma Mel 28 (figure 4.09) and Ma Mel 26a (figure 4.10) were tested with cisplatin and vindesine. All three cell lines revealed a concentration dependent effect with a drop in ATP RLUs observed with the ViaLight® Plus assay as the cisplatin dose increased. As seen previously with the first three cell lines tested, the cytotoxic effects with cisplatin was more severe than with vindesine using the ViaLight® Plus assay, with Ma Mel 28 cells (in figure

4.09; B) revealing little change in RLUs with vindesine exposure. The effects of the drug cisplatin were noticeable after only 24 h with the RLUs at 50% of that in the control in all the cell lines. After 72 h, the RLUs further decreased to a much lower level than seen with vindesine.

The results obtained from the ToxiLight® assay in figure 4.09 (A & B) mirror the results previously seen with the Ma Mel 28 cells exposed to doxorubicin, revealing no killing with either cisplatin or vindesine. The RLUs decrease slightly with increasing concentration of drug, illustrating cell cytostasis with fewer cells present in the culture. MEWO and Ma Mel 26a cells showed a slight increase in RLUs, suggesting some cell death had occurred after 48 and 72 h with cisplatin, but the RLUs nearly doubled 72 h after treatment with vindesine. This was an unexpected result as the ViaLight® Plus data revealed a more severe drop in RLUs with cisplatin than vindesine. Comparing all six cell lines, most cell death was observed with COLD 794 cells treated with vindesine; however, comparison of the two drugs overall revealed variable results, with some cells responding better to cisplatin (WM 1205 cells) and others to vindesine (COLD 794 and MEWO cells). Comparing the vindesine and cisplatin results with the initial data obtained with doxorubicin, less cell death was observed overall with cisplatin and vindesine. The Ma Mel 28 cells remained consistent, showing no cell death (cytotoxicity) with either doxorubicin or vindesine and very little effect with cisplatin (cytostasis). The Ma Mel 28 cells were therefore considered resistant to all 3 of the drugs used.

From all the chemo sensitivity assays carried out, it was decided to choose 3 cell lines for further investigation. The Ma Mel 28 cells appeared resistant to the chemotherapeutic agents and were the prime choice. In contrast, the Ma Mel 26a cells appeared to be more sensitive and could be used as a direct comparison to the resistant Ma Mel 28 cells. The cell lines Ma Mel 26a and 28 had known clinical history and patient outcome

which could be used in further data interpretation. To confirm this difference in drug effect, both cell lines were exposed to a further three in-house drugs (Lonza Ltd) to assess their effects with both the ToxiLight® and ViaLight® Plus assays. Dexamethasone is a glucocorticoid anti-inflammatory agent, camptothecin is a DNA topoisomerase I inhibitor and arabinosylcytosine (Ara-C) is a selective inhibitor of DNA synthesis. Cells were prepared in 100 µl volumes in 96 well culture plates with an initial cell density of 1×10^5 cells.ml⁻¹. Three drugs were tested at 0, 5 and 10 µM.ml⁻¹ with an exposure time of 72 h prior to testing with ToxiLight® and ViaLight® Plus assays. The vehicle control shown in figures 4.11 is DMSO into which all three of the drugs had been reconstituted. Although no interference had been seen on the ToxiLight® and ViaLight® Plus assays previously with DMSO, it was decided to confirm this by including a control to ensure no interference was seen with the assays. Complete media containing 0.1% DMSO (i.e. highest concentration used in the experiments) was added to a 96 well plate in 100 µl volumes and tested with both assays. A 100% lysis control was included to obtain a percentage of AK release figure 4.11.

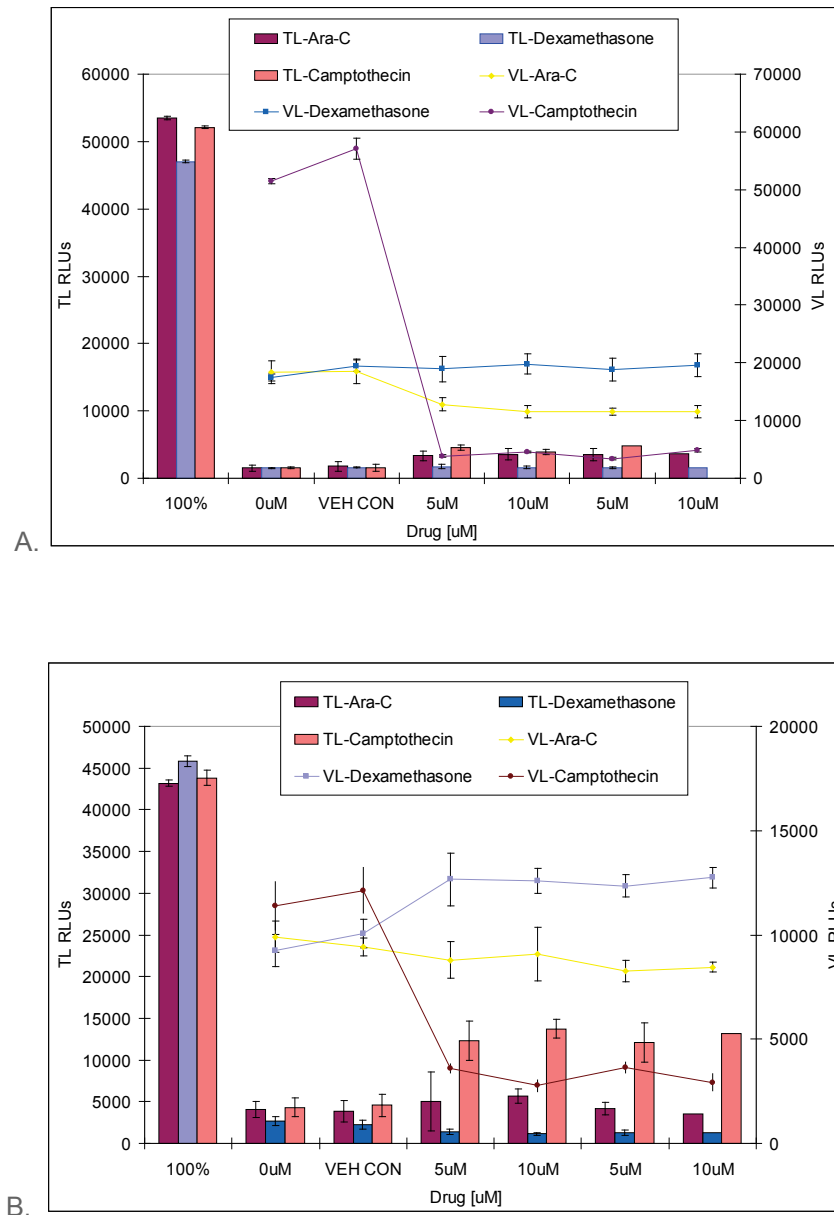


Figure 4.11: The effects of ara-C, dexamethasone and camptothecin on the primary Ma Mel 28 cells (A), and Ma Mel 26a cells (B), tested using the ToxiLight® and ViaLight® Plus kits. The resulting RLUs were measured using bioluminescence on a Berthold MPL-2 luminometer to obtain an ATP/RLU (VL RLUs) and an AK/RLU (TL RLUs) +/- the standard deviation.

N = number of experiments.

The results in figure 4.11 confirmed that the Ma Mel 28 cell line (A) was resistant to drug therapy with dexamethasone, with no drop in ATP observed at all with the ViaLight® Plus assay and consequently no killing was detected with the ToxiLight® assay. The drug did not even produce a cytostatic effect. In the presence of ara-C and camptothecin, there was an observable drop in ATP RLUs with the ViaLight® Plus assay but the ToxiLight® assay revealed little change and therefore no significant cell death. This result showed that some of the cell population were in growth arrest. In comparison, Ma Mel 26a cells did show an effect with camptothecin and ara-C. However as seen with Ma Mel 28, no change in RLUs was observed with dexamethasone with either of the assays. Ara-C revealed a small reduction in RLUs with the ViaLight® assay and a small increase in RLUs with the ToxiLight® assay, concluding that some cell death had occurred. Ma Mel 26a cells treated with camptothecin on the other hand revealed that 25% of cells had been killed after 72 h when compared to the 100% lysed control using the ToxiLight® assay. In addition, the ViaLight® RLUs dropped significantly confirming this cell killing within the culture. These results confirmed the choice of Ma Mel 28 and Ma Mel 26a cells for further investigations. In addition, to these results, it was concluded that the vehicle control (DMSO), did not have any adverse effects on either the ToxiLight® or ViaLight® Plus assays with no significant change in RLUs observed with either assay. As the results did not reveal any of the remaining cell lines to be conclusively resistant or sensitive throughout the experiments, MEWO cells were selected as a third cell line for further investigation, due to current research which investigated it's sensitive and resistant nature to various drugs (Kissel, 2006).

4.2.2 Investigation into the effects of trichostatin A on melanoma cells.

Trichostatin A (a reversible inhibitor of histone deacetylase; HD) is thought to be a possible drug for future melanoma therapy either alone or used in combination (La Porta, 2007). It inhibits cell proliferation, thereby allowing a possible second drug to target the cells in growth arrest resulting in apoptosis. The effect of melanoma cell growth of this drug was assessed using a combination of the ToxiLight® and ViaLight® Plus assays to monitor cell death. The three selected cell lines Ma Mel 28, Ma Mel 26a cells and MEWO cells were assessed after 24, 48 and 72 h of exposure to trichostatin A. The results obtained were verified with FACScan analysis, trypan blue uptake and visually using a light microscope.

The number of replicate samples taken at each time point was n=18 for MEWO, n=10 for Ma Mel 28 and n=14 for Ma Mel 26a cells. All cell based experiments were completed within 5 passages to ensure as few cellular changes within the populations as possible. All cells were prepared either in 100 µl volumes in 96 well culture plates with an initial cell density of 1×10^5 cells.ml⁻¹ or in T25 cell culture flasks in 10 ml volumes at 1×10^5 cells.ml⁻¹. The ToxiLight® assay incorporated a 100% lysis control to quantify the amount of cell killing. Trichostatin A was added to the cells at 0, 1 and 5 µM with an exposure time of 24, 48 and 72 h prior to testing with ToxiLight® and ViaLight® Plus assays. The cells prepared in flasks were scraped, lysed and frozen for further proteomics analysis (see chapter 5).

4.2.2.1 Effect of trichostatin A on MEWO cells

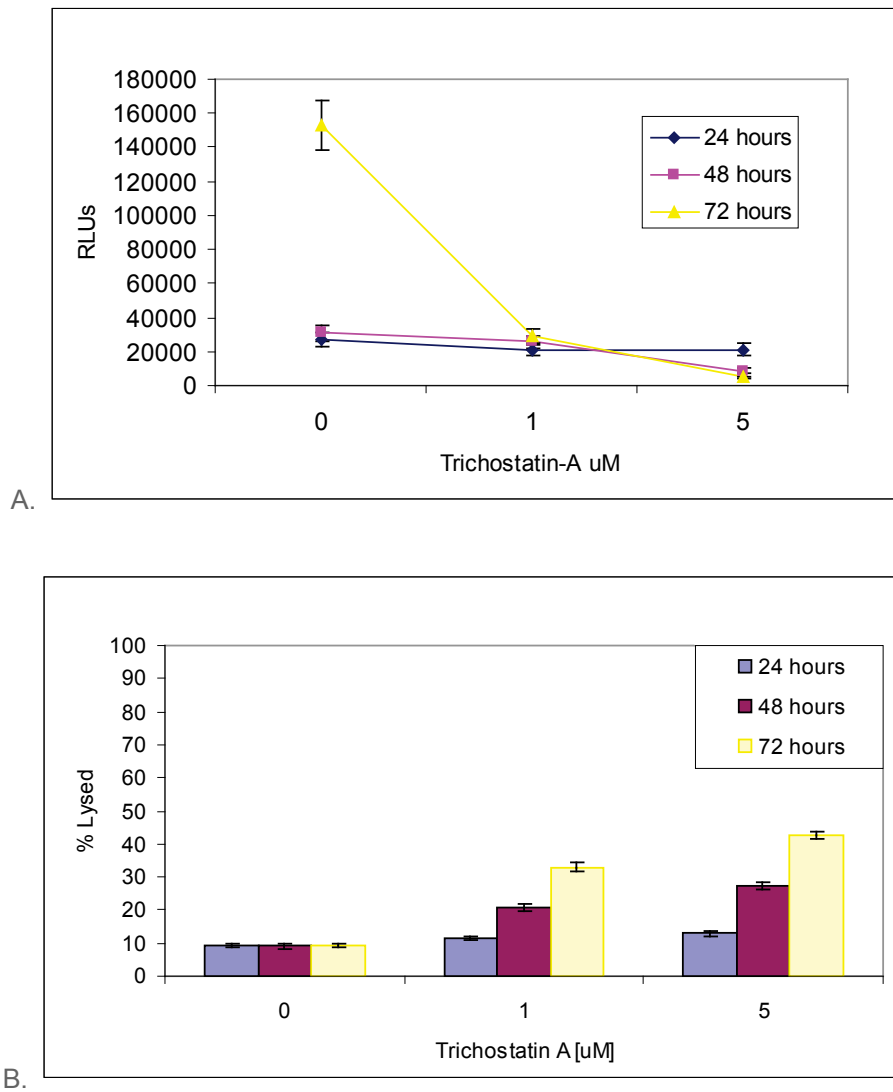


Figure 4.12 MEWO cells were treated with trichostatin A, incubated at 37°C for up to 72 hours and tested every 24 hours for the effects of the drug. A represents the ViaLight® Plus assay; B contains the ToxiLight® data. The resulting RLUs were read on a Berthold MPL-2 luminometer showing ATP/RLUs +/- standard error of the mean where n=18.

N = number of experiments.

Figure 4.12 summarises the effects of trichostatin A on MEWO cells over 72 h. The ViaLight® data reveals a concentration dependent effect with a dramatic reduction in RLUs with increasing drug concentration at 72 h; no

noticeable effect was observed after 24 h in either assay. In addition, the ToxiLight® assay demonstrated that the drug resulted in cell death in 22% of cells after 48 h and 41% of cells after 72 h of incubation. This is represented by the increase in ToxiLight® RLU which indicates necrosis and therefore irreversible cell death. Although cells had been killed it appeared that the majority could be in growth arrest or remain unaffected by the drug.

Microscope examination of the MEWO cells was performed at 72 h as a visual aid in monitoring the state of the cells:

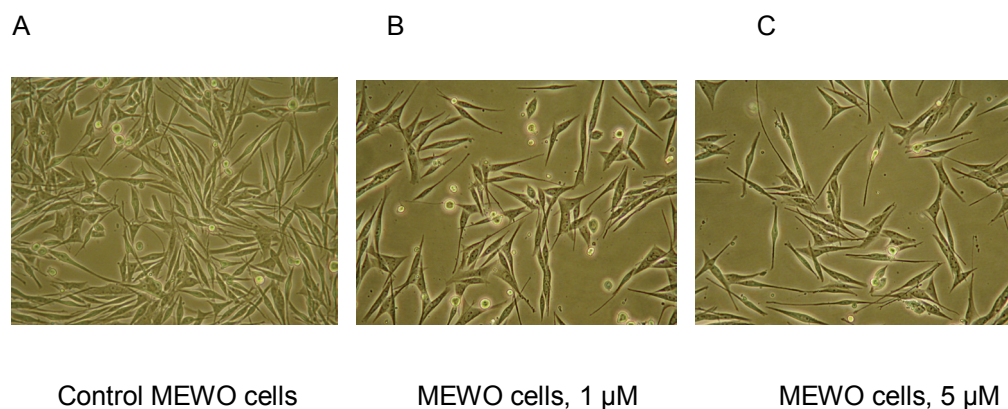


Figure 4.13 Microscopy of MEWO cells dosed with trichostatin A after 72 hours and taken with a light microscope (x10 lens).

The results in figure 4.13, taken at 72 h (1 and 5 μ M trichostatin A) clearly show that there are fewer cells present (figure 4.13, B and C). Some dead cells can be seen suspended in the culture media which may account for the 41% increase in RLU (cell death) with the ToxiLight® assay after 72 h. The remainder of the cells; although in fewer number, remain adherent and healthy confirming the ViaLight® and ToxiLight® data which implies cytostasis.

To correlate the ToxiLight® data, propidium iodide (PI) FACScan staining was carried out. The ability of the cells to exclude various dyes indicates

the maintenance of cell membrane integrity and hence the viability of the cell. PI fluoresces red when it binds to DNA but is excluded from cells with intact plasma membranes. 200 μl of cell culture were sampled and mixed with 200 μl of PI ($50 \mu\text{g}\cdot\text{ml}^{-1}$) and incubated for 10 min at room temperature. The cells were analysed to assess PI uptake with a Becton Dickinson FACScanTM Flow Cytometer and the results are illustrated in table 4.03 at 24, 48 and then 72 h; each experiment consisting of control cells, and cells treated with 1 and 5 μM of trichostatin A.

	% PI Uptake	% Trypan Blue Uptake
Control Cells		
Time (h)		
24	2.24	3
48	4.62	2
72	5.62	4
1 μM TRICHOSTATIN A		
Time (h)		
24	9.20	4
48	18.56	9
72	31.90	18
5 μM TRICHOSTATIN A		
Time (h)		
24	9.56	6
48	39.46	24
72	47.22	32

Table 4.03: MEWO cells treated with trichostatin A (0, 1 and 5 μM) for 24, 48 and 72 h and stained with propidium iodide and compared with trypan blue uptake. The resulting PI uptake was measured by FACS, scanning a population of 5000 cells.

The above data is representative of one experiment (n=1)

Table 4.03 shows a composite of the data produced after monitoring the effects of trichostatin A on MEWO cells for 24, 48 and 72 h. As can be seen in the controls, the MEWO cells appear healthy at 24, 48 and 72 h. After 24 h only 2.24% of the cell population have taken up the propidium iodide dye increasing to only 5.26% after 72 h. MEWO cells dosed with 1 μM trichostatin A after 24 h reveal the percentage of cells taking up the dye to have increased significantly from 2.24% to 9.20% and the highest concentration (5 μM) of trichostatin A concludes that there has been no further increase in cell death with this increase in drug exposure when compared to the 1 μM dose of trichostatin A.

The effect after a 48 h incubation with 1 μM trichostatin A; reveals a shift in the MEWO cell population with 18.56% of the overall population of cells becoming more permeable over time, taking up the dye into the cell membrane. Trypan blue uptake also increased from the control although only 9% uptake. With an increase in trichostatin A concentration to 5 μM , over a 48 h period of exposure, 39.46% of the cells have taken up the dye signifying a further increase in cell death over time, with the trypan blue count also increasing. MEWO cells treated with 1 μM trichostatin A after 72 h reveal a substantial increase in cell death with prolonged drug exposure. The percentage of cells that have taken up the PI has increased to 31.90% and 18% with trypan blue. An even higher number of necrotic cells were recorded after prolonged treatment with 5 μM trichostatin A (72 h) demonstrating that 47.22% of the cells are necrotic with PI staining and 32% with trypan blue uptake. As the FACS data shows in table 4.03, a concentration dependent increase was observed with cells treated with trichostatin A for 48 and 72 h. After 24 h, only a few cells were necrotic, whereas this increased to nearly 50% after 72 h with 5 μM trichostatin A.

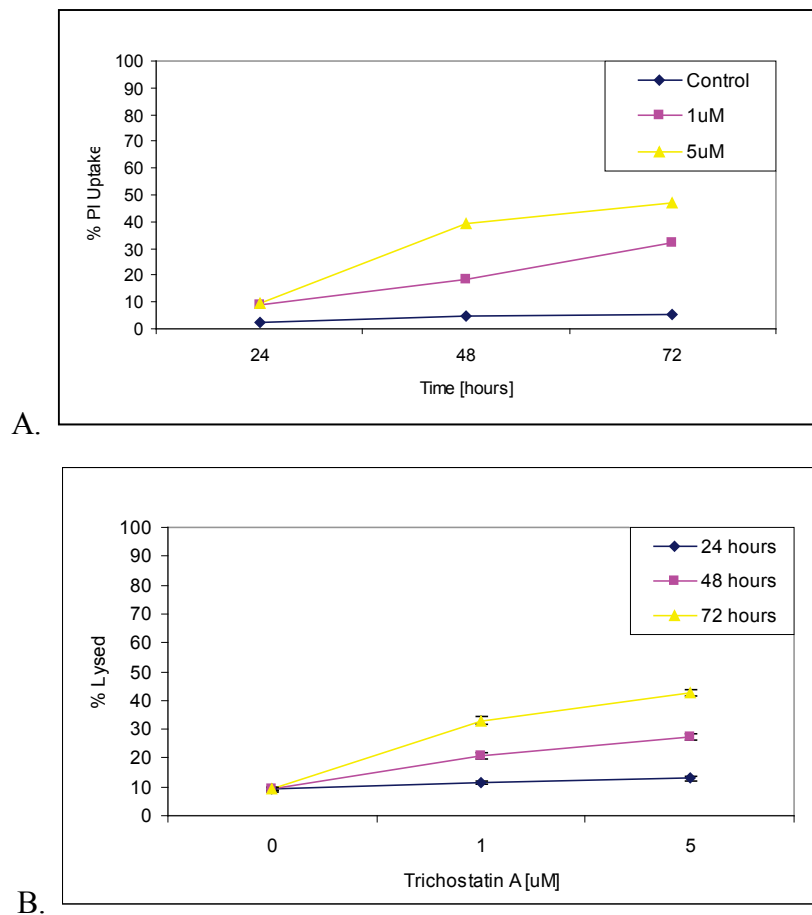


Figure 4.14 Summary comparing the PI uptake data (A) with the ToxiLight data (B). MEWO cells treated with trichostatin A (0, 1 and 5 μM) for 24, 48 and 72 h.

The percentages obtained by FACS analysis, although slightly higher with PI uptake, show similar results to that observed with the ToxiLight® assay (figure 4.14). Trypan blue uptake did correlate with both PI uptake and the ToxiLight® data although the results remained lower throughout all the experiments due to cells disintegrating; therefore not visible by trypan blue exclusion.

4.2.2.2 Effect of trichostatin A on Ma Mel 28 cells

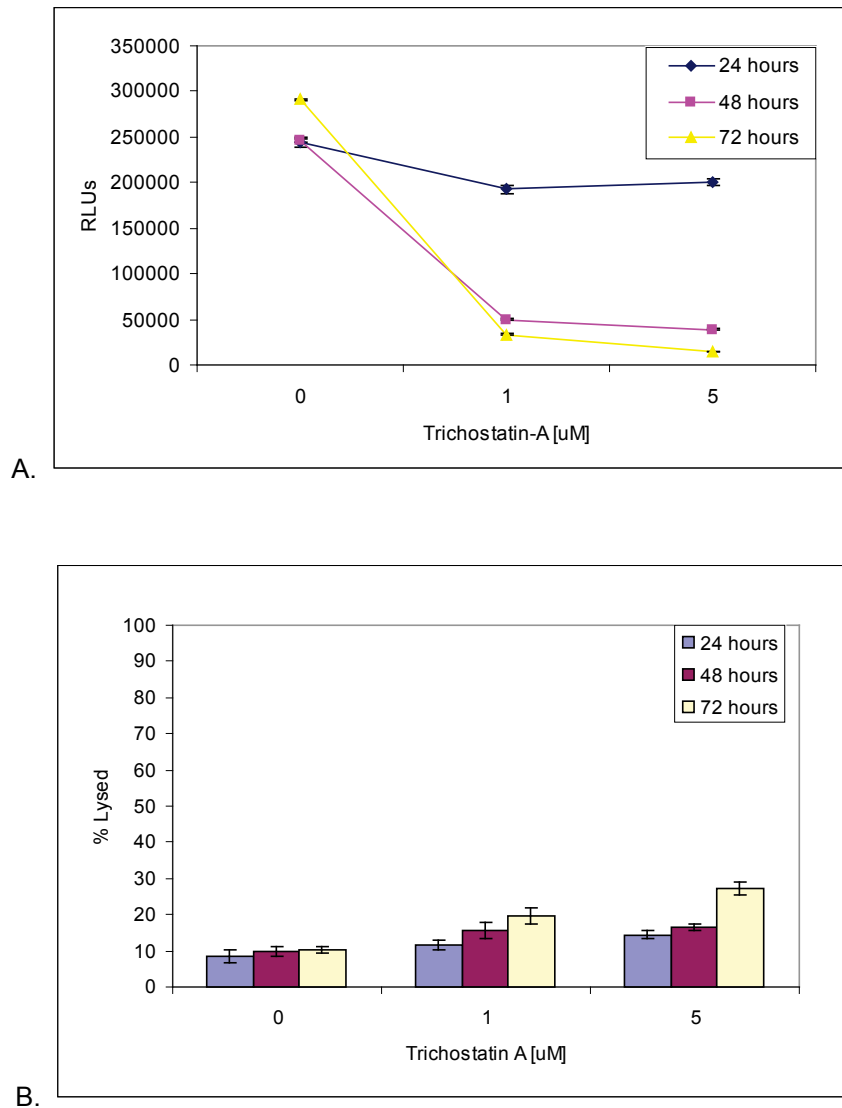


Figure 4.15 Ma Mel 28 cells were treated with trichostatin A and incubated at 37°C for up to 72 h and tested every 24 h for the effects of the drug. Figure A represents the ViaLight® Plus assay; (B) contains the ToxiLight® data. The resulting RLU values on an MPL-2 luminometer, show ATP/RLUs +/- standard error of the mean where n=10.

N = number of experiments.

The results in figure 4.15 summarise the effects of dosing Ma Mel 28 cells with trichostatin A over 72 h. The ViaLight® data reveals only a slight drop in RLUs with 1 and 5 μM trichostatin A at 24 h, but a concentration dependent effect with increasing drug concentration observed at 48 and 72 h. In contrast to the MEWO cells however, the ToxiLight® assay did not demonstrate any significant cell death at 24 or 48 h. After 72 h, there was a significant difference with the percentage of lysed cells increasing from 13% in the control, to 23% after 48 h, and 31% after a 72 h incubation time. This data combined with the ViaLight® Plus assay, which showed a dramatic drop in RLUs at 72 h, suggest that the majority of the cells were in growth arrest.

Microscopic examination of the Ma Mel 28 cells was performed at 72 h as a visual aid in monitoring the state of the cells.

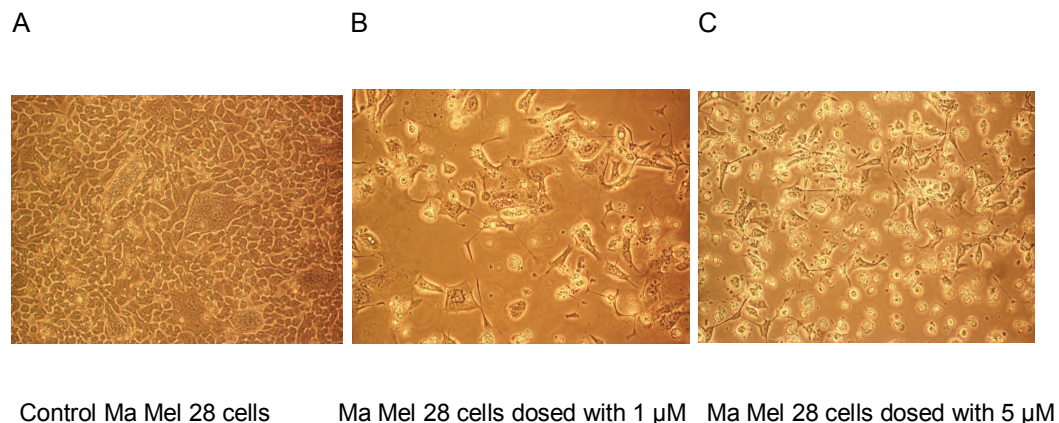


Figure 4.16 Microscopy of Ma Mel 28 cells dosed with trichostatin A after 72 h and taken with a light microscope (x10 lens).

Figure 4.16 shows the effect of trichostatin A at 72 h demonstrating that there are fewer cells present at 1 and 5 μM doses (figure 4.16, B and C) compared with the control. Although the pictures do not represent this clearly due to a lack of picture quality, there were many cells observed suspended in the culture media (4.16, C), accounting for the 31%

increase in RLU with the ToxiLight® assay after 72 h and many of the cells seen lack the cellular junction that connects adherent cells with their adjacent neighbours. The remaining cells are shown to be adherent and appear healthy, although fewer in number compared to the control; this correlates with the ViaLight® and ToxiLight® data, indicating cytoostasis. To further confirm the data, propidium iodide (PI) staining and trypan blue exclusion was carried out.

	<i>% PI Uptake</i>	<i>% Trypan Blue Uptake</i>
Control Cells		
Time (h)		
24	7.06	4
48	8.97	4
72	10.43	7
1 µM TRICHOSTATIN A		
Time (h)		
24	7.56	3
48	12.34	6
72	17.49	11
5 µM TRICHOSTATIN A		
Time (h)		
24	9.95	5
48	14.08	9
72	27.41	16

Table 4.04: Ma Mel 28 cells treated with trichostatin A (0, 1 and 5 µM) for 24, 48 and 72 h and stained with propidium iodide and compared with trypan blue exclusion.

The above data is representative of one experiment (n=1)

As observed with the ToxiLight® assay (figure 4.15; B), there was little change in PI uptake over a 24 h period. The percentage obtained with PI uptake after 48 h (5 µM trichostatin A) revealed a 14% increase and at 72 h (5 µM trichostatin A), a 27% increase in PI uptake (table 4.04). This confirmed the ToxiLight® data, demonstrating that very few cells were undergoing cell death as a result of trichostatin A exposure (figure 4.17). Despite this, the ViaLight® Plus assay had RLUs which reduced considerably after 72 h, revealing the drug is having some effect on the cells, albeit a cytostatic effect. The results with trypan blue uptake, although lower, correlated with PI uptake and the ToxiLight® data, which showed a slight increase in necrotic cells with an increase in drug exposure over time.

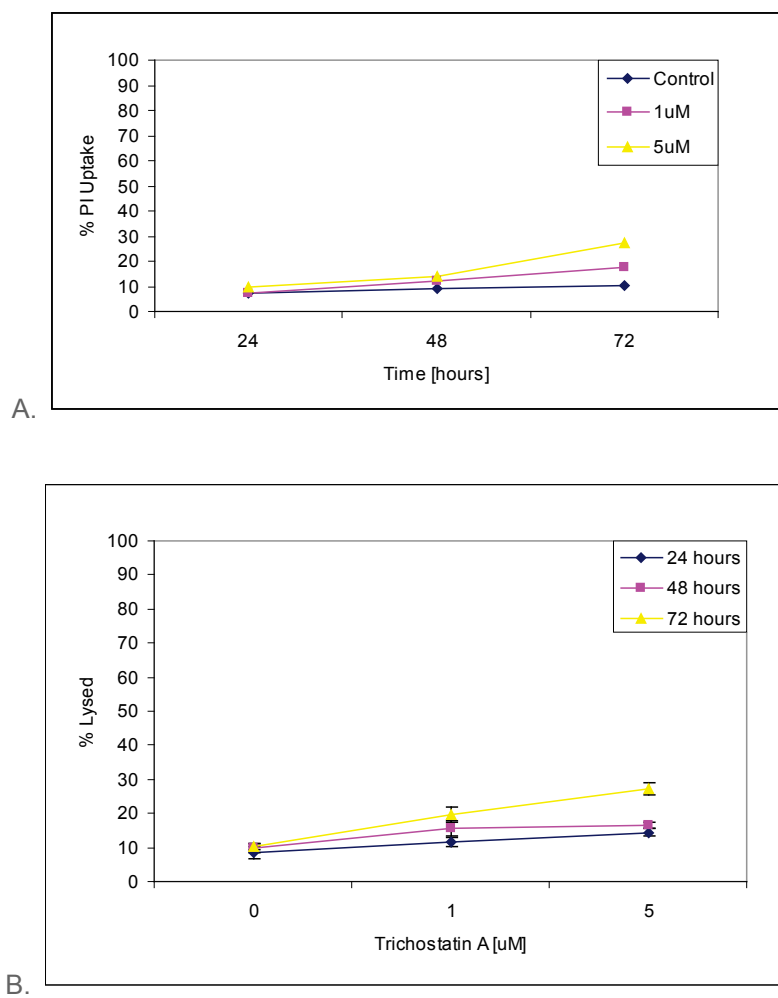


Figure 4.17: Summary comparing the PI uptake data (A) with the ToxiLight data (B). Ma Mel 28 cells treated with trichostatin A (0, 1 and 5 μ M) for 24, 48 and 72 h.

4.2.2.3 Effect of trichostatin A on Ma Mel 26a cells

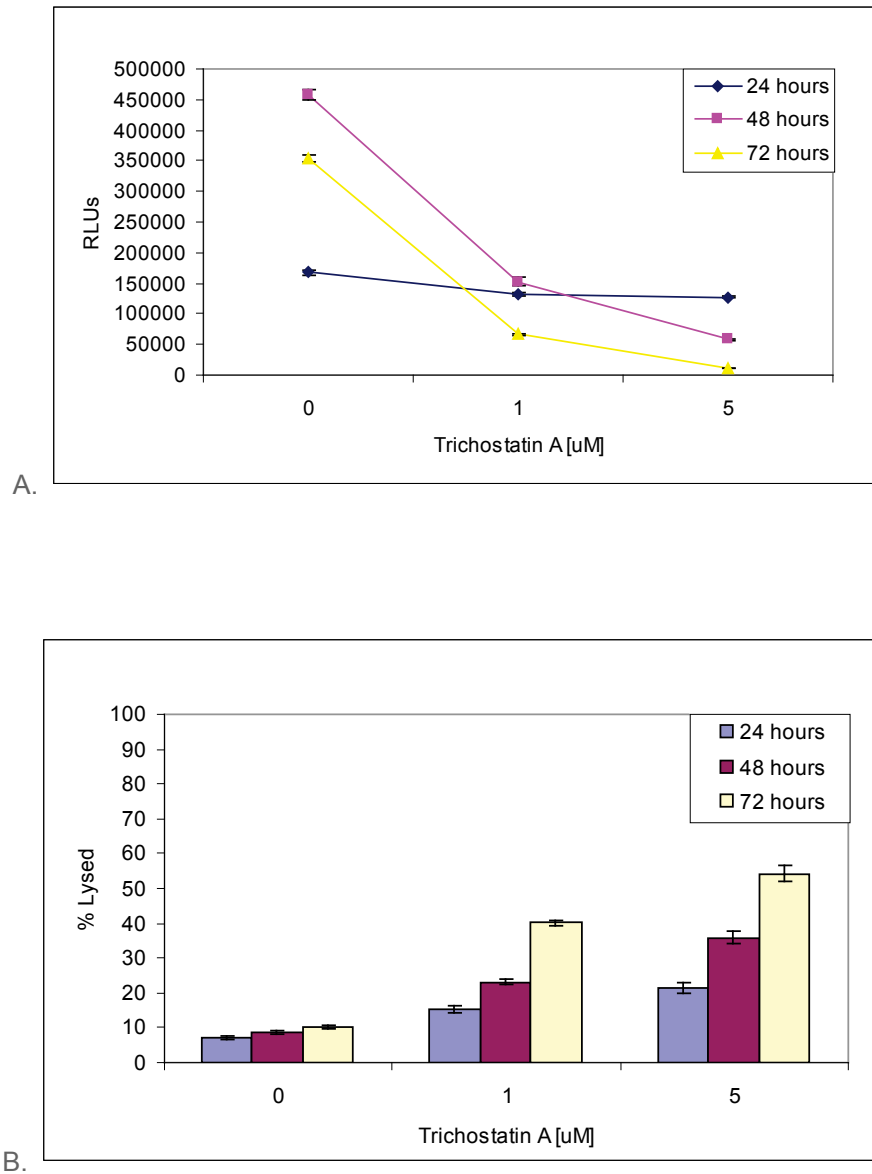


Figure 4.18 Ma Mel 26a cells were treated with trichostatin A and incubated at 37°C for up to 72 h and tested every 24 h for the effects of the drug. Figure A represents the ViaLight® Plus assay, figure B contains the ToxiLight® data. The resulting RLUs were read on an MPL-2 luminometer, show ATP/RLUs +/- standard error of the mean where n=14.

N = number of experiments.

The Ma Mel 26a cells were the final cell line to be tested with trichostatin A. The results summarised in figure 4.18, B revealed this cell line to have the highest observed cell death with the ToxiLight® assay. A concentration dependent increase in AK release could be seen at 24, 48 and 72 h. After 24 hours the % lysed cells had increased from 9% in the control, to 18% and 23% with 1 μM and 5 μM trichostatin A respectively. By 72 h this had further increased to nearly 60% cell death with 5 μM of trichostatin A. Although this still was not 100% cell death, it was a significant change to the previous results observed with MEWO and Ma Mel 28 cells. The ViaLight® Plus data correlated with the ToxiLight®, with a slight decrease in RLUs after 24 h, continuing to drop at 48 and 72 h until the RLUs had fallen to a very low level following treatment with 5 μM trichostatin A.

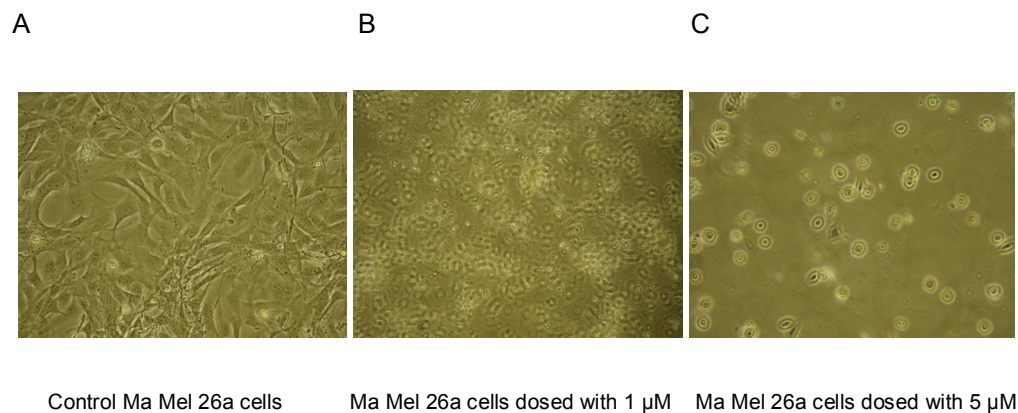


Figure 4.19: Microscopy assessments of Ma Mel 26a cells treated with trichostatin A after 72 h and taken with a light microscope (x10 lens).

The cell morphology in figure 4.19 after 72 h of treatment with 1 and 5 μM trichostatin A clearly shows that there has been a large amount of cell death occurring within the cell population. Although the above pictures are not of good quality, it could be seen that the adherent junctions are no longer visible with 1 μM trichostatin A (B) with very few cells seeming to be adherent with 5 μM trichostatin A (C). This was a very promising result correlating with the large increase in cell death observed with the

ToxiLight® assay. It can be seen clearly from in figure 4.19 that cell morphology had deteriorated more than previously seen with the MEWO and Ma Mel 28 cells. To correlate the ToxiLight® data, propidium iodide (PI) staining and trypan blue exclusion assays were carried out.

	% PI Uptake	% Trypan Blue Uptake
Control Cells		
Time (h)		
24	3.75	2
48	5.79	4
72	10.76	7
1 µM TRICHOSTATIN A		
Time (h)		
24	15.82	8
48	20.72	28
72	47.82	39
5 µM TRICHOSTATIN A		
Time (h)		
24	27.49	19
48	39.95	42
72	67.82	82

Table 4.05: Ma Mel 26a cells dosed with trichostatin A (0, 1 and 5 µM) at 24, 48 and 72 h of incubation and stained with propidium iodide and compared with trypan blue exclusion.

The above data is representative of one experiment (n=1)

The data obtained with Ma Mel 26a cells treated with trichostatin A and stained with PI is shown in table 4.05, revealing a large proportion of the cell population to be necrotic. The percentage cell death assessed with PI uptake and trypan blue staining was greater than that in the ToxiLight® assay (60%) with nearly 70% stain with PI and 82% with trypan blue after 72 h (5 µM trichostatin A). After 24 h a significant difference was

observed, even with 1 μM trichostatin A. The results with PI, although slightly higher correlated with the ToxiLight[®] assay (figure 4.20). The results with trypan blue uptake produced significantly higher results than both the ToxiLight[®] and PI staining. It appeared that nearly all of the cells were necrotic after 72 h of treatment with very few viable cells remaining.

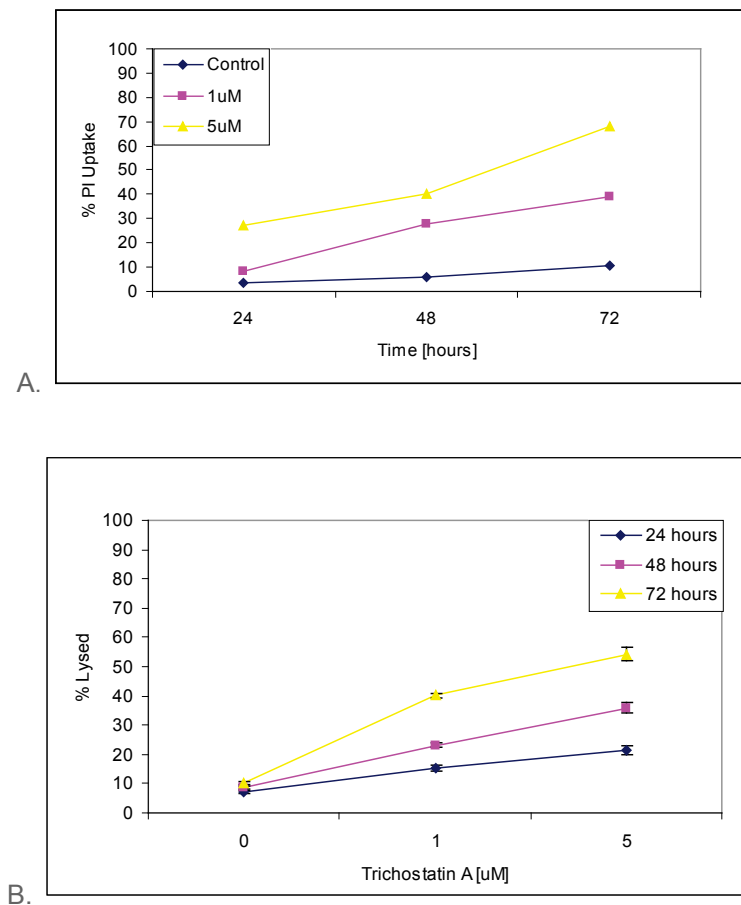


Figure 4.20: Summary comparing the PI uptake data (A) with the ToxiLight data (B). Ma Mel 26a cells treated with trichostatin A (0, 1 and 5 μM) for 24, 48 and 72 h.

Below is a summary table of all experimental results carried out in this chapter:

<i>Cells Tested</i>	<i>Drug Treatment</i>	<i>Published Result</i>	<i>Result from this research</i>
MEWO	Cisplatin	Sensitive/resistant	Cytostatic
	Vindesine	Sensitive/resistant	Cell death
	Doxorubicin	Sensitive/resistant	Cell death
	Trichostatin A	Used in combination therapy (sensitive)	Cell death
ESTDAB 105	Cisplatin	Not published	Resistant
	Vindesine	Not published	Resistant
	Doxorubicin	Not published	Cell Death
WM 1205	Cisplatin	Not published	Cell death
	Vindesine	Not published	Cell death
	Doxorubicin	Not published	Cell death
COLD 794	Cisplatin	Not published	Cytostatic
	Vindesine	Not published	Cell death
	Doxorubicin	Not published	Cell death
Ma Mel 26a	Cisplatin	Not published	Cell death
	Vindesine	Not published	Cell death
	Doxorubicin	Not published	Cell death
	Camptothecin	Not published	Cell death
	Dexamethasone	Not published	Resistant
	Ara-C	Not published	Cytostatic
Trichostatin A	Not published	Cell death	
Ma Mel 28	Cisplatin	Not published	Cytostatic
	Vindesine	Not published	Cytostatic
	Doxorubicin	Not published	Cytostatic
	Camptothecin	Not published	Cell Death
	Dexamethasone	Not published	Resistant
	Ara-C	Not published	Resistant
	Trichostatin A	Not published	Cell death

Table 4.06: Summary of the results found in this research

4.3 Discussion

The work included in this chapter has examined the potential of using the novel bioluminescent assay ToxiLight®; and the ViaLight® Plus assays in parallel with a view to investigating the susceptibility of cells to various known chemotherapeutic agents. The study incorporated six melanoma cell lines, to analyse the effects chemotherapy agents have on cell survival using the ToxiLight®, ViaLight® Plus assay and subsequently P.I. uptake, trypan blue staining and light microscopy to confirm the assay data.

The main objective of this chapter was to obtain further understanding of tumour chemo-sensitivity assays. The response of patients to chemotherapy varies immensely within the same histological tumour type (tumour heterogeneity). Human malignant melanoma, a tumour with a high potential to metastasise, is well known for its resistance to various anti-cancer agents (Nessling *et al.*, 1999). The role of p53 and drug resistance in melanoma has been extensively studied; however, a full understanding of the molecular mechanisms occurring within these cells has not been obtained (Li *et al.*, 1998). An investigation was undertaken to discover sensitive and resistant cell lines to various toxic chemotherapy agents; the selected cells can then be further investigated at the molecular level to ascertain the mechanism(s) of resistance (chapter 5).

Assessment for mycoplasma contamination on all the melanoma cells gave a negative result, and all the drugs (doxorubicin, vindesine and cisplatin) were screened at their working concentrations with both the ToxiLight® and ViaLight® Plus assays to ensure there was no interference with either assay. The standards for both AK and ATP, with and without the drugs showed no significant difference.

4.3.1 Effect of doxorubicin on melanoma cells

The four cell lines, COLD 794, ESTDAB 005, WM 1205 and MEWO and the recently established Ma Mel 28 and Ma Mel 26a were all exposed to the anti-tumour antibiotic doxorubicin, with a view to establishing their drug sensitivity / resistance. It was concluded that the most sensitive cell line to doxorubicin was MEWO. The data with doxorubicin treatment is new and has not been found in published data. All of the cell lines showed a concentration dependent effect with the drug, revealing that doxorubicin had prevented replication of the cells. Doxorubicin is known to interact with DNA by intercalation and inhibition of macromolecular biosynthesis (Momparler *et al.*, 1976). It inhibits the progression of the enzyme topoisomerase II, which “unwinds” DNA for transcription. Doxorubicin stabilises the topoisomerase II complex after it has broken the DNA chain in readiness for replication, preventing the DNA double helix from being resealed and thereby inhibiting the process of replication. Due to the consistent effects of this drug on the melanoma lines tested, it was difficult to differentiate sensitive from resistant cell lines.

In contrast, the data produced from dosing the cells with doxorubicin, revealed two varying results. Doxorubicin had a cytotoxic effect on the Ma Mel 26a cells assessed by the ViaLight® Plus assay but no change was observed in the ToxiLight® assay, concluding that the drug was cytostatic for cell growth. The cells had been prevented from proliferating but no cell death was occurring. The Ma Mel 28 cell line proved to be the most resistant of the six lines tested and was used in subsequent experiments.

4.3.2 Effect of cisplatin and vindesine on melanoma cells

Subsequent data with cisplatin and vindesine on all six cell lines demonstrated cell death in COLD 794 and WM 1205 and Ma Mel 26a cells by the ToxiLight® assay. WM 1205, Ma Mel 26a and MEWO cells were consistently sensitive to doxorubicin, cisplatin and vindesine with an increase in AK release in all experiments compared to the other cell lines. As previously mentioned MEWO cells had been previously published with cisplatin and vindesine (Nessling *et al.*, 1999) revealing the sensitive nature of the cells to these drugs. In comparison however, no cell death was seen in either the ESTDAB 005 or Ma Mel 28 cells, which were resistant to both cisplatin and vindesine. This is new data that has not been published. The Ma Mel 28 cells revealed resistance to all three drugs tested, while ESTDAB 005 cells were only sensitive to one drug; doxorubicin. This led to the belief that apoptosis and cell death within melanoma cells could be drug specific as shown previously by Kissel (2006) who investigated sensitive and resistant strains of MEWO cells to etoposide and cisplatin.

The data presented in this study suggests that the Ma Mel 28 cells could be used as a resistant cell line, at least in the context of cisplatin, doxorubicin and vindesine. Ma Mel 26a cells were sensitive to all three drugs and were chosen as a sensitive cell line. Both these cell lines were obtained from known patients with no previously published data. The history of the individual patients in respect to their individual therapy was available although the research was conducted blindly. To confirm this hypothesis of drug sensitive and resistant cells, three in-house drugs (camptothecin, ara-C and dexamethasone) were used against Ma Mel 26a and 28 cell lines. Ma Mel 28 cells demonstrated resistance to all drugs except camptothecin used in the study and in addition there was no concentration dependent reduction in ATP with increasing exposure to

dexamethasone, implying the cells were also resistant to cytostasis. Ma Mel 26a cells were also resistant to dexamethasone, an effect not previously reported with these cells. With ara-C a slight drop in ATP was observed with both cell lines with an increase in drug exposure but no cytolysis observed. Camptothecin on the other hand, caused cell death in Ma Mel 26a cells with a drop in ATP and a significant increase in RLUs with the ToxiLight® assay. The conclusion from these results was that melanoma cells respond differently to various chemotherapeutic agents. One cell line may respond positively to one toxic agent but not another, and demonstrates that individual patients may respond differently to the agents used for treatment. The basis for drug resistance in melanoma is most likely dysregulation of apoptosis, although other mechanisms including drug transport, detoxification, and enhanced DNA repair may also play a role (Grossman and Altieri, 2004).

4.3.3 An investigation into the effects of trichostatin A on melanoma cells.

Histone deacetylase inhibitors (HDACIs) are a promising group of compounds inducing differentiation, growth arrest and apoptosis in tumour cells. The latter part of this study uses a combination of the ToxiLight® and ViaLight® Plus assays to monitor the effectiveness of the HDACI, trichostatin A on three melanoma cell lines. Previous studies concluded that the two cell lines Ma Mel 26a and Ma Mel 28 would be suitable for these experiments. These cells originate from patients with melanoma and no published has been found using them. The patient history is accessible for this study which was carried out blindly. A third cell line, MEWO, was selected for its sensitivity and its reported drug sensitivity in previous research (Kiesel, 2006). From the data it can be seen that trichostatin A does have an effect on MEWO cells, resulting in 50% necrosis upon exposure to 5 µM; this result correlated with the

FACSCalibur™ and trypan blue exclusion data demonstrating although trypan blue uptake remained much lower than both PI and the ToxiLight® data, throughout the experiment, probably due to many of the dead cells degrading to form apoptotic bodies, not being accountable in this methodology. ToxiLight® on the other hand measures a stable enzyme in culture and should therefore be more sensitive and accurate.

The most sensitive cell line was Ma Mel 26a, resulting in nearly 60% necrosis, again correlating with the data gained from the FACSCalibur™ analysis and trypan blue uptake. Ma Mel 28 cells proved to be resistant to trichostatin-A, although cytostasis was achieved with a reduction in ATP being observed. This was an encouraging result and suggests that histone deacetylase inhibitors (HDACIs) could be used in future research with melanoma cells. Histone acetylation is the subject of both research and clinical investigation (Haggarty *et al.*, 2003). Response to HDACIs has also been observed by Peltonen *et al.*, (2005), in studying the cellular effects of trichostatin A (TSA), on a panel of melanoma cell lines and its mechanism of action in relation to p53. While growth arrest was induced in all cell lines studied and apoptosis in the majority, these cellular effects were independent of the p53 status of the cells. The results from Peltonen *et al.* indicated that trichostatin A activated the apoptotic pathway in two out of the three cell lines tested; this could therefore provide alternative therapeutic approaches for melanoma treatment, whether alone or in combination therapy.

The next phase of this study was to use frozen samples of all the cell lines treated with and without trichostatin A and analyse changes in the cell proteome correlating with cytotoxicity/viability. MALDI-TOF MS analysis will be used to derive protein/peptide profiles. The results from the MALDI analysis will then be subjected to bioinformatic analysis, using artificial neural networks to identify potential biomarkers that may associate with melanoma cell apoptosis.

Chapter 5: Identification of important ions using proteomics and bioinformatics analysis which could be associated with drug response.

5.1 Introduction

In the UK alone, more than 10,000 people are diagnosed with skin cancer each year. About 3 out of every 100 cancers diagnosed (3%) are melanomas. Although not a common cancer, melanoma is important because it is easily curable if diagnosed early. Primary treatment involves surgical removal of the melanoma which results in 98% of low-risk patients being cured. However, if the disease has progressed current treatment is still experimental and effective only in a small number of cases. There is no recent evidence to show that survival rates have improved due to adjuvant therapy. Serum biomarkers that are currently used clinically, with the ability to differentiate between high and low stage melanoma patients are lactate dehydrogenase (LDH), S100B and melanoma-inhibitory activity (MIA). These tests lack sensitivity and are unreliable predictors of asymptomatic and metastatic cancer (Matharoo-Ball *et al.*, 2007). This has resulted in a large amount of research being undertaken to search for melanoma biomarkers that predict a patients' risk of cancer or metastasis and to monitor those receiving adjuvant therapies. Phenotypic expression patterns could hold the key to certain pathological conditions resulting in the discovery of novel biomarkers or as a target for new therapies. Techniques involving molecular profiling are not only confined to identifying macromolecules (e.g peptides/proteins) that could form the basis of new treatment regimes (Mian *et al.*, 2003), they can even be applied as a novel methodology for the pathological classification of diseased tissue such as cancer (Koomen *et al.*, 2005; Matharoo-Ball *et al.*, 2007; Ball *et al.*, 2001).

One approach that shows great promise is proteomic profiling, in which new methods for sensitive and reproducible identification and quantification of thousands of different proteins in cells and serum are being applied to analyse molecular changes in melanoma (Bernard *et al.*, 2003). The availability of new mass spectrometers capable of high-throughput protein analysis has brought about powerful screening methods for identifying protein signatures with disease stage. The two most popular approaches in analysing and identifying proteins that are present in biological samples are MALDI (matrix assisted laser desorption ionisation) and SELDI (surface enhanced laser desorption ionisation) mass spectrometry (MS). These methods are capable of measuring protein profiles as a “top-down” approach, analysing intact proteins in complex mixtures, and peptides, a “bottom-up” approach. The robustness of MALDI-TOF-MS facilitates the investigation of complex samples and has been applied successfully using a variety of statistical pattern-recognition tools for early cancer detection in ovarian, colorectal, breast, prostate, astrocytoma/glioblastoma and melanoma cancers (Mian *et al.*, 2005; Petricoin *et al.*, 2002; Li *et al.*, 2002; Matharoo-Ball *et al.*, 2007). SELDI, introduced by Hutchens and Yip, utilises a sample platform using solid phase supports or “chips” coated with a selection of chemical or biochemical agents for protein separation prior to analysis by MALDI (Li *et al.*, 2002). A limitation of MALDI-MS and SELDI-MS analysis is that identification of proteins cannot be carried out by measuring the protein molecular weight or m/z without the incorporation of protein digestion. This is usually carried out separately following 2-DE analysis of proteins or as in solution digestion prior to MS analysis.

There has been much controversy about the methodology used regarding biological, technological and data mining tools that could introduce bias. These mainly refer to the way samples are collected, processed and

stored, instrumentation and data analytical methods used. The research team at Nottingham Trent University has employed a combination of an automated robotic chromatographic ZipTip™ methodology combined with MALDI-TOF-MS generating a powerful and sensitive analysis of samples (Matharoo-Ball *et al.*, 2007). This method enables measurement at the protein level, with the same sample tryptically digested for measuring peptides (bottom-up) for identification as demonstrated in figure 5.01. Measurement of proteins alone would require further investigation by additional techniques to confirm identification.

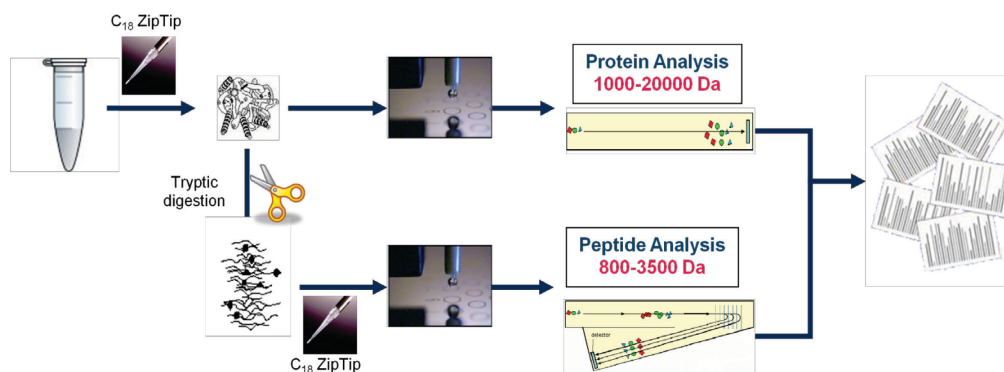


Figure 5.01 A flow diagram to illustrate the procedure of mass spectrometry

Due to the high number of samples and the quantity and dimensionality of the data produced by MALDI-TOF MS, data mining tools are essential in order to sort through the data for protein or peptide patterns. To produce accurate and sensitive predictions of important ions, the statistical methods used have to be very powerful. Some of the methods assessed include Bayesian analyses, fuzzy logic, and the computational tool employed in this study, artificial neural networks (ANNs). ANNs are divided into two main classes; supervised and unsupervised methods (Lancashire *et al.*, 2005). Supervised learning involves a dataset consisting of both input and output data which is presented to the ANN during a training phase. The ANN tries to find a link between the data that

results in the least error adjusting the weighted links until this error falls below a certain threshold. Once the ANN has established a connection between the inputs and outputs, the model can then be utilised for unseen data. In comparison, unsupervised learning uses only the input dataset and the ANN is free to search for hidden relationships amongst this data (Tafeit *et al.*, 1999). Recent studies have shown that the application of ANN-based approaches can be used to identify patterns strongly associating with specific disease stages (Matharoo-Ball *et al.*, 2007; Ball *et al.*, 2002; Petricoin *et al.*, 2002). The ANNs used in the present study, uses the supervised approach, learning predictive patterns contained within complex datasets, by adjusting and updating the connecting weights between the layers of the network using the back propagation (BP) algorithm applied to the multi-layer perceptron (MLP).

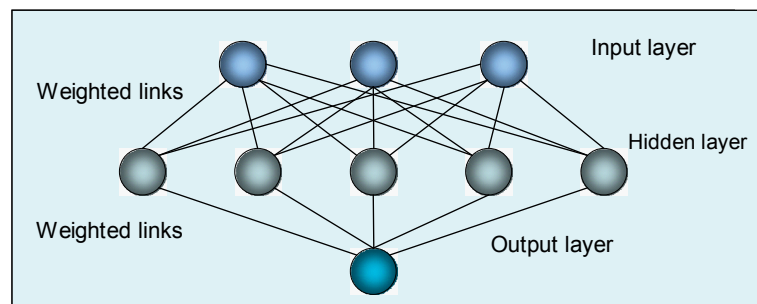


Figure 5.02 To show the structure of the multi-layer perceptron ANN

- **Input layer:** Receives input from the raw data, corresponding to one of the variables i.e. control (1) or drug treated (2).
- **Hidden layer:** It is a feature detector which can classify non-linear data.
- **Output layer:** The data from this section are the final results.

As illustrated in figure 5.02, the ANNs are trained using the input layer (representing independent variables), and given the resulting output or correct sample group. The input layer could represent the m/z value and intensity from a set of mass spectral profile data. (Note: The ion values (m/z) represent $[M+H]^+$ ions from the MALDI-MS). The hidden layer represents the mathematical mechanism of the model and it learns by processing all the data and information it receives to find patterns between sample groups and passes it to the output layer via weighted links. The output layer is calculated by the network based on the data inputted, and is then compared with the actual known output. For example, in a classification model an output of 1 would represent a control sample and an output of 2 would represent a cancer-treated sample, and then the error between the predicted and actual outputs is calculated. This error demonstrates how well the ANNs are working.

When using ANNs, analysing the data can be separated into three groups; (1) the training data as previously mentioned; (2) the test data where the ANNs are checked and validated for its outputs on the test set whilst the training occurs and (3) once training has been completed, it is validated by a further set of completely blind data which are applied and an output calculated based upon the new data (Basheer *et al.*, 2000; Lancashire *et al.*, 2005). The performance on unseen data indicates whether a generalised model has been obtained or not. By using multiple models with different unseen datasets (random sample cross validation) a more generalised model may be obtained with only a small sample number. ANNs are based on biological neurons which are highly organised, processing information which contains high levels of noise and redundancy (Ball *et al.*, 2002). Their ability to learn and adapt, allow the system to modify itself enabling analysis of unseen data. ANNs have been used in a variety of applications including modeling, classification,

pattern recognition, and multivariate analysis. The stepwise approach used in this study is a detailed method of parameterisation, whereby ions are added step by step for the determination of the best subset of ions to predict a particular outcome. Interactions between the ions may also be identified in this way. The analysis is based on the hypothesis that the change in performance when an input is added indicates its influence on the model. Multiple sub models are run with input 1, then with 2, and then with input 3 and so on until all of the inputs are modeled separately. The error known as “test error” is determined for each sub model and the input that gives the best “test performance” and the lowest “test error” is selected. This is then placed with all of the remaining inputs sequentially in a number of sub models once more. This process continues adding more inputs until there is no improvement in the error revealing a subset of identified ions.

The aim of the research in this chapter was to identify molecular factors that may be associated with the drug-resistant or sensitive phenotypes of three pre-selected malignant melanoma cell lines. To minimise criticisms involving bias in biomarker identification a validated, robust, and reproducible methodology based on MALDI-TOF-MS combined with bioinformatics to profile tryptic peptides was used. The three human melanoma cell variants exhibiting low and high levels of resistance to various drugs tested in chapter 4 were exposed to the histone deacetylase inhibitor, trichostatin A. Its effect on these cells was characterised using MALDI-TOF MS for peptide identification. Alterations in the various protein expressions were monitored over time and at different dose concentrations of the drug, thus simulating a situation close to clinical chemotherapy. ANNs were applied to the data for the cell lines and a panel of peptide biomarkers obtained correlating to the dose and time of drug exposure.

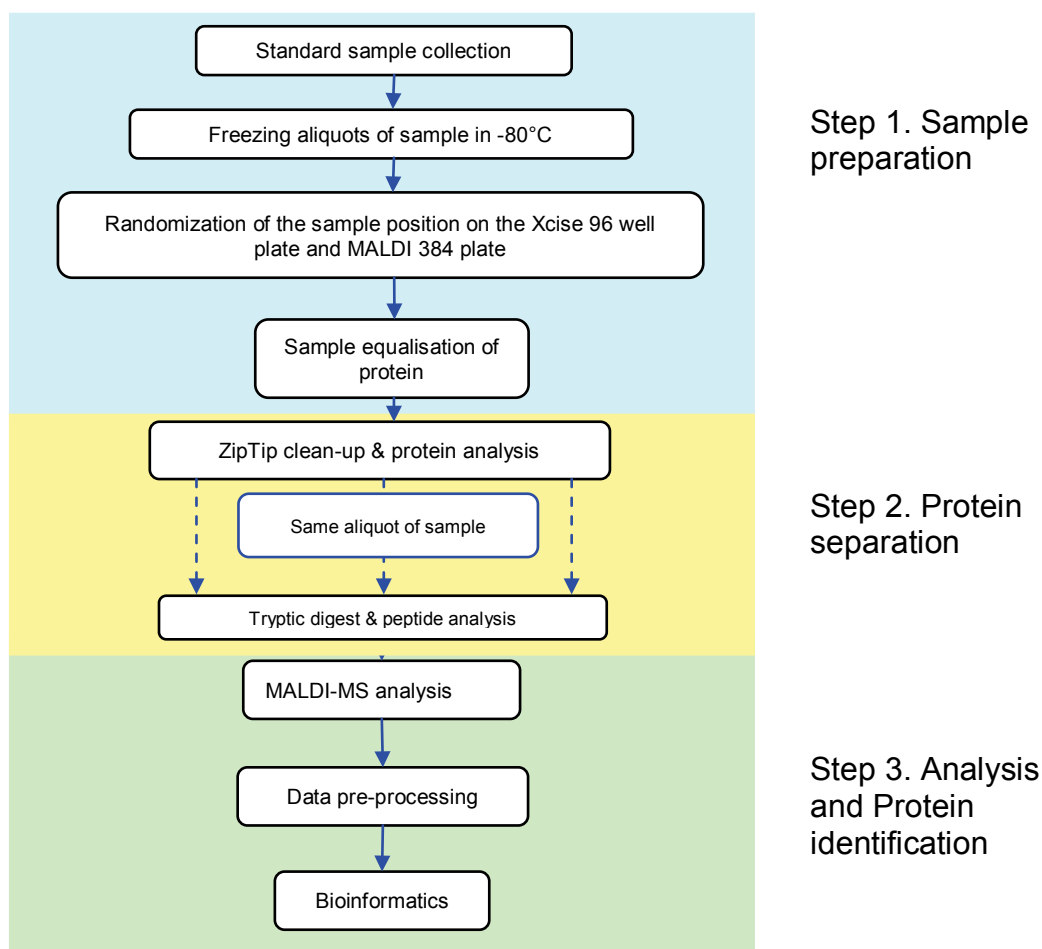


Figure 5.03 Schematic flow chart outlining the methodology carried out in this study for biomarker identification.

The aims of this chapter will be to:

- Prepare and optimise the samples for analysis.
- Separate the proteins using C_{18} ZipTips, utilising an automated methodology (Xcise, Proteome Labs, Shimadzu, Manchester, UK), followed by tryptic digestion of the cellular proteins and a second C_{18} ZipTip for desalting and concentration of the sample.
- To analyse the samples by MALDI-TOF MS and then visually inspect the data.

- Pre-process the MALDI-TOF MS spectra ready for bioinformatic analysis using ANNs.
- Train and test the ANNs and allow the trained network to recognise key differences between drug-treated and untreated melanoma cells using a blind dataset.
- Carry out MALDI-TOF MS/MS for protein identification of the tryptic peptide ions predicted by ANNs.

5.2 Results

5.2.1 Protein quantification of melanoma samples

Protein quantification was performed using the Bio-Rad protein micro assay as described in chapter 2.9.2. The standard curve used for the quantification of protein in the MEWO cell samples is illustrated in the graph below (figure 5.04). As can be seen an R^2 value of 0.98 was achieved from this experiment with the standard curves for Ma Mel 26a and Ma Mel 28 cells resulting in an R^2 value of 0.97 and 0.98 respectively.

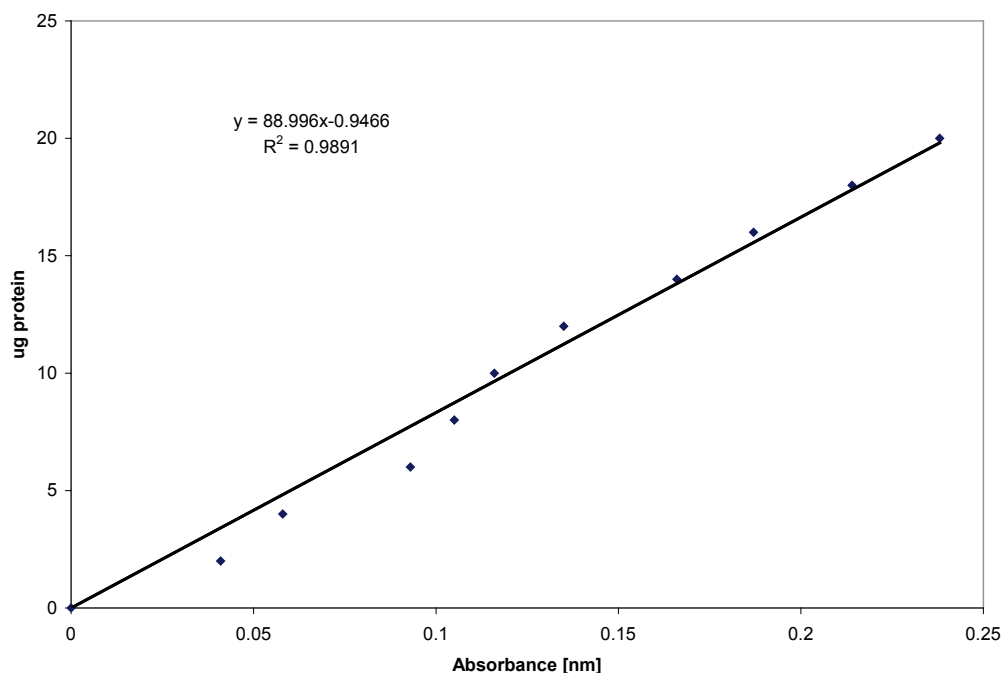


Figure 5.04 An illustration of the BSA standard curve obtained after measurement on a plate reader at an absorbance of 595 nm.

5.2.2 Sample optimisation

Once the amount of protein was quantified on all 3 cell lines, the frozen aliquots of the Ma Mel 26a cell lysates were corrected to 0.1 mg.ml^{-1}

using 0.1% TFA prior to analysis on the MALDI-TOF MS. This concentration was chosen because the majority of the samples had very low starting protein concentrations. Samples were optimised as explained in chapter 2.9.3 and 2.9.4 prior to sample randomisation on the MALDI target plate using Microsoft Excel 2003. Once randomised and diluted the samples were processed on the robotic system Xcise (Shimadzu, Manchester, UK).

5.2.3 MALDI-TOF-MS

The samples were analysed using an Axima CFR⁺ MALDI-TOF mass spectrometer (Shimadzu, Manchester UK) operated in reflectron mode mass range of 800-3500 Da for peptide analysis. Mass spectra acquisition was performed using autoquality mode, with the accumulation of 100 profiles and using per 5 shots per profile. After data acquisition by MALDI-MS, all spectra were checked visually to ensure the quality and if they resembled a blank profile then these were removed prior to ANN analysis. Figure 5.05 shows the spectra observed from six QC samples at various positions on the same MALDI target plate demonstrating the reproducibility of the MALDI-TOF MS method. There is still some slight variation in the intensities of some peaks even though they have been subjected to the same MALDI MS run, laser power and matrix. However, these samples undergo a cleaning procedure twice on the robotic system prior to MALDI analysis which may increase the variability between samples. Another observation of the QC samples in figure 5.05 is that although the spectrum obtained is highly reproducible, it is also very complex making many individual peaks difficult to compare and identify without closer inspection.

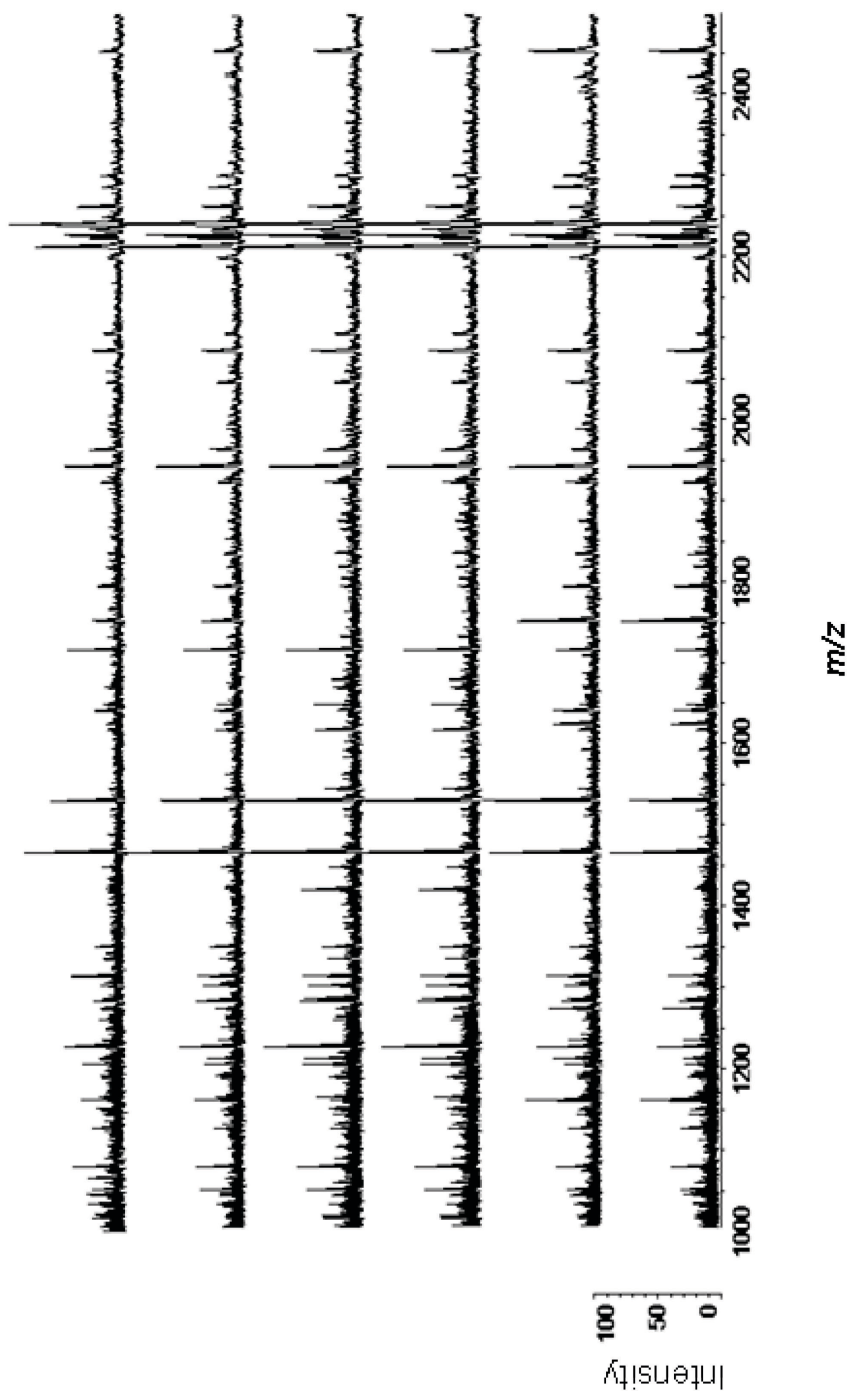


Figure 5.05 Example of the reproducibility of MALDI MS profiles in the 1000-2500Da mass range. The figure shows six random QC samples after tryptic digest, run in reflectron mode. Each spectrum is representative of a QC sample run on different positions of the MALDI target plate.

5.2.4 Ma Mel 26a cells

Preliminary work was carried out on the Ma Mel 26a cells to investigate the proteomic profile differences between drug-treated and untreated cells after initial dose (day 0), day 1, day 2 and day 3 after drug exposure for identification of biomarkers that could correctly classify differences between these groups. Upon visual inspection, differences were observed between the tryptic peptide spectra obtained from treated and untreated cells. The representative spectra for the peptides with 1 μM and 5 μM trichostatin A are shown in figures 5.06 and 5.07 respectively. As can be seen, these spectra are too complex and the pattern differences between the groups are ambiguous by eye. Any visual differences seen between the treated and untreated cells may not necessarily mean that they will be important predictive markers.

Differences seen in ions m/z 1321 and 1468 (figure 5.06) appear to show the protein being expressed less in the drug-treated cells with the intensity dropping at each time point measured from day 0 to day 3. Figure 5.07 shows an ion at 1568 which appears to increase in intensity over time, showing expression within the cells as they are treated with trichostatin A. After day 3 the intensity of the ion appears to drop again. Even though the samples were equalised for the initial protein concentration the general spectra at day 3 appeared to have a trend of lower intensity peptide peaks compared with days 1 and 2 of exposure. It was however noted from the spectra that the protein levels needed to be more concentrated than the 0.1 mg.ml^{-1} that was used, as very few peptide peaks could be visually seen with even less observed after 3 days as mentioned above. There are other peaks that could also be said to have differences within the spectra but due to the number of samples

analysed and complexity of the data the application of ANN analysis was necessary for full data analysis.

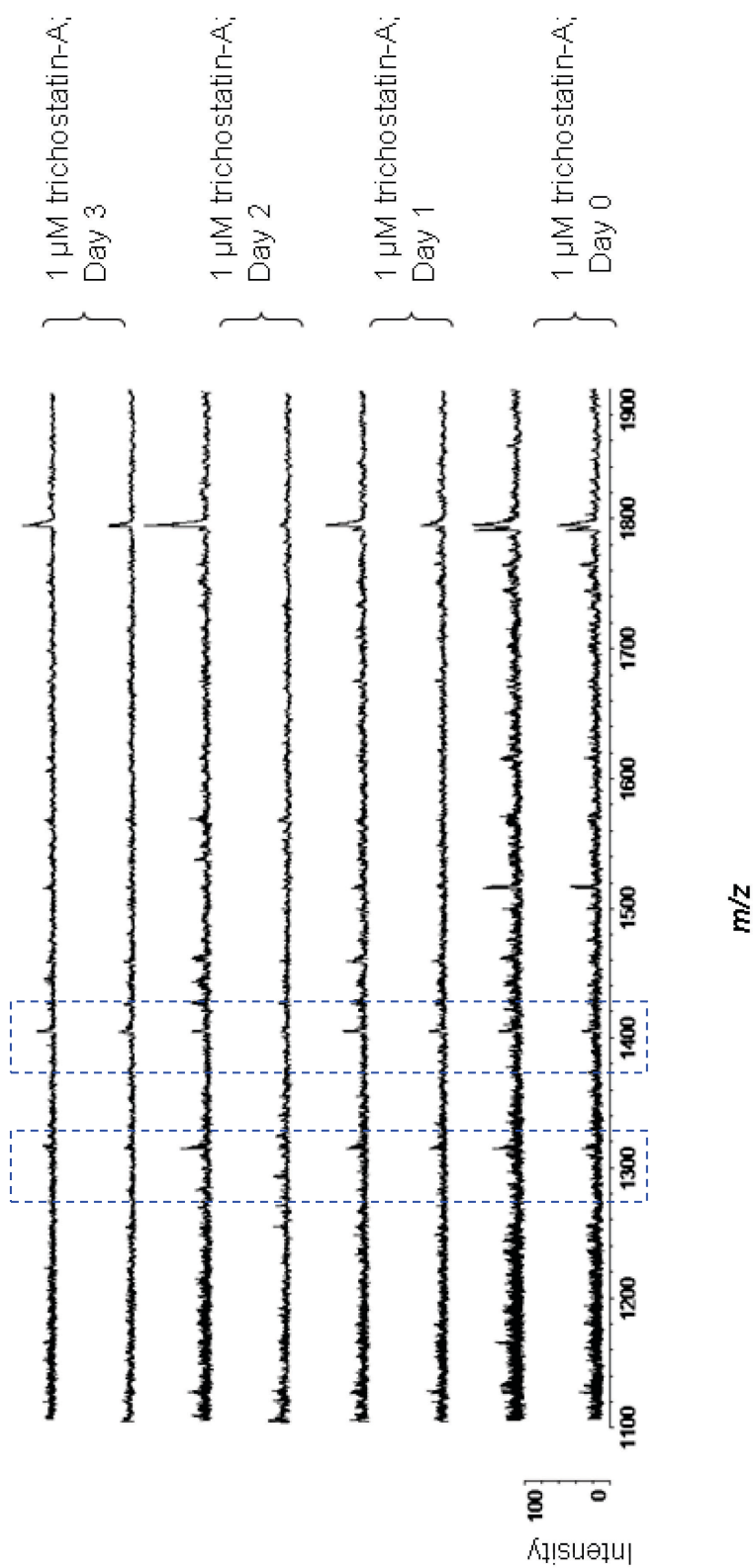


Figure 5.06 Representative spectra of Ma Mel 26a cell tryptic peptides, after treatment with 1 μ M trichostatin A, acquired in reflectron mode. The regions highlighted show visual differences.

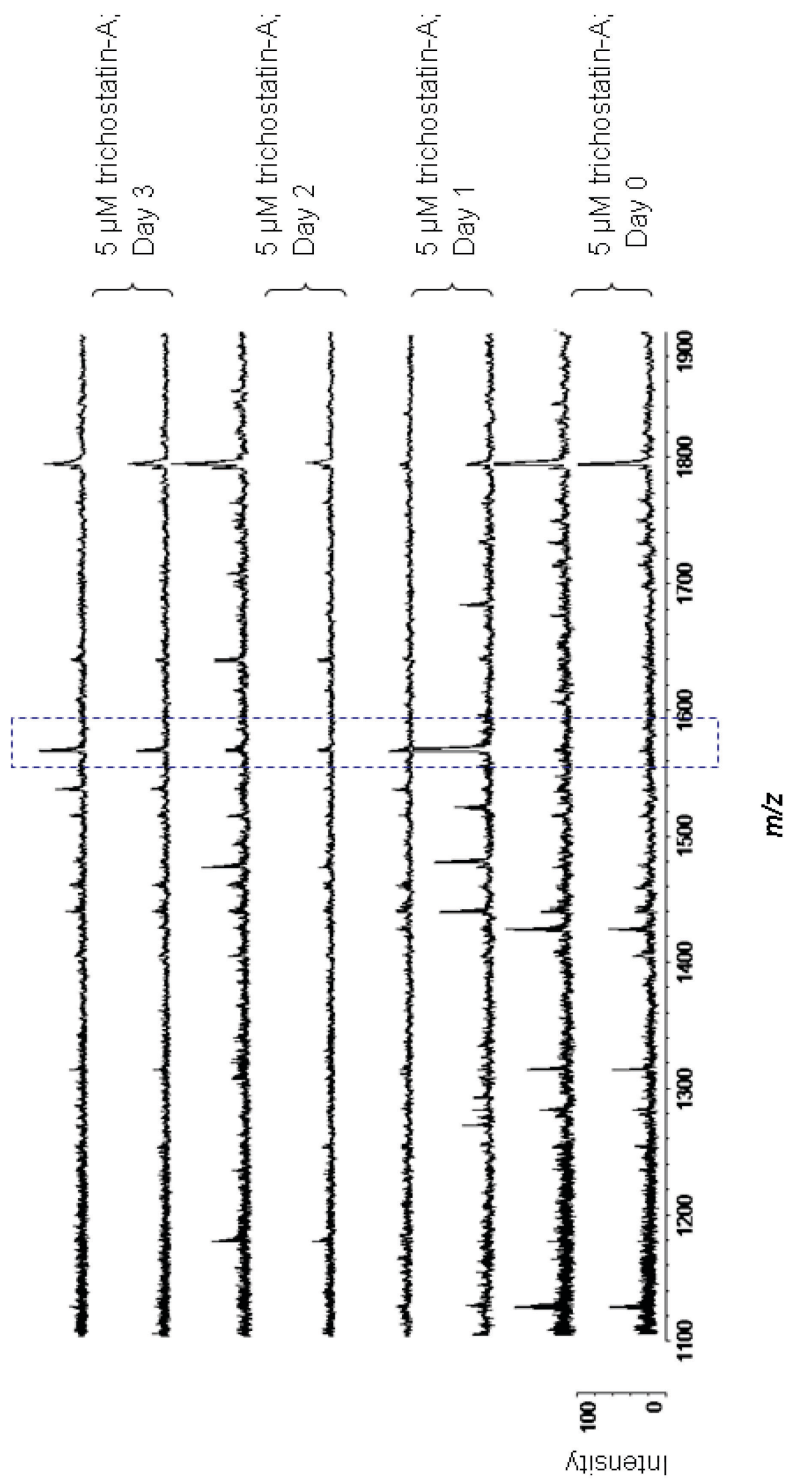


Figure 5.07 Representative spectra of Ma Me1 26a cell tryptic peptides after treatment with 5 μM trichostatin A, acquired in reflectron mode. The regions highlighted show visual differences.

5.2.4.1 Bioinformatic analysis of Ma Mel 26a cells using ANNs

Bioinformatic analysis was carried out to compare the different profiles obtained by MALDI-MS, using a stepwise approach. To interpret this highly complex data, a sophisticated algorithm (i.e. ANNs) was employed. Prior to ANNs analysis it was essential to reduce the data points by rounding (binning) the m/z values to the nearest Dalton, to increase the accuracy and efficiency of the analysis. Any spectra that looked like blank profiles or not having consistent peaks were removed prior to ASCII file conversion and bioinformatic analysis. A stepwise approach was utilised to train the data to recognise key peptide profiles that differentiated untreated cells versus the cells treated with the drug to give a panel of important biomarkers. A multi-layer perceptron ANN with a back propagation was used for this study as described by Lancashire *et al.* (2005) and demonstrated in figure 5.02. The m/z MALDI-MS data were used to train, test and validate the ANN model which was developed using random sample cross validation where the data is randomly split into three subsets. The data consisted of $n=14$ experiments with each time point (0, 24, 48 and 72 hours) and drug treatment (0, 1, 5 μM) (i.e. 168 datapoints (14x12)). 60% of samples from each cell line were set aside for training, with 20% used to test the performance of the ANNs and then a final 20% of the samples used as a blind or validation set of data. The primary ion identified by the model was used as a single input and for each model 50 random training/test/validation bootstrapped subsets were used. The model with the lowest predictive error determined the most important input. This identified input was then combined with a second input (two inputs) to train the models as described above and accordingly the second important ion was identified. This process was continued until no significant improvement in the performance of the model was obtained by adding new inputs. This methodology resulted in the production of a list of key ions, as shown in table 5.01 for Ma Mel 26a cells. These ions

are the most important for correctly classifying the two classes of samples: untreated and treated cells.

Stepwise steps	m/z [M+H]⁺	Test Performance (%)	Test Error
Day 1 Control vs 1 μM			
1	1082	75	0.166
2	1680	83	0.141
Day 2 Control vs 1 μM			
1	844	71	0.193
2	1793	85	0.126
3	3163	86	0.089
4	1666	100	0.059
Day 3 Control vs 1 μM			
1	2782	75	0.191
2	2955	75	0.149
3	1429	88	0.126
Day 1 Control vs 5 μM			
1	3334	79	0.157
2	2355	79	0.132
3	1476	86	0.114
Day 2 Control vs 5 μM			
1	3235	71	0.191
2	1025	85	0.139
3	2553	86	0.109
4	1107	100	0.068
Day 3 Control vs 5 μM			
1	1062	85	0.859
2	2155	86	0.135

Table 5.01 Artificial Neural Network results of Ma Mel 26a cells (n=14). Table to show the test performances and the mean squared error for the test data sets as each input is added to the model. The results show the top ions that gave the best accuracy of prediction with the error failing to improve with subsequent additions.

N = number of experiments

As can be seen in table 5.01, several ions have been identified as important in each of the models. In the control versus treatment exposure (1 μ M) for day 1, the first step of the model identified the ion at m/z 1082 which shows a significant difference in 75% of the data analysed; this was demonstrated to be the most important ion. The addition of the second ion at m/z 1680 increased the performance to 83% after which the addition of further ions did not improve the model. After day 2 of drug treatment a new set of ions were shown to be important with ion m/z 844 showing a 71% performance. The addition of ions 1793, 3163, 1666 produced a 100% performance rate. At day 3, three ions were identified, ion m/z 2782 being the most important with the addition of the ions 2955 and 1429 giving a model performance of 88%. Treatment with 5 μ M trichostatin A showed ion m/z 3334 between the groups to differentiate with a 79% accuracy, ions 2355 and 1476 resulted in 86% performance; day 2 identified four ions; 3235 (most important), 1025, 2553 and 1107, combined gave a 100% performance rate and at day 3, 1062 and 2155 gave an 86% performance rate.

5.2.4.2 Validation of ANNs with blind data set

After training and testing of the model was completed, a new independent blind set of data, not previously incorporated into the model was presented to validate the results by evaluating the ability of the model to assign these new samples to the correct class. Validation samples $n=5$ of treated and $n=5$ of untreated for each drug concentration and drug exposure time were used for data analysis. For the untreated compared to the treated cells with 1 μ M trichostatin A, the model correctly classified only 55% of the day 1 dataset, 45% of the day 2 dataset and 60% of the day 3 dataset. This series of experiments questioned the validity of the model and predicted ions (table 5.01) to associate and define the class of

samples. For the untreated compared to the treated cells with 5 μ M trichostatin A the model also failed to predict unseen samples accurately, 38% were correctly classified for the day 1 dataset, 48% correct for the day 2 dataset and only 33% classified correctly for day 3. With the original spectra proving inconclusive visually, due to the low concentration of protein, and the additional lack of good quality ANNs data, the biomarker ions identified within these models were considered to be inaccurate and were not analysed by MS/MS. The cell line could not be repeated at a higher protein concentration due to a lack of cell samples remaining. Time permitting the original experiments would have been repeated.

5.2.5 Ma Mel 28 cells

Due to the low quality of spectra produced for the Ma Mel 26a cells using a protein concentration of 0.1 mg.ml^{-1} , the starting protein concentration was increased to 0.5 mg.ml^{-1} for subsequent experiments. After a visual inspection of the peptide spectra (shown in figures 5.08 and 5.09), it can be seen that the increased protein levels led to a better quality spectra when compared to the Ma Mel 26a data (figures 5.06 and 5.07). Visual differences were possible because cell spectra were equalised for the same peak intensity. Due to the large amount of data, only a few peaks were identified visually as showing differences between the treated and untreated cells. Ions m/z 1346, 1439 and 1618 were seen to have an increasing intensity when the cells were treated with $1 \text{ }\mu\text{M}$ trichostatin A as shown in figure 5.08. Ions m/z 1482 and 1676 were the two peaks shown to increase in intensity (figure 5.09) with the increase in drug-treatment to $5 \text{ }\mu\text{M}$ trichostatin A. As seen previously with the Ma Mel 26a cells, after day 3 of treatment with $5 \text{ }\mu\text{M}$ trichostatin A, the spectra has significantly less peptide peaks. The ions m/z 1482 and 1676 appear to decrease in expression in this spectrum possibly due to the secretion of the protein into the surrounding media or initiation of apoptotic mechanisms which may suggest cell death following drug exposure.

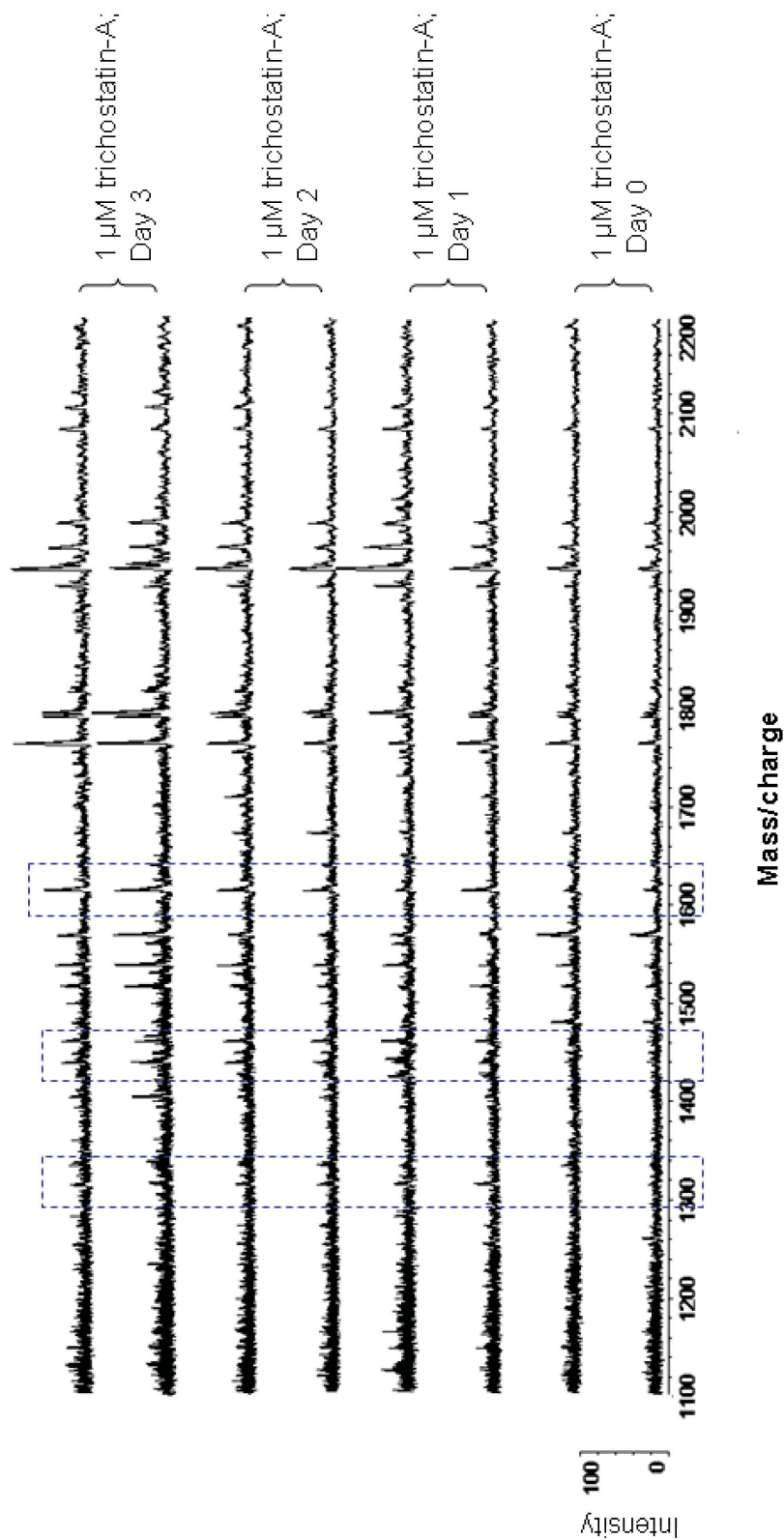


Figure 5.08 Representative spectra of Ma Mel 28 cell tryptic peptides, after treatment with 1 μM trichostatin A, acquired in reflectron mode. The regions highlighted show visual differences.

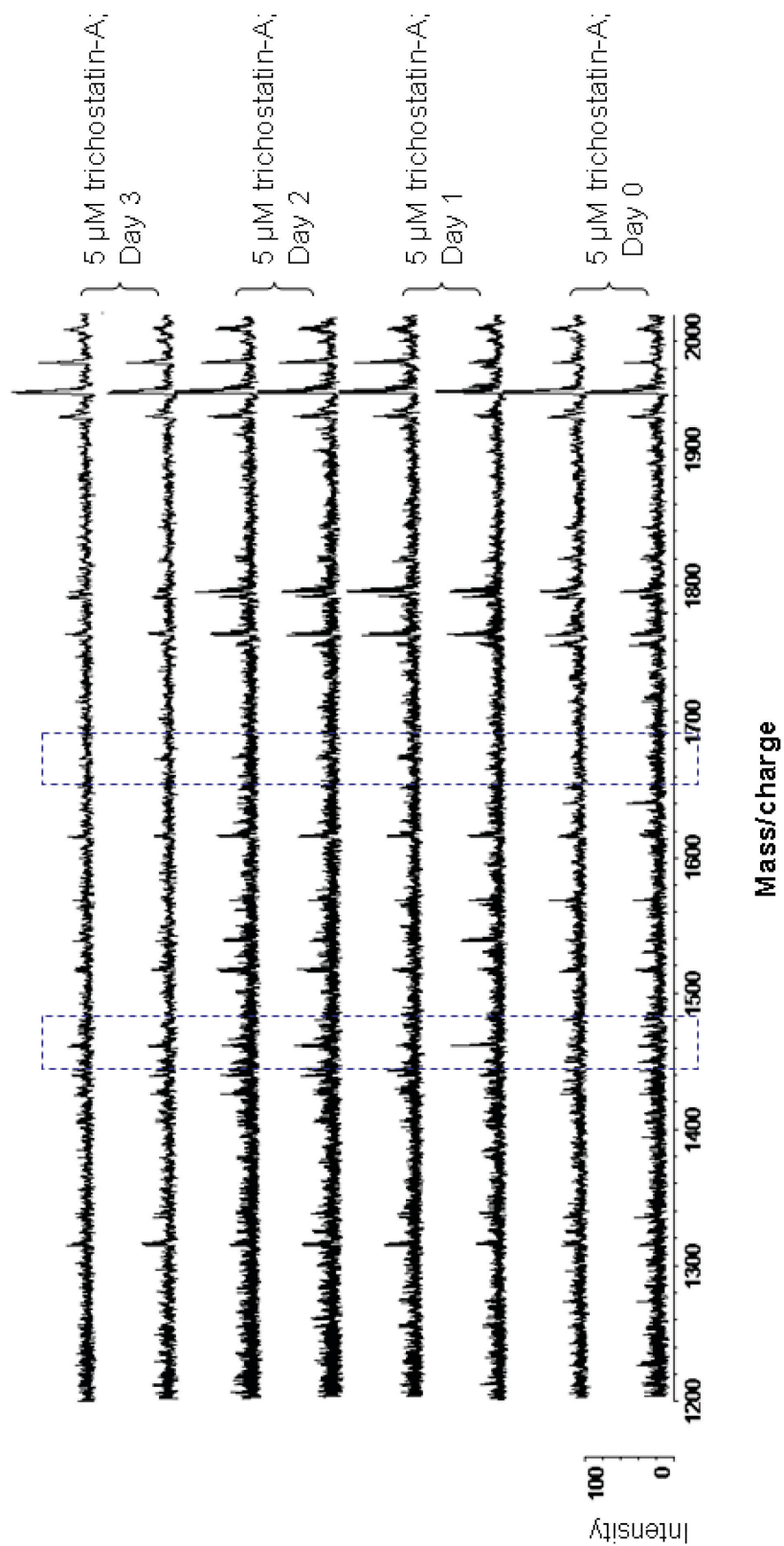


Figure 5.09 Representative spectra of Ma Mel 28 cell tryptic peptides after treatment with 5 μM trichostatin A, acquired in reflectron mode. The regions highlighted show visual differences.

5.2.5.1 Bioinformatic analysis of Ma Mel 28 cells using ANNs

As for Ma Mel 26a cells, data mining was conducted using ANNs to derive and recognise patterns that associate with drug treated and control cells. As can be seen in table 5.02, the ANNs have performed well in all the models tested. After day 1 of treatment with 1 μM trichostatin A, three ions were identified to be of importance. The most important ion m/z 1541 resulted in an 88% performance rate and the addition of m/z 2191 and m/z 3383 gave additional support to the model resulting in a 100% performance. After day 2, the ion m/z 1440 gave a performance of 83% with the addition of the second ion m/z 2840 giving a 100% performance. At day 3 a single ion, m/z 1378, gave a 100% test performance. When treated with 5 μM trichostatin A, some of the ions seen previously with 1 μM trichostatin A re-appeared. After day 1, ion m/z 1817 (with a singular performance of 80%), combined with ions m/z 2566 and 1884 gave a performance of 90%. Day 2 resulted in the most important ion m/z 1430 (81%), together with ions m/z 1440 and 1618 giving a 100% performance. The m/z 1440 ion had been previously identified after day 2 of treatment with 1 μM trichostatin A where it was the most important ion (see ion in red, table 5.02). Day 3 of treatment with 5 μM trichostatin A again showed the re-appearance of the ion m/z 1430 where it was now seen to be the most important ion giving a 100% performance.

Stepwise steps	m/z [M+H]⁺	Test Performance (%)	Test Error
Day 1 Control vs 1 μM			
1	1541	88	0.127
2	2191	88	0.098
3	3383*	100	0.060
Day 2 Control vs 1 μM			
1	1440	83	0.120
2	2840	100	0.049
Day 3 Control vs 1 μM			
1	1378	100	0.077
Day 1 Control vs 5 μM			
1	1817	80	0.162
2	2566	90	0.149
3	1884	90	0.100
Day 2 Control vs 5 μM			
1	1430*	81	0.130
2	1440	94	0.076
3	1618*	100	0.035
Day 3 Control vs 5 μM			
1	1430*	100	0.017

*No identity found

Table 5.02 Artificial Neural Network results on Ma Me1 28 cell line (n=10). Table to show the test performances and the mean squared error for the data sets as each input is added to the model. The results show the top ions that gave the best accuracy with the error failing to improve with subsequent additions; highlighted in red are the ions which appear in more than one model as a top predictive ion.

N = number of experiments

A population chart was generated to test the ANNs ability to predict the peptide profiles correctly for individual sample. Over 50 models the ANNs predicted this model with an accuracy of 100%. Figure 5.10 is based on the single ion m/z 1430 obtained from untreated and 5 μM trichostatin treated cells after 72 h of treatment. The results show the model correctly predicted 91 % of the individual cell lines as either a control or drug-treated sample; the misclassified samples have been circled. The ratios below 0.5 are assigned to the untreated control group and a ratio above 0.5 is classified as the treated samples. It can be seen from the chart that all of the drug-treated cells were classified correctly (red bars) with a ratio of >0.5 however; the control cells had four samples misclassified with the remaining predicted correctly with a ratio <0.5 .

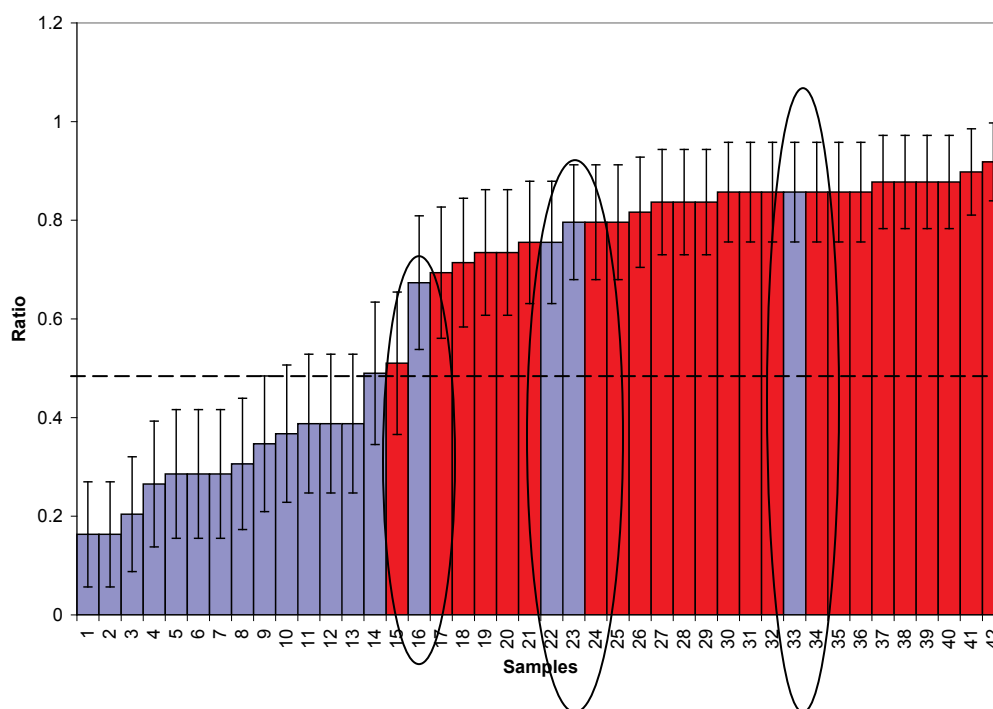


Figure 5.10 Predictive capability of ANNs trained to recognise tryptic peptide profiles based on the ion m/z 1430 for Ma Mel 28 cells versus control. The error bars represent the confidence interval. The blue bars correspond to the control samples and the red indicate drug treated samples. A predicted value below 0.5 indicates a control sample, whilst a prediction greater than 0.5 indicates a treated sample.

5.2.5.2 Validation of ANNs with blind data set

To test the validity of the trained model further we used a completely independent blind dataset that had not been included in the model previously. This validation set to test the model included MALDI spectral data from n=4 treated and n=4 of untreated cells for each drug treatment and incubation period. For treatment of 1 μ M trichostatin A compared to untreated cells, the samples were correctly assigned to a median accuracy of 84% for day 1; 96% for day 2 and 100% for day 3. Treatment with 5 μ M trichostatin A gave a median accuracy of 66% for day 1, 94% for day 2 and 100% for day 3. These results suggested that the model was performing well and that the predictive ions identified could be used as biomarkers discriminating between untreated and drug treated cells. This proof of principle study has important implication for tailoring the drug treatment to patient response and a move toward personalised therapy. To investigate this further, it would mean repetition of experiments to see if the same biomarkers appear. If they do these markers could be representative of response to therapy. To clinically evaluate the data, serum samples would have to be collected in conjunction with these experiments as this would be more realistic at a clinical level i.e. cells obtained from biopsies is not an easy option.

5.2.5.3 Identification of predicted biomarkers for Ma Mel 28 cells

The results from the blind dataset revealed the ANN model to have good predictive capabilities; the only exception being the control and drug-treated cells (5 μ M) at day 1, which only classified 66% of the blind data correctly. Therefore the biomarker ions within these models were considered to be those which most accurately distinguished between

control and treated melanoma cells for this dataset. The predictive peptide ions in table 5.02 were analysed by MS/MS on the Ultraflex III (Bruker), a more sensitive machine than the initial MALDI data which was run on the Shimadzu AXIMA-CFR. Due to the complexity of biological samples a more rigorous pre-fractionation of the samples was carried out prior to MALDI-MS/MS analysis. The samples were manually C₁₈ ZipTipped and eluted with increasing concentrations of ACN. Only a few peptides were identified using the MALDI-MS-MS methodology due to the minimal fractionation using C₁₈ ZipTip. This may have led to several overlapping peptide peaks making classification of these proteins difficult. Therefore the MEWO and Ma Mel 28 cell line samples were sent to Bruker Daltonics (Bremen, Germany) for analysis. Prior to MS/MS analysis a comprehensive Liquid Chromatography separation was carried out so that one sample was fractionated over the 384 MALDI target plate ensuring separation of the peptides to allow protein identity.

To identify the peaks following MS/MS analysis the Mascot database search engine was used and the search parameter settings for the Mascot sequence query routine were as follows: 4 maximum missed cleavage, 0.8 Da tolerance was used for the singly and doubly charged precursor ion and 0.9 Da for the fragment ion mass. Swissprot was used as the reference database (human taxonomy) and trypsin was set as the proteolytic enzyme.

The biomarker with m/z 1440 identified by ANNs as discriminatory between day 2 control and 1 μ M and 5 μ M trichostatin-A treatment was identified as ATP synthase with a measured m/z of 1439.7783. Protein identities were also found for the measured peptide with an m/z value of 1540.77 as alpha enolase for the ANN ion m/z 1541. The predicted peptide ion m/z 1817 resulted in three possible identities which were ATP

synthase subunit beta (m/z 1815.86), tropomyosin alpha-3 chain (m/z 1815.88) and m/z 1815.99 which belonged to 78 kDa glucose regulated protein. The tryptic peptide biomarker with m/z 1884 had two possible identities which were pyruvate kinase isozymes M1/M2 with a measured peak at m/z 1883.88 and a second protein identified as glutathione S-transferase P with an m/z 1883.94. The last predicted ion identified in drug-treated samples from the ANNs analysis was m/z 2840 which was identified as trifunctional enzyme subunit beta, mitochondrial (m/z 2840.32). All the ions with an m/z of 1541, 1817, 1884 and 2840 were found in drug-treated samples only and were not found in any control cell lines.

For the peptide ion 1378 two possible peptides were identified – heterogeneous nuclear ribonucleoproteins A2/B1 (m/z 1377.61) and poly ADP-ribose polymerase 1 (m/z 1377.73). The ion with m/z 2191 was also identified as a component of heterogeneous nuclear ribonucleoproteins A2/B1 (m/z 2189.88) whilst the ion m/z 2566 from the ANN analysis was identified as staphylococcal nuclease domain-containing protein 1 (m/z 2565.25). Both these peptide peaks were only found in the control samples. A summary of the results are shown in table 5.03. These results would have to be re-analysed to assess the reproducibility of the data.

For the ANN ions m/z 1430, 1618 and 3383 no peptide sequences were identified upon database searching using the appropriate MS/MS spectra. The identified proteins and the associated peptide peaks were noted and checked to ensure the peaks were present in the original MALDI-TOF-MS peptide spectra. Peptide profiles of m/z 1439.77 (ATP synthase) are shown in figure 5.11.

Ma Me 28 ions (combined)					
ANN Ion	m/z Identified	Peptide sequence	Mowse Score	Protein Identified	Samples
1378	1377.6183	GGGGNFGPGPSNFR	75	Heterogenous nuclear ribonucleoproteins A2/B1	CON
	1377.7368	TTNFAGILSQGLR	42	Poly ADP-ribose polymerase 1	
1440	1439.7783	VALTGLTVAEYFR	92	ATP synthase subunit beta, mitochondrial	TR
1541	1540.7742	VVIGMDVAASEFFR	124	Alpha enolase	TR
1817	1815.8639	IMDPNIVGSEHYDVAR	99	ATP synthase subunit beta, mitochondrial	TR
	1815.8888	HIAEEADRKYEEVAR	53	Tropomyosin alpha-3 chain	
	1815.9924	IINEPTAAAIAYGLDKR	70	78kDa Glucose regulated protein	
1884	1883.8853	LNFSHGTHEYHAETIK	87	Pyruvate kinase isozymes M1/M2	TR
	1883.9447	FQDGLTLYQSNTILR	129	Glutathione S-transferase P	
2191	2189.8857	NMGGPYGGGNYGPGSGSGGGYGR	209	Heterogenous nuclear ribonucleoproteins A2/B1	CON
2566	2565.2588	VLPAQATEYAFAFIQVPQDDAR	33	Staphylococcal nuclease domain-containing protein 1	CON
2840	2840.3223	FNFLAPELPAVSEFSTSETMGHSADR	62	Trifunctional enzyme subunit beta, mitochondrial	TR

TR = drug-treated samples CON = Control samples

Table 5.03 Table to show the peptides identified by MS/MS using ions predicted by ANNs for discrimination between untreated and drug-treated cells.

The identified peptides peaks were checked for presence with the original spectra to confirm their presence in the samples. The peak at m/z 1439.77 was present in most of the spectra in drug treated cell samples. Figure 5.11 demonstrates that this peak was observed at both 1 μM and 5 μM trichostatin A after day 2 of treatment as identified by the ANN analysis.

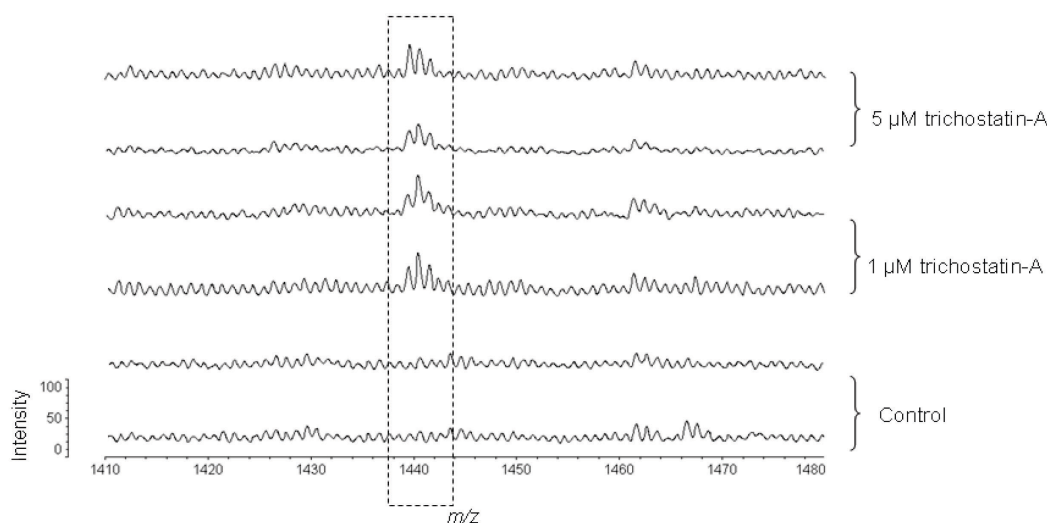


Figure 5.11 Representative mass spectra of peptides magnified using fractionated Ma Mel 28 cell lysate from control and trichostatin-A treated samples after day 2 of treatment. This spectrum illustrates the observed intensity differences of ion at m/z 1440, present in treated melanoma but not in the control samples.

The ion identified at m/z 1541 by ANNs predicted 88 % of the cells after day 1 of treatment with 1 μM trichostatin A versus control cells. Its presence was found in many of the samples treated with both 1 μM and 5 μM of drug with no peaks observed in the untreated cells. Although figure 5.12 shows the presence of ion m/z 1541 in both concentrations of trichostatin treated samples after day 1 of drug treatment in the raw MALDI spectra; this ion was not found to be an important predictive ion

using the stepwise ANNs in the 5 μM treated cells versus control samples for any of the drug exposure times.

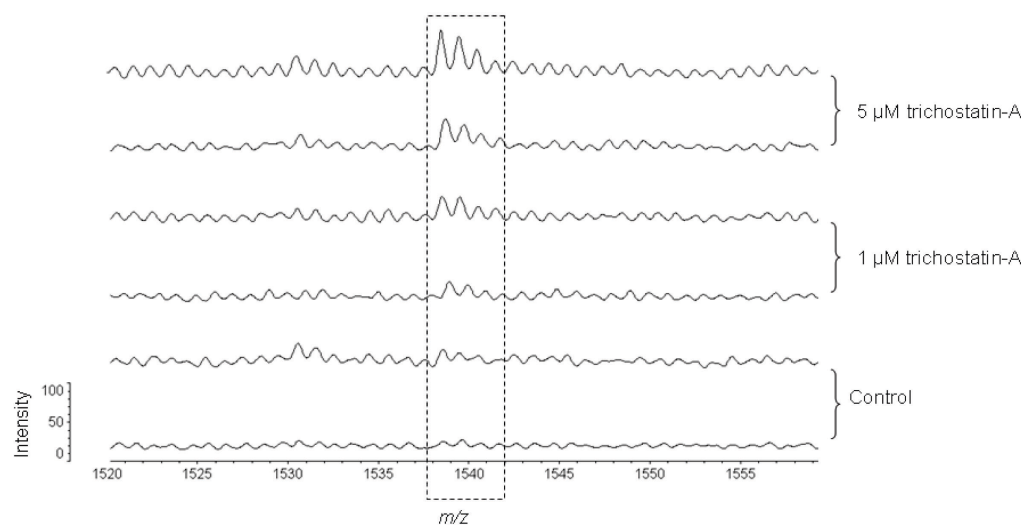


Figure 5.12 Representative mass spectra of peptides magnified using fractionated Ma Mel 28 cell lysate from control and trichostatin-A treated samples after day 1 of treatment. This spectrum illustrates the observed intensity differences of ions at m/z 1541, present in treated melanoma but not in the control samples.

The identified ion at m/z 1884 was observed in only 4 treated samples out of 42, where it was identified by ANNs after day 1 of treatment with 5 μM trichostatin A versus control melanoma Ma Mel 28 cells (figure 5.13). This result is not unexpected as the stepwise ANNs model predicted the top ion m/z 1817 which predicted 80% and the addition of 2566 increased the predictive performance to 90% and the third ion m/z 1884 also predicted 90% of the cells. The ion at m/z 2566 only added 10 % of the population to the overall model which resulted in the presence of this ion in only 4 drug treated samples. The ion m/z 1430.78 was found only in untreated cells at low intensity in the control melanoma cells only when compared with days 2 and 3 of drug treatment with trichostatin A but not in cells exposed to day 1 of treatment.

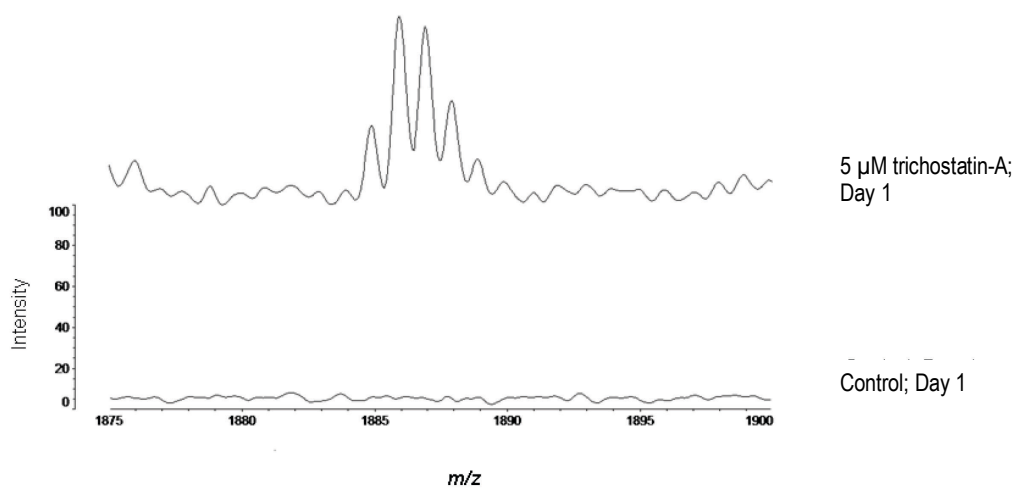


Figure 5.13 Representative mass spectra of peptides magnified using C₁₈ ZipTip fractionated Ma Mel 28 cell lysate from an untreated control sample and a trichostatin-A treated sample after day 1 of treatment with 5 μM. This spectrum illustrates the observed intensity differences of ion at m/z 1884.04, present in treated melanoma but not in the control samples.

5.2.6 MEWO cells

As the protein concentration of 0.5 mg.ml^{-1} resulted in improved spectra that were of good quality for the Ma Mel 28 cells, the protein concentration was equalised to 0.5 mg.ml^{-1} for all melanoma MEWO cells in the following experiments. Figures 5.14 and 5.15 illustrate the peptide spectra obtained. The spectra were observed visually and differences between the treated and untreated cells are highlighted in figures 5.14 and 5.15. Decreasing intensity of ion m/z 1310 can be seen in figure 5.14 for cells that were treated with $1 \text{ }\mu\text{M}$ trichostatin A. As observed with the other two melanoma cell lines the spectra at day 3 for MEWO cells also contained very few peaks compared to the other days tested as shown in figure 5.15 with $5 \text{ }\mu\text{M}$ trichostatin A. Another ion at m/z 1440 was observed in figure 5.15 increasing in intensity but reduced after day 3. This ion may represent a drug effect resulting in the cells going into apoptotic death as a result of drug exposure.

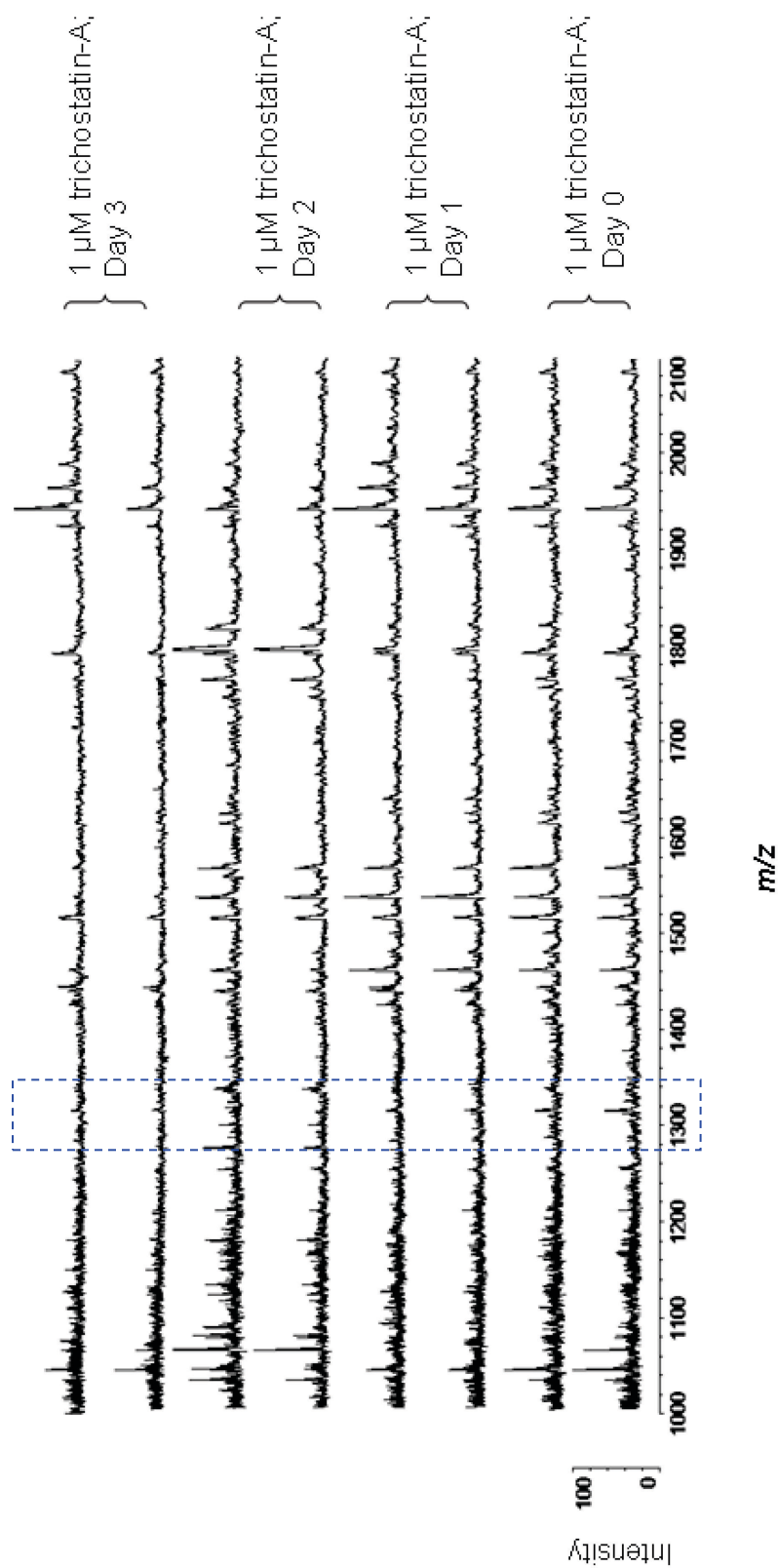


Figure 5.14 Representative spectra of MEWO cell tryptic peptides, after treatment with 1 μM trichostatin A, acquired in reflectron mode. The regions highlighted show visual differences.

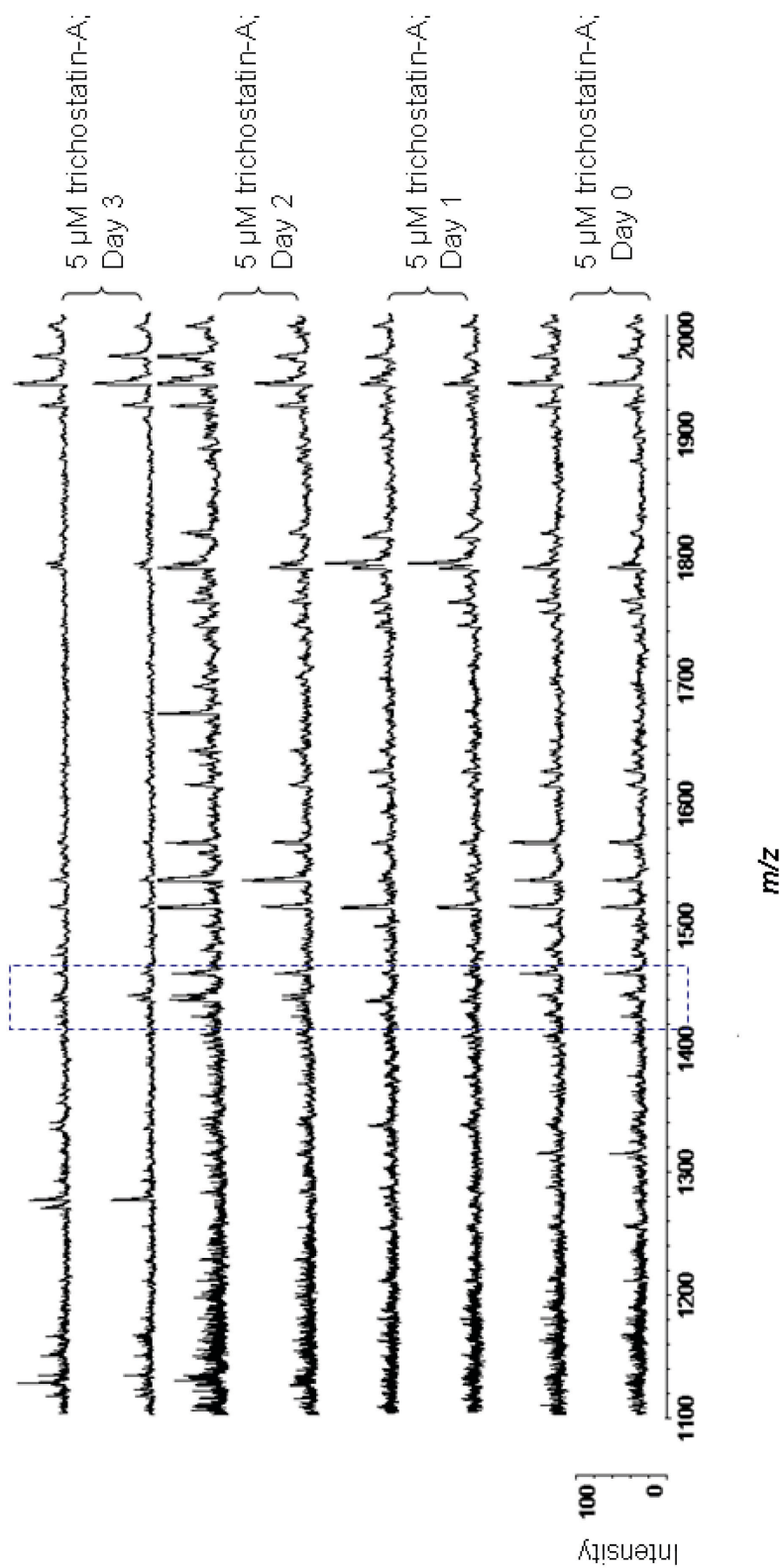


Figure 5.15 Representative spectra of MEWO cell tryptic peptides after treatment with 5 μM trichostatin A, acquired in reflectron mode. The regions highlighted show visual differences.

5.2.6.1 Bioinformatic analysis of MEWO cells using ANNs

ANN analysis of the MEWO data in table 5.04 revealed one ion m/z 1439/1440 which repeatedly appeared as the most important ion. The 1 Da mass difference in the m/z value is due to the fact that prior to ANNs analysis the raw MALDI data was rounded to the nearest Da to reduce the amount of data for bioinformatic analysis so the two m/z ions may belong to the same peptide. i.e. a m/z ion of 1439.4 would be rounded down to 1439 and a m/z value of 1439.8 would be rounded up to 1440. Peaks corresponding to the ions at m/z 1440 and 1439 were seen to be present as the first ion in day 1, day 2 and day 3 with 5 μM trichostatin A and in the day 1 samples of cells treated with 1 μM trichostatin A. In addition the same ion that was also seen and identified in the Ma Mel 28 cells. With 1 μM trichostatin A after day 1 of dosing this ion gave a performance of 83% with the ion 2570 increasing this performance to 89%. Day 2 revealed two ions, 1531 and 1677 giving a combined test performance of 86%. Day 3 resulted in 1133 giving 71% performance with the addition of the ions m/z 1934, 3082, and 1828 increasing this to 93%. Treatment with 5 μM trichostatin A gave the ion m/z 1439 a performance of 94% with the ion m/z 2266 increasing this to 100% at day 1. Again at day 2, ion m/z 1440 gave a performance of 88% with the second ion m/z 3372 taking this to 100%. Day 3 revealed m/z 1440 (90% performance) and although ion m/z 2939 did not improve the model performance, addition of ion m/z 1729 resulted in a 100% performance of the model.

Stepwise steps	m/z value	Test Performance (%)	Test Error
Day 1			
Control vs 1 μM			
1	1439	83	0.157
2	2570*	89	0.108
Day 2			
Control vs 1 μM			
1	1531	85	0.176
2	1677	86	0.128
Day 3			
Control vs 1 μM			
1	1133	71	0.198
2	1934	79	0.125
3	3082*	89	0.120
4	1828	93	0.075
Day 1			
Control vs 5 μM			
1	1439	94	0.101
2	2266	100	0.062
Day 2			
Control vs 5 μM			
1	1440	88	0.102
2	3372*	100	0.058
Day 3			
Control vs 5 μM			
1	1440	90	0.126
2	2939	90	0.078
3	1729*	100	0.049

* No Identify found

Table 5.04 Artificial Neural Network results on MEWO cell line (n=18). Table to show the test performances and the mean squared error as each input is added to the model. The results show the top ions that gave the best accuracy with the error failing to improve with subsequent additions. The highlighted ions in red show the same value re-appearing as the most important ion particularly when treated with 5 μM trichostatin A.

N = number of experiments

The validity of the ANNs model was tested by generating a population chart for each individual melanoma sample assignment as drug treated or control using the stepwise predicted ions. Figure 5.16 is based on ions m/z 1439 and 2266 obtained from untreated and treated cells after day 1 of drug treatment with 5 μM trichostatin A. The results show that the ANNs model correctly predicted 97% of the data as either a control or drug-treated sample; the misclassified samples have been circled. The ratios below 0.5 are assigned to the untreated control group and ratios above 0.5 are classified as treated samples. It can be seen that the majority of the control cells, with the exception of one sample, were classified correctly (blue bars) with a ratio of <0.5 . The drug treated cells had two misclassified samples with the remaining predicted correctly with a ratio >0.5 .

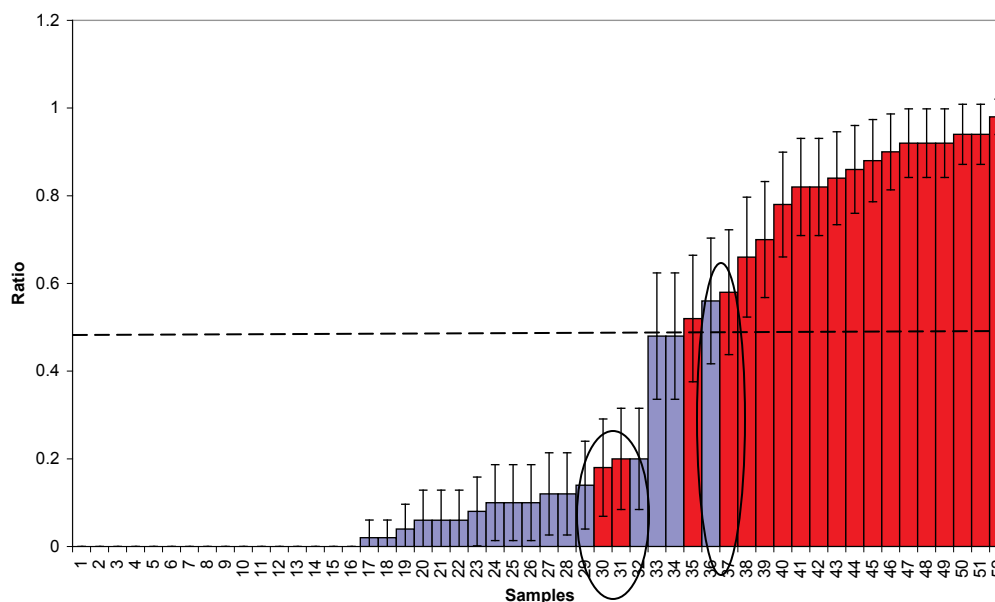


Figure 5.16 Predictive capability of ANNs trained to recognise tryptic peptide profiles based on the ions m/z 1439 and 2266. The error bars represent the confidence interval. The blue bars correspond to the control samples and the red indicate drug treated samples. A predicted value below 0.5 indicates a control sample, whilst a prediction greater than 0.5 indicates a treated sample.

5.2.6.2 Validation of ANNs with a blind data set

MEWO cell samples (n=5) for each treatment and exposure time and control cell samples (n=5) at each time period were used to predict the ANN models generated as an independent blind data set. The trained models were tested with a completely blind dataset to determine the validity of the results. For cells treated with 1 μ M trichostatin A, compared to untreated cells, the samples were correctly assigned to a median accuracy of 97% for day 1; 77% for day 2 and 48% for day 3. Treatment with 5 μ M trichostatin A gave a median accuracy of prediction 57% for day 1, 80% for day 2 and 88% for day 3. The high accuracy of prediction observed in table 5.04 infer that the model was performing well and that the ions identified represent possible biomarkers for drug treatment and exposure time.

5.2.6.3 Identification of predicted biomarkers for MEWO cells

The blind data was correctly classified in most of the samples except between control cells and treated cells (with 5 μ M of drug) for day 1 (57%) and at 1 μ M trichostatin after 3 days of incubation. Therefore the biomarker ions within these models were considered to be those which most accurately distinguished peptide patterns between control and treated melanoma cells for this dataset. The predicted peptide ions (table 5.05) were analysed by MS/MS to obtain the sequence and subsequent identity of the protein. Due to the complexity of the biological samples, a pre-fractionation was required before MALDI analysis. As with Ma Mel 28 cells, the original samples were manually fractionated using a C₁₈ column and eluted from the column sequentially using increasing concentrations of ACN diluted in 0.1% TFA. Each of the eluted samples were analysed by MALDI-TOF MS/MS analysis. As already mentioned in section 5.2.5.3

above for the Ma Mel 28 cell line, the samples for MEWO were also sent to Bruker Daltonics (Bremen, Germany) for further identification of predictive peptide ions from the ANNs analysis.

A mascot search (Swissprot database) identified all three ANNs ions with m/z 1440/1439, 2266 and 1677 as ATP synthases with the peaks observed in the drug-treated samples (m/z 1439.7827; 2266.0762 and 1676.8289). Analysis of the ANNs biomarker at m/z 1531 and 1934 were identified as 10 KDa heat shock protein (with a measured peak of m/z 1529.7858) or haemoglobin subunit alpha (measured peak of m/z 1529.7205) and GRP78 precursor respectively (measured peak m/z 1933.9866). The ANNs ion m/z 1531 was shown to be at high intensity in the control cell lysates whilst the ion at m/z 1934 was present only in the drug-treated samples. The ANNs ion at m/z 1133 had two possible identities of actin, cytoplasmic 1 (with an observed peak at m/z 1132.51) or m/z 1132.62 as ADP/ATP translocase 2. Upon visual inspection of the spectra the peaks were observed in the drug-treated samples. The predictive tryptic peptide ions m/z 1828 and 2939 with measured peaks of m/z 1827.9164 belonged to eukaryotic initiator factor 4a-1 and m/z 2928.3254 was identified as elongation factor 1-alpha 1. Very few peaks were observed in the original spectra for the ANNs ion m/z 1828 but where it was observed, it was present only in the drug-treated samples. The ANNs ion m/z 2939 was also observed only in drug-treated samples. The predictive peptide ions m/z 1729, 2570, 3082 and 3372 did not yield significant sequence matches (<0.05) using the MASCOT search engines. A summary of the identified proteins and their respective sequences are given in table 5.05. As previously mentioned with the Ma Mel 28 data, the ANNs would have to be repeated to verify the identities and thus the reproducibility of this methodology.

MEWO Ions					
ANN Ion	m/z Identified	Peptide sequence	Mowse Score	Protein Identified	Samples identified
1133	1132.6202 1132.5128	QIFLGGVDKR GYSFTTTAER	56 60	ADP/ATP translocase 2 Actin, cytoplasmic 1	TR
1439 1440	1439.7827	VALTGLTVAEYFR	67	ATP synthase subunit beta, mitochondrial	TR
1531	1529.7858 1529.7205	VVLDDKDYFLFR VGAHAGEYGAEALER	113 75	10kDa heat shock protein, mitochondrial Haemoglobin subunit alpha	CON
1677	1676.8289	FEDEKFEVIEKPQA.	61	ATP synthase coupling factor 6, mitochondrial MOST DOSED	TR
1828	1827.9164	GIYAYGFEEKPSAIQQR	83	Eukaryotic initiation factor 4a-I	TR
1934	1933.9866	DNHLLGTFDLTGIPPAPR	74	GRP78 Precursor	TR
2266	2266.0762	IPSAVGYQPTLATDMGTMQER	71	ATP synthase subunit beta	TR
2939	2938.3254	SGDAAIVDMVPGKPMCBESFSDYPPLGR	43	Elongation factor 1-alpha 1	TR

TR = drug-treated samples CON = Control samples

Table 5.05 Table to show the peptides identified by MS/MS using ions predicted by ANNs for discrimination between untreated and drug-treated cells.

All of the identified ions were confirmed to be present in the original MALDI-TOF MS peptide spectra. Figure 5.17 shows the ATP synthase ion at m/z 1439.7827. The peak was observed in the majority of the samples after treatment with 5 μM trichostatin A as predicted by the ANNs revealing both 1439 and 1440 to be a key first ion. The ion was also observed in some samples treated with 1 μM trichostatin A after day 1 of drug-treatment. No peaks were seen in the control samples. The spectra in figure 5.17 demonstrate the peak seen at m/z 1439.7827 revealing its presence in drug-treated cells but not in control cells.

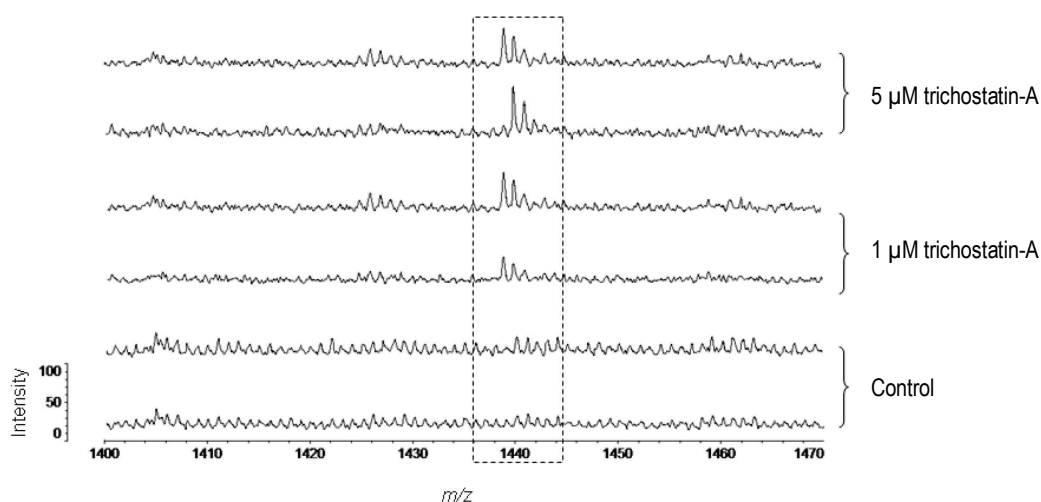


Figure 5.17 Representative mass spectra of peptides magnified using fractionated MEWO cell lysate from control and trichostatin-A treated samples after 24 h of treatment. This spectrum illustrates the observed intensity differences of ions at m/z 1439.79, present in treated melanoma but not in the control samples.

5.3 Discussion

Currently there is a lack of biomarkers which predict whether a patients' treatment has been successful. If peptide "fingerprints" and a panel of biomarkers from proteomic studies can be identified, then this would be of great clinical benefit to the patient (personalised medicine). *In vitro* cultured cells are currently used in many studies due to the scarcity of patient tissue and the results of this chapter reveal that it is possible to identify biomarkers from cell lines that correlate with drug treatment and exposure. This work examined the potential of MALDI MS based proteomics combined with ANN analysis to determine whether melanoma cell lines expressed altered peptidomic profiles following treatment and exposure times with the histone deacetylase inhibitor, trichostatin A.

5.3.1 Sample preparation and analysis

Prior to analysis by MALDI MS, the melanoma samples were adjusted to 0.1 mg.ml^{-1} (Ma Mel 26a) and 0.5 mg.ml^{-1} (MEWO and Ma Mel 28 cell lines). Although analysis by MALDI MS is not quantitative, protein adjustment has to be carried out to identify differential intensities of the peaks and establish patterns between the data points. Measurement of the protein standards using the Bio-Rad micro-assay, gave a R^2 value of over 0.98 on all cell lines, enabling accurate measurement of the cell lysate samples. The cells were then adjusted to their respective concentrations using 0.1% TFA; this dilution buffer was used through out the MALDI MS analysis.

5.3.2 Importance of QC in MALDI-MS analysis

There has been a considerable amount of debate surrounding the use of SELDI-MS and MALDI-MS protein analysis, particularly with regard to the reproducibility of the methods (Diamandis, 2004). Critics have argued that reported discriminatory protein profiles have been based largely on experimental artefacts rather than biological differences (Matharoo-Ball *et al.*, 2007). However, the methods used in this study for MALDI MS analysis were optimised for sample preparation and analysis carried out using the in-house protocol (Matharoo-Ball *et al.*, 2007). Processing time, clotting times, centrifugation speeds, pre-aliquoting, storage temperature and the number of freeze-thaw cycles are all critically important as well as variation in ZipTip fractionation, MALDI crystallisation, laser irradiation, and sample preparation all of which influence protein/peptide outcomes. All samples in this study were centrifuged at a set speed and time and stored at -80°C until use. Freeze-thaw was limited to two cycles with sample preparation of each cell line carried out on ice prior to sonication and MALDI analysis. Sample bias reported by Petricoin *et al.*, (2002) regarding the reproducibility of MALDI based approaches were tackled by randomising the position of samples on the target plate prior to analysis. Appropriate blanks, QC and BSA samples were also randomised and included on all plates. The blanks (0.1% TFA and matrix) were included to monitor contamination of the target plate; QC samples ensured a robust and reproducible methodology and BSA controls were used to confirm the efficiency of the tryptic digest and peptide acquisition. Close external calibration for peptides was used where the data was acquired from a calibration mixture spotted adjacent to each group of four sample spots. Poor or infrequent calibration can lead to a significant shift in the m/z values for the mass spectral peaks.

5.3.3 MALDI-MS analysis

The spectra produced by MALDI MS revealed some visual differences between drug-treated and control melanoma and the reproducibility of the QC samples in figure 5.05 revealed a good correlation between all spectra captured on the MALDI MS. The spectra for Ma Mel 26a cells contained the worst peptide profiles, with very few peaks present visually due to the low starting protein concentration. This concentration as previously mentioned was chosen because the majority of the Ma Mel 26a cells had very low total protein concentrations. This was rectified for the MEWO and Ma Mel 28 cells which resulted in a significantly improved spectral profile. When sufficient sample was available, the protein concentration was increased further (1 mg.ml^{-1}) resulting in improved peptide spectral profile which enabled identification of the ANNs predicted biomarkers. The spectra for MEWO and Ma Mel 28 cells at day 3 showed low intensity peptide peaks compared with days 1 and 2 of drug treatment. Comparing this data to the results obtained in chapter 4, a correlation between the data can be seen. The MEWO cells were shown to have 50% cell death compared to 30% in the Ma Mel 28 cells after treatment for 3 days with $5 \text{ }\mu\text{M}$ trichostatin A (chapter 4) when measured using the ToxiLight® and ViaLight Plus® assays. The MEWO spectra analysed by the MALDI-TOF MS in this study revealed very low intensity peptide peaks at day 3 with both $1 \text{ }\mu\text{M}$ and $5 \text{ }\mu\text{M}$ of drug. This may imply that drug treatment induces the initiation of the apoptotic pathway resulting in down-regulation of most proteins in drug exposed cells compared to untreated melanoma cells. The Ma Mel 28 cells which were more resilient to the drug treatment only showed a reduction in the peptide peaks with MALDI-TOF MS after day 3 and then only with the higher concentration ($5\mu\text{M}$) of trichostatin A. At this time the combinatorial

assays ToxiLight® and ViaLight Plus® also showed cell death due to drug exposure but less so with shorter drug exposure times.

5.3.4 Analysis by ANNs

Bioinformatic analysis acceptance criteria was based on visual inspection of mass spectrometric, BSA, and calibration profiles and those deemed to have a poor signal were removed from bioinformatic data assessment. The noisy and highly dimensional data obtained through proteomic analysis requires all aspects of data interrogation to be optimised including spectra pre-processing, quality control and dimensionality reduction. The biggest challenge in analysing data is the development of algorithms that can predict samples accurately into their correct groups for unseen or blind data. There are many data mining methods that can be employed and presently no single method can provide the most accurate and reliable analysis.

The results in this study using ANN analysis, failed to validate the model for Ma Mel 26a cells for untreated compared to drug treated cells with 1 μM trichostatin A and correctly classified only 55% of samples of the day 1 dataset, 45% of the day 2 dataset and 60% of the day 3 dataset. This was disappointing but not unexpected due to the poor peptide spectral quality and the low starting protein concentration. However; it has to be noted that with the current and improved MS instrumentation (Bruker Ultraflex III) a starting concentration of 0.1 mg.ml^{-1} would generate good quality spectral profiles (unpublished data). Ma Mel 28 cells, on the other hand, performed well when analysed using ANNs for both the modelling set of samples and when tested with an independent blind dataset. ANNs analysis showed good predictions with the exception of one model which

resulted in only 66% of samples being correctly classified but the remaining five models assigned > 84% of samples correctly into their respective groups (drug-treated (both 1 and 5 μ M) and untreated cells).

For the MEWO cells the modelling data resulted in good prediction for all models between the trichostatin (1 and 5 μ M) treated samples with increasing drug incubation times versus controls. For the blinded MEWO samples the ANNs predicted ions accurately classified >77% of samples in four of the six models, with the remaining 2 models underperforming (<77%). The application of blinded validation and test data in the modelling approach produced models with good performance on blind data and prevented over-fitting. In the Ma Mel 28 and MEWO melanoma cell lines the ion at m/z 1439/1440 appeared as predictive peptide ions in more than one model for both drug concentrations and exposure times. This ion may therefore be reflective of a marker of cell toxicity through apoptosis following drug exposure.

Due to the poor results obtained with Ma Mel 26a cells, no further analysis was carried out for identification of predicted ions. Time and samples permitting, these cells would have been re-tested at a higher protein concentration. The top ions identified by the ANNs could have been identified following pre-fractionating the samples to further separate the proteins prior to MS/MS analysis. Identification of peptide ions was however; conducted for Ma Mel 28 and MEWO cell line. MALDI-TOF MS/MS was carried out following sample fractionation using sequential elutions of increasing organic solvent to resolve the peptide ions in order to help with the identification of the peptide and therefore parent protein. Further identification was carried out by LC-MALDI followed by MALDI-TOF MS/MS (Bruker).

Protein identification of the tryptic peptide biomarker ions was achieved for the MEWO cells using MALDI-TOF MS/MS and LC-MALDI with the ANN discriminatory ion m/z 1439 identified as a peptide from protein ATP synthase (m/z 1439.78). Two further peptide ions were also identified from the protein ATP synthase (m/z 2266.0762 and 1676.8289) providing further evidence for its presence with the peaks observed in the spectra belonging to drug-treated samples only. Two identities were found for the ANNs ion at m/z 1133 with possible identities of beta actin (m/z 1132.51) or ADP/ATP translocase 2 (m/z 1132.62). Multiple identities were found for many of the ANNs ions in both cell lines. These proteins provided significant scores through the MASCOT database and because prior bioinformatic analysis requires reduction of the number of data points by binning the m/z to the nearest Dalton, it means that the ANNs predicted ions could represent either of the two identified proteins. A second reason may be due to the resolution and mass accuracy of the older MALDI instrument which was used for the initial MS analysis for discovery of the biomarkers correlating to drug treatment. However; the identity of the ions was carried out on a MALDI instrument with a much higher resolution and mass accuracy leading to a more comprehensive coverage of the proteome and higher protein identification rate. To confirm significance of the proteins immunoassays (ELISA, western blotting or immunohistochemistry) would have to be carried out which was beyond the investigations of this study. It was not possible to achieve protein identification of all the predictive ANNs ions using MALDI MS/MS and LC-MALDI. A more sensitive method using ESI-MS/MS would have to be employed to identify these ions.

Successful protein identification from the tryptic peptide biomarker ions was gained for the Ma Mel 28 cells using MALDI-TOF MS/MS and LC-MALDI with sequences of the ANN discriminatory ion at m/z 1440 being identified as a peptide belonging to the protein ATP synthase subunit beta (m/z 1439.7827) which was present in the drug-treated samples only. As already stated with the MEWO cells, multiple identities were also found for the Ma Mel 28 cell line for the ANN ions at m/z 1817 and 1884. The ANNs discriminatory ion m/z 1817 had three possible identities with peptides belonging to the protein ATP synthase subunit beta (observed in peak m/z 1815.86); tropomyosin alpha-3 chain (m/z 1815.88) or 78 kDa glucose regulated protein (m/z 1815.99). The final ANNs ion with m/z 1884 had two possible identities with a peptide sequence observed for pyruvate kinase isozymes M1/M2 (m/z 1883.88) and glutathione S-transferase P (m/z 1883.94). The reason for multiple identities as previously explained could have been due to binning the m/z to the nearest Dalton prior to ANN analysis and/or the mass and resolution accuracy of the new improved MALDI mass spectrometer. This means that the predictive m/z value identified by ANNs could potentially represent all of the identified proteins. In order to find out conclusively which protein was the “true biomarker” a further investigation would need to be carried out using Immunoassay methods.

5.3.5 Clinical relevance of identified ions

Protein identities from both Ma Mel 28 and MEWO cell lines revealed similar differentials between control and drug-treated samples by ANNs analysis with many peptide ions belonging to ATP synthases. This added confidence to the possibility that this biomarker could be used to predict therapeutic response in melanoma cells. ATP synthase or ATP5B (beta subunit) or H⁺ transporting, mitochondrial F1 complex are human genes.

These genes encode a subunit of mitochondrial ATP synthase which catalyzes ATP synthesis, during oxidative phosphorylation. There are two linked subunits of ATP synthase composed of the soluble catalytic core, F1, and the membrane-spanning component, F0, and together they comprise the proton channel. The catalytic portion of mitochondrial ATP synthase where the identities were found consists of 5 different subunits (alpha, beta, gamma, delta and epsilon). Recent studies on melanoma have demonstrated that malignant melanoma show abnormal redox regulation, and although the molecular mechanisms involved are not well characterised, they seem to be related to oxidative stress (Locatelli *et al.*, 2009). ATP synthase has been demonstrated to be up regulated during apoptosis in a time-linked manner. This up regulation ensures that there is sufficient intracellular ATP levels and therefore efficient functioning of the mitochondrial respiratory chain for successful completion of the apoptotic pathway (Singh and Khar, 2005). The presence of this protein in both MEWO and Ma Mel 28 cells treated with trichostatin A could indicate that the treatment is having a positive effect on the cells and they are undergoing or preparing for apoptosis. This could imply that prolonged exposure of the drug past the 3 days monitored in this study may result in a larger percentage of cells being killed. The presence of ATP synthase is therefore very promising especially combined with the ViaLight Plus™ data in chapter 4. As ATP was demonstrated to have dramatically reduced in the majority of the experiments tested by the ViaLight Plus™ assay, the implication that the mitochondria were being affected by the drug-treatment could imply that apoptosis is occurring and adds further confidence to the fact that the protein ATP synthase (which is involved in apoptosis) has been discovered by MALDI MS in conjunction with ANN analysis and identified by MALDI-MS/MS in the drug-treated samples. This could be a marker for apoptosis illustrating

that a cytotoxic drug is having a positive effect for a patient undergoing treatment and should be investigated further. This study also illustrates that using multiple assay platforms can identify biomarkers which could be used for patient tailored treatments. Further investigations to monitor the reproducibility of this work would involve repeating the experiments using serum samples from patients rather than cells to see if ATP synthase can be found as a marker after treatment. Even though cells are the closest way of monitoring the tissue *in vitro* this is not always feasible due to the difficulties in obtaining cells by biopsy. Serum is easy to obtain from a blood sample and can be monitored over a patient's treatment.

Two proteins identified in the drug-treated MEWO cell lysates were beta actin and 10 kDa heat shock protein. Beta actin (gene name ACTB) is one of six different actin isoforms which have been found in humans. This is one of two non-muscle cytoskeletal actins. Actins are highly conserved proteins that are involved in cell motility, structure and integrity. The actin cytoskeleton controls multiple cellular functions, including cell morphology, movement and growth. A recent article by Dundr *et al.*, earlier this year (2009) suggested that neural crest-derived tumours had shown expression of smooth muscle actin on some occasions but not consistently. It has however; been shown to play a role in metastasis by coordinating changes of the filaments. Yang *et al.*, revealed the role actin played in stabilising the space generated by the membrane deformation ensuring efficient protrusion (Yang *et al.*, 2009). Although a transient space can be formed without actin playing a part, the filaments were required to fill the space to allow the cells to protrude. Actin (if the correct identity for the ANNs ion – it was one of two possible identities for the ANNs ion) was only present in drug-treated samples in this study and not controls which could imply that the cell cytoskeleton was being broken down due to the effects of the drug.

Heat shock proteins are a class of functionally related proteins whose expression is increased when cells are exposed to elevated temperatures or other stress to try to restore immature proteins or denatured proteins, thus protecting the cell. The expression of heat shock proteins has been observed in hepatocellular carcinoma (HCC) where correlation with tumour severity and poor outcomes of HCC patients has been observed (Lu *et al.*, 2009). The presence of the heat shock protein in this study (10 kDa heat shock protein) was present only in the control melanoma samples. This could be a normal house keeping protein that monitors the cell ensuring proper protein conformation. In addition, to the 10kDa heat shock protein, both the cell lines (MEWO and Ma Mel 28) revealed the 78 kDa glucose regulated protein, a heat shock protein belonging to the heat shock protein-70 family. The 70 kDa heat shock protein was present in only drug-treated samples indicating that the cell was under stress. If further investigations into heat shock proteins on a larger population size identifies its relationship to severe melanoma cases, it may enable this protein to be used as a prognostic biomarker. The presence of these proteins has been observed in many malignant tumours, but their expression in association with melanoma has yet to be studied (Park *et al.*, 2009). A review was published by Lee in 2007 discussing the role that GRP78 plays in many cancers. It was stated that the protein GRP78 or BIP (immunoglobulin heavy-chain binding protein) is induced under conditions of stress which then promotes tumour proliferation, survival, metastasis and resistance (Lee, 2007). Its presence is indicative of poor patient survival and higher pathological grade. This could be the reason for the presence of this protein in the melanoma samples in this study as it was potentially identified in both cell samples. The results from the ToxiLight™ assay in chapter 4 revealed only very low levels of cell death especially in the Ma Mel 28 cells implying resistance. Given the

importance of this protein in cancer cell survival, it could represent a prime target for anticancer agents.

The ANNs ion m/z 1828 was identified as a peptide from the protein eukaryotic initiator factor. Protein synthesis can be divided into three phases: initiation, elongation and termination. Initiator factors are proteins that bind to the small subunit of the ribosome during the initiation of translation, a part of protein biosynthesis. Protein synthesis has been shown to considerably reduce during programmed cell death (Bushell *et al.*, 2004). The presence of this protein in only a few drug-treated samples at low intensity could also be an indicator of apoptosis. The majority of the potential protein identities in both cell lines fall into three main categories: metabolic proteins (e.g. ATP synthase), cytoskeleton proteins (e.g. actin) and nuclear proteins (e.g. heterogeneous nuclear ribonucleoproteins A2/B1). They all imply that the cell is under stress and beginning to break down further supporting the previous cell assay data with ToxiLight™ and ViaLight™ Plus in chapter 4. The drug-treated cells were showing signs of stress by the decrease in ATP observed and an increase, although only a low percentage, in cell death.

The cell lines used in this study were mostly derived from metastases meaning that many of the identified ions could be associated with metastatic disease, and may have a connection with drug response/treatment and exposure time (see table 5.06). Unfortunately the patients had little history to compare the data with due to their low survival rate after tissue extraction.

<i>Tissue Number</i>	<i>Patient Number</i>	<i>Cell Line Code</i>	<i>Tissue Origin</i>	<i>Survival (months) since tissue extraction</i>
285	MA 000263	Ma Mel 26a	Lymph node	6.30
284	MA 000336	Ma Mel 28	Squamous cell (skin)	4.59

Table 5.06 Clinical information of the cell lines used in this study

The identified ATP synthases mainly in the treated cells could be an indicator of apoptosis and thus cytotoxicity occurring *in vivo* for a patient receiving treatment. This could help in monitoring drug toxicity levels to prevent unnecessary over-exposure of the drug and hence drug side-effects for the patient. To further clarify these findings further investigations would be required to define the *in vivo* role and impact of the identified proteins after trichostatin-A drug treatment and exposure. Although the study was carried out within a low passage number, it should be noted that changes in both the proteome and genome may have occurred during *in vitro* culture and hence there are likely to be differences between the original tissue and the cell line.

5.3.6 Conclusion

Due to the limitations of tumour tissue, the research carried out on cell lines is of importance to identify diagnostic and prognostic markers. Other studies have been carried out on drug resistant cells. Urbani *et al.*, (2005) examined etoposide resistance to chemotherapy in human neuroblastoma, discovering a number of over-expressed proteins; and Craven *et al.*, (2004) studied proteins induced in response to interferon α . The results obtained from work presented in this chapter have revealed how cell lines can be used to provide useful information on markers that associate with drug treatment for a particular disease, especially at the protein level. It provides a proof of principle study that markers can be identified by MALDI MS analysis in conjunction with ANNs associated with drug-sensitive and drug-resistant cell samples. These findings could lead to the discovery of proteins that are of prognostic and therapeutic benefit with the long term outcome leading to personalised treatments for individuals in which a decision can be made on the best suited treatment.

Chapter 6: Discussion

6.1 ToxiLight® and its use as a cytotoxicity assay

The research presented in this thesis has demonstrated the design, optimisation and effective use of a novel bioluminescent assay for the analysis of cell death. The initial work illustrated the production of a novel assay that is sensitive, rapid and homogeneous competing against current methodologies already commercially available. The use of bioluminescence as a measurement of cell viability and cell death has been proven in this study to be a reliable alternative to the conventional methods. ToxiLight® was found to be highly sensitive both in detecting AK standards and low cell numbers with excellent reliability. It was able to measure a 96 well white walled luminometer plate in less than 5 min (dependent upon the transport mechanism of the luminometer used) showing detection limits of 10 cells per well. This sensitivity has to the best of my knowledge, not been identified in an assay previously making this assay the most sensitive measurement of cell death. Due to the low signal to noise levels of bioluminescence, the assay demonstrated better sensitivity than both fluorescent (LDH) and colorimetric assays (WST-1, MTT, MTS) currently utilised and does not contain any harmful radioactive components present in the well-renowned chromium⁵¹ release assay. The overall evaluation of the kits tested within this study illustrated that ToxiLight® proved to be the best cytotoxicity assay tested. This study did however highlight the need for combination assays to gain maximal information on the cells tested and as a result the bioluminescent kits ViaLight® and ToxiLight® were found to work well in conjunction with each other. This combination of a viability and cell death assay was discussed by Miret (2006) stating the need to analyse both apoptotic and necrotic forms of cell death. By measuring and comparing the relative amounts of AK and ATP within a population of cells, it was found that it

was possible to screen for all outcomes in a cell viability study. An increase in ATP values above that of the control sample would indicate proliferation in the cell sample, whereas samples giving lower ATP/RLUs to the control and showing a decrease / no change in the levels of AK would indicate growth arrest and a decrease in ATP and an increase in AK would conclude that the cells are necrotic. A good example of the need to measure cell viability and cell death was shown by measuring the effects of dacarbazine on melanoma cells. Neither the ToxiLight® assay nor the ViaLight® Plus assays on their own could identify the true effects of the drug on the cells. It was only when the two assays were used in combination with each other that a conclusion of cell cytostasis could be drawn from the experiment (figure 3.18).

Cell-based assays are being adopted with increasing frequency in drug discovery programs because cell systems are often inherently predictive of *in vivo* response. The use of technical optimisation in the combined kits allows an increase in the relevance of correlation testing, to enhance the chances of detecting precisely the cytotoxicity effects of drugs and to reduce the overall handling time and the amount of test compounds needed. It also allows optimal use of rare and valuable cell samples, such as primary cell cultures. Multiple endpoint kits may also provide hints of the mechanisms of toxicity. Since its launch in 2005, ToxiLight® has been utilised successfully by researchers for detecting the effects of drugs on cells in studying many diseases including cancer (Daniels *et al.*, 2006; Kumarasuriyar *et al.*, 2007; Morgan-Lappe *et al.*, 2007; Si *et al.*, 2008). In addition a paper published in 2006 by Miret compared many *in vitro* assays of cellular toxicity in HepG2 cells and concluded the ViaLight® Plus, ToxiLight® and caspase 3 fluorometric assays to be the most useful combination, again confirming the need for more than one assay to fully evaluate the cellular effects of a drug. Since the production of ToxiLight®,

a novel assay has been produced which is a 2 in 1 assay measuring both cell viability and cell death known as MultiTox-Fluor, it incorporates both fluorescence and luminescence measurements of proteases. Although it was not assessed in this study, this assay would be beneficial if its claims of sensitivity and rapid throughput are correct. However, it does possess obvious disadvantages, including the instability of the protease released upon cell death after 9 h in cell culture (Promega, 2009). This would result in ineffective and inconsistent measurements over a prolonged period of time. Future work for improving the ToxiLight® assay would be the inclusion of a “stop” solution which would allow for a more accurate measurement over time, to overcome the very rigid time restriction (of no more than 30 min) after addition of the AK detection reagent for analysing by luminometry. Ideally, a stop solution would improve the reproducibility for users and prevent any adverse effects of this reversible reaction.

6.2 Cytotoxicity assays and melanoma study

One of the main aims of the research was to obtain a drug sensitive and resistant melanoma cell line for further investigations into cellular proteomics. The combination of the ToxiLight® and ViaLight® Plus assays successfully identified the Ma Mel 28 cells as a vindesine, camptothecin and dexamethasone resistant cell line (chapter 4 of this thesis). The assays also revealed that the response observed with these cells was mainly due to a cytostatic effect to their treatment with the drugs ara-C, cisplatin and doxorubicin. In contrast to the Ma Mel 28 cell line, the Ma Mel 26a and MEWO cell lines proved to be more sensitive overall to the exposure to drugs ara-C, doxorubicin, camptothecin, cisplatin and trichostatin A used in this study. However, not all the drugs resulted in the same cellular effects throughout, with responses varying within the same cell line. Resistance is known to occur with many chemotherapy drugs

and experimentally, acquired resistance has been reported to various compounds (Kerbel *et al.*, 2001). Goldie and Coldman (1979) suggest that spontaneous mutations occurring during tumour evolution are responsible for the presence of intrinsically resistant cells before exposure of a tumour to a cytotoxic drug and this hypothesis continues to play a crucial role in the application of treatments (Poprach *et al.*, 2008). The results gained from studies presented in this thesis revealed that melanoma cells respond differently to various chemotherapeutic agents. A cell line may respond positively to one toxic agent but not another, and it may be inferred that individual patients respond differently to the agents used for their treatment. This highlights the need for “personalised” therapy for all patients so they can be screened individually for their potential response to a given cytotoxic drug prior to administration.

Melanomas are known to be intrinsically resistant to both chemotherapy and radiotherapy (Seetharamu *et al.*, 2009) and assays capable of detecting drug-resistance before commencement of treatment would be of benefit to patient management. The ToxiLight® and ViaLight® Plus assays could be utilised in these settings, but would rely on the use of techniques that reproducibly allowed primary cell cultures to be established. This represents an area that in the past has been difficult to address successfully. Current research is looking into the role cancer stem cells play in the resistance observed when patients undergo treatment. These cells are a small population of the tumour that possess the stem cell property of self renewal and proliferation (Gao, 2008). The cancer cells that undergo apoptosis when treated with a cytotoxic agent may be the tumour cells that have limited proliferation properties and are unable to renew. It is reported that cancer stem cells can resist apoptosis (Wei *et al.*, 2006) and it is therefore these resistant cells which should be

used in the screening for biomarkers and should be considered for future research.

6.3 The use of trichostatin A in the treatment of melanoma

Previously, trichostatin A, the most potent inhibitor of histone deacetylase, was shown to strongly suppress growth of pancreatic adenocarcinoma cells (Donadelli *et al.*, 2003). More recently the effects of trichostatin A on cancers including melanoma, have been widely tested and demonstrated to induce growth arrest and apoptosis in many studies (Koh *et al.*, 2007; Khan *et al.*, 2008). The data presented by Khan *et al.* (2008) revealed that abnormalities observed in some tumours, for example in the expression of MHC class I antigens may result from epigenetic repression. The use of trichostatin A has been shown to convert a tumour cell to an “antigen presenting cell” capable of activating IFN-gamma secreting T cells via the class I pathway (Khan *et al.*, 2008). This is most likely due to T-cell engagement which without the presence of co-stimulatory molecules e.g. B7, would lead to T-cell apoptosis and clonal deletion/peripheral tolerance (Zamorano *et al.*, 2001). Trichostatin A has also been shown to stabilise wild-type p53, although this was not proven to be the cause of the observed growth arrest (Peltonen *et al.*, 2005). The results indicate that while the action of TSA is independent of p53, the activation of the apoptosis pathway by the HDAC inhibitors may provide further therapeutic approaches for melanoma treatment (Peltonen *et al.*, 2005). The results in this thesis replicated the results observed in the study by Peltonen *et al.*, where all the cell lines responded to treatment with the drug. Although Ma Mel 28 cell death was not observed until after 72 h (using 5 μ M trichostatin A) the cells were non-replicating, indicating growth arrest.

It is not possible to mimic *in vitro* the exact condition of drug therapy, since many factors need to be taken into account. Melanoma patients undergo long treatment regimes whereas drug treatment *in vitro* is time restricted usually 24 – 72 h. The concentration of the drug at the tumour site will be variable depending on where the tumour is in the body, and the drugs pharmacokinetics: the extent and rate of absorption, distribution, metabolism and excretion of the drug (ADME); although in recent years pharmacokinetics has been better described as LADME:

- Liberation - the drugs release from the formulation.
- Absorption - the drug entering the body.
- Distribution - the dispersion or dissemination of the drug throughout the fluids and tissues of the body.
- Metabolism - the irreversible transformation of parent compounds into daughter metabolites.
- Excretion - the elimination of the substances from the body. In rare cases, some drugs irreversibly accumulate in a tissue in the body.

Future work on melanoma cells would investigate the undamaged cells by re-growing this hypothetically resistant population by exposing cells to trichostatin A over a prolonged period of time. This would prove whether or not a longer incubation time (beyond 3 days) would result in additional cytotoxic effects or whether a resistant population survives. This can then be compared to the original drug sensitive population for changes in the proteome and molecular pathways which may lead to a greater understanding of events within a cancer cell *in vivo*. This method would be a better way of monitoring differences between sensitive and resistant cells *in vitro* as this research resulted in findings related to ‘drug-induced’ effects. If the melanoma cells fail to respond to additional exposure of trichostatin A, a second agent in combination with trichostatin A could be

tested. Touma *et al.*, (2005) combined the use of retinoic acid and trichostatin A, which led to increased growth inhibition in renal cell carcinoma. Before confirmation of the overall effects of trichostatin A, the results obtained in this melanoma study could be repeated on different cancer cell types to determine whether the same heterogeneous response occurs. If these results conclude a lack of commonality within a larger homogeneous patient population then it may be concluded that there is a need for assays for drug sensitivity testing: personalised medicine (Marko-Varga *et al.*, 2007).

6.4 The cancer cell lines proteome

Proteomics has proven to be a useful tool in this study to extend our understanding to the molecular mechanisms associated with drug treated and untreated cancer cells. MS and bioinformatic analysis were introduced to interrogate the proteome of melanoma cells. The cell lines studied have revealed proteomic profiles that can be used to identify cellular changes resulting from the use of the chemotoxic drug, trichostatin A. Differences in the peptide fingerprinting profiles was observed that reflected the results obtained with the ToxiLight® and ViaLight Plus® assays. This led to the hypothesis that the differences in the profiles (drug treated versus control) would correlate with drug-response and the development of resistance to drug treatment. To further this aspect of the study, the reproducibility of the MALDI-TOF MS analysis was explored. The duplication of MS data is a contentious subject between many researchers, as highlighted in earlier studies by Petricoin *et al.*, (2002) which indicated that the data produced was not always replicated in further studies. However, the original work by Petricoin lacked vigorous quality control and standard operating procedures using robotic and automated sample processing. The MS

work carried out in chapter 5 were rigorously controlled and standardised including the use of an automated Xcise robotics for sample preparation; the inclusion of quality control to check for reproducibility; BSA controls to ensure the proteins had been tryptically digested; blanks to confirm there had been no contamination on the MALDI target plate and the randomisation of the samples on the MALDI plate. A problem that is often highlighted in proteomic research is the cut off for peak discrimination. Small peaks are often the same peak intensity as the baseline peaks themselves, but could contain important information not readily identified due to the lack of sensitivity of the methodology.

To corroborate the peptide profile data obtained in this study, future work should include validation by other operators on the same and other instruments at more than one centre. An added parameter to consider upon analysing the results for peptide profile differences between the cell lines is that each individual cell line should undergo assay on different days to establish the in built error of analysis at different time points. Other parameters associated with cell culture and freezing conditions will be important to understand and crucial in removing any bias that may be introduced to a study.

Cell lines are proving to be a valuable alternative and a pre-requisite to the use of tissue for genetic and proteomic studies. The availability of tissues to researchers has been problematic for a number of reasons: the lack of adequately characterized high quality tissues, increasing concerns due to privacy issues and the inability to obtain follow-up or clinical outcome of patients. Protein profiles between areas of the tissue mass can also alter, similar to the alteration seen with cell lines during their time in culture. A number of proteomic studies have been conducted whereby the authors have utilised cell lines to identify proteins of possible clinical

significance. Mian *et al.*, (2003) studied the effects of the chemotherapeutic agent taxol, in resistant and sensitive breast cancer cell lines by examining their protein expression patterns over a treatment period of 96 h. Analysis of a resistant gastric cancer cell line by MALDI-TOF MS identified nine differential expression proteins between the parental and resistant strains enabling the sensitization of the cells by the construction of a vector for Triosephosphate isomerase (TPI) which was found to be down-regulated (Wang *et al.*, 2008). After transfection with the vector, the cells became more sensitive to several drugs and the resistance was shown to be reversed.

6.5 Use of bioinformatics as a tool in biomarker identification

Due to the enormous quantity of data obtained by proteomics it was necessary to evaluate the results by means of statistical algorithms capable of handling the dimensionality of large data sets. This prevents both bias and promotes faster analysis of data establishing differences or commonalities in protein profiles for biomarker identification. As previously mentioned, data pre-processing is important for reproducible data (Carlson *et al.*, 2005; Petricoin *et al.*, 2002). Although ANNs has not been used directly in patient treatment, the results show that it has huge potential to be of benefit to patients for personalised therapy in the future. Larger populations would improve the predictive performance of the ANNs resulting in a larger validation set if the data were analysed in the same manner as in this study i.e. 60% training set; 20% test data set and a 20% blind data set (Schwarzer *et al.*, 2000).

The majority of proteins identified by proteomic profiling were associated with either metabolic, cytoskeletal or nuclear responses in this investigation (ATP synthase was identified as a prominent response).

However, such high abundance molecules are often produced as a reaction to tumour presence, but could still represent valid biomarkers of the disease process or response to therapy (Diamandis, 2002). As revealed in this study the presence of ATP synthase in both Ma Mel 28 and MEWO cells was indicative of cell death, and it can be suggested that protein could be of use in diagnosis or prognosis with this or other drugs. Whether other drugs produce the same protein anti-inflammatory response or not remains to be established. Further research using a broader range of drugs, patient samples and different cancers should be conducted. A larger patient population would also benefit accuracy and reproducibility of ANN analysis allowing further differences and new cancer biomarkers to emerge; these biomarkers could provide valuable information that may aid in a more effective diagnosis, prognosis, and response to therapy.

From the results obtained here using mass spectrometry and ANN analysis, the identity and correlation of patterns of melanoma response to trichostatin A has revealed differences between drug-treated and control melanoma cells. The responses identified upon drug exposure (e.g. ATP synthase in drug-treated cells) revealed that the cells had been damaged by the drug treatment replicating the results observed with the cytotoxicity assays; ViaLight® Plus and ToxiLight®. Further research investigating trichostatin A as a future potential agent in patient treatment would be required using a larger patient sample population, obtained from various centres. The protein identities in this study should also be confirmed by other methodologies including western blotting and ELISA.

This methodology of using MALDI-MS and the combinatorial cell death assays could provide a way of monitoring the treatment of patients in the future. At present, there are limitations to the methodologies. The MALDI-

MS and ANNs analysis is time consuming, equipment is expensive and the software requires specialist knowledge and interpretation. The techniques would need to be reproducible, robust, user-friendly and easily adapted for the high throughput screening (HTS) of therapeutic drugs. The biomarkers identified in this research could have potential in monitoring the effects of drug treatment. If ATP synthase is confirmed to be consistently up regulated after a patient has a positive response to drug treatment, then this biomarker could be a potential maker for drug therapy. The research would have to be repeated on a larger population, in different clinics and monitored using patient serum as tissue is not easily accessible or optional for regular monitoring.

6.6 Personalised medicine

Recent advances in science offers the potential to define an individuals risk based on their own personal “genetic make-up”. Currently, cancer treatment is based upon standards of care that are determined by averaging the response rates of clinical trials across large cohorts i.e. a treatment plan that is similar for the analysis of clinical trials in different cancer types (Mansour *et al.*, 2008; Van't Veer *et al.*, 2008). The emergence of subtypes of disease adds to the difficulty of determining the prognosis of patients and recommendation of the most appropriate treatment; the stage, grade and histological type of the cancer can affect how drugs localise in cancer tissue and should be taken into account. Personalization of treatment should be based on an individual patient's clinical status, taking into account age, gender, height, weight, diet and environment that could be used to stratify disease status; select between different medications and/or tailor their dosage; provide a specific therapy for an individual's disease; or initiate a preventative measure that is particularly suited to that patient at the time of administration. Several

examples of approaches to personalized medicine have already been established in practice, such as the testing for disease-causing mutations in the BRCA1 and BRCA2 genes implicated in familial breast and ovarian cancer syndromes (Tonin *et al.*, 2006) and the well documented herceptin therapy (Germano and O'Driscoll, 2009). It is hoped that in the future with the use of proteomic and genomic approaches to diagnosis, drug development and individualized therapy will improve the quality of life for patients with cancer (Marko-Varga *et al.*, 2006). Better diagnosis and prediction of treatment outcome will prevent patients undergoing treatments that are unnecessary and identify, with a higher degree of accuracy, appropriate (personalised) therapies.

References

Aalinkeel R, Nair MPN, Sufrin G. *et al.* Gene expression of angiogenic factors correlates with metastatic potential cancer cells. *Cancer Research*. 2004; **64**: 5311-5321.

Adam BL, Qu Y, Davis JW *et al.* Serum protein fingerprinting coupled with a pattern-matching algorithm distinguishes prostate cancer from benign prostate hyperplasia and healthy men. *Cancer Research* 2002; **62 (13)**: 3609-3614.

Agarwala SS, Keilholz U, Gilles E *et al.* LDH correlation with survival in advanced melanoma from two large, randomized trials. *European Journal of Cancer* 2009; **45 (10)**: 1807-1814.

Ahmed N, Barker G, Oliva KT *et al.* Proteomic-based identification of haptoglobin-1 precursor as a novel circulating biomarker of ovarian cancer. *British Journal of Cancer*. 2004; **91 (1)**: 129-140.

Alarcon-Vargas D. and Ronai Z. The p53–Mdm2—the affair that never ends. *Carcinogenesis*. 2002; **23 (4)** 541-547.

Alberts B, Bray D, Lewis J *et al.* Molecular biology of the cell. 2nd edn. Garland Publishing, New York. 1989.

Alexandrova R. Tumour heterogeneity. *Experimental Pathology and Parasitology*. 2001; **4 (6)**: 57-67.

Amiri KI, Horton LW, La Fleur BJ *et al.* Augmenting chemo sensitivity of malignant melanoma tumours via proteasome inhibition: implication for bortezomib (VELCADE, PS-341) as a therapeutic agent for malignant melanoma. *Cancer Research* 2004; **64 (14)**: 4912-4918.

Ang IL, Poon TC, Lai PB *et al.* Study of serum haptoglobin and its glycoforms in the diagnosis of hepatocellular carcinoma: a glycoproteomic approach. *Journal of Proteome Research* 2006; **5 (10)**: 2691-2700.

Ashcroft AE. Recent developments in electrospray ionization mass spectrometry: noncovalently bound protein complexes. *National Product Reports* 2005; **22 (4)**: 452-464.

Baak JPA, Path FRC, Hermsen MAJA *et al.* Genomics and proteomics in cancer. *European Journal of Cancer* 2003; **39**: 1199-1215.

- Balch CM, Reintgen DS, Kirkwood JM *et al.* Cutaneous melanoma: In: VT DeVita; S Hellman; SA Rosenberg, editors *Cancer: principles and practice of oncology*. 5th edn. Philadelphia Pa: Lippincott; 1997; pp1935-1993.
- Bachy M, Bonnin-Rivalland A, Tillet V *et al.* Beta galactosidase release as an alternative to chromium release in cytotoxic T-cell assays. *Journal of Immunological Methods*. 1999; **230**: 37-46.
- Baggerly KA, Morris JS, Edmonson SR *et al.* Signal in noise: evaluating reported reproducibility of serum proteomic tests for ovarian cancer. *Journal of the National Cancer Institute* 2005; **97 (4)**: 307-309.
- Balch CM, Buzaid AC, Soong SJ *et al.* Final version of the american joint committee on cancer staging system for cutaneous melanoma. *Journal of Clinical Oncology* 2001; **19 (16)**: 3635-3648.
- Ball G, Mian S, Holding F *et al.* An integrated approach utilizing artificial neural networks and SELDI mass spectrometry for the classification of human tumours and rapid identification of potential biomarkers. *Bioinformatics* 2002; **18 (3)**: 395-404.
- Basheer IA, Hajmeer M. Artificial neural networks: fundamentals, computing, design, and application. *Journal of Microbiological Methods* 2000; **43 (1)**:3-31.
- Baumforth KR, Young LS, Flavell KJ *et al.* The Epstein-Barr virus and its association with human cancers. *Molecular Pathology*. 1999; **52**: 307-322.
- Becton Dickinson, Facscalibur Training Manual; 1997
- Bensmail H, Haoudi A. Data mining in genomics and proteomics. *Journal of Biomedicine and Biotechnology* 2005; **2**: 63-64.
- Berger AJ, Kluger HM, Li N *et al.* Subcellular localisation of activating transcription factor 2 in melanoma specimens predicts patient survival. *Cancer Research*. 2003; **63**: 8103-8107.
- Berking C, Takemoto R, Binder RL *et al.* Photocarcinogenesis in human adult skin grafts. *Carcinogenesis*. 2002; **23 (1)**: 181-187.
- Bernard K, Litman E, Fitzpatrick JL *et al.* Functional proteomic analysis of melanoma progression. *Cancer Research* 2003; **63 (20)**: 6716-6725.

- Berridge MV, Herst PM, Tan AS. Tetrazolium dyes as tools in cell biology: new insights into their cellular function. *Biotechnology Annual Review* 2005; **11**: 127-152.
- Berwick M, Orlov I, Mahabir S *et al.* Estimating the relevant risk of developing melanoma in INK4A carriers. *European Journal of Cancer Prevention* 2004; **13 (1)**: 75-80.
- Bossuyt R. A five minute ATP platform test for judging the bacteriology quality of raw milk. *Netherlands Milk Dairy Journal* 1982; **36**: 335-338.
- Bradbury DA, Simmons TD, Slater KJ *et al.* Measurement of the ADP:ATP ratio in human leukaemic cell lines can be used as an indicator of cell viability, necrosis and apoptosis. *Journal of Immunological Methods*. 2000; **240**: 79-92.
- Bromberg ME, Konigsberg WH, Madison JF *et al.* Tissue factor promotes melanoma metastasis by a pathway independent of blood coagulation. *Proceedings of the National Academy of Science USA* 1995; **92 (18)**: 8205-8209.
- Burns DA, Breathnach SM, Cox N *et al.* Rooks Textbook of Dermatology. 7th edn. Wiley-Blackwell; 2004.
- Bushell M, Stoneley M, Sarnow P, Willis AE. Translation inhibition during the induction of apoptosis: RNA or protein degradation? *Biochemical Society Transactions*. 2004; **32 (4)**: 606-610.
- Campana D, Coustan-Smith E. Minimal residual disease studies by flow cytometry in acute leukemia. *International Journal of Haematology*. 2004; **112 (1-2)**: 8-15.
- Carbone A, Gloghini A, Dotti G. EBV-associated lymphoproliferative disorders: classification and treatment. *The Oncologist*. 2008; **13 (5)**: 577-585.
- Carlson SM, Najmi A, Whitin JC *et al.* Improving feature detection and analysis of surface-enhanced laser desorption/ionization-time of flight mass spectra. *Proteomics* 2005; **5 (11)**: 2278-2788.
- Cazares LH, Dias JI, Drake RR *et al.* MALDI/SELDI protein profiling of serum for the identification of cancer biomarkers. *Methods in Molecular Biology*. 2008; **428**: 125-140.

- Chautan M, Chazal G, Cecconi F *et al*. Interdigital cell death can occur through a necrotic and caspase-independent pathway. *Current Biology* 1999; **9 (17)**: 967-970.
- Collie-Duguid ESR, Petty RD, Kerr KM. Cancer therapy prognosis and target. Published patent application 2007, in press, BOA: 0519405.5.
- Cooper GM. *The Cell – A molecular approach*. Oxford University Press. 1997
- Craven RA, Stanley AJ, Hanrahan S *et al* Identification of proteins regulated by interferon-alpha in resistant and sensitive malignant melanoma cell lines. *Proteomics*. 2004; **4 (12)**: 3998-4009.
- Cree IA, Pazzagli M, Mini E *et al*. Methotrexate chemosensitivity by ATP luminescence in human leukaemia cell lines and in breast cancer primary cultures: comparison of the TCA-100 assay with a clonogenic assay. *Anticancer Drugs* 1995; **6**: 398-404.
- Cree IA, Kurbacher CM, Untch M *et al*. Correlation of the clinical response to chemotherapy in breast cancer with *ex vivo* chemosensitivity. *Anticancer Drugs*. 1996; **7**: 630-635.
- Cree IA, Kurbacher CM, Christian M. ATP-based tumour chemosensitivity testing: assisting agent development. *Anticancer Drugs*. 1999; **10 (5)**: 51-57.
- Crouch SPM, Kozlowski R, Slater KJ *et al*. The use of ATP bioluminescence as a measure of cell proliferation and cytotoxicity. *Journal of Immunological Methods*. 1993; **160**: 81-88.
- Darkes MJM, Plosker GL, Jarvis B. Temozolomide: a review of its use in the treatment of malignant gliomas, malignant melanoma and other advanced cancers. *American Journal of Cancer* 2002; **1 (1)**: 55-80.
- Dahl C, Guldberg P. The genome and epigenome of malignant melanoma. *Scandinavian Societies for Medical Microbiological and Pathology (APMIS)* 2007; **115 (10)**: 1161-1176.
- Daniels I, Abulayha AM, Thomson BJ *et al*. Caspase-independent killing of Burkitt lymphoma cell lines by rituximab. *Apoptosis* 2006; **11 (6)**: 1013-1023.
- Darzynkiewicz Z, Bruno S, Bino GD *et al*. Features of apoptotic cells measured by flow cytometry. *Cytometry* 1992 ; **13** : 795 - 808

- de Noo ME, Tollenaar RAEM, Deelder AM *et al.* Current status and prospects of clinical proteomics studies on detection of colorectal; cancer: hopes and fears. *World Journal of Gastroenterology* 2006; **12 (41)**: 6594-6601.
- Decker T, Lohmann-Mathes ML. A quick and simple method for the quantification of lactate dehydrogenase release in measurements of cellular cytotoxicity and tumour necrosis factor (TNF) activity. *Journal of Immunological Methods*. 1988; **15**: 61-69.
- Désilets A, Gheorghiu I, Yu SJ *et al.* Inhibition by deacetylase inhibitors of IL-1-dependent induction of haptoglobin involves CCAAT/Enhancer-binding protein isoforms in intestinal epithelial cells. *Biochemical and Biophysical Research Communications* 2000; **276 (2)**: 673-679.
- DeWitt N. Angiogenesis. *Nature*. 2005; **438**: 931.
- Diamandis EP. Proteomics patterns in serum and identification of ovarian cancer. *Lancet* 2002; **360 (9327)**: 170; author reply 170-171.
- Diamandis EP, Identification of serum amyloid a protein as a potentially useful biomarker for nasopharyngeal carcinoma. *Clinical Cancer Research* 2004; **10 (15)**: 5293-5294.
- Diamandis EP, Analysis of serum proteomic patterns for early cancer diagnosis : drawing attention to potential problems. *Journal of the National Cancer Institute*. 2004; **96 (5)**:353-356.
- Dieplinger H, Ankerst DP, Burges A *et al.* Afamin and apolipoprotein A-IV: novel protein markers for ovarian cancer. *Cancer Epidemiology, Biomarkers and Prevention* 2009; **18 (4)**: 1127-1133.
- Dolken G. Detection of minimal residual disease. *Advanced Cancer Research* 2001; **82**: 133-185.
- Donadelli M, Costanzo C, Faggiolo L *et al.* Trichostatin A, an inhibitor of histone deacetylases, strongly suppresses growth of pancreatic adenocarcinoma cells. *Molecular Carcinogenesis* 2003; **38 (2)**: 59-69.
- Dowling P, O'Driscoll L, Meleady P *et al.* 2-D difference gel electrophoresis of the lung squamous cell carcinoma versus normal sera demonstrates consistent alterations in the levels of ten specific proteins. *Electrophoresis* 2007; **28 (23)**: 4302-4310.

Dothager RS, Putt KS, Allen BJ *et al.* Synthesis and identification of small molecules that potently induce apoptosis in melanoma cells through G1 cell cycle arrest. *Journal of the American Chemical Society Articles* 2005; **127**: 8686-8696.

D'Souza G, Kreimer AR, Viscidi R. Case control study of human papillomavirus and oropharyngeal cancer. *The New England Journal of Medicine* 2007; **356 (19)**: 1944-1956.

Dundr P, Povysil C, Tvdik D. Actin expression in neural crest cell-derived tumours including schwannomas, malignant peripheral nerve sheath tumours, neurofibromas and melanocytic tumours. *Pathology International* 2009; **59 (2)**: 86-90.

Dworzak MN. Immunological detection of minimal residual disease in acute lymphoblastic leukaemias. *Oncology*. 2001; **24**: 442-448.

Esteller M. Cancer epigenomics: DNA methylomes and histone-modification maps. *Nature Reviews Genetics*. 2007; **8**: 286-298.

Ewaschuk JB, Naylor JM, Zello GA. D-lactate in human and ruminant metabolism *Journal of Nutrition* 2005; **135 (7)**: 1619-1625.

Fenech M. Biomarkers of genetic damage for cancer epidemiology. *Toxicology* 2002; **181-182**: 411-416.

Fenech M. Chromosomal biomarkers of genomic instability relevant to cancer. *Drugs Discovery Today*. 2002; **7 (22)**: 1128-1137.

Fiers W, Beyaert R, Declercq W *et al.* More than one way to die: apoptosis, necrosis and reactive oxygen damage *Oncogene* 1999; **18 (54)**: 7719-7730.

Finucane DM, Waterhouse NJ, Amarante-Mendes *et al.* Collapse of the inner mitochondrial transmembrane potential is not required for apoptosis of HL60 cells. *Experimental Cell Research*. 1999; **251**: 166-174.

Florenes VA, Skrede M, Jorgensen K *et al.* Deacetylase inhibition in malignant melanomas: impact on cell cycle regulation and survival. *Melanoma Research* 2004; **14 (3)**: 173-181.

Fogel GB. Computational intelligence approaches for pattern discovery in biological systems. *Brief Bioinformatics* 2008; **9 (4)**: 307-316.

Forman SB, Ferringer TC, Peckham SJ *et al.* Is superficial spreading melanoma still the most common form of malignant melanoma *Journal of American Academy of Dermatology* 2008; **58 (6)**: 1013-1020.

Fuks A, Banjo C, Shuster J *et al.* Carcinoembryonic antigen (CEO): molecular biology and clinical significance. *International Journal of Biochemistry, Biophysics and Molecular Biology* 1975; **417 (2)**: 123-152.

Fung ET, Weinberger SR, Gavin E *et al.* Bioinformatics approaches in clinical proteomics. *Expert Review of Proteomics* 2005 ; **2 (6)** : 847-862.

Furumai R, Komatsu Y, Nishino N *et al.* Potent histone deacetylase inhibitors built from trichostatin A and cyclic tetrapeptide antibiotics including trapoxin. *Proceedings of the National Academy of Science of the USA* 2001; **98 (1)**: 87-92.

Gadduci A, Marrai R, Baicchi U *et al.* Prothrombin fragment F1+2 and thrombin-antithrombin III complex (TAT) plasma levels in patients with gynecological cancer. *Gynecological Oncology* (2002); **61 (2)**: 215-217.

Gao J. Cancer stem cells: the lessons from pre-cancerous stem cells. *Journal of Cell and Molecular Medicine* 2008; **12 (1)**: 67-96.

Garbe C. Chemotherapy and chemo immunotherapy in disseminated malignant melanoma. *Melanoma Research* 1993; **3 (4)**: 291-299.

Germano S, O'Driscoll L. Breast cancer: understanding sensitivity and resistance to chemotherapy and targeted therapies to aid in personalised medicine. *Current Cancer Drug Targets* 2009; **9 (3)**: 398-418.

Ginsberg D. E2F1 pathways to apoptosis. *FEBS Letters* 2002; **529(1)**: 122-5.

Goldie JH, Coldman AJ. A mathematical model for relating the drug sensitivity of tumours to their spontaneous mutation rate. *Cancer Treatment Reports* 1979; **63 (11-12)**: 1727-1733.

Gonda TJ, Sheiness DK, Bishop MJ. Transcripts from the cellular homologs of retroviral oncogenes: distribution among chicken tissues. *Molecular and Cellular Biology* 1982; **2 (6)**: 617-624.

Gorman A. Morphological assessment of apoptosis in: Techniques in apoptosis. *Portland Press*; 1996

Gottifredi V, Karni-Schmidt O, Shieh S *et al.* p53 down-regulates CHK1 through p21 and the retinoblastoma protein. *Molecular and Cellular Biology*. 2001; **21 (4)**: 1066-1076

Green DS, Bodman-Smith MD, Dalglish AG *et al.* Phase I/II study of topical imiquimod and intralesional interleukin 2 in the treatment of accessible metastases in malignant melanoma. *British Journal of Dermatology* 2007; **156 (2)**: 337-345.

Grell P, Svoboda M, Simickova M *et al.* Trastuzumab in the breast cancer treatment: efficacy and resistance mechanisms. *Clinical Oncology* 2009; **22 (2)**: 45-51.

Grossman D, Altieri DC. Drug resistance in melanoma: mechanisms, apoptosis, and new potential therapeutic targets. *Cancer Metastasis Reviews* 2004; **20 (1-2)**: 3-11.

Habold C, Poehlmann A, Bajbouj K *et al.* Trichostatin A causes p53 to switch oxidative-damaged colorectal cancer cells from cell cycle arrest into apoptosis. *Journal of Cellular and Molecular Medicine* 2008; **12 (4)**: 1421.

Hainaut P. and Wiman KG. 25 years of p53 research. 2nd edn: Springer. 2007.

Hemann MT, Lowe SW. p53 links tumour development to cancer therapy In: 25 years of p53 research. Edited by Hainaut P, Wiman K. 2005; chapter 15.

Hanahan D, Weinberg RA. The hall marks of cancer. *Cell* 2000; **100 (1)**:57-70.

Harrison SL, MacLennan R, Speare R *et al.* Sun exposure and melanocytic naevi in young Australian children. *Lancet*. 1994; **344**: 1529-1532.

Hassan MM, Spitz MR, Thomas MB *et al.* The association of family history of liver cancer with hepatocellular carcinoma: a case-control study in the united states. *Journal of Hepatology*. 2008; **50 (2)**: 334-341.

Hastings JW. Biological diversity, chemical mechanisms and the evolutionary origins of bioluminescent systems. *Journal of Molecular Evolution*. 1983; **19**: 309-321.

- Herrera DJ, Morris K, Johnston C *et al.* Automated assay for plasma D-lactate by enzymatic spectrophotometric analysis with sample blank correction. *Annals of Clinical Biochemistry* 2008; **45 (Pt 2)**: 177-183.
- Hodgson S. Mechanisms of inherited cancer susceptibility. *Journal of Zhejiang University Science* 2008; **9 (1)**: 1-4.
- Hoover-Plow J, Hart E, Gong Y *et al.* A physiological function for apolipoprotein(a): a natural regulator of the inflammatory response. *Experimental Biology and Medicine* 2009; **234 (1)**: 28-34.
- Horner SM, DeFilippis RA, Mannelidis L *et al.* Repression of the human papillomavirus E6 gene initiates p53-dependent, telomerase-independent senescence and apoptosis in HeLa cervical carcinoma cells. 2004; **78 (8)**: 4063-4073.
- Huang LF, Liang YZ, Guo FQ *et al.* Simultaneous separation and determination of active components in *Cordyceps sinensis* and *Cordyceps militaris* by LC/ESI-MS. *Journal of Pharmaceutical and Biomedical Analysis* 2002; **33 (5)**: 1155-1162.
- Hirsch T, Susin SA, Marzo I. Mitochondrial permeability transition in apoptosis and necrosis. *Cell Biology and Toxicology*. 1998; **14**: 141-145.
- Hutchens TW, Yip TT. New desorption strategies for the mass spectrometric analysis of macromolecules. *Rapid Communications in Mass Spectrometry* 1993; **7**: 576-580.
- Jiao W, Lin HM, Datta J *et al.* Aberrant nucleocytoplasmic localization of the retinoblastoma tumor suppressor protein in human cancer correlates with moderate/poor tumor differentiation. *Oncogene* 2008; **27** 3156-3164.
- Kaplan DE, Chang K. Current status of vaccine therapy for hepatitis C infection. *Current Hepatitis Reports*. 2006; **5 (2)**: 68-74.
- Karas M, Hillenkamp F. Laser desorption ionisation of proteins with molecular masses exceeding 10,000 daltons. *Analytical Chemistry* 1988; **60 (20)**: 2299-2301.
- Khan AN, Gregorie CJ, Tomasi TB. Histone deacetylase inhibitors induce TAP, LMP, Tapasin genes and MHC class I antigen presentation by melanoma cells. *Cancer Immunology Immunotherapy* 2008; **57 (5)**: 647-654.

- Kawada K, Yonel T, Ueoka H *et al.* Comparison of chemosensitivity tests: clonogenic assay versus MTT assay. *Okayama University Medical School.* 2002; **56 (3)**: 129-134.
- Kebarle, P. A brief overview of the present status of the mechanisms involved in electrospray mass spectrometry. *Journal of Mass Spectrometry.* 2000; **35 (7)**: 804 - 817.
- Kerbel RS, Yu J, Man S *et al.* Possible mechanisms of acquired resistance to anti-angiogenic drugs: implications for the use of combination therapy approaches. *Cancer Metastasis Reviews* 2001; **20 (1-2)**: 79-86.
- Khan AN, Gregorie CJ, Tomasi TB. Histone deacetylase inhibitors induce TAP, LMP, Tapasin genes and MHC class I antigen presentation by melanoma cells *Cancer Immunology, Immunotherapy* 2008; **57 (5)**: 647-654.
- Kiaris H. Understanding Carcinogenesis: An introduction to the molecular basis of cancer. Wiley-VCH, Weinheim. 2006.
- Kim CJ, Dessureault S, Gabrilovich D *et al.* Immunotherapy for melanoma. *Cancer Control.* 2002; **9 (1)**: 22-30.
- Kim CJ, Dessureault S, Gabrilovich D *et al.* Immunotherapy for melanoma. *Cancer Control* 2002a; **9 (1)**: 22-30.
- Kim CJ, Reintgen DS, Balch CM. The new melanoma staging system *Cancer Control* 2002b; **9 (1)**: 9-15.
- Kim H, Yoon SC, Lee TY *et al.* Discriminative cytotoxicity assessment based on various cellular damages. *Toxicology Letters* 2009; **184 (1)**: 13-17.
- Kim HR, Kim EJ, Yang SH *et al.* Trichostatin A induces apoptosis in lung cancer cells via simultaneous activation of the death receptor-mediated and mitochondrial pathway? *Experimental and Molecular Medicine* 2006; **38 (6)**: 616-624.
- Kissel CK, Schadendorf D, Rockmann H. The altered apoptotic pathways in cisplatin and etoposide-resistant melanoma cells are drug specific. *Melanoma Research* 2006; **16 (6)**: 527-535.
- Klatt EC and Kumar V. Review of pathology. 3rd edn: WB Saunders Company, Pennsylvania. 2009.

- Klisovic DD, Katz SE, Efron D *et al.* Depsipeptide (FR901228) inhibits proliferation and induces apoptosis in primary and metastatic human uveal melanoma cell lines. *Investigative Ophthalmology and Visual Science* 2003; **44 (6)**; 2390-2398.
- Koeller KM, Haggarty SJ, Perkins BD *et al.* Chemical genetic modifier screens: small molecule trichostatin suppressors as probes of intracellular histone and tubulin acetylation. *Chemistry and Biology* 2003; **10 (5)**: 397-410.
- Koh E, Bandle R, Clair T *et al.* Trichostatin A and 5-aza-2'-deoxycytidine switch S1P from an inhibitor to a stimulator of motility through epigenetic regulation of S1P receptors. *Cancer Letters* 2007; **250 (1)**: 53-62.
- Koomen JM, Shih LN, Coombes KR *et al.* Plasma protein profiling for diagnosis of pancreatic cancer reveals the presence of host response proteins. *Clinical Cancer Research*. 2005; **11 (3)**: 1110-1118.
- Korzeniewski C, Callewaert DM. An enzyme-release assay for natural cytotoxicity. *Journal of Immunological Methods* 1983; **64**: 313-320.
- Krebs HA. The history of the tricarboxylic acid cycle. *Perspectives in Biology and Medicine*. 1970; **14**: 157-170.
- Kroemer G, Zamzami N, Susin SA *et al.* Mitochondrial control of apoptosis. *Immunology Today*. 1998; **18**: 44-51.
- Kumarasuriyar A, Dombrowski C, Rider DA *et al.* A novel use of TAT-EGFP to validate techniques to alter osteosarcoma cell surface glycosaminoglycan expression. *Journal of Molecular Histology* 2007; **38 (5)**: 435-437.
- Kurbacher CM, Cree IA, Bruckner HW *et al.* Use of an *ex vivo* ATP luminescence assay to direct chemotherapy for recurrent ovarian cancer. *Anticancer Drugs*. 1998; **9 (1)**: 51-57.
- Kurth KH. Diagnosis and treatment of superficial transitional cell carcinoma of the bladder: facts and perspectives. *European Urology* 1997; **31**: 10-19.
- Lage H, Helmbach H, Grottke C *et al.* DFNA5 (ICERE-1) contributes to acquired etoposide resistance in melanoma cells. *FEBS Letters* 2001; **494 (1-2)**:54-59.
- Lamkanfi M, Kalai M, Vandenabeele P. Caspase-12: an overview. *Cell Death and Differentiation* 2004; **11**: 365-368.

- Lancashire L, Schmid O, Shah H *et al.* Classification of bacterial species from proteomic data using combinatorial approaches incorporating artificial neural networks, cluster analysis and principal components analysis. *Bioinformatics* 2005; **21 (10)**: 2191-2199.
- La Porta CA. Drug resistance in melanoma: new perspectives. *Current Medicinal Chemistry* 2007; **14 (4)**: 387-391.
- Larkin JM, Norsworthy PJ, A'Hern RP *et al.* Anti-alphaGal-dependent complement-mediated cytotoxicity in metastatic melanoma. *Melanoma Research* 2006; **16 (2)**: 157-163.
- Le L, Chi K, Tyldesley S *et al.* Identification of serum amyloid A as a biomarker to distinguish prostate cancer patients with bone lesions. *Clinical Chemistry* 2005; **51 (4)**: 695-707.
- Lee AS. GRP78 induction in cancer: therapeutic and prognostic implications. *Cancer Research* 2007; **67** 3496-3499
- Leman ES, Getzenberg RH. Biomarkers in prostate cancer. *Journal of Cellular Biochemistry* 2009; **(epub ahead of print)**.
- Leonetti C, Biroccio A, Candiloro A *et al.* Increase of cisplatin sensitivity by c-myc antisense oligodeoxynucleotides in a human metastatic melanoma inherently resistant to cisplatin. *Clinical Cancer Research* 1999; **5 (9)**: 2588-2595.
- Lesk AM. Introduction to bioinformatics. 2nd edn Oxford University Press, New York 2005; pp298, 199.
- Li G, Tang L, Zhou X *et al.* Chemotherapy-induced apoptosis in melanoma cells is p53 dependent. *Melanoma Research* 1998; **8 (1)**: 17-23.
- Li J, Zhang Z, Rosenzweig J *et al.* Proteomics and bioinformatics approaches for identification of serum biomarkers to detect breast cancer. *Clinical Chemistry* 2002; **48 (8)**: 1296-1304.
- Li J, Zhang Z, Rosenzweig J *et al.* Proteomics and bioinformatics approaches for identification of serum biomarkers to detect breast cancer. *Clinical Chemistry*. 2002; **48 (8)**: 1296-1304.
- Li M, Brooks CL, Wu-Baer F *et al.* Mono-versus polyubiquitination: differential control of p53 fate by Mdm2. *Science* 2003; **302**: 1972-1975.

Liebler DM. Introduction to proteomics: tools for the new biology. Humana Press, NJ. 2002; Chapter 1.

Lindenbach BD, Evans MJ, Syder AJ *et al.* Complete replication of hepatitis C virus in cell culture. *Science*. 2005; **309 (5734)**: 623-626.

Liotta LA, Petricoin EF. Serum peptidome for cancer detection: spinning biologic trash into diagnostic gold. *Journal of Clinical Investigations*. 2006; **116**: 26-30.

Little KJ, LaRocco KA. ATP screening method for presumptive detection of microbiologically contaminated carbonated beverages. *Journal of Food Science*. 1986; **51**: 474-476.

Lobner D. Comparison of the LDH and MTT assays for quantifying cell death: validity for neuronal apoptosis? *Journal of Neuroscience Methods* 2000; **96 (2)**: 147-152.

Locatelli C, Leal PC, Yunes RA, Nunes RJ, Creczyuski-Pasa TB. Gallic acid ester derivatives induce apoptosis and cell adhesion inhibition in melanoma cells: the relationship between free radical generation, glutathione depletion and cell death. *Chemico-Biological Interactions* 2009; **181 (2)**: 175-184.

Lu WJ, Lee NP, Fatima S *et al.* Heat shock proteins in cancer: signaling pathways, tumour markers and molecular targets in liver malignancy. *Protein Peptide Letters* 2009; **16 (5)**: 508 – 516.

Lugovic L, Situm M, Kos L. Malignant melanoma - future prospects. *Acta Dermatovenerologica Croatica*. 2005; **13 (1)**: 36-43.

Lundin A. Luminescent Assays: perspectives in endocrinology and clinical chemistry. Applications of firefly luciferase. Raven Press. 1982

Lundin A. Optimised assay of firefly luciferase with stable light emission, In: Bioluminescence and chemiluminescence: Status report. (Szalay, A. A., Krika, L. J. and Stanley, P. E. Eds) John Wiley, Chichester, UK. 1993. Pp 291-295.

Mann M, Hendrickson RC, Pandey A. Analysis of proteins and proteomes by mass spectrometry. *Annual Review of Biochemistry* 2001; **70**: 437-473.

Mansour JC, Schwarz RE. Molecular mechanisms for individualized cancer care 2008; *Journal of the American College of Surgeons* 2008; **207 (2)**: 250-258.

- Markey MK, Tourassi GD, Floyd CE Jr. Decision tree classification of proteins identified by mass spectrometry of blood serum samples from people with and without lung cancer. *Proteomics* 2003; **3 (9)**: 1678-1679.
- Markiewski MM, Lambris JD. Is complement good or bad for cancer patients? A new perspective on an old dilemma. *Trends in Immunology* 2009; **30 (6)**: 286-292.
- Marko-Varga G, Ogiwara A, Nishimura T *et al.* Personalised medicine and proteomics: lessons from non-small cell lung cancer. *Journal of Proteome Research* 2007; **6 (8)**: 2925-2935.
- Marshall NJ, Goodwin CJ, Holt SJ. A critical assessment of the use of micro culture tetrazolium assays to measure cell growth and function. *Growth Regulation* 1995; **5 (2)**: 69-84.
- Matharoo-Ball B, Ratcliffe L, Lancashire L *et al.* Diagnostic biomarkers differentiating metastatic melanoma patients from healthy controls identified by an integrated MALDI-TOF mass spectrometry/bioinformatic approach. *Proteomics and Clinical Applications*. 2007; **1**: 605-620.
- Matharoo-Ball B, Miles AK, Creaser CS *et al.* Serum biomarker profiling in cancer studies: a question of standardisation? *Veterinary and Comparative Oncology* 2008; **6 (4)**: 224-247.
- McCarthy NJ, Jacobson MD. Why be interested in death? In: Apoptosis the molecular biology of programmed cell death. Oxford University Press. 2002. Chapter 1.
- McCarthy NJ Bennett MR. Death signaling by the CD95/TNFR family of death domain containing receptors in: The molecular biology of programmed cell death. Oxford University Press 2002; chapter 8.
- McCluskey C, Quinn JP, McGrath JW. An evaluation of three new generation tetrazolium salts for the measurement of respiratory activity in activated sludge microorganisms. *Microbial Ecology*. 2005; **49 (3)**: 379-387.
- McLaughlin-Drubin ME, Huh K and Munger K. Human papillomavirus type 16 E7 oncoprotein associates with E2F6. *Journal of Virology*. 2007; **82 (17)**: 8695-8705.
- Meyskens FL Jr., Buckmeier JA, McNulty SE *et al.* Activation of nuclear factor- κ B in human metastatic melanoma cells and the effect of oxidative stress. *American Association for Cancer Research*. 1999; **5**: 1197-1202.

Mian S, Ball G, Hornbuckle J *et al.* A prototype methodology combining surface-enhanced laser desorption/ionization protein chip technology and artificial neural network algorithms to predict the chemoresponsiveness of breast cancer cell lines exposed to paclitaxel and doxorubicin under *in vitro* conditions. *Proteomics* 2003; **3 (9)**: 1725-1737.

Mian S, Ugurel S, Parkinson E *et al.* Serum proteomic fingerprinting discriminates between clinical stages and predicts disease progression in melanoma patients. *Journal of Clinical Oncology* 2005 ; **23 (22)**: 5088-5093.

Miret S, De Groene EM, Klaffe W. Comparison of *in vitro* assays of cellular toxicity in the human hepatic cell line HepG2. *Journal of Biomolecular Screening* 2006; **11 (2)**: 184-193.

Momparler RL, Karon M, Siegal SE *et al.* Effect of adriamycin on DNA, RNA and protein synthesis in cell-free systems and intact cells. *Cancer Research* 1976; **36 (8)**: 2891-2895.

Monte M, Simonatto M, Peche LY *et al.* MAGE-A tumour antigens p53 transactivation function through histone deacetylase recruitment and confer resistance to chemotherapeutic agents. *Proceedings of the National Academy of Science USA* 2006; **103 (30)**:11160-11165.

Motoko I, Akihiro K. *In vitro* chemosensitivity assays of retinoblastoma cells. *International Journal of Clinical Oncology* 2004; **9 (1)**: 31-35.

Morgan-Lappe SE, Tucker LA, Huang X *et al.* Identification of Ras-related nuclear protein, targeting protein for xenopus kinesin-like protein 2, and stearyl-CoA desaturase 1 as promising cancer targets from an RNAi-based screen. *Cancer Research* 2007; **67 (9)**: 4390-4398.

Mostaghel EA, Montgomery B, Nelson PS. Castration-resistant prostate cancer : targeting androgen metabolic pathways in recurrent disease. *Urology Oncology* 2009 ; **27 (3)** : 251-257.

Mtynarczyk-Biaty I, Roeckmann H, Kuckelkorn U *et al.* Combined effect of proteasome and calpain inhibition on cisplatin-resistant human melanoma cells. *Cancer Research* 2006; **66 (15)**: 7598-7605.

Munshi A, Kurland JF, Nishikawa T *et al.* Histone deacetylase inhibitors radiosensitize human melanoma cells by suppressing DNA repair activity. *Clinical Cancer Research* 2005; **11 (13)**: 4912-4922.

Muscolini M, Cianfrocca R, Sajeve A *et al.* Trichostatin A up-regulates p73 and induces Bax-dependent apoptosis in cisplatin-resistant ovarian cancer cells. *Molecular Cancer Therapeutics* 2008; **7 (6)**: 1410-1419.

Nessling M, Kern MA, Schadendorf D *et al.* Association of genomic imbalances with resistance to therapeutic drugs in human melanoma cell lines. *Cytogenetics and Cellular Genetics* 1999; **87 (3-4)**: 286-290.

Nicholson DW. Caspase structure, proteolytic substrates and function during apoptotic cell death. *Cell Death and Differentiation* 1999; **6**: 1028-1042.

Nociari MM, Shalev A, Benias P *et al.* A novel one step, highly fluorometric assay to evaluate cell-mediated cytotoxicity. *Journal of Immunological Methods*. 1998; **213**: 157-167.

Norris JL, Cornett DS, Mobley JA *et al.* Processing MALDI mass spectra to improve mass spectral direct tissue analysis. *International Journal of Mass Spectrometry* 2007; **260**: 212-221.

Nouri K. Skin Cancer. McGraw-Hill Professional Publishers 2007; p49

O'Day SJ, Christina KJ, Reintgen DS. Metastatic melanoma : chemotherapy to biochemotherapy. *Cancer Control*. 2002; **9 (1)**: 31-38.

Ormerod MG. Review: The study of apoptotic cells by flow cytometry. *Leukemia* 1998; **12**: 1013-1025.

Omerod MG. Investigating the relationship between the cell cycle and apoptosis using flow cytometry. *Journal of Immunological Methods*. 2002; **265**:73-80.

Osborne C, Wilson P, Tripathy D. Oncogenes and tumour suppressor genes in breast cancer: potential diagnostic and therapeutic applications. *Oncologist* 2004; **9 (4)**:361-377.

Panneerselvam M, Bredehorst R, Vogel CW. Resistance of human melanoma cells against the cytotoxic and complement-enhancing activities of doxorubicin. *Cancer Research* 1987; **47 (17)**: 4601-4617.

Park HS, Park CH, Choi BR *et al.* Expression of heat shock protein 105 and 70 in malignant melanoma benign melanocytic nevi. *Journal of Cutaneous Pathology* 2009; **36 (5)**: 511 – 516.

- Parkin DM. The global health burden of infection-associated cancers in the year 2002. *International Journal of Cancer*. 2006. **118 (12)**: 3030-3044.
- Pazzagli M. Bioluminescence and chemiluminescence studies and application in biology and medicine. Wiley Publishers, NewYork. 1988
- Pecorino L. Molecular biology of cancer: mechanisms, targets and therapeutics. Oxford University Press. 2005
- Peltonen K, Kiviharju TM, Jarvinen PM *et al*. Melanoma cell lines are susceptible to histone deacetylase inhibitor TSA provoked cell cycle arrest and apoptosis *Pigment Cell Research* 2005; **18 (3)**: 196-202.
- Petricoin EF, Liotta LA. Proteomic analysis at the bedside: early detection of cancer. *Trends in Biotechnology* 2002; **20 (12)**: s30-34
- Petty RD, Sutherland LA, Hunter EM *et al*. Comparison of MTT and ATP-based assays for the measurement of viable cell number. *Journal of Bioluminescence and Chemiluminescence* 1995; **10**: 29-34.
- Plummer ER, Middleton MR, Jones C *et al*. Temozolomide pharmacodynamics in patients with metastatic melanoma: DNA damage and activity of repair enzymes O⁶ -alkylguanine alkyltransferase and poly(ADP-ribose) polymerase-1. *American Association for Cancer Research Research* 2005; **11**: 3402-3409.
- Poprach A, Michalova E, Pavlik T. Actual state of *ex vivo* chemo resistance testing of malignant tumors in Masaryk Memorial Cancer Institute Brno. *Clinical Oncology*. 2008; **21 (3)**: 116-121.
- Ragnarsson-Olding B, Platz A, Olding L *et al*. P53 protein expression and TP53 mutations in malignant melanomas of sun-sheltered mucosal membranes versus chronically sun-exposed skin. *Melanoma Research*. 2004; **14 (5)**: 395-401.
- Reed RJ, Martin P. Exploding Myths: melanocytic neoplasms. *Seminars in Cutaneous Medicine and Surgery* 1997; **16 (2)**: 137-158.
- Richards IS. Principles and Practice of Toxicology in Public Health. Jones and Bartlett Publishers, Canada. 2008
- Rieber MS, Zangemeister-Wittke U, Rieber M. p53-independent induction of apoptosis in human melanoma cells by a bcl-2/bcl-xL bispecific antisense oligonucleotide. *Clinical Cancer Research* 2001; **7**: 1446-1451.

Ries L, Eisner M, Kosary C *et al.* Surveillance, epidemiology and end results (SEER): *Cancer Statistics Review 1975-2000*. Bethesda, MD: National Cancer Institute. 2003

Rosenfelt J, Hubler K. Adenylate Kinase. 1999

Roy N, Cardone MH. The caspases: consequential cleavage. In apoptosis the molecular biology of programmed cell death in: *Frontiers in cell apoptosis research* Oxford University Press 2002. Pp93-135

Sagnelli E, Coppola N, Pisaturo M *et al.* HBV super infection in HCV chronic carriers, a disease that is frequently severe but associated with the eradication of HCV. *Hepatology* 2009; **49 (4)**: 1090-1097

Sanchez C, Mendoza P, Contreras HR *et al.* Expression of multidrug resistance proteins I prostate cancer is related with cell sensitivity to chemotherapeutic drugs. *Prostate* 2009; **(epub ahead of print)**.

Sasaki T, Kawai K, Saijo-Kurita *et al.* Detergent cytotoxicity: simplified assay of cytolysis by measuring LDH activity. *Toxicology in vitro*.1992; **6 (5)**: 451-457.

Sauter ER, Klein-Szanto AJ, Atillasoy E *et al.* Ultraviolet B-induced squamous epithelial and melanocytic cell changes in a xenograft model of cancer development in human skin. *Molecular Carcinogenesis*. 1998; **23 (3)**: 168-174.

Schulz, WA. *Molecular Biology of Human Cancers*. Springer Publishing, The Netherlands. 2007.

Schwabe M, Lubbert M. Epigenetic lesions in malignant melanoma. *Current Pharmaceutical Biotechnology* 2007; **8 (6)**: 382-387.

Schwarzer G, Vach W, Schumacher M. On the misuses of artificial neural networks for prognostic and diagnostic classification in oncology. *Statistics for Medical Research* 2000; **19 (4)**: 541-561.

Scotto KW. Transcriptional regulation of ABC drug transporters. *Oncogene* 2003; **22**: 7496-7511.

Seeff LB and Hoofnagle JH. Peginterferon and ribavirin for chronic hepatitis C. *The New England Journal of Medicine*. 2006; **355 (23)**: 2444-2451.

Seetharamu N, Ott PA, Pavlick AC. Novel therapeutics for melanoma. *Expert Review of Anticancer Therapy*. 2009; **9 (6)**: 839-849.

- Sersa G, Stabuc B, Cemazar M *et al.* Electro chemotherapy with cisplatin: the systemic antitumour effectiveness of cisplatin can be potentiated locally by the application of electric pulses in the treatment of malignant melanoma skin metastases. *Melanoma Research* 2000; **10 (4)**: 381-385.
- Shabbits JA, Hu Y, Mayer LD. Tumor chemo sensitization strategies based on apoptosis manipulations. *Molecular Cancer Therapeutics* 2003; **2 (8)**:805-813.
- Sharpless NE, Kannan K, Xu J *et al.* Both products of the mouse Ink4a/Arf locus suppress melanoma formation *in vivo*. *Oncogene*. 2003; **22**: 5055-5059.
- Shih CS, Laurie N, Holzmacher J *et al.* AAV-mediated local delivery of interferon-beta for the treatment of retinoblastoma in preclinical models. *Neuromolecular Medicine* 2009; **11 (1)**: 43-52.
- Shuster S. Is sun exposure a major cause of melanoma? No. *British Medical Journal* 2008; **337**:a764.
- Si T, Guo Z, Hao X. Immunologic response to primary cryoablation of high-risk prostate cancer. *Cryobiology* 2008; **57 (1)**: 66-71.
- Sidawi D, Derra S. Fueled by large government grants, researchers are honing techniques that will help defend against bio-terror attacks and the spread of infectious diseases. *Research and Development Magazine*, May 2009.
- Singh S, Khar A. Differential gene expression during apoptosis induced by a serum factor: role of mitochondrial F0-F1 ATP synthase complex. *Apoptosis* 2005; **10 (6)**: 1469-1482
- Squirrel DJ, Murphy MJ. Adenylate kinase as a cell marker in bioluminescent assays In: bioluminescence and chemiluminescence: fundamental and applied aspects. John Wiley & Sons 1995: pp486-489
- Squirrel DJ, Murphy MJ. Rapid detection of very low numbers of microorganisms using adenylate kinase as a cell marker in: A practical guide to industrial uses of ATP luminescence in rapid microbiology. *Cara Technology Limited* 1997; pp107-113.
- Soengas MS, Lowe SW. Apoptosis and melanoma chemo resistance. *Oncogene* 2003; **22**: 3138-3151.

- Song H, Li Y, Lee J *et al.* Low-density lipoprotein receptor-related protein 1 promotes cancer cell migration and invasion by inducing the expression of matrix metalloproteinases 2 and 9. *Cancer Research* 2009; **69 (3)**: 879-886.
- Sorace JM, Zhan M. A data review and re-assessment of ovarian cancer serum proteomic profiling. *BMC Bioinformatics* 2003; **4**: 24-37.
- Stannard CJ, Wood JM. The rapid estimation of microbial contamination of meat by measurement of adenosine triphosphate. *Journal of Applied Bacteriology* 1983; **55**: 429-435.
- Steck K, McDonnell T, Sneige N *et al.* A flow cytometric analysis of apoptosis and Bcl-2 in primary breast carcinomas: clinical and biological implications. *Cytometry* 1996; **24**: 116-122.
- Subramanian A, Mokbel K. The role of herceptin in early breast cancer. *International seminars in surgical oncology*. 2008; **28 (5)**: 9
- Suter R, Marcum JA. The molecular genetics of breast cancer and targeted therapy. *Biologics* 2007; **1 (3)**: 241-258.
- Tafeit E, Reibnegger G. Artificial neural networks in laboratory medicine and medical outcome prediction. *Clinical Chemistry and Laboratory Medicine* 1999; **37 (9)**: 845-853.
- Taylor RC, Cullen SP, Martin SJ *et al.* Apoptosis: controlled demolition at the cellular level. *Nature Review of Molecular and Cell Biology*. 2008; **9 (3)**: 231-241.
- Testori A, Soteldo J, Sances D *et al.* Cutaneous melanoma in the elderly. *Melanoma Research* 2009; **19 (3)**: 125-134.
- Thakkar, NS, Potten CS. Inhibition of doxorubicin-induced apoptosis *in vivo* by 2-deoxy-D-glucose. *Cancer Research* 1993; **53 (9)**: 2057-2060.
- Thompson MP, Kurzrock R. Epstein-Barr virus and cancer. 2004; **10**: 803-821
- Tian HM, Shi XY, Fu J *et al.* Correlation between ATP bioluminescence tumour chemo sensitivity assay and clinical response in ovarian cancer. *Chinese Journal of Oncology* 2005; **27 (5)**: 296-298.

- Tonin PN. The limited spectrum of pathogenic BRCA1 and BRCA2 mutations in the French Canadian breast and breast-ovarian cancer families, a founder population of Quebec, Canada. *Cancer Bulletin* 2006; **93 (9)**: 841-846.
- Toth KF, Knock TA, Wachsmuth M *et al.* Trichostatin A-induced histone acetylation causes decondensation of interphase chromatin. *Journal of Cell Science* 2004; **117(Pt 18)**: 4277-4287.
- Touma SE, Goldberg JS, Moench P *et al.* Retinoic acid and the histone deacetylase inhibitor trichostatin A inhibit the proliferation of human renal cell carcinoma in a xenograft tumor model. *Clinical Cancer Research* 2005; **11 (9)**: 3558-3566.
- Traub F, Feist H, Kreipe HH *et al.* SELDI-MS-based expression profiling of ductal invasive and lobular invasive human breast carcinomas. *Pathology Research and Practice*. 2005; **201**: 763-770.
- Truong CD, Feng W, Li, W *et al.* Characteristics of epstein-barr virus-associated gastric cancer: a study of 235 cases at a comprehensive cancer center in USA. *Journal of Experimental and Clinical Cancer Research*. 2009; **3 (28)**: 14
- Tsujimoto Y. Apoptosis and necrosis: intracellular ATP levels a determinant for cell death modes. *Cell Death and Differentiation*. 1997; **4**: 429-434.
- Urbani A, Poland J, Bernardini S *et al.* A proteomic investigation into etoposide chemo-resistance of neuroblastoma cell lines *Proteomics* 2005; **5 (3)**: 796-804.
- Valentovic MA, Ball JG. 2-aminophenol and 4-aminophenol toxicity in renal slices from sprague-dawley and fischer 344 rats. *Journal of Toxicology and Environmental Health* 1998; **55 (3)**: 225-240.
- Van't Veer LJ, Bernards R. Enabling personalised cancer medicine through analysis of gene-expression patterns. *Nature* 2008; **452 (7187)**: 564-570.
- Varmus H. The Harold Varmus papers: Retroviruses and the genetic origins of cancer, 1970-1993.
- Veenstra TD, Conrads TP, Hood BL *et al.* Biomarkers: mining the biofluid proteome. *Molecular Cell Proteomics* 2005; **4 (4)**: 409-418.

- Wang X, Lu Y, Yang J *et al.* Identification of triosephosphate isomerase as an anti-drug resistance agent in human gastric cancer cells using functional proteomic analysis. *Journal of Cancer Research and Clinical Oncology* 2008; **134 (9)**: 995-1003.
- Wei C, Guo-min W, Yu-jun L. Apoptosis resistance can be used in screening the markers of cancer stem cells. *Medical Hypotheses* 2006; **67**: 1381-1383.
- Weinberg RA. Oncogenes and tumour suppressor genes. *CA: A Cancer Journal for Clinicians* 1994; **44 (3)**: 160-170.
- Weinberg RA. How cancer arises. *Scientific American* 1996; **275 (3)**: 62-70
- Weinberg RA. The biology of cancer. Garland Science Publishers. 2007.
- Westhead DR, Twyman RM. Bioinformatics. BIOS Scientific Publishers Ltd. 2002
- Westphal CH. Cell cycle signaling: Atm displays its many talents. *Current Biology* 1997; **7**: R789-R792.
- Wittig R, Nessling M, Will RD *et al.* Candidate genes for cross resistance against DNA-damaging drugs. *Cancer Research*. 2002; **62**: 6698-6705.
- Wolnicka-Glubisz A, Damsker J, Constant S *et al.* Deficient inflammatory response in UVB in neonatal mice. *American Association for Cancer Research*. 2006; **47 (7)**: 1120.
- Wu B, Abbott T, Fisherman D *et al.* Comparison of statistical methods for classification of ovarian cancer using mass spectrometry data. *Bioinformatics* 2003; **19 (13)**: 1636-1643.
- Wyllie AH, Kerr JF, Currie AR. Cell death: the significance of apoptosis. *International Review of Cell and Molecular Biology* 1980; **68**, 251-306.
- Yanagisawa K, Shyr Y, Xu BJ *et al.* Proteomic patterns of tumour subsets in non-small cell lung cancer. *Lancet* 2003; **362 (9382)**: 433-439.
- Yang C, Hoelzle M, Disanza A, Scita G, Svitkina T. Coordination of membrane and actin cytoskeleton dynamics during filopodia protrusion. *Public Library of Science* 2009; **4 (5)**: 5678
- Yasuhara N, Eguchi Y, Tachibana T *et al.* Essential role of active nuclear transport in apoptosis. *Genes to Cells* 1997; **2 (1)**: 55-64.

Young LS and Rickinson AB. Epstein-Barr virus: 40 years on. *Nature Reviews Cancer*. 2004; **4 (10)**: 757-768.

Zamorano J, Mora AL, Boothby M *et al*. NF-kappa B activation plays an important role in the IL-4 induced protection from apoptosis. *International Immunology* 2001; **13 (12)**: 1479-1487.

Zanetti R, Franceschi S, Rosso S *et al*. Cutaneous melanoma and sunburn in childhood in a southern european population. *European Journal of Cancer*. 1992; **28A (6-7)**: 1172-1176.

Zhang Z, Bast RC Jr, Yu Y *et al*. Three biomarkers identified from serum proteomic analysis for the detection of early stage ovarian cancer. *Cancer Research* 2004; **64 (16)**: 5882-5890.